INTERACTION OF GASEOUS MULTIPLE SWIRLING FLAMES.

A Thesis Submitted to the
University of Sheffield for
the Degree of
Doctor of Philosophy.

by

Günay Apak, B.Sc.Tech.,M.E.T.U.,Ankara.

Department of Chemical Engineering
and Fuel Technology,
University of Sheffield.

1974.

SUMMARY

This thesis is based on a study of the behaviour of the multiple burner systems. The influence of number of burners, their separation and degree of swirl on the interaction of multiple gaseous turbulent diffusion flames, for different configurations chosen, has been investigated. A single flame has been studied as a reference flame to provide information for the comparison with multiple systems.

The temperature and concentration profiles within the flames have been determined using thermocouples and a semi-continuous gas sampling system in conjunction with a gas chromatograph.

Three orthoganol mean velocity components in the annular air stream of a single isothermal swirling jet have been measured using a hot wire anemometer and by the application of a four point measurement technique developed within the department.

Multiple flame systems were found to be less stable against blow-off compared to single flames and the blow-off limit shifted towards the fuel rich region as the swirl was reduced. At low swirl levels and minimum separation the centre flames were lifted off the burner rim and were frequently blown-off.

At separations of less than four exit diameters, the overall flame length increased with a decrease in burner separation and increase in number of burners. At larger separations the flame length of the group reduced to that of a single flame at the same swirl level.

Flame temperature was found to be very sensitive to burner spacing and number of burners. Burner crowding is shown to reduce the entrainment of the ambient air and the rate of mixing

within the flames thus resulting in delayed combustion. Nevertheless the temperature profile of a multiple system was found to approach that of a single burner as the separation was increased to more than two exit diameters.

At the minimum separation concentration profiles showed high unburnt fuel and low oxygen concentrations on the axis between the flames where the turbulence intensities were expected to be low. Significantly high carbonmonoxide concentrations were recorded in the multiple flames due to improper combustion.

The multiple flame systems showed a slower approach to complete combustion. When the adjacent burners are far apart the large scale mixing between the fuel and the air is increased greatly.

A dilution factor has been described and computed using the measured gas concentration data which indicates the degree of dilution as a consequence of the entrainment of the surrounding air into the flame. The degree of dilution at a flame point is decreased as the number of burners is increased and the degree of swirl is decreased.

For flames separated by more than two burner exit diameters there was no significant interaction. When the burners are adjacent to one another interaction reaches a maximum.

ACKNOWLEDGEMENTS

The author would like to express her gratitude and appreciation to all those who have given help and advice during the course of this research. In particular she is indebted to Dr. N.A. Chigier for his guidance and continuous support on the project, without which this thesis would never have been completed.

Special thanks must also go to Professor J.M. Beér who helped to initiate the research, and Mr. G.N. Critchley for his invaluable guidance.

Thanks are also due to the Staff of the Department for their assistance throughout the course of this study, especially to Mr. C. Simpson and Mr. T. Galaj and the rest of the staff of the workshop who helped to build the experimental apparatus; to Mr. A. Reynolds, Mr. V.E. Reilly and Mr. D.J. Hancock for their willingness to help at all times and to Mr. R. Thompson and Mr. M. Wilde for all the photographic work; Mr. A. Sanby for the preparation of the sampling probes.

The author specially would like to thank Mrs. J. Czerny for the typing of this thesis.

The author also wishes to acknowledge the financial support of the Ministry of Defence (Ships) for the development of the project.

TABLE OF CONTENTS

LIST OF FIGURES

CHAPTER 6.

37. Effect of burner crowding on axial gas concentrations.

a - CH_4, O_2 conc.
b - CO, CO_2 conc.
c - H_2 conc.

38. Effect of burner crowding on axial gas concentrations at low swirl level.

a - CO, O_2 conc.
b - CH_4 - CO_2 conc.

39. Effect of swirl on O_2, CH_4, CO concentrations in a three burner system.

40. Effect of separation on axial gas concentrations in a three burner system.

a - O_2 - CO conc.
b - CH_4 - CO_2 conc.

41. Effect of separation on axial gas concentrations in a three burner system at low swirl level (S = 0.2).

a - O_2 - CO conc.
b - CH_4 - CO_2 conc.
c - H_2 conc.

42. Radial profiles of gas concentrations for a single flame at three axial positions.

a - CH_4 conc. b - CO conc.
c - H_2 conc. d - O_2 conc.
e - CO_2 conc. f - N_2 conc.

43. Isothermal velocity distributions in the annular section of a single jet (S = 0.37).

a - relative mean axial velocity.
b - relative mean tangential velocity.
c - relative mcan radial velocity.

44. Isothermal velocity distributions in the annular section of a single jet at high swirl level (S = 0.57).

a - relative mean axial velocity.
b - relative mean tangential velocity.
c - relative mean radial velocity.

45. Amplitudes of temperature fluctuations for a single flame (from C. Apak).

a - at S = 0.37.
b - at S = 0.57.

LIST OF PLATES

NOMENCLATURE

a	separation between the burners; distance to apparent origin of jet in diameters.
$\bar{a}$	separation constant.
A,B,C	calibration constants.
A',B',C'	second set of calibration constants.
A_p	orifice throat area.
c_p	specific heat.
C	nozzle fluid concentration.
C_m	mole fraction of nozzle fluid in an unburned stoichiometric mixture of nozzle fluid and air.
$\overline{(C'^2)}^{\frac{1}{2}}$	unmixedness factor.
C_p	orifice discharge coefficient.
d	wire diameter of the hot wire probe.
d_e	equivalent nozzle diameter in double concentric jets.
d_g	gas nozzle diameter.
D	jet nozzle diameter; D, inner diameter of the annular orifice; D_2 outer diameter of the annular orifice; side of an approximately square array.
D_E	burner exit diameter.
D_{eq}	equivalent nozzle diameter.
D_T	burner throat diameter.
D_W	thermocouple wire diameter.
e	excess air.
E	instantaneous voltage from anemometer; activation energy.
E_c	bridge voltage in the absence of any temperature change.
E_m	bridge voltage at temperature T_a.
E_s	stoichiometric combustion air requirement of the jet fuel.

f	mass fraction.
F	unmixedness factor; frequency factor.
g	gravitational constant.
G	momentum flux, $(\bar{w}_{mo}/\bar{u}_{mo})$ ratio of tangential/axial velocity maximum at nozzle exit.
G,K	probe direction constants.
G_x	axial flux of linear momentum.
G_ϕ	axial flux of angular momentum.
h	heat transfer coefficient between the wire and the flame; enthalpy.
H	heat of combustion.
id	inner diameter.
I	turbulent intensity.
I_x,I_y,I_z	local turbulent intensities.
J	proportionality factor, for laminar flames proportional to the exit velocity, for turbulent flames a constant; turbulent flux vector.
k	thermal conductivity, wave number.
K	orifice constant; numerical proportionality constant.
KE	kinetic energy of turbulence.
ℓ	wire length.
L	flame length; burner length.
L_R	relative flame length, %.
m	time mean chemical species' mass fraction; mass flow rate across a section at right angles to the jet axis.
M	mass flow rate; excess momentum flux of the jet; molecular weight.
M_A	aerodynamic mixing factor.
M_D	dilution factor.
M_e	entrained mass flow rate.
M_s	stoichiometric mixing factor.

M_s	stoichiometric mixing factor.
n	number of burners; a constant ($\approx$ 0.5).
N	degree of oxidation; number of moles.
Nu	Nusselt Number, (h.d/k).
P	pressure; distance between jet centres (pitch)
$\bar{P}$	pitch constant.
Pr	Prandtl Number, (c_p μ/k).
q	total volumetric flow.
Q_o	volume flux of injected fuel.
Q_p	volumetric flow through probe.
r	radial distance from central jet axis; radial co-ordinate.
R	jet radius; mass rate of creation per unit volume.
Re	Reynolds Number, (ρuD/μ).
R_E	jet exit radius.
R_T	jet throat radius.
R_s	separation ratio, (a/D_E)
R_w	wire resistance.
S	swirl number.
t	time.
T	temperature.
T_a	ambient temperature; temperature of the flow around the wire.
T_G	true gas temperature.
T_R	relative temperature rise, %.
T_w	wire temperature.
T_∞	semi-infinite equilibrium temperature.
u	component velocity in x direction.
u_m	maximum velocity.

$\bar{u}$	mean velocity in x direction.
u'	fluctuating velocity component in x direction.
$u'v'$	shear stress component in x-y plane.
$u'w'$	shear stress component in x-z plane.
U	mean resolved velocity acting on hot-wire sensor.
v	component velocity in y direction; time mean velocity.
$\bar{v}$	mean velocity in y direction.
v'	fluctuating velocity in y direction.
$v'w'$	shear stress component in y-z plane.
V	molecular volume.
w	component velocity in z direction.
$\bar{w}$	mean velocity in z direction.
w'	fluctuating velocity in z direction.
x	axial co-ordinate.
x,y,z	three mutually perpendicular axes (cartesian co-ordinate system).
x_c	critical distance.
X	mole fraction; axial distance.
y	transverse co-ordinate.
z	axial co-ordinate in the polar co-ordinate system.
Z	an additive constant ($\approx 2/3$)

Greek Symbols.

α	absorption coefficient.
Γ	turbulent exchange coefficient.
δE	variation in the bridge voltage with the temperature change.

$\delta r,\ z$	small distances in r - and z - directions.
ε	$(T_{a_1} - T_{a_2})/T_{a_1}$
ϵ	emissivity.
θ	overheat ratio; polar co-ordinate.
λ	annular to central jet velocity ratio of coaxial jets.
μ	viscosity.
ν	kinematic viscosity.
π	pi.
ρ	density; ρ_s ambient fluid density; ρ_o density of the nozzle fluid; ρ_F mean flame density; ρ_a air density.
σ	$\theta - 1$; Stefan-Boltzman constant.
τ	stress tensor; τ_{rr}, $\tau_{\theta\theta}$, τ_{xx}, $\tau_{r\theta}$, $\tau_{z\theta}$, τ_{rz} components of the stress tensor.
Φ	dissipation function.
ψ	stream function; ψ_T total value at particlar axial station.

Subscripts.

a	annular.
c	central.
co	centre jet to outer jet.
h	relating to enthalpy.
i,j	relating to chemical species i and j.
m	multiple.
mo	maximum values at the orifice exit.
max	maximum.
min	minimum.

o	initial value at nozzle exit.
oo	outer jet to outer jet.
s	single.
T	total.
TOT	total.
z,r,0	components of vector in co-ordinate directions.
1,2,3,4	measuring planes of hot wire probes.

Superscripts.

-	time mean average values.
'	fluctuating values.

CHAPTER 1.

INTRODUCTION TO THE PROBLEM AND AIMS OF THE STUDY

1.1 The General Picture.

In engineering practice groups of burners are often used rather than a large single burner of the same capacity. It is required to maintain high mixing rates in the individual jets in order to achieve stable conditions which are easily controllable for variations in fuel and air flow rates. In a single turbulent diffusion flame, chemical reaction and heat and mass transfer processes in the flame are largely controlled by the turbulent mixing properties of the flow. Heat, mass and momentum transfer within the flow is dependent upon the random turbulent motion superimposed on the time-mean flow. When a group of such flames is considered, it is advantageous to know how adjacent flames will behave and which are the major parameters affecting the rate of reaction and heat and mass transfer processes in such systems.

Although a multiple burner system has advantages over a large single burner, such a system has neither been fully studied or understood. In the past, emphasis was directed mainly toward single flame study. A large amount of information on single laminar and turbulent flames exists but these have not answered many of the fundamental questions concerning multiple flame behaviour. In recent years, multiple flame studies received more attention. Emphasis has been placed on obtaining information on these variables which will lead to a basic understanding of the behaviour and characteristics of multiple flames.

When the individual jets of the multiple flame system are distant from each other, the flame from each jet can be considered as a single flame and analyzed as such. As the distance between each jet is reduced, the flames will start to influence one another. Such conditions will be termed "interacting flames". As the separation is reduced, each flame starts touching the adjacent ones and they can even combine together to form a single flame. This condition is termed as "merging".

1.2 The Particular Interest.

Multiple burner systems are commonly used in industrial size boilers, reheating furnaces, process heating furnaces and rockets. The Admiralty, who initially proposed this research topic, uses multiple burners in Marine type boilers with the requirements of very high heat output in a considerably small volume. A typical marine type boiler as shown in plate (1-a) has closely packed multiple burners positioned on one wall firing directly into the cubic combustion chamber. Some of the methods used in firing of marine boilers are given by Hardcastle (1). The type of air registers used by the Admiralty have swirlers and the resultant jet is stabilized by a recirculation zone downstream of the swirler (2),(3).

The general reason for the preference of a multiple burner system is the numerous advantages it can provide over a single burner. These advantages can be summarized as follows:

a) Ease of obtaining a more uniform combustion and heat flux distribution within the furnace.

b) Avoiding the technical difficulties which are associated with making very large single burners during the design of high capacity furnaces.

c) Increased operating range owing to the possibility of turning one or more burners off to decrease furnace capacity.

d) Avoiding the dangers of burner failure which could result in serious losses if a single burner is used.

e) Possibility of changing burners or even the type of fuel used without seriously interrupting the furnace operation.

In spite of these advantages, problems arising from flame interaction can be quite detrimental to the combustion system. Some of the important effects can be summarized as follows:

a) Low frequency oscillations within the combustion chamber which could damage the system.

b) Flame switching, where the overall flame configuration may change and cause uneven heat distribution.

c) Preferential crowding of the flames to one wall of the combustion chamber.

d) Blow-off of one or more of the flames and subsequent reduction in the efficiency of energy output.

e) Lengthening or shortening of the flames resulting in wall impingement and bad heat distribution.

f) Poor mixing giving rise to improper combustion.

1.3 The Objectives of the Study.

The aerodynamic interaction of a multiple jet system is considered to be the most important factor which governs the overall interference. Allen (4) studied the principal factors which effect the interference of multiple jets under isothermal conditions. In order to achieve a better understanding of the extent of jet interaction in multiple jet systems it was decided to study the multiple jets under burning conditions. When the results of this research are coupled with Allen's (4) results on aerodynamic factors governing the system, wider

information about multiple flame processes can be obtained. To achieve this it was necessary to discover how a burning turbulent jet would behave in the presence of other similar neighbouring jets at close proximity. Since the mass flow rate of fuel and air were kept constant in each burner the increased flame lengths and changes in gas concentrations and flame temperatures along the flames in the group arrangements could be attributed to flame interaction in such systems.

The main objectives of this research programme are to study both quantitatively and qualitatively the effects of burner separation, degrees of swirl and number of burners for different arrays of turbulent swirling gaseous jet diffusion flames.

1.4 Outline of the Research Programme.

The research programme can be divided into two main categories: "Single jet investigations" and "Multiple flame studies". These can also be subdivided within themselves as follows.

a) Single jet investigations.

   i) Isothermal flow studies of the single jet with varying degrees of swirl.

   ii) Flame studies of a single flame at different swirl levels.

b) Multiple flame studies at various swirl levels.

   i) Two burner system with various separations.

   ii) Three burners in line with two different separations.

   iii) Four burners in square form.

   iv) Five burners (four burners forming a square and the fifth at the centre).

More details of the burner configurations studies are given in Chapter (4).

1.5 General Concepts Applied to Turbulent Jet Flows.

1.5.1 Two Dimensionality in Jets.

Physically all jets are three dimensional. Velocities may only be defined by assigning three components generally in the axial (u), radial (v) and tangential (w) directions. The axial velocities are in general dominant and velocity fluctuations and turbulent stresses are always present in all three dimensions; although they are non-isotropic, i.e. the three components of velocity fluctuations and turbulent stresses are not equal in all three directions. In the case of round jets, a cylindrical co-ordinate system (x, r, $\emptyset$) is generally convenient to use. In axi-symmetric jets which remain symmetrical about the central axis, at any one axial position the jet properties are only dependent upon the radial position. Therefore in practice, since $d/d\emptyset \neq 0$, it is only necessary to obtain measurements in any plane passing through the jet axis, thus axi-symmetric jets are mathematically described as being two dimensional.

1.5.2 Regions and Properties of a Swirling Axi-Symmetric Jet.

The tangential and axial velocity profiles of a jet with strong swirl will be as in Fig.(1). This swirl is produced near the jet exit either by a system of vanes in the path of the jet fluid or by introduction of a fluid, (mostly air) tangentially at the same point. Within the jet, the centrifugal forces and the pressure forces balance each other so that the equation $dp/dr = \rho w^2/r$ is satisfied. This radial pressure gradient results in a central core within the jet which has a lower pressure than the ambient pressure at the nozzle. This, in turn, results in an adverse axial pressure gradient so that

the flow reverses in direction and a central torroidal vortex is set up when the degree of swirl is sufficiently high. Under the effects of this vortex the outer boundaries of the jet expand rapidly. Due to this vortex, the potential core breaks down much faster and thus the flame is fully developed at much closer proximities to the nozzle of a jet with strong swirl as compared to a non-swirling jet. References (4,5,6,7,8,9) contain experimental and theoretical investigations of weakly to very strongly swirling jets.

The recirculation zone in a swirling jet increases the flame stability by the recirculation of hot combustion products into the cold fuel-air stream and by acting as a direct heat supply. It also decreases the axial velocities to a sufficiently low level to prevent blow-off and thus the jet flame which results is shorter wider and more intense. Near the jet axis the swirling flow is of the type termed "forced vortex" or "solid body rotation" where the tangential velocity component increases linearly with the radial distance from the axis. At positions away from the axis the swirling flow is of the type termed "free vortex" in which the tangential velocity decreases hyperbolically with the radial distance from the burner axis.

The degree of swirl of a jet can be quantitatively defined by deriving a dimensionless swirl number S (5) depending on axial flux of linear and angular momentum (G_x and G_ϕ respectively) as well as R, the jet radius.

Thus swirl number will be

$$S = \frac{G_\phi}{G_x \cdot R} \qquad \ldots\ldots\ldots \qquad (1.1)$$

The values of G_ϕ and G_x for the case of a forced vortex flow with a uniform distribution of the axial velocity at the orifice (when $\bar{w} = \bar{w}_{m_o} \cdot (\frac{r}{R})$ and $\bar{u} = \bar{u}_{m_o}$) are determined from the following equations (5),

$$G_\phi = 2\pi\rho \int_o^R r^2 \overline{uw}\, dr = \tfrac{1}{2}\pi \cdot \rho \cdot \bar{u}_{m_o} \cdot \bar{w}_{m_o} \cdot R^3 \quad \ldots(1.2)$$

$$G_x = 2\pi\rho \int_o^R r(\bar{u}^2 - \tfrac{1}{2}\bar{w}^2)\, dr = \pi\rho\bar{u}^2_{m_o} \cdot R^2(1-\frac{G^2}{4}) \quad \ldots (1.3)$$

where $G = \dfrac{\bar{w}_{m_o}}{u_{m_o}}$

So

$$S = \frac{G_\phi}{G_x \cdot R} = \frac{\frac{1}{2}G}{1 - \frac{G^2}{4}} \qquad \ldots\ldots\ldots \qquad (1.4)$$

Where the subscript O refers to maximum values at the orifice. A plot of S calculated from $S = (G/2)/(1-G^2/4)$ vs G is given in Fig.(2). When compared with the experimental values of S it is seen that the agreement although excellent below $G = 0.4$, is not as good at higher G values and in this range $S = (G/2)/(1-(G/2))$ fits the points much better.

1.5.3 Definitions Applied to Describe Turbulent Flows.

A Cartesian co-ordinate system (x,y,z) is used to define the system, the x axis coinciding with the axis of symmetry of the jet. Assuming that the flow field can be split into three component mean velocities ($\bar{u}$, $\bar{v}$, $\bar{w}$) and instantaneous fluctuating velocities (u', v', w') in the x, y and z directions respectively, at a point at any instant of time the instantaneous velocities can be given as

$$u = \bar{u} + u' \quad ; \quad v = \bar{v} + v' \quad ; \quad w = \bar{w} + w' \quad ;$$

Thus the time mean average terms can be given as

$$\overline{u^2} = \bar{u}^2 + \overline{u'^2} \quad ; \quad \overline{v^2} = \bar{v}^2 + \overline{v'^2} \quad ; \quad \overline{w^2} = \bar{w}^2 + \overline{w'^2}$$

If the root mean squares (RMS) of velocity fluctuations in x,y and z directions are represented by

$$(\overline{u'^2})^{\frac{1}{2}} \quad ; \quad (\overline{v'^2})^{\frac{1}{2}} \quad ; \quad (\overline{w'^2})^{\frac{1}{2}} \qquad \text{respectively}$$

then a local turbulence intensity can be defined for each direction as:

$$I_x = \frac{(\overline{u'^2})^{\frac{1}{2}}}{\bar{u}} \quad ; \quad I_y = \frac{(\overline{v'^2})^{\frac{1}{2}}}{\bar{v}} \quad ; \quad I_z = \frac{(\overline{w'^2})^{\frac{1}{2}}}{\bar{w}}$$

For a swirling jet the velocity fluctuations in all three directions are comparable in magnitude and the total local turbulence intensity is defined as:

$$I_{(TOT)} = \frac{(\overline{u'^2} + \overline{v'^2} + \overline{w'^2})^{\frac{1}{2}}}{(\bar{u}^2 + \bar{v}^2 + \bar{w}^2)^{\frac{1}{2}}}$$

Similarly there will be stresses formed within the flow field and the turbulent normal stresses are defined as:

$$-\rho\overline{v'^2} \quad ; \quad -\rho\overline{w'^2} \quad ; \quad \rho\overline{u'^2} \quad ;$$

the turbulent shear stresses are defined as:

$$-\rho\overline{u'v'} \quad ; \quad -\rho\overline{u'w'} \quad ; \quad -\rho\overline{w'v'} \quad ;$$

and the local kinetic energy of turbulence is defined as:

$$KE = \frac{\overline{u'^2} + \overline{v'^2} + \overline{w'^2}}{\bar{u}^2 + \bar{v}^2 + \bar{w}^2} = I^2_{(TOT)}$$

Because the kinetic energy of matter is proportionalto the square of the velocity the numerator is proportional to the energy of fluctuation whereas the denominator is proportional to the energy due to mean velocity.

The average direction of motion of molecules within a jet can be defined using the stream function ψ which may be defined as

$$\psi = \int_o^r \rho \, \bar{u} \, . \, r \, . \, dr \qquad \ldots\ldots\ldots \qquad (1.5)$$

and the total stream function ψ_T can be calculated by

$$\psi_T = \int_o^\infty \rho \, \bar{u} \, . \, r \, dr \qquad \ldots\ldots\ldots \qquad (1.6)$$

Since the total axial mass flowrate at any cross section downstream of the nozzle exit may be defined as:

$$M_T = \int_o^\infty \rho \, . \, 2\pi \, . \, \bar{u} \, . \, r \, . \, dr = 2\pi \, \psi_T \ldots\ldots \qquad (1.7)$$

and also the original mass flowrate from the nozzle may be defined as:

$$M_o = \int_o^r \rho \, . \, 2\pi \, . \, \bar{u} \, r \, dr = 2\pi \, \psi_o \qquad \ldots\ldots\ldots \qquad (1.8)$$

where ψ_o is the value of ψ_T evaluated at the nozzle exit. Thus the relative total axial mass flowrate will be

$$\frac{M_T}{M_o} = \frac{\psi_T}{\psi_o} \qquad \ldots\ldots\ldots \qquad (1.9)$$

A jet entrains the surrounding fluid across its boundaries as a result of momentum exchange between the jet and surroundings. The amount of entrainment will mainly depend upon the exchange coefficients and the local velocity gradient. The amount of

surrounding fluid entrained can be quite considerable, i.e. a turbulent jet entrains fluid equivalent to the nozzle fluid mass flow rate for about every three nozzle diameters' distance along the jet axis. For a constant density system (10), entrained mass is given as:

$$\frac{M_e}{M_o} = 0.32 \frac{x}{d} - 1 \quad \ldots\ldots\ldots \quad (1.10)$$

A more general equation for a non-constant density system is similarly given as

$$\frac{M_e}{M_o} = 0.32 \left(\frac{\rho_a}{\rho_o}\right)^{\frac{1}{2}} \frac{x}{d} - 1 \quad \ldots\ldots\ldots \quad (1.11)$$

where

M_e : Mass entrained downstream of the nozzle.

x : axial position.

d : nozzle diameter.

By applying the concept of the equivalent nozzle diameter based on the conservation of momentum flux, Beér and Chigier (11) extended several general relationships of round free jets to more complex systems. With no external forces acting, the axial momentum flow at the nozzle exit will be

$$G_x = G_o = \text{const} = \frac{\pi d^2}{4} \rho_o \bar{u}_o^2 \quad \ldots\ldots\ldots \quad (1.12)$$

For a non-constant density system the jet entrains ambient fluid of density ρ_s and due to high entrainment rate the density within the jet boundaries approaches the density of the surroundings within a short distance from the nozzle exit. The momentum flux for this system is given as:

$$G_o = \frac{d_e^2 \pi}{4} \rho_s \bar{u}_o^2 \quad \ldots\ldots\ldots \quad (1.13)$$

From eq. (1.12) and (1.13)

$$d_e = d \left(\frac{\rho_o}{\rho_s}\right)^{\frac{1}{2}} \qquad \ldots\ldots\ldots \qquad (1.14)$$

it is possible to calculate the equivalent nozzle diameter from the following equation if the mass flow rate and the momentum flux are known.

$$d_e = \frac{2\, M_o}{(G_o\, \pi\, \rho_s)^{\frac{1}{2}}} \qquad \ldots\ldots\ldots \qquad (1.15)$$

1.5.4 Characteristics of Double Concentric Jets.

Double concentric jets are compound jets consisting of a central jet surrounded by a coaxial annular jet. In their fully developed regions (8-10 nozzle diameters downstream) the two jets combine and show flow patterns similar to those of round jets. In this region the behaviour of the combined jet can be predicted from the combined mass flow rates and jet momenta. The region close to the nozzle is strongly affected by the size and geometry of the interface separating the central and annular jets. Because of its effect on flame stability, this region has a special importance for combustion studies.

In coaxial jets there is a displacement of the jet origin. Values of the displacement of the origin of the jet for a wide range of values of the annular to central jet velocity ratio λ of coaxial jets have been determined experimentally by Chigier and Beér (12). The value of the equivalent nozzle diameter d_e' for a double coaxial jet system was calculated as

$$d_e' = \frac{2(M_c + M_a)}{\pi\, \rho\, (G_c + G_a)^{\frac{1}{2}}} \qquad \ldots\ldots\ldots \qquad (1.16)$$

where:

M_c = mass flow rate of the central jet.

M_a = mass flow rate of the annular jet.

G_c = momentum flux of the central jet.

G_a = momentum flux of the annular jet.

Mean exit velocity $\bar{u}_{c_o}$, through the central nozzle of diameter d, is taken as the characteristic velocity of the central jet. The nozzle geometry and intensity of turbulence generated prior to the nozzle exit control the length of the potential core. Fig.(3) shows that for very low values of λ, i.e. $\lambda = 0.08$, the centre line velocity remains constant approximately for a distance of four central nozzle diameters, and then follows the hyperbolic decay of

$$\frac{\bar{u}_m}{\bar{u}_{c_o}} = 6.4 \frac{d_e'}{x + a} \quad \text{.....} \quad (1.17)$$

In Fig.(3) it is also shown that while the value of λ is increased the length of the potential core is decreased and velocity decays much faster. For the case of $\lambda = 2.35$ where the central jet is completely absorbed by the annular jet, at a distance of 3 d reverse velocity is measured on the centre line. The annular jet can be treated similarly by taking $\frac{1}{2}(D_2 - D_1)$ as the characteristic length and the annular mean exit velocity $\bar{u}_{a_o}$ as the characteristic velocity, where D_1 and D_2 are the inner and outer diameters of the annular orifice respectively. To specify the potential core of the annular jet is not very easy. Chigier and Beér (12) have shown in Fig.(4) that as the central jet velocity is increased, the length of the annular potential core is reduced and the decay of the maximum annular velocity is increased until $\lambda = 0.08$,

and the annular jet is absorbed, after a distance of $(D_2-D_1)=1$, within the confines of the central jet.

1.6 General Information on Flames.

1.6.1 General Behaviour of Turbulent Diffusion Flames.

Large industrial furnaces usually employ diffusion type flames in which fuel and oxidant are issued either unmixed or only partly premixed and the mixing occurs within the combustion chamber in conjunction with the combustion process. Under such conditions mixing properties of the turbulent flow are solely responsible for the mass transfer and most of the heat transfer within the flame. Heat, mass and momentum transfer within the flow is dependent upon the random turbulent motion superimposed on the time-mean flow. The rate controlling step in such a process is the turbulent "disintegration" of the reactants and the mixing is completed by molecular diffusion of the reactants into the cores of very small turbulent eddies. The oxidant and fuel must be sufficiently mixed at the root of the flame for any combustion to be possible. But even with a thoroughly mixed combustible, sufficient sensible heat must be supplied to provide the energy of activation for ignition. This is supplied by the back flow of the heat of combustion to the fresh mixture by convection and radiation. The contribution due to radiation is often negligible in gas flames. At the vicinity of the ignition zone owing to the turbulent exchange across the ignition front there is sufficient convective back flow of heat for flame stabilization. This mechanism is much faster than the molecular heat conduction in laminar combustion waves and becomes dominant totally as the stream velocities are increased beyond a certain critical value. This turbulent exchange is

not always fast enough to stabilize the flame at the burner exit and the mixture can either blow-off or the flame front can move some distance away from the burner where the stream velocities are lower. Therefore to enable the use of smaller combustion chambers and to ensure the ignition of the mixture, the generation of high turbulence intensities near the burner exit is quite desirable.

In practice one or more reverse flow zones will achieve this objective by carrying hot combustion products back to the fresh mixture just leaving the burner.

The reverse flow regions could be either external or internal to the flame. In external recirculation hot gases in the combustion chamber surrounding the flame are recirculated through the external flame boundary and merge into the main flame thus heating the mixture. In the case of internal reverse flow, recirculation occurs within the main forward flow of the jet. This can either be in the form of a wake flow behind a bluff body as in Fig. (5.). or by the static pressure defect which can cause the flow on the jet axis to be reversed due to a swirling motion imparted to the combustion air stream before it issues from the burner as in Fig. (6.).

Changes in flame shape will occur as the flow rate of fuel issuing from a nozzle is progressively increased. The diffusion flames increase in length as the nozzle velocity is increased up to a critical value, then the tip of the flames becomes unsteady and begins to flutter. As the velocity is increased a noisy turbulent flame brush starts forming at a definite point along the flame where breakdown of the laminar flow occurs and a turbulent jet develops. The distance from

the nozzle to the beginning of that turbulent brush is called the breakpoint length. With further increase in velocity, the breakpoint length decreases, and the fully developed turbulent flame condition is reached when the breakpoint shifts close to the nozzle. Hottel and Hawthorne (13), (20) determined characteristic flame length and breakpoint length curves as a function of jet velocity.

The length of a turbulent diffusion-free flame is generally dependent upon the fuel properties and the diameter of the burner used. Guenther (21) derived the following semi-empirical formula giving the flame length in terms of nozzle diameter.

$$\frac{L}{d} = 6\,(E_s + 1)\,\left(\frac{\rho}{\rho_F}\right)^{\frac{1}{2}} \qquad \text{.....} \qquad (1.18)$$

where E_s = Stoichiometric air/fuel weight ratio.

ρ = Fuel gas density.

ρ_F = Mean flame density.

Since mean flame density is found to be almost the same for various gaseous fuels, L/d varies with E_s and ρ only. For natural gas expected flame length within 10% accuracy is:

$$\frac{L}{d} = 6\,(17.25 + 1)\,\left(\frac{0.0423}{0.0128}\right)^{\frac{1}{2}} = 199$$

For the type of burners used in this research, the above formula does not apply. First of all, it does not cover the fully turbulent flame conditions and secondly the burner geometry is not taken into consideration.

1.6.2 Flame Stabilization and the Influence of Swirl on Flame Properties.

A stable flame is defined to be one that neither flashes back nor blows off after the ignition of the combustible mixture.

Under certain conditions the flame front is at a considerable distance away from the burner exit; such flames are still considered to be stable but the ones which are stable close to the nozzle exit are preferable. An unstable flame can be made stable by creating a zone or boundary layer within the flame in which the velocities are different from that in the main stream and are lower than the velocity of flame propagation. Velocity gradients must not exceed the critical boundary velocity gradients at which flame stretch occurs. Although flames can be stabilized using several different means, setting up recirculating flows in enclosed jet systems, in the central region of swirling jets and in the wake of bluff bodies are the most effective and practical methods of achieving this objective.

In systems used in practice, the relative variations of burning velocity as well as the variations of the flow velocity must be considered owing to the fact that the burning velocity will vary as a function of space. Several workers have devised models to predict the limits between which a flame will be stable (14-19). They are all similar except for the relative importance they have placed on the fluid mechanics and the chemical kinetics aspects of their approach. The main concern of these models is to restrict the stable region between the blow-off and flash back velocities at a given mixture ratio.

The main effect of imparting a swirling motion to the combustion air stream is the production of an internal reduced or reversed velocity region within the flow system. There are very high intensities of turbulence on the boundaries between this reverse flow region and the forward flowing main stream. Because the fuel is generally injected into the reverse flow

region, the main action of the swirl is to accelerate the mixing between the fuel and the oxidant and thus increase the combustion intensities. Such a system will be self stabilizing whatever the load on it might be owing to the increase in the reversed mass flow rate caused by any increase in the forward flow. The flame may still blow off at very high loads but this will be due to effects of reaction kinetics. In Fig.(7) a typical streamline pattern of a swirling jet issuing from a cylindrical annular nozzle into a large combustion chamber obtained by Chigier and Beér (22) is shown. In such a burner fuel would be injected through the central pipe into the reversed flow region. The resultant jet flame would be shorter and wider than a corresponding non-swirling flame and the overall combustion intensity will be much greater. The size and shape of such a flame can be varied between wide limits by changing the degree of swirl imparted to the jet. The generation of reverse flow zones by swirl has been demonstrated by photographs in flames by Swithenbank and Chigier (23).

For the type of system investigated maintaining the stability by swirl in particular when combined with a divergent burner exit was found to be very effective. Even though a swirler requires more fan power compared to a disc or wedge type stabiliser it has the advantage that in contrast to bluff body wakes the blockage in swirling jets is entirely aerodynamic and there is no need for a solid surface that is exposed to high temperature and to the effects of coke deposition which occurs on bluff bodies in heterogeneous combustion systems. There are two main methods of producing swirl; by supplying the fluid to the jet tangentially or by positioning a swirler with vanes to

impart a rotational motion to the fluid passing through the swirler.

The flame stability and the mixing rate of a multiple flame system is higher if swirling jets are used and the adjacent jets are "out of mesh" where the swirl velocity of the adjacent jets oppose each other rather than "in mesh" where the swirl velocities of the adjacent jets concur. To obtain this stability "out of mesh" swirling jets are used in this research.

Fricker and Leuckel (26) investigated swirl stabilisation of high jet momentum natural gas flames and provided detailed information on burner design.

1.6.3 Concentration of Species in Flames.

Combustion is a rapid process, and within a flame several reactions occur at a very rapid rate. Information on the rate of mixing and the reaction kinetics of combustion can be obtained by determining complete concentration profiles of different gas components at every point within the flame. During the evaluation of the gas composition Hawthorne et al. (13) have derived a quantity named significant concentration based on a conversion of the gas sample to its equivalent composition prior to any combustion, and identified the fraction of the converted sample which came from the nozzle. The mole fraction of nozzle fluid in a sample (C) is known as the nozzle fluid concentration. The mole fraction of nozzle fluid in an unburned stoichiometric mixture of nozzle fluid and air is C_m. In this research a similar correlation is made by using the carbon from the fuel as a tracer and making a carbon balance to calculate the amount of air entrained at each point.

The mass fraction of species i is defined as:

$$f_i = m_i / \sum m_i$$

The mole fraction of species i is defined as:

$$X_i = N_i / \sum N_i$$

Where $N_i = m_i / M_i \, V$

Therefore $$X_i = \frac{f_i / M_i}{\sum f_i / M_i}$$

Where M_i represents the molecular weight of species i.

The concentration data in this research is represented as percentage where % concentration of species i = X_i x 100.

1.6.4 Some Concepts of Flame.

The velocity with which a plane flame front moves normal to its surface through the adjacent unburnt gas is called the burning velocity. It varies with the nature and concentration of the gas mixture and initial gas temperature. Dugger and Heimel (24) found that burning velocity, S_u, of methane-air mixtures rises from 40 cm/sec at 320° K to 120 at 580° K. Burning velocity has a practical importance in flame stabilization and theoretical importance in the flame propagation theories. Since a plane flame front can only be observed under extremely special conditions several complications arise in measuring burning velocity. In general the flame front is either curved or it is not normal to the velocity of the gas stream. Several methods of measurement are given by Gaydon and Wolfhard (25).

The back pressure of a flame is imparted due to the acceleration of the flame gases as they pass through the reaction

zone. It varies with the burning velocity and for slow flames back pressure will be too small to measure; thus for natural gas-air flames it will only be at most about 0.001 mm of water. For fast flames, however, back pressure will be considerable and may even be used to determine the burning velocity.

1.6.5 Notations Used to Define Mixing in Flames.

Some derived quantities have been defined by Hemsath (27) to aid in the quantitative description of some properties of flames such as the amount of mixing, the effectiveness of mixing and the extent of combustion at any specific point within the flame. These quantities are defined as follows:

a) The aerodynamic mixing factor M_A: This value compares the air to fuel ratio at a flame point to that at the burner input. It is defined as:

$$M_A = \frac{(\text{Mass of air/Mass of fuel})_{\text{flame point}}}{(\text{Mass of air/Mass of fuel})_{\text{input}}}$$

Theoretically

$M_A < 1$ indicates an excess of fuel.

$M_A = 1$ indicates complete mixing.

$M_A > 1$ indicates an excess of air.

But in practice and especially at the outer regions of an open burner, this ratio is always higher than unity due to entrainment of atmospheric air into the flame.

b) The stoichiometric mixing factor M_s: This value compares the air to fuel ratio at a flame point to the stoichiometric air to fuel ratio of the fuel being used, it is defined as:

$$M_s = \frac{(\text{Mass of air/Mass of fuel})_{\text{flame point}}}{(\text{Mass of air/Mass of fuel})_{\text{stoichiometric}}}$$

These two mixing factors are not linearly independent and the relation between them can be given as

$$M_s = (1 + e) M_A$$

where e is the fraction of excess air employed. It is evident that

$M_s < 1$ indicates insufficient air for the completion of the fuel combustion.

$M_s = 1$ indicates just sufficient air to complete the combustion.

$M_s > 1$ indicates an excess of air over that required to complete the combustion at the point in question.

These two factors can represent the extent of large scale mixing quite satisfactorily but the determining factor in combustion is the mixing at the molecular level. This unfortunately is not directly observable but because the rate of combustion is on the average an order of ten higher than that of molecular diffusion, mixing at the molecular level can be assumed to be the rate determining step in combustion reactions and the scale can be estimated depending upon the extent of possible combustion.

c) Degree of oxidation N: This is a measure of the extent of the combustion. It is given as:

$$N = \frac{\text{Mass of } O_2 \text{ reacted.}}{(\text{Mass of } O_2 \text{ reacted} + \text{Mass of } O_2 \text{ required to complete the reaction})}$$

$N = 0$ indicates no combustion,

$N = 1$ indicates complete combustion,

and N will be between these two values in case of incomplete combustion. The combustion can be incomplete owing to two factors:

i) The stoichiometric mixing factor at the point in question can be below 1 meaning that there is not enough oxygen to take the reaction to completion.

ii) Although the oxygen required for combustion is present, either it is too much so that the mixture lies outside the inflammibility limits or it is not mixed with the fuel at a molecular level to enable combustion. A factor which takes into account both these variables will be the following

d) Unmixedness factor F: This is defined as

$$F = 1 - \frac{N}{M_s} \quad \text{for} \quad M_s < 1$$

$$F = 1 - N \quad \text{for} \quad M_s \geq 1$$

The reason for defining the unmixedness by two different expressions is to differentiate between incomplete combustion due to lack of oxygen and that due to poor molecular mixing. If there is an excess oxygen, the amount of oxygen makes very little difference therefore M_s is omitted from the expression for $M_s \geq 1$.

e) Dilution factor M_D : In a free turbulent flame there is extensive entrainment of the atmospheric air into the flame. The concentration profiles for combustion products all decay after a certain point, as one moves away from the burner in any direction, due to dilution effects. To explain the extent of this, a dilution factor is derived by the Author which gives a measure of the gas at a flame point which originally came from the nozzle. It is given as:

$$M_D = 1 + \left(\frac{X_{air}}{X_{fuel}} \right)_{input} \cdot \left(X_{fuel} \right)_{\substack{flame \\ point}} - \left(X_{Air} \right)_{\substack{flame \\ point}}$$

where X denotes mole fraction.

M_D = 0 indicates that the medium is only entrained air.

M_D = 1 indicates zero entrainment.

The real practical application of M_D is that when the measured concentration of a combustion product or combustible component at the flame point is divided by M_D, the result will represent the concentration without any entrainment present.

Values $M_D > 1$ indicates that the region is fuel rich.

CHAPTER 2.

LITERATURE SURVEY

2.1 Introduction

The present state of knowledge on multiple jet systems is very limited. Only a few references are available in the literature on the multiple flame systems. Even among the single jet studies information on double-concentric-swirling jets is quite rare. In the following chapter the relevant information available related to the subject of this research is reviewed. Although this research deals with a system of multiple jets, some information on single jets - the building blocks of a multiple jet system - is also included in order to help in the understanding of the behaviour of the individual jets used.

2.2 Single Swirling Jets.

2.2.1 Single Isothermal Swirling Jets.

For the purpose of improving flame stabilization and overall combustion characteristics in industrial burners, a swirling motion is imposed - generally on the combustion air stream. The extensive practical difficulties of obtaining detailed accurate measurements in flames limited the initial jet studies to isothermal models but recent developments in technology have made many measurements in flames possible.

Chigier and Beér (22) measured the mean velocity and static pressure distributions in swirling air jets issuing from annular and divergent nozzles into stagnant surroundings and found that a region of sub-atmospheric pressure was generated in the central region of the jet. An increase in the degree

of swirl of the air increased this static pressure defect. Flow reversal and the formation of an internal torroidal vortex was detected above some critical value of swirl. Associated with any progressive increase in swirl level there was an increase in the angle of spread of the jet as well as increases in the rates of decay of the axial, tangential and radial components of the mean velocity. Chigier and Chervinsky (5),(28), further studied a similar system and proved that the empirical constants describing the physical characteristics of a fluid jet like the decay of velocity and spread of the jet were all functions of the degree of swirl. The authors concluded that with increase in the degree of swirl the velocity constants decreased progressively whereas the rate of spread of the jet increased. The rate of spread of the jet is generally described by means of the jet half angle which is defined by the angle of the line drawn through the point at which $u/u_m = 0.5$.

Craya and Darrigol (7) made an extensive investigation of turbulent isothermal and heated swirling jets. Eight jets, each having different degrees of swirl from weak (S = 0) to very strong (S = 1.58) have been employed systematically during the investigation. Mean axial and swirl velocities, mean temperature fields in the heated jets, kinematic fluctuations and thermal intensity of turbulence have been measured. Maximum axial velocities near the axis and a reversed recirculating flow in the vicinity of the nozzle have been recorded for strongly swirling jets. The kinematic and thermal expansion of a strongly swirling jet up to 20 orifice diameters downstream was found to be more rapid than in a non-swirling jet. The observed axial velocity and turbulent shear stress profiles were explained

theoretically and the theoretical limiting case where similar profiles are possible is discussed. It is found that similar velocity profiles are possible only for a jet having zero axial momentum flux change.

Laurence (8) measured intensity of turbulence, longitudinal and lateral scales, and the spectra of turbulence in the mixing region of a free subsonic jet with a hot-wire anemometer. The intensity of turbulence, expressed as a percentage of the core velocity, gave a maximum at about 1 jet radius away from the centreline and decreased with an increase in Mach and/or Reynolds number. The lateral and longitudinal scales of turbulence were found to be almost independent of Mach and Reynolds number and varied proportionally with distance from the jet exit. The lateral scale was found to be much smaller than the longitudinal scale and did not vary with distance from the centreline of the jet, while the longitudinal scale was a maximum at a distance from the centreline of about 0.7 to 0.8 of the jet radius.

Rose (9) studied a swirling round turbulent jet of air generated by flow issuing from a rotating pipe into a reservoir of stagnant air. The velocity field of the swirling jet down to a distance of fifteen pipe diameters from the exit was measured by a constant-temperature hot-wire anemometer. The results of his measurements show that very nearly similar Gaussian profiles exist for the axial velocity at all measured axial stations beyond $1\frac{1}{2}$ diameters. The distribution of the swirling velocity at all measured axial stations assumes the same similar profile which is related to the corresponding similar profile for the axial velocity distribution at the same

axial station through a characteristic radius of the swirling jet. Rose also reported the decay of the maximum axial and the maximum swirling velocities and the effect of swirl on jet spread.

Ricou and Spalding (10) developed a technique for measuring the axial mass flow rate in a turbulent jet formed when a gas is injected into a reservoir of stagnant air at uniform pressure. From the experimental measurements an entrainment law relating jet momentum, mass flow rate, axial station and density of the surroundings, including the effects of buoyancy was determined. For high Reynolds numbers when the fluid density is uniform and x is much larger than the diameter of the orifice, a proportionality between m and x was existed as follows:

$$K = \frac{m}{x \; M^{\frac{1}{2}} \; \rho_s^{\frac{1}{2}}}$$

where

m	:	mass flow rate across a section at right angles to the jet axis.
x	:	axial distance from the nozzle.
M	:	excess momentum flux of the jet.
ρ_s	:	density of the surrounding fluid.
K	:	numerical proportionality constant.

The value of K was determined as 0.282 for different jet fluids under isothermal conditions. The above equation was valid for non-uniform density systems provided that buoyancy effects are negligible. Measurements under burning condition of propane and hydrogen showed that the rate of entrainment was lower under burning conditions than isothermal system. They also showed a considerable effect of buoyancy.

Allen (4) studied a turbulent swirling jet using a constant temperature hot wire anemometer and measured turbulent intensities, shear stresses. kinetic energy of turbulence and other important turbulence parameters. With the introduction of swirl the velocity gradients within the jet were found to increase and associated with that, mixing rates close to the nozzle also improved; therefore swirling jet entrained surrounding air at a greater rate than a corresponding non-swirling jet, consequently the length of the jet and the time required for mixing is reduced. At about four jet diameters downstream, the normal and shear stress terms were found to be less than those in a non-swirling jet, but the area over which the jet had spread was wider.

Lee (6) has obtained a simple closed-form solution for an axisymmetrical turbulent swirling jet issuing from a circular source into a semi-infinite motionless ambient fluid. Assumptions of similar axial and swirl velocity profiles and lateral entrainment of ambient fluid have been made in the derivation of the integrated governing equations of state. There is a close agreement between theoretically calculated results for the decays of axial and swirling velocities and the spread of the jet, and experimental results.

2.2.2 Single Swirling Jet Flames.

Narain and Uberoi (29) developed a new analytical entrainment model for an axisymmetric buoyant swirling turbulent plume in a quiescent homogeneous density environment, by assuming density differences between the plume and the ambient surroundings. They further assumed streamwise similarity of the mean axial and swirl velocities, as well as the turbulent stresses. The

latter assumptions have been confirmed experimentally by several authors. However, such similarity assumptions are only valid at large distances from the orifice of the jet and for small degrees of swirl. The entrainment is found to be a function of the Reynolds stress, the form of various similarity profiles, the local Froude number, and the swirl ratio of the swirling plume. The rate of entrainment across the boundaries of the plume were found to be increased with an increase in degree of swirl. The numerical results agree well with the existing experimental investigations for the axial and swirl velocity decays and the jet spread.

Chigier and Chervinsky (30) further investigated turbulent swirling free flames in a similar flow system as in their isothermal studies. The flames investigated were lifted and stabilised approximately four diameters from the burner exit in the form of an annular ring. The relatively cold, high velocity core persisted over almost the whole length of the flame and the temperature maximum was found in the main reaction zone in an annular region. The turbulent burning velocity was found to be eighty times greater than the laminar burning velocity. The decay of axial velocities in the flame was slower than isothermal model.

Bafuwa and Maccallum (19) have worked on stabilising swirling jets with 30°, 45°, 60° vanes, using town-gas as fuel. They found that in fuel rich flames stability depended on secondary combustion with entrained air. Work was mainly concentrated on weak flames in which the stability depended on the central recirculation zone, and it was concluded that the stabilization of the flames in the central recirculation zones of

swirling jets is greatly influenced by entrainment of ambient air into the central zone which increases with degree of swirl. By plotting the absolute component of velocity at the swirler exit against the temperature at the edge of the recirculating zone nearest to the swirler, the weak stability limits can be correlated. The mass ratios of entrained air to total gases in the recirculation zone were found to be 0.26, 0.40 and 0.53 for the 30°, 45° and 60° swirlers respectively.

Beér and Chigier (31); Beér (32); Kerr and Fraser (33); Fricker and Leuckel (34); Leuckel (35) and Beltagui and Maccallum (36) have all studied swirling flame systems with different types of swirlers and different fuels. All their results show increased combustion intensities with increasing swirl and improved flame stability.

2.3 Multiple Jets.

2.3.1 Multiple Non-swirling Isothermal Jets.

Laurence and Benninghoff (37) have determined turbulence and mean-flow characteristics of several noise-suppression multiple jet nozzles such as four slotted nozzles in line with different separation and three sector nozzles. The authors aimed to determine the effect of nozzle configurations on the intensity and the scale of the turbulence in the mixing zone common to two or more interfering jets. Turbulent mixing was found to be increased by dividing the flow into interfering multiple-jet nozzles. Maximum turbulent intensities occurred at the outer fringes of the jets. The scale and intensity of turbulence were less in the common mixing zone of two interfering jets than in the mixing zone of a single jet. The study of the turbulent spectra of the noise generated showed that the effect of multiple slots or sectors was to shift energy from high to low frequencies and to eliminate or reduce spectral peaks in certain frequencies and to increase them in others.

Corrsin (38) studied a parallel two dimensional jet system. Each jet issued from slots in a grid which was made up of a row of parallel rods with a grid density (solid area/total area) of 0.83. The system as a whole was unstable. Immediately after exit from the slots grouping of adjacent jets occurred which caused vigorous eddying flow. Subsequently neighbouring groups combined together and the phenomenon was non-stationary and switched from one configuration to another. A fine mesh grid, placed close to the nozzle exit helped to stabilize the flow. In the mixing region between the jets, low turbulence intensities were recorded at the regions having high velocities and low velocity gradients and high turbulence intensities occurred at the regions having low velocities and high velocity gradients.

Jung Von (39) studied the stability of a single jet in a long enclosure. He also performed a series of experiments showing the instability of four of these jets when placed parallel to each other. Due to crowding of the combined jets upon one wall or the other an asymmetric flow distribution was obtained which could be controlled by adjusting the direction of the jets in such a manner that combination of adjacent jets was encouraged.

Knystautas (40) investigated the turbulent jet system issuing from a series of holes in line with a pitch (distance between jet centres/jet diameters) of 1.5 and 3. A comparison between measured mean velocity profiles and theoretical profiles was made. Some preliminary theoretical work was presented on the formation af a quasi-two dimensional jet.

Koestel and Austin (41) derived a set of equations, depending on the principle of addition of momentum, to estimate

the maximum jet velocites at any distance from two adjacent parallel air jet nozzles.

Whaley (42) made an investigation of multiple jet systems. He studied the flow characteristics in a multiple burner arrangement and showed that there is a close resemblance between axial velocity decay and recirculation of enclosed multiple jets and that of an enclosed single jet. Close to the nozzle exit both a single jet and closely spaced multiple jets were found to behave similarly. At the downstream positions of multiple systems, the jets combined and could be treated as a single jet from a source along the common axis. By placing a wire mesh grid into the flow field at an axial station away from the jet exit recirculation towards upstream of the jet could be increased.

Miller and Comings (43) studied dual jet flows issuing from a plane wall and their force momentum fields. Near the nozzle exits and in the region of jet convergence the flow structure in the core of either jet was found to be similar to that of a single free jet allowing for the static pressure differences. The two jets tended to converge due to creation of a sub-stmospheric pressure region between the jets. The jets combined to form a single jet after the convergence and the combined jet was nearly symmetrical about the centre line and behaved similarly to that of a single jet. In the sub-atmospheric region between the jets, due to flow reversal, two stable contra-rotating vortices were formed with a free stagnation point on the centre plane.

Glahn et al (44) have obtained peak-velocity decay data for several circular and non-circular single element and multi-

element nozzles for reducing the jet-flap interaction noise from an externally-blown-flap Stol aircraft. The data were found to be useful for nozzle design in order to improve the mixing between the jet exhaust and the surrounding air. The multi-element nozzle formed from small individual elements promoted an initially rapid mixing with the surrounding air resulting in a rapid axial velocity decay. The peak axial-velocity decay curves for several categories of multi-element nozzles at different configurations were obtained. The multi-element nozzle types used were coplanar multitube nozzles including single and multiple rings of tubes, single ring coplanar multi-lobe nozzles, and several special non-coplanar nozzles. Empirical equations were developed, in particular for the nozzle geometries tested, to correlate the peak axial-velocity decay in multi element systems in terms of flow regime and nozzle dimensions.

2.3.2 Multiple Non-Swirling Jet Flames and Multiple Fires.

Wright (45) made an investigation of multiple flameholders to increase flame spreading rates relative to the rate possible with a single flameholder. He has reported that, with multiple arrangements, relatively shorter combustion chambers are needed, but since the blockage of the flameholder in the small duct is high, and since blockage adversely affects flame blow-off speeds, the blow-off speeds for multiple arrays are relatively low. Due to flame interaction in multiple flameholder systems, some of the flames are usually pinched down and blown-off prematurely, particularly for closely spaced flameholders and for conditions approaching blow-off. The flames were found to have the same average flow conditions.

Godridge (46) studied flame temperature, heat fluxes, emissivities and carbon concentrations on large scale oil fired burners in single and group arrangements. He has shown that burners fired in groups gave higher temperatures and heat fluxes but less grit concentrations. Heat fluxes are shown to be increased by a factor of two and three in going from a single burner in the test facility to the multiple system in the plant. If these high heat fluxes occur close to off-load burners, the burner components could easily be damaged. Since the formation of SO_3 increases relative to the amount of excess air in the furnace, the cooling of the off-load burners by introducing large amount of air is not recommended.

Miss Macnair (3) reports some of the problems related to multiple burners, such as the effect on register draught loss, flame length and heat transfer, air distribution between the individual burners. Recommendations are made on further research to find an optimum separation which will give rapid and complete combustion.

Zeitz et al (47) investigated the properties of high speed enclosed propane-air diffusion flames for burners with fuel slits lying in between the air slits. Jet arrangements with 2, 3 or 4 air jets and 1, 2, or 3 fuel jets respectively were used. A radioactive tracer (Kr 85) was used to find the flow path of the fuel and its mixing with the air jet. Both symmetrical and asymmetrical flow configurations could be obtained in a cold three slit system as a consequence of wake formation in between the air slits. In a five slit system, first two jets mix and subsequently the remaining two jets merge into this stream to form one single jet which leans towards one of the walls and

creates a large recirculation swirl on the opposite side of the chamber, thus resulting in an assymmetrical flow pattern. In contrast to the isothermal system, under burning condition symmetrical profiles were obtained for both 3 and 5 slit arrangements. However, complete stabilization still was not possible even though the mass of the jet was accelerated by combustion. Slightly higher recirculation velocities were recorded in flames but the whole mass sucked in by the air jets on a certain length was reduced because of the lower density of the recirculated flow. The centre jet showed a slight pendulum motion from one wall jet to the other. Countercurrent velocity in the central wake was found to increase linearly with increasing inlet velocity, but the length of the recirculation zone remained independent of the air jet velocity. The stability of a flame was characterized by the blow-off velocity which was a function of air discharge velocity since this dominated the flow field in diffusion flames. For the range studied the fuel velocity had no influence on blow-off velocity since the flow rate of the fuel was only 1 - 5% of that of the air. The maximum blow-off velocity for the three slit burner was seen to decrease with increased slit width whereas it was increased in case of the five slit burner; but the range of the maximum velocities for the five-slit burner was lower (40 - 80 m/s) than it was for the three slits (150 - 330 m/s). The corresponding maximum fuel/air ratios have shown a similar behaviour. In the case of the three slit burner a stable flow with strong wall jets was even possible under isothermal conditions and this stability was increased further with combustion. When the air slit width was increased a smaller

wake was formed between the slits which led to a lower recirculating flow and thus lower blow-off velocities. Measurements also showed that the ratio of maximum recirculating velocity to inlet air velocity was decreased as the separation between air and fuel slit centres was decreased and less amount of fuel could be preheated. In case of the five slit burner the centre air jet had to propagate against a strong pressure gradient which was created by the two side jets and under isothermal conditions a stable symmetrical flow was not possible at all. Although combustion increased the stability there was still a high tendency for the centre jet to merge with one of the side jets. The system was unstable and showed a slight pendulum motion. Consequently the level of blow-off velocities was greatly reduced compared with the three slit burner. The reason in this case for a decrease in the air slit width being not accompanied by an increase in the fuel/air ratio was given as follows: The tendency of instability was increased with decreasing air-slit width when the centre to centre separation was kept constant, because lower recirculation flows and lower blow-off velocities due to the presence of unstable recirculation zones were more sensitive to opposite fuel flow within their own centre which always had the tendency to slow down the recirculation flow. The observations for burners with more slits gave the same unstable asymmetrical flow patterns.

Putnam and Speich (48) have studied effects of interaction in buoyancy controlled gaseous multiple turbulent diffusion flames for the purpose of modelling such flames. A gaseous fuel was preferred in order to keep the fuel flow rate under control and to eliminate the fuel flow rate as an independent

variable in the establishment of modelling laws. Several flame arrays have been studied in terms of number of jets, flame height, source shape factor, flame spacing and fuel flow rate. The ratio of flame height of group jet flames to single jet flame was found to change as a function of jet spacing, the number of jets, and source shape factor. At a critical spacing factor of about two, the jet flames changed abruptly from acting as single jet flames to acting as a mass fire. A semi-empirical correlation of the array flame height indicates that flame height reaches a finite maximum as the number of jets in a line is increased. The experimental data have been presented and analyzed from two different view points. First considering the total flame source as a series of small or point sources of fuel, and secondly considering the total flame source on an area basis. A range of flow rates and nozzle diameters was found so that the Reynolds number would be large enough for turbulent flow yet the Froude number would be small enough that the flame would be buoyancy controlled. For multiple fires considered as point sources, Putnam and Speich correlated flame lengths as

$$L_m/L_s = \text{function}\left[\text{source shape factor}, n, \frac{a}{(Q_o^2/g)^{1/5}}\right]$$

where Q_o = volume flux of injected fuel.

g = gravitational constant.

L_m = multiple fire height.

L_s = single fire height.

n = number of jets.

a = spacing between jets.

A plot of the data as a flame height function $[(L_m/L_s)-1]/(n^{2/5} - 1)$ versus a spacing function $[a/(Q_o{}^2/g)^{1/5}]$ showed that the flame height function was increased as the spacing function was decreased which was considered to be caused by mutual entrainment. Treating the total flame source on an area basis, a correlation was obtained by plotting L/D vs $q^2/g\ D^5$ where q is the total flow rate and D is the side of an approximately square array.

Thomas, et al (49) also studied the flame heights of buoyancy controlled merging fires. A highly simplified theory was developed which considered entrainment and the motion of the flames. An expression for the flame height at the onset of merging of two rectilinear fuel burners was derived. It was noted that a column of hot rising gases entrains air from its surroundings, so that when one flame is placed in the neighborhood of another, the resulting restriction of the air flow causes a pressure drop in the space between the two. This pressure drop causes the air to flow toward the low pressure space, which in turn causes the flames to be deflected from the vertical.

Huffman (50) made some experimental studies to obtain data on the interaction and merging of flames from various liquid fuels in several spatial configurations. The work was mainly concentrated on studying the burning rate and radiation flux to the fuel and surroundings with special relevance to heat feedback. The burning rate data was correlated in such a manner that it could be used to predict the behaviour of multiple fires in situations involving other liquid fuels and other numbers and arrangements of fuel sources.

Braunschweig (51) made an analysis of the multiple flame behaviour to find a proportionality factor which could help to predict the interaction of multiple flame systems. The ratio x/L was accepted as a good measure for the degree of completion of all the flame processes where x was the axial distance measured from the nozzle exit and L was the "stoichiometric" flame length. The combustion was completed at $x/L = 1$. In a similar manner, the ratio a/L was given as a measure for the interaction of several parallel flame-jets. Where a was the separation between the flame axis of neighbouring flames. The interaction of flames increased as a/L was reduced. The region close to the nozzle exit was defined as the "near region" whereas the region at a larger distance from the exit was defined as the "far region". In the "far region" the mass and momentum flux resulting from a multi burner system was not different from that of a single burner with an equivalent diameter D_{eq} and with the initial mass flow and the momentum flux equal to the sum of the mass flow and momentum flux from the multiple system. The approximate length of a laminar or non-swirling turbulent diffusion flame could be calculated from the following equations:

$$L = JD(Z + E_s) \approx JDE_s$$

where
- J : proportionality factor; for laminar flames proportional to the exit velocity; for turbulent flames - a constant.
- E_s : The stoichiometric combustion air requirement of the fuel jet. (m^3 air/m^3 fuel).
- Z : An additive constant ($\approx 2/3$).(Z is normally much smaller than E_s and thus negligible.)
- D : diameter of the burner nozzle.

In the multiple systems when the combustion in the far region was not complete, then a single "resulting" flame was formed. Its length could be approximated as

$$L_m = J D_{eq} (Z + E_s) \approx D_{eq} \cdot E_s$$

where $L_m > L$.

The ratio x/L_m was taken as the measure for the progress of the flame process in the "resulting" flame where $x/L_m < x/L$. When the individual flames of the multiple system were combined to form one big flame in the far region the progress in combustion process slows down. A critical distance x_c was taken as a limit between two defined regions where the "near region" was at $x < x_c$ and the "far region" was at $x > x_c$. The magnitude of x_c increased as the separation between the burners increased. The following relation was obtained

$$\frac{L}{x_c} \sim \frac{L}{a} \sim \frac{D E_s}{a}$$

where L/x_c showed the performance of an individual flame in a multiple-jet system such that the ratio is smaller than 1 if burnout occurred in the "near region" and greater than 1 if the burnout occurred in the "far region". The aim was to find a proportionality factor (J'), in the following equation

$$x_c = J' \cdot a$$

2.4 Multiple Swirling Jets and Flames.

Allen (4) investigated the aerodynamic behaviour of isothermal multiple jet systems with relevance to flame interaction. Both swirling and non-swirling jets were used for the

configurations studied. A hot wire anemometer was used to measure the mean velocity and turbulence quantities and a technique was developed based on a voltage velocity relationship. Multiple jet systems were found to produce a "damping"of the turbulent motion of the fluid particles between the jets due to aerodynamic interaction which lead to a reduction in turbulence level and consequently poorer mixing. These interaction effects were increased with decreasing separation between the jets and vanished beyond 3 diameters separation. As the swirl level was decreased, the jet interaction greatly increased. Simple relationships between the velocity gradients and the shear stress terms were no longer valid and effective viscosity terms varied quite markedly within the flow field. Non-swirling jet systems showed more interaction than the corresponding swirling jet systems. In swirling jets at regions close to the nozzle exit the turbulence quantities were still very much higher in value than those found in the non-swirling jet systems and the effect of the "damping" of the turbulent fluid motion between adjacent jets was less pronounced. The reduction in the turbulence quantities has been more marked for jets swirling "in mesh" than "out of mesh" due to the fact that the swirl velocity gradients and corresponding shear terms were very much greater for "out of mesh" swirling jets since the swirl velocity directions are opposed in the region between adjacent jets.
In order to understand the behaviour of interacting flames and to help in the interpretation of the aerodynamic results, Allen performed a series of simple multiple flame studies. When three identical burners, supplied with premixed propane air gas mixture, were brought close together, the overall visible flame

length started to increase and, further, bringing the flames closer together, the central flame tended to be unstable, lifted off the burner rim and was either stabilised further downstream or the flame blew-off.

Hardcastle (2) has studied various heat transfer characteristics within a marine boiler. The type of burners employed were swirling "out of mesh" (the same direction of rotation). He has investigated the effects of number of burners used and the total heat supplied on the heat transfer characteristics. He has reported that increasing the heat input in the boiler by the addition of another burner led to a decrease in the observed flame length instead of an increase. That behaviour was not fully understood.

Tucker (52) developed a simple mathematical model for a burner with swirl in order to prevent impingement on furnaces having side fired multiple flame systems. He has suggested that when swirling jets are used to transfer radiant heat in the furnaces swirl direction must be chosen in such a way that flame impingement will be avoided.

At the International Flame Research Foundation, Ijmuiden, a series of experiments have been performed on multiple burner systems using natural gas as fuel (53). Groups of two, three, four and five burner systems, having linear, triangular and square arrays, have been studied under both swirling and non-swirling flame conditions. Burner spacing, burner array, degree of swirl and direction of swirl were the major parameters considered to affect flame stability, flame length, flow and combustion patterns, flame temperatures, cross lighting between burners and uniformity of burner draft losses in a bank of burners.

Two types of flames were used during investigation. The ones which were called type I were produced when an axial fuel gas jet of sufficiently high velocity is injected at the centre of the swirl induced internal reverse flow so that the gas jet penetrates through the reverse flow zone leaving an annular region of reverse flow to stabilize the flame. These were long comparatively quiet flames. Type II flames were produced when the swirl induced internal reverse flow zone is able to force the fuel injected on the flame axis to spread radially outwards so that it mixes rapidly with the combustion air giving a short and intense noisy flame. Three types of exchangeable gas nozzles were used for the fuel supply, one with a single hole giving an axial fuel jet of approximately 100 m/sec velocity which produced a long (type I) flame and the other two injecting the gas through sixteen diverging gas jets with a half angle of divergence either 20° or 90° which produced a short (type II) flame. The one which has diverging gas jets at 90° half angle had a gas jet velocity of about 220 m/sec. Swirl was generated by a vane type swirler which was placed in the throat section of the burners. The burners were mounted on a thick water cooled plate which had nine cylindrical burner holes in 3 x 3 square array with the maximum possible centre to centre distance between two burners being four burner exit diameters, while the minimum distance available was $\sqrt{2}$ burner exit diameters.

It was reported that there were no problems of flame stability or flame jet deflection due to flame interaction. In the cases of close proximity of burners, increase in gas temperature occurred in or downstream of the flames. This was attributed to a reduction in the entrainment of cooled furnace

gases by the confined flames. Flame lengthening was observed only in the most extreme circumstances. For the short (type II) flames when three or more burners were used at the minimum separation of $\sqrt{2}D_E$ between the burner axes, some flame lengthening was found to occur. For the long (type I) flames there was a definite tendency for the centre flame of three and five burner combinations to get longer when the burners were brought closer, giving a maximum of approximately 30% of the original flame length. Part of that lengthening was considered due to delayed mixing between fuel and air. Cross lighting between thermally equally loaded swirling flames was possible at the burner spacings less than 2 exit diameters provided that the furnace temperature was above 250° C. Under no conditions was the cross lighting of non-swirling flames possible. Swirling "in mesh" or "out of mesh" had no effect on cross lighting.

The results of this investigation are only applicable to a very narrow range of industrial uses owing to the choice of individual flames with very high momentum. The aim of this choice was to eliminate the confining effects of the furnace walls. This also reduced, if not eliminated, the aerodynamic interference between the jets, which would be expected from a multiple burner system with moderate or low momentum. In case of the non-swirling flames investigated, the gas was injected into the air stream through multihole divergent nozzle having a divergent half angle of 90°, at a velocity of 220 m/sec. to increase the air-fuel mixing rate. In case of the swirling flames the swirl levels used were very high (0.5 - 1.0).

It is evident that under these conditions there will be very little or no interaction between multiple burners.

Another disadvantage this system may represent is the high power needed to give the required momentum to the fuel stream. This energy can easily exceed that required to induce a swirl in a jet and therefore the user will loose the advantage gained from using a non-swirling flame.

CHAPTER 3.

THEORETICAL CONSIDERATIONS

3.1 Introduction to the Theory of Combustion.

At the present there is no universally accepted theory which accounts for all aspects of combustion process. Although a great amount of research has been done on the nature and laws governing turbulent combustion, no single theory which adequately describes turbulent burning processes has yet been established. The reason for this condition is the great complexity of these processes. For instance, the chemical reactions which occur during combustion are extremely complicated and very rapid and moreover the reactions occur in a field where the temperature and the composition varies rapidly. Both turbulence theory and combustion theory have recently been enriched by a certain amount of new data obtained by highly developed techniques which permits a revision of the basic concepts of turbulent combustion.

Up to the present two types of combustion have been quite extensively studied. The first type is normal combustion, in which a heat wave, velocity of which is determined by the laws of thermal conduction, diffusion, and kinetics of chemical reactions in a flame, propagates throughout the mixture, heating it in the process, and preparing conditions for completion of the chemical reaction. The propagation velocities of such flames vary from several centimeters to several meters per second. The second type of combustion is detonation. In this case the chemical reaction in the initial mixture is induced by a shock wave, which propagates with a velocity of the order of several thousand meters per second. These are two limiting cases of

combustion. In practice, however, combustion processes may develop with any intermediate burning velocities (several centimeters to several meters per second). This type of combustion obeys neither the laws of normal combustion nor those of detonation. At the present time it is still not clearly known how the turbulent burning velocity varies with the basic parameters of turbulent flow (the fluctuating velocity and its distribution over a scale spectrum), or with the basic physico-chemical characteristics of a combustible mixture (the laminar burning velocity and the fundamental kinetic parameters). Also nothing much is known about the structure of the reaction zone of turbulent flames. A comprehensive theory of turbulent combustion can apparently be constructed only on the basis of joint consideration of both flame propagation and volume reaction, which develops wherever turbulent mixing leaves flame propagation behind. The problem consists in deciding which occurs more rapidly, the burning of an eddy at its surface, or its ignition after a certain delay determined both by the temperature and by the degree of dilution of the fresh mixture with combustion products.

3.2 General Equations Related to the Flow and Mixing of Turbulent Fluids.

The equations which are used to describe the behaviour of a turbulent fluid, namely the Reynolds equations of motion and the equation of continuity of mass, have been derived from a similar set of equations initially developed to describe the laminar flow of Newtonian fluids, where the equations of motion are known as the Navier-Stokes equations. Basically, the Navier-Stokes equations were derived by applying Newton's

Second Law of Motion to an infinitesimal volume element which was assumed to be immersed in the fluid and subjected to typical forces and fluxes of momentum. The Reynolds' equations start from Navier-Stokes equations and generalize these equations for turbulent flow by assuming that the instantaneous velocity at any point is made up of a time-mean value and a fluctuating component. Therefore the Reynolds' equations are similar to the Navier-Stokes equations and the only difference is the turbulence stress terms added onto the set of differential equations. The development of the Reynolds' equations are fully discussed by other workers (54),(55),(56).

For a system of turbulent, chemically reacting, multicomponent mixtures, in which heat and mass transfer are occurring the basic Reynolds' equations of conservation of mass, momentum, enthalpy and chemical species can be written in the cylindrical polar co-ordinate system (z,r,θ) as follows:

$$\frac{\partial}{\partial z}(\rho v_z) + \frac{1}{r}\frac{\partial}{\partial r}(r \rho v_r) = 0 \qquad \ldots\ldots\ldots \qquad (3.1)$$

$$\rho\left(v_z \frac{\partial}{\partial z} v_z + v_r \frac{\partial}{\partial r} v_z\right) = \frac{\partial}{\partial z}(\tau_{zz}) + \frac{1}{r}\frac{\partial}{\partial r}(r \tau_{rz}) - \frac{\partial P}{\partial z} \quad \ldots \quad (3.2)$$

$$\rho\left(v_z \frac{\partial}{\partial z} v_r + v_r \frac{\partial}{\partial r} v_r - \frac{v_\theta^2}{r}\right) = \frac{\partial}{\partial z}(\tau_{rz}) + \frac{1}{r}\frac{\partial}{\partial r}(r \tau_{rr}) - \frac{\tau_{\theta\theta}}{r} - \frac{\partial P}{\partial r} \qquad \ldots\ldots\ldots \qquad (3.3)$$

$$\rho\left(v_z \frac{\partial}{\partial z} v_\theta + v_r \frac{\partial}{\partial r} v_\theta + \frac{v_r v_\theta}{r}\right) = \frac{\partial}{\partial z}(\tau_{\theta z}) + \frac{1}{r^2}\frac{\partial}{\partial r}(r^2 \tau_{r\theta}) \qquad (3.4)$$

$$\rho\left(v_z \frac{\partial h}{\partial z} + v_r \frac{\partial h}{\partial r}\right) = -\frac{\partial}{\partial z}\left((J_h)_z\right) - \frac{1}{r}\frac{\partial}{\partial r}\left(r(J_h)_r\right) + \Phi \quad \ldots\ldots \qquad (3.5)$$

$$\rho\left(v_z \frac{\partial m_j}{\partial z} + v_r \frac{\partial m_j}{\partial r}\right) = -\frac{\partial}{\partial z}\left((J_j)_z\right) - \frac{1}{r}\frac{\partial}{\partial r}\left(r(J_j)_r\right) + R_j \quad \ldots\ldots (3.6)$$

where:

v_z : time mean velocity in z direction.

v_r : time mean velocity in r direction.

v_θ : time mean velocity in θ direction.

h : time mean enthalpy.

J : turbulent flux vector.

m : time mean chemical species' mass fraction.

R : mass rate of creation per unit volume.

P : time mean pressure.

r : radial co-ordinate.

t : time.

v : time mean velocity.

z : axial co-ordinate.

θ : polar co-ordinate.

ρ : time-mean density.

$\tau_{rr};\tau_{zz};\tau_{\theta\theta}$: turbulent normal stress components.

$\tau_{rz};\tau_{r\theta};\tau_{z\theta}$: turbulent shear stress components.

Φ : dissipation function which is given in eq. (3.7).

subscripts:

h : relating to enthalpy.

jj : relating to chemical species j.

z,r,θ : components of vector in co-ordinate directions.

$$\Phi = \tau_{zz}\frac{\partial v_z}{\partial z} + \tau_{rr}\frac{\partial v_r}{\partial r} + \tau_{\theta\theta}\frac{v_r}{r} + \tau_{rz}\left(\frac{\partial v_z}{\partial r} + \frac{\partial v_r}{\partial z}\right)$$

$$+ \tau_{r\theta}\left(\frac{\partial v_\theta}{\partial r} - \frac{v_\theta}{r}\right) + \tau_{z\theta}\left(\frac{\partial v_\theta}{\partial z}\right) \quad \text{.....} \quad (3.7)$$

In the derivation of the above equations the motion is assumed to be quasi-steady ($\partial/\partial t = 0$) axisymmetric ($\partial/\partial\theta = 0$). There is an equation of type (3.6) for each chemical species present. No external forces are acting on the system and the internal energy has been equated with enthalpy. Since the molecular contributions being considered very small in fully turbulent flows only turbulent contributions to the fluxes are considered and they are given as follows:

$$\tau_{zz} = -\rho\,\overline{v'_z v'_z} \qquad \tau_{rz} = \tau_{zr} = -\rho\,\overline{v'_r v'_z}$$

$$\tau_{rr} = -\rho\,\overline{v'_r v'_r} \qquad \tau_{r\theta} = \tau_{\theta r} = -\rho\,\overline{v'_r v'_\theta}$$

$$\tau_{\theta\theta} = -\rho\,\overline{v'_\theta v'_\theta} \qquad \tau_{z\theta} = \tau_{\theta z} = -\rho\,\overline{v'_z v'_\theta} \qquad \ldots\ldots\ldots (3.8)$$

$$(J_h)_z = \rho\,\overline{v'_z h'} \qquad (J_h)_r = \rho\,\overline{v'_r h'} \qquad (J_h)_\theta = \rho\,\overline{v'_\theta h'} \qquad \ldots\ldots\ldots (3.9)$$

$$(J_j)_z = \rho\,\overline{v'_z m'_j} \qquad (J_j)_r = \rho\,\overline{v'_r m'_j} \qquad (J_j)_\theta = \rho\,\overline{v'_\theta m'_j} \qquad \ldots\ldots (3.10)$$

where (') terms represent the turbulent fluctuating components.

For an isotropic system these fluxes become:

$$\tau_{zz} = 2\mu\,\frac{\partial v_z}{\partial z} \qquad \tau_{rz} = \tau_{zr} = \mu\left(\frac{\partial v_z}{\partial r} + \frac{\partial v_r}{\partial z}\right)$$

$$\tau_{rr} = 2\mu\,\frac{\partial v_r}{\partial r} \qquad \tau_{r\theta} = \tau_{\theta r} = \mu r\,\frac{\partial}{\partial r}\left(\frac{v_\theta}{r}\right)$$

$$\tau_{\theta\theta} = 2\mu\,\frac{v_r}{r} \qquad \tau_{z\theta} = \tau_{\theta z} = \mu\,\frac{\partial v_\theta}{\partial z} \qquad \ldots\ldots\ldots (3.11)$$

$$(J_h)_z = -\Gamma_h\,\frac{\partial h}{\partial z} \qquad (J_h)_r = -\Gamma_h\,\frac{\partial h}{\partial r} \qquad (J_h)_\theta = 0 \qquad \ldots\ldots\ldots (3.12)$$

$$(J_j)_z = -\Gamma_j\,\frac{\partial m_j}{\partial z} \qquad (J_j)_r = -\Gamma_j\,\frac{\partial m_j}{\partial r} \qquad (J_j)_\theta = 0 \qquad \ldots\ldots\ldots (3.13)$$

where

Γ : turbulent exchange coefficient.

μ : turbulent viscosity.

The equations given so far are not sufficient to close the system to solve for P, v, T and m_j. Following thermodynamic relationships provide extra equations to help for the solution of the above equations:

$$P = \rho\,\frac{R}{M}\,T \qquad \ldots\ldots\ldots (3.14)$$

$$h = c_p T + \sum_j (H_j M_j) \qquad \ldots\ldots\ldots (3.15)$$

$$R_j = -F_j \exp(-E_j/RT) \qquad \ldots\ldots\ldots (3.16)$$

where

H = heat of combustion.

E = activation energy.

c_p = specific heat.

T = temperature.

F = frequency factor.

There is an equation of type (3.16) for each chemical species present.

3.3 Boundary Layer Approximations.

Some simplifying assumptions about the characteristics of the flow can be made to allow some of the terms to be omitted in the Reynolds' equations. If the flow has no swirl or low degrees of swirl with no recirculation the flow can be considered to be mainly predominant in one direction and the flux components of this flow can be considered to be significant only in directions at right angles to this predominant direction. By considering the relative orders of magnitude of the terms the following approximations can be made:

$$\frac{\partial}{\partial r} \gg \frac{\partial}{\partial z} \quad \text{and} \quad \bar{v}_r \ll \bar{v}_z$$

Therefore it is usually possible to simplify the Reynolds' equations. However these conditions do not apply to flows with high swirl and such approximations cannot be applied to such flows.

3.4 Generation and Decay of Turbulence and Mixing in Turbulent Flames.

In practice most of the flows encountered are turbulent where there is a very irregular, random fluctuation from the mean values present in the flow. Owing to the extreme complexity of the detail of this motion only in the recent years it has become possible to treat it mathematically.

In a field of turbulent flow the pressure and velocity at a fixed point, fluctuate around their mean at a high frequency rather than remaining constant. The small pockets of fluid which perform these oscillations can be considered to be "fluid particles". The motion of these so called particles bear a similarity to that of the molecular motion in that they are both random in nature. This analogy is not readily applicable due to the mass of fluid particles and their mean free path not being constant in a certain medium. But since these variables are very large compared to their analogues at the molecular level, the mixing effect on the turbulent diffusion is much stronger than that of molecular diffusion.

When two or more viscous fluids of different mean velocities come into contact a set of shear stresses are formed by the mixing of different streams and as a result of this a turbulent motion is set up. First large eddies are formed due to this motion. These eddies drain away the energy from the bulk flow through the intermediary of the so-called turbulent shearing stresses, and pass it on to the turbulent motion. Nevertheless these large eddies mutually interact to give a spectrum of eddies of a wide range in size and energy as seen in Fig.(8). Also the non-isotropic character of the eddies decreases as the directions of fluctuations get more and more random. The eddies having smaller wave lengths dissipate to release their turbulence energy as heat whereas the larger ones with high wave lengths transfer their energy to the smaller eddies. Thus the band of the spectrum known as the universal equilibrium range stays independent of the conditions under which the eddies have formed and since the eddies of this region contain eighty percent of

the total turbulence energy (57), it is these eddies that are responsible for the molecular mixing mentioned above. Such eddies are also produced from the eddies of air formed in the surrounding atmosphere being drawn into the flame. These larger eddies are subsequently broken up into smaller eddies under the shear forces within the jet. As mentioned before, the number of large eddies depend upon the geometry of the system whereas the small eddies are independent of the origin of formation and are almost isotropic (54).

In general, turbulent mixing mainly depends upon the total turbulence energy content of the system which is given as:-

$$\text{Turbulent kinetic energy per unit mass} = \int_0^\infty E(k)\, d\, k$$

$$= \frac{1}{2}\left(\overline{u'^2} + \overline{v'^2} + \overline{w'^2}\right) \qquad \ldots\ldots\ldots \qquad (3.17)$$

For isotropic turbulence this can be approximated to:

$$= \frac{3}{2}\, u'^2 \qquad \ldots\ldots\ldots \qquad (3.18)$$

The factors which affect the efficiency of turbulent mixing are:

a) Intensity of turbulence ($v'/\bar{u}$).

b) The scale of turbulence (ℓ).

c) The length of the mixing region (L).

d) The lateral distances through which the injected fluid must travel.

e) The velocity of the gas through the mixing system.

It has been shown (13) that a flame can be about fifty percent longer than the point at which the time-mean concentration on the flame axis becomes stoichiometric. Because for the combustion to take place the fuel and gas has to be mixed in the molecular level, and this is governed by molecular diffusion. In turbulent flames due to the presence of a flame envelope surrounding the eddies the area available for combustion to occur is larger than that of a laminar flame. To be able to specify the mixing system completely, fluctuating values of local gas composition must be known as well as the time-mean values.

The case when the air sufficient for combustion is mixed with the fuel at a macro scale but the final intimate mixing has not yet taken place is called the phenomena of "unmixedness". In turbulent combustion systems a time-mean sample enables the measuring of the mean concentrations as well as allowing explanation of the details of the mixing taking place during combustion. An unmixedness factor, analogous to the root mean square of the fluctuating velocity component, given as $(\overline{C'^2})^{\frac{1}{2}}$ was derived by Hawthorne et al. (13). This factor could readily be obtained from a time-mean sample provided that both oxygen and unburned fuel gas were present together in the sample. This factor can be a measure of the intimacy of mixing; the smaller the value the better will be the intimacy of mixing.

3.5 Theoretical Analysis of Flow Systems.

In the theoretical analysis of a flow system the aim is to provide a set of equations which will enable predictions to be made of properties within the flow such as temperature, velocities and concentration. Reynolds equations giving a complete description of the flow system can be written but even

after a number of assumptions have been made to simplify them, the solution of the reduced equations also requires knowledge of a number of empirical constants.

It is not within the scope of this thesis to enter into a detailed description of the prediction procedure for turbulent swirling or recirculating flows starting from basic fluid dynamics, nor indeed to attempt to predict such flows, since the complexity of such a prediction procedure is considered to merit an entirely independent study. However the experimental data presented later in this thesis is shown to be of particular relevance for the establishment of the coefficients of turbulent mixing equation that is derived through such prediction procedures. Lilley (68) has developed a technique for solving the system of equations governing multicomponent boundary layer flows with turbulence, swirl and chemical reaction. He has shown that the effects of swirl on the physical properties of flames like flame size, shape and combustion intensity may be represented by turbulence models depending on non-isotropic mixing - length and energy length as well as by an eddy-break-up turbulence-controlled reaction model.

There are certain difficulties involved in the theoretical modelling of turbulent flames. It is usually the case that there are more number of unknowns than the number of equations existing. Bray (75) has derived a set of rigorously based, time-averaged balance equations for mass, momentum and energy of the mixture, for the concentrations of individual species, for the fluctuation intensities of vorticity, density, temperature and species concentration and for the kinetic energy of turbulence; for a chemically reacting turbulent flow system. An ideal gas mixture with each constituent having constant heat of formation

and specific heats have been assumed. The equations for turbulent quantities previously have been modelled as if the flow was cold, incompressible and non-reacting. As an improvement on this situation Bray (75),(76),(77) has provided information on the importance of some of the neglected terms which plays an important role in a more realistic description of the processes involved.

To simplify the general equations presented in (75), for the case of a two-dimensional, premixed, free burning flame of low Mach number and high Reynolds number Bray (76) has given the boundary layer approximation. He has stated that chemical reactions contribute several terms containing the rates of production of species and fluctuations of these rates. The terms containing the velocity divergence and its fluctuations have a high dependence on heat release and reaction rates. Bray (76) with an order-of-magnitude analysis, has shown that some of the terms neglected in most of the modelling studies of turbulent combustion could be important in turbulent flame studies. Relative fluctuation intensities in temperature, enthalpy, composition and density are all assumed to have the same order of magnitude. For thermodynamic variables, he has suggested two simple alternative descriptions of intensity levels and described as the small fluctuation case and the large fluction case respectively. It was assumed that the relative fluctuation intensities of temperature, enthalpy, composition and density have same order of magnitude as velocity fluctuations in small fluctuation case and have order of unity in large fluctuation case.

Finally, Bray (77) has derived an approximate form of the turbulence kinetic energy balance equation for a stationary,

two-dimensional, premixed, turbulent flame at low Mach number and high Reynolds number, by using the exact equations of turbulent reacting flow and closure hypotheses, which could partially explain experimentally observed effects of turbulence on the propagation of open flames, ducted flames and spherical, non-stationary flames. The method presented applies only to premixed flames. It is not directly applicable to turbulent diffusion flames.

Although the amount of data presented in Chapter (6) provides considerable information in the field of turbulent chemically reacting systems with recirculation, it is not sufficient to solve the complete set of Reynolds' equations of conservation of mass, momentum, enthalpy and chemical species. Dvorak (70) has measured mean and fluctuating velocities and turbulence intensities in a single burner, having the same design specifications and air-fuel input, under burning and cold conditions at several swirl levels. In addition to that Apak (69) has measured oxides of nitrogen and fluctuating temperatures in the same single burner, with the same input variables and swirl levels.

These three sets of data will provide valuable and sufficient information for testing the validity of existing models for a single swirling diffusion flame with recirculation. Although the prediction of recirculating flows, especially under burning condition is highly complicated, any attempt made to predict such flow systems would be a valuable contribution to science. Predictions of the multiple flames cannot be made with the existing data available. Flame velocity measurements are required to complete the set, but the multiple swirling flame

systems will raise additional difficulties in modelling associated with complexity involved as a consequence of flame interaction. Where swirl is concerned some difficulty with entrainment leading to incorrect mass flow rate predictions could result (68). In multiple swirling flame systems, in addition to the entrainment of the ambient fluid, each flame could entrain unburned fuel and combustion products from the adjacent flames and could lead to incorrect predictions.

CHAPTER 4.

DESIGN AND DESCRIPTION OF EXPERIMENTAL APPARATUS

4.1 Experimental Arrangements.

A general schematic flow diagram of the experimental setup is shown in Fig.(9). In the design of the apparatus the following features have been taken into consideration:

(a) The burner plate was designed to enable the change of burner separation between a = 0.25 D_E to a $\geq$ 4 D_E for two and three burners in line arrangements. For four burners in square and five burner (four in square and one at the centre) groupings the possible burner separations were less.

(b) Natural gas, tangential air and axial air were supplied to each burner with a separate monitoring device such that identical quantities of each of these could be fed to individual burners.

(c) An additional support plate, parallel to the burner plate, was used to keep the burners in a vertical position.

4.2 Design and Description of the Apparatus.

4.2.1 Experimental Burners.

Swirling double concentric jets have been employed throughout the investigation. The jets were designed Fig.(10) with a 20° half angle diffuser exit so as to enable generation of recirculation even at low swirl levels and lead to better mixing of fuel and combustion air. Natural gas was supplied through a 0.955 cm i.d., 1.23 cm o.d., 110 cm long copper tube having a central single hole nozzle terminating at the burner throat and fixed to the axial air pipe with a support spider. Axial air was fed through 3.19 cm i.d., 3.45 cm o.d., 100 cm long copper tube with a sharp right angle air entry at the bottom. A sharp

right angle entry and a tube length of about 30 D_T were used to obtain a uniform flow pattern at the nozzle exit.

In order to assure the close packing of the jets and at the same time to enable the introduction of air tangentially into an inner annulus to produce swirl, diffuser exits were used. In references (5) and (30), it was shown that one of the most convenient and successful ways of producing swirl is to introduce air from an outer annulus tangentially into an inner annulus. Tangential air was fed through two supply pipes into the swirl chamber which had 4 slots for the tangential entry of the air into the inner annulus through which axial air was also introduced. The slots were at 2 throat diameter upstream from the burner exit plane and 2 throat diameters in length. The inner wall of the swirl chamber and the diffuser exit were machined from a single piece of brass bar and then soldered to a copper axial air pipe and the outer walls of the swirl box. The use of two tangential air supply pipes was found necessary to overcome a slight assymetric flow distribution of the resultant jet when only one supply pipe was used.

4.2.2 Burner Plate and Burner Support.

The burners were mounted on a burner plate consisting of three rectangular sections each having three mounting holes in line with a 0.25 exit diameter separation, Fig. (11). Thus by moving the outer plates the separation between the adjacent burners could be varied without dismantling the burners. Burner ports not in use were blanked off. Possible group arrangements were as follows:

(a) Two burner arrangements with a minimum separation of $a = 0.25\ D_E$ and maximum $a \geq 4\ D_E$. It was possible to increase the separation continuously from minimum to maximum, Fig. (12.a).

(b) Three burners in line grouping with $a_{min} = 0.25\ D_E$ and $a_{max} \geq 4\ D_E$, Fig.(12-b).

(c) Four burners in square arrays: only two possibilities existed with $a_{min} = 0.77\ D_E$ and $a_{max} = 1.5\ D_E$, Fig.(12.c)

(d) Five burner arrays (four in square and one at the centre) had only one possible position.

Fig.(12.d), which had a separation of the centre burner to the outer burners $a_{co} = 0.77 D_E$ with the separation between the outer burners being $a_{oo} = 1.5\ D_E$.

To keep the burners in a vertical position a wooden support plate parallel to the burner plate was used.

4.2.3 Air and Fuel Supply.

The tangential and axial air supplied to each jet was monitored separately by means of orifice plates. The degree of swirl was varied by altering axial and tangential air flow rates. The total air supply was maintained 20% in excess of the stoichiometric requirement.

Natural gas from the main supply line was introduced through a safety valve into a manifold which in turn distributed the natural gas through separate valves to each rotameter and jet. The composition of the natural gas is given in (Appendix 1.), the experimental apparatus is shown in P.(1-b).

4.3 Probe Traversing Mechanism.

A lathe bed was used for the probe traversing which enabled traverses to be made in each of the 3 mutually perpendicular directions.

Gas sampling probes were attached directly to the lathe bed. The four point anemometer measurement technique (58) used, for the isothermal annular air velocity measurements, required rotation of a straight hot wire probe around its axis at 45°

intervals. Instead of using a protractor a special probe-support-holder was designed to accommodate the probe and its connections and to enable the desired probe rotation around its axis at definite angles.

As can be seen in Fig.(13) the probe support was placed into the holding chuck (1) and its electrical connections passed through the stainless steel extension tube (2) to the anemometer. A brass indicator rod (6) was pulled into the milled grooves on the index head (5) by the spring (4) working under compression between the index head and the spring guide (3). 5 grooves at 45° to each other were milled on the index head to ensure accuracy of rotation. The whole attachment was held on the lathe bed through the extension rod (7).

CHAPTER 5.

MEASUREMENT TECHNIQUES AND INSTRUMENTATION

5.1 Measurement in Flames.

To be able to determine rates of heat, mass and momentum transfer within the flame and heat transfer from the flame to its surroundings detailed measurements of velocity, pressure, temperature, concentration of gases and solid or liquid particles, heat transfer, turbulence and physical properties are required. In turbulent systems measurements are usually tedious and time consuming. To enable the determination of local heat, mass and momentum flux values in a turbulent system, instantaneous values are necessary which could be resolved into time mean average values, root mean square values and time mean average correlations. While choosing a measuring instrument and measurement technique, dependability and reproducibility of the results must be considered. Even though the required accuracy depends on the system being studied the aim must be to achieve the highest possible accuracy. In ref's (11), (25), (59), (60) several methods of measurement, design and construction details are given.

5.2 Temperature Measurements.

5.2.1 Introduction.

To find a perfect method of flame temperature measurement is quite impossible. All possible methods are subject to some practical and theoretical limitations, and the choice of the most convenient and reliable method will depend on the type of flame being studied. Between the basic methods of measurement, optical methods in general have the advantage over wire methods

in that they do not disturb the flame gases. On the other hand they often have the disadvantage that it is not possible to make a point by point study of the temperature distribution in the flame, the methods only giving a mean value along the path of the light-beam.

5.2.2 Measurement with Fine Wire Thermocouples.

For the system studied fine wire thermocouples were found suitable and chosen as the primary temperature measuring instrument. The basic advantages of fine wire thermocouples considered are:

(a) High precision of electrical measurements.

(b) Extremely small thermocouples can be constructed so that high resolution can be obtained and aerodynamic disturbance of the flame front is minimized.

(c) High temperature resistant materials can be used.

(d) No costly and complex equipment is needed because of its simplicity and convenience.

Besides the above advantages there are a number of sources of error involved in the measurements. The wire will normally be cooler than the flame gases owing to heat losses by radiation to the flame surroundings, and by conduction along the leads. The radiation error of a thermocouple wire decreases as the size of the wire is decreased. A wire of zero diameter would give the true gas temperature. Because of their fragility fine wires are not very practical and usually have to be supported by thicker wires of the same material. Since the radiation from the probe increases with the fourth power of the probe temperature, the correction which must be made for this loss increases very sharply with temperature. Bradley and Matthews (61) showed that at a gas temperature of 1300° K, a 0.127 mm

diameter platinum wire probe may have a radiation correction of 5° rising to 60° for a gas temperature of 2100° K, the corresponding values of the correction for a 0.508 mm diameter probe would be 35° and 200°. In cases where it is impossible to use fine wires because of strength limitation, the velocity over the sensing elemcnt can be increased as in a suction pyrometer, thereby reducing the radiation correction. The measurements can also be corrected for the effect of stream velocity, since as the Reynold's number increases the conduction error decreases.

5.2.3 Type of thermocouple used and coating of the thermocouple bead.

Temperature measurements were taken with a bare Pt/Pt-Rh fine wire thermocouple, having a wire diameter of 0.10 mm and junction diameter 0.40 mm. To protect the wires from catalytic effects and chemical attack it is necessary to coat the wires with an inert coating. A coating suitable for flame temperature measurement should have the following general properties:

(a) It must be noncatalytic toward the flame.

(b) It must be inert toward the thermocouple material at all temperatures.

(c) It must be impermeable to gases so as to afford protection from the environment.

(d) It must be a poor conductor of electricity, especially at high temperatures; otherwise the thermocouple will be short circuited.

(e) It should be stable, particularly at high temperatures. Forms of instability include oxidation, reduction, hydration, volatization, and crystalline change.

(f) It must be capable of being applied evenly and smoothly to the thermocouple surface and must cover it completely.

(g) The thickness of the coating should be minimal to avoid appreciable losses through conduction.

A very thin coating of silica may successfully be used at temperatures up to 1300° C. It can easily be deposited on the wire surface as a continuous layer, provided that the junctions are well formed, without protruding wire ends. At higher temperatures, however, the silica is reduced by hydrogen in the flame, and diffusion of free silicon into platinum produces embrittling silicide. Therefore it is necessary to eliminate silica completely for temperature measurements higher than 1300° C. A combination of ytrium oxide and beryllium oxide was developed as a very successful coating material, by Kent (66), which gave good results at high temperatures.

During this investigation the maximum recorded temperature was about 1300° C and a very thin coating of hexamethylone-disiloxane was used successfully without having any fragility problem.

5.2.4 Temperature Correction.

The heat received (or lost) by the thermocouple by convection is equal to the heat lost (or gained) from the thermocouple by radiation plus heat lost by conduction along the wires from the junction. The steady state heat transfer equation for an uncoated wire can be written as follows:

$$\frac{d}{dx}\left(k\frac{dT}{dx}\right) + \frac{4h}{D_W}(T_G - T) - \frac{4\sigma}{D_W}(\epsilon T^4 - \alpha T_W^4) = 0 \quad \ldots\ldots \qquad 5.1$$

where k = Thermal conductivity.

D_W = Diameter of the wire

T_G = True gas temperature.

T_W = Wall temperature.

T = Hot junction temperature.

h = Heat transfer coefficient between the wire and the flame.

σ = Stefan-Boltzman Constant.

ϵ = Emissivity of bare thermocouple junction.

α = Absorption coefficient.

In deriving the above equation the surrounding walls are assumed to be black to radiation from the wire and radiant energy exchange between the wire and the gases is negligible. Since the gases do not contain suspended particles it is not necessary to add an extra term to allow for the emissivity of the particles. By using sufficiently long thermocouple wires, heat loss due to conduction can be eliminated and then the wire will be at its 'semi-infinite equilibrium temperature', T_∞. The difference between T_∞ and T_G is the radiation correction. So the equation (5.1) becomes

$$\frac{4h}{D_w}(T_G - T_\infty) - \left(\frac{4\sigma}{D_w}\right)(\epsilon T_\infty^4 - \alpha T_w^4) = 0 \quad \ldots\ldots\ldots \quad (5.2)$$

For wire temperatures above 1000° C and low wall temperatures the absorption term is usually negligible.

So the equation reduces to

$$T_G = T_\infty + \frac{\sigma \epsilon T_\infty^4}{h} \quad \ldots\ldots\ldots \quad (5.3)$$

T_G = True gas temperature, °K.

T_∞ = Wire temperature, °K.

ϵ = Emissivity of silica coated thermocouple junction.

Gas property data and the values of h and ϵ were calculated using the procedures and data recommended by Bradley and

Mathews (61). For coated wires the emittance depends on the diameter of the wire and the thickness of the coating. Bradley and Entwistle (62),(63) give the theoretical and experimental values of total hemispherical emittance for silica coated platinum - 10% rhodium wires. The emittance is close to the uncoated wire emissivity at high temperatures. A computer program was written for the correction of recorded gas temperatures. A flow chart of the computer program is given in Appendix 3. As seen from the computed results the correction was significant at high temperatures whereas at low temperatures the recorded temperatures represented the true gas temperature.

5.3 Gas Concentration Measurements.

5.3.1 Introduction.

The majority of combustion processes take place in the gaseous phase and the products (end-products or intermediates) are usually gaseous. Gas sampling was therefore considered to be suitable means for detailed investigations. The fundamental problem which has to be solved in gas sampling is to obtain a sample which will be representative of the composition of the fluid at the sampling point. In gas and solid particle concentration measurements the sampling from the flames appears to be the most important part of the process. In sampling from the flames care must be taken:

(a) to ensure that the sampling probe does not obstruct the flow pattern upstream of the sampling nozzle - the sampling should be "iso-kinetic".

(b) to prevent any further reaction after sampling, the gases must be quenched as soon as they pass the probe nozzle.

Direct probe sampling is found to be the most successful and convenient method for the determination of the concentrations of stable species in flames.

There are four basic methods of analyzing a flame sample:

(a) Manometric analysis (it has very limited application).

(b) Infrared analysis (it has very limited application).

(c) Mass spectrometer (it has very high sensitivity and accuracy but, it is costly and complex in use).

(d) Gas chromatographic analysis. With recent developments, gas chromatographs are now commercially available to suit almost any type of analysis. They are simple to use and can be highly sensitive.

5.3.2 Choice of System.

For the system being investigated analysis of large numbers of samples from the flames were required. With its rapid response the Penny and Giles gas chromatograph (67) was found quite satisfactory. The main purpose of analysis was to obtain quantitative information on the degree of completion of combustion and the mixing rates rather than the kinetics of the reactions. For that purpose a simple method of analysis was found satisfactory. With the chosen system it was possible to analyse a gas sample for CO_2, H_2, O_2, N_2, CH_4, and CO in four minutes. The gas chromatograph was also capable of analysing H_2O vapour and higher hydrocarbons such as C_3H_8, with only small changes and a slight increase in time.

5.3.3 The Gas Chromatograph.

The flow diagram for the chromatograph is shown in Fig.(14). The sample continuously passes through the sample loop and an automatic timing mechanism causes the sampling valve to actuate, thus injecting the sample contained at that instant within the loop into the analyzing columns together with argon carrier stream. The sample with the carrier gas first passes through a porapak-Q column at 50° C where any carbon dioxide present is

retarded with respect to all other constituents. The Katharometer detector follows this first column and thus an "overall peak" is first detected followed by a carbon dioxide peak. The "overall peak" contains all gases present except CO_2. After the detector a column packed with soda asbestos and magnesium perchlorate removes all the CO_2 from the rest of the sample. The remaining sample then passes through a molecular sieve 5A column at the same temperature which separates hydrogen, oxygen, nitrogen, methane and carbon monoxide. The separated sample then passes again through the Katharometer and the gases are detected as they pass in the order mentioned above. A typical chromatogram is shown in Fig.(15-a). At the end of the cycle a fresh sample is automatically injected.

5.3.4 Probe Sampling.

It is necessary to introduce a fresh sample, at or near atmospheric pressure, into the gas chromatograph every four minutes in order to assure its maximum operating efficiency. The most suitable system would be the method of continuous probe sampling. In this method the sample is withdrawn, quenched to stop any further reaction and then passed through the gas chromatograph continuously from which the chromatograph could take a sample every four minutes. Because of the very small size of the quartz microprobes, only a few micrograms of sample per second are withdrawn and the flame is not disturbed, but another major problem arises which is the conversion of a very low pressure sample from the micro probe into a sample at atmospheric pressure. This can be overcome by the use of a peristaltic pump which is capable of evacuating a closed system down to approximately 0.1 to 5 mm Hg. by squashing a rubber tube

continuously with three rotating pins against a semi-circular track. The use of the peristaltic pump also solved the problem of contamination of the sample or any effect of preferential diffusion such as would be obtained by the use of a diffusion pump. A pressure drop of 10:1 across the orifice has generally been found to be sufficient in order to provide a sonic flow and thus freeze the sample composition at the probe orifice. For an atmospheric pressure flame therefore sampling pressure up to 70 mm Hg. could safely be used. With a suitably chosen size of tubing for the peristaltic pump the size of the orifice controls the pressure obtained within the probe.

5.3.5 Design and Construction of Sampling Probes.

To minimize the disturbance arising both from sample withdrawal and from the bulk of the probe itself, and also to assure the rapid decompression and withdrawal of the sample to a cool region outside the flame the full design and construction procedures were adopted as set out by Fristrom and Westenberg (59). The probes were made of tapered quartz tube and consisted of three sections:

(a) Sonic orifice inlet: its size was determined by the rate of sampling and required pressure drop.

(b) The expansion nozzle following the orifice: tapers between 15 - 45° were found to assure a rapid decomposition and cooling of the sample. No additional cooling of the probe was necessary.

(c) Connecting tubing; its size was chosen to allow 10:1 pressure drop across the inlet orifice.

The probes were bent at right angles to about 2-3 cm from the tip of the probe in order to position the orifice inlets in the main flow direction.

The probes were constructed from 3 mm o.d. quartz tube by pulling a taper carefully while heating the quartz tube in an oxy-hydrogen flame. The tapered tube was then cut at a suitable diameter and the tip was fused in the flame to obtain the final orifice.

The flow through the orifice was estimated by the critical orifice relation:

$$Q_p = C_p A_p K P \quad \ldots\ldots\ldots \quad (5.4)$$

where

Q_p = Volumetric flow, cm^3/sec.

A_p = Orifice throat area, cm^2.

K = Contains all the constants for a given gas and standard temperature and pressure, (cm/sec-atm) 10^4.

P = Upstream pressure, atmosphere.

C_p = Constant factor, discharge coefficient $\simeq 0.5$ for a fine orifice.

5.3.6 Operating Procedure.

The schematic flow diagram of the sampling system is shown in Fig.(16). A 3 mm. o.d. quartz probe was joined to a 6 mm. i.d. ceramic tube with ceramic cement to enable easy positioning of the sampling probe onto the traversing mechanism. The ceramic tube was joined to a 9 mm. i.d. neoprene tubing with additional rubber tubing. A vacuum gauge measured the pressure within this line at a point as near as possible to the probe end. Neoprene tubing passed through the pins of the peristaltic pump. After the pump a drying column containing concentrated $H_2 SO_4$ was placed in order to remove water vapour from the sample being injected into the chromatograph. The sample was then passed through a needle valve to damp the fluctuations in the flow due

to the action of the pump, and was fed into the chromatograph. The pressure at this point was also monitored and kept just above atmospheric. After passing through the sample loop within the chromatograph the sample passed out into the atmosphere through a water trap, a water bubbler and rotameter. The rotameter measured the pumping rate and the water bubbler enabled a slight positive pressure to be maintained within the chromatograph and also acted as a check on the sample flow rate. The water trap prevented this water from being sucked back into the chromatograph when the pump was switched off.

The calibration of the gas chromatograph is dependent upon the sample gas pressure. The pressure drop and the flow rate of the sample across the micro probe orifice is dependent upon the conditions of the sampling point, such as temperature and viscosity. The pressure was therefore maintained constant during use and whilst calibrating.

To maintain an efficient pumping rate the tubing of the peristaltic pump had to be changed periodically. To increase the life time of the tubings, silicone grease was used to soften them and minimize friction. Due to the formation of high amounts of water vapour, the contents of the drying bottle had to be changed frequently in order to keep its efficiency high enough. A leak test was essential before each experiment for the accuracy of the analysis. Zero flow through the system was checked by switching off the pump with the orifice still blocked, and checking that the vacuum was maintained. Also a final check had to be made by taking a sample from a pure gas containing no oxygen and checking for zero oxygen in the analysis.

5.3.7 Calibration.

The present chromatograph which was used throughout the research was equipped with an automatic timing and attenuator unit which attenuated the sensitivity of the chromatograph to suit each component as they were detected. For calibration, a standard sample of known composition was injected into the instrument, and the attenuators were adjusted to give a suitable size peak on the recorder for each constituent. Whenever a wide range of compositions of a particular component are likely, a number of sensitivity settings may be required, but each setting must be calibrated with at least one standard sample. It is preferable to maintain a number of samples of known composition so that two or three points on a graph of peak height against percentage can be obtained. The linearity of the response was good for all ranges and constituents used. The calibration of the instrument varied very little with time, but calibrations were made before and after each session which lasted 5 to 6 hours. Fig.(15-b) shows typical calibration data.

5.4 Isothermal Velocity Measurements.

5.4.1 Introduction.

Local gas velocity is one of the primary aerodynamic variables which characterizes a flow system. For a complete description of the flow system the distribution of velocity throughout the system is one of the first requirements. Stream lines of gas flow, mass flow rates within stream tubes or annuli, mass flow rates within recirculation eddies, and total entrained mass flow rates can all be calculated from integration of measured mean velocity distributions. In three dimensional flow systems such as flows having swirl or recirculation it is necessary to measure both the magnitude and the direction of mean velocity, as well as turbulent fluctuations. The hot wire anemometer has the necessary high frequency response and high sensitivity at low flow velocities for measurements in the high turbulence levels encountered in three dimensional flow systems. A hot wire anemometer operating at constant temperature mode measures basically the rate of heat loss from a heated wire to a gas stream. In general this heat loss is interpreted in terms of the velocity of the gas stream.

5.4.2 Constan Temperature Hot Wire Anemometer.

The anemometer consists of a Wheatstone bridge, of which the probe forms part, and a D.C. amplifier. The bridge is in exact balance at a certain bridge voltage supplied by the servo amplifier. A slight change in the probe resistance, such as a change in the convective cooling of the wire, will cause a small unbalance voltage, which, after considerable amplification is used to adjust the bridge voltage (probe current) in such a way as to keep the bridge close to balance. In this way the temperature variations of the wire are kept extremely small, even when high frequencies of the fluctuating velocity occur.

The instantaneous value of the electrical power applied to the probe may be assumed to equal the instantaneous heat loss to the surrounding fluid. This heat loss is dependent upon the physical properties of the surrounding fluid and, assuming these are all constant then the gas velocity is the only variable. The electrical power can thus be used as a direct measure of the velocity. The mean (D.C.) and the root mean square (A.C.) components of the total instantaneous voltages existing across the probe are measured by meters connected across the bridge terminals.

5.4.3 The Hot Wire Probes.

The probes used in the present work were manufactured by D.I.S.A., and consisted of platinum coated tungsten wire, 5 microns in diameter, which was connected to the nickel supports by a combined method of welding and electroplating. This wire when positioned in a gas stream is primarily sensitive to the component of the flow velocity which is normal to the wire axis. If the wire is inclined at some angle to the mean flow direction, then it has been usual to assume a simple cosine relationship for the normal cooling component. However, deviations from cosine law become significant as the ℓ/d ratio of the wire is reduced, where ℓ is the length and d is the diameter of the wire.

In order to measure the turbulence characteristics of three dimensional flows it is essential to incline the wire in the plane of the total mean velocity vector. It is also essential to take into account the response of the wire to all three orthagonal velocity components. Existing heat transfer relationships are derived for wires which are effectively infinitely long and then the heat transfer is dependent solely on the normal components of the velocity to the wire axis. It should be noted that many of the cooling laws used in anemometry are derived for wires that are

effectively infinitely long with regard to their diameter, and it is therefore essential that the wires be calibrated rather than the wire constants determined by calculation from theoretical considerations.

Several expressions have been derived and applied for calibration purposes. The general equation is in the form of

$$E^2 = A + B\,(U)^n \qquad \ldots\ldots\ldots \qquad (5.5)$$

where

E = Mean voltage.

U = Mean velocity.

n = Constant between 0.45 - 0.5.

Over a large cooling range this expression yields unsatisfactory results. Higher order polynomials have been found to give better curve fits to the experimental calibration curves of E vs U (4),(71). The expression which is commonly used is as follows:

$$E^2 = A + BU^{\frac{1}{2}} + CU \qquad \ldots\ldots\ldots \qquad (5.6)$$

In calibration, a much better curve fit is obtained if the zero velocity voltage is excluded since a spurious value of A is generated owing to free convection effects. The probes generally have different calibration constants when they are facing in different directions. The instantaneous cooling velocity is given by:

$$U^2 = w^2 + G^2\,u^2 + K^2\,v^2 \qquad \ldots\ldots\ldots \qquad (5.7)$$

where K factor arises from cooling along the wire and G factor arises from wire support interference effects. For miniature D.I.S.A. probes these values generally are G = 1.15 and K = 0.25 (72);but G and K must be determined for each individual probe since these values are affected by small manufacturing variations.

5.4.4 Method used for Signal Analysis.

The method used was developed by Syred (58) requires only one probe with four point measurements and has proved to be much more accurate method of evaluating velocity levels in highly turbulent flows compared to six position methods. In six position methods two probes are necessary for measurement at the same point which may not be placed in quite the same position and since it usually requires longer time, the flow state and calibration constants may alter. Another disadvantage of these methods is that all six output voltages are assumed to be in similar regular shape and frequency distribution and also in phase (4), (71). For the method applied a straight hot wire probe was used which was mounted parallel to v direction. As it is shown in Fig. (17-a) the probe was rotated about its axis of symmetry at four measuring points each having 45° separations in between.

5.4.5 Calibration of the Probes.

The aim of wire calibration is to determine the coefficients of the heat transfer relationship adopted for the wire. For accuracy, the calibration must be frequently repeated, since the wire characteristics drift rather quickly with age, due principally to the deposition of dust. In principle, the requirements of a calibration system are that it should provide a controllable, turbulent free flow of accurately known velocity and temperature.

The probes were mounted in the potential core of a free air jet issuing from a round nozzle, with the wire normal to the flow direction. It was ensured that the full length of the wire was in a uniform velocity field and that the turbulence intensity of the calibration jet was as low as possible. The jet velocity was measured with a standard N.P.L. pitot tube. The jet

velocity was varied and voltage readings were taken for each known velocity.

A hot wire probe with three components of a total velocity vector acting in directions parallel to the three orthogonal axes is shown in Fig.(17-b).

The wire response equations which was found to give the best description of the calibration data over the entire cooling range was quadratic in $(U)^{\frac{1}{2}}$.

$$E^2 = A + BU^{\frac{1}{2}} + CU$$

The calibration constants A, B, C were calculated for a least squares fit on the calibration data. The response of the hot wire to the three velocity components is as in (eq.5.7).

$$U^2 = w^2 + G^2u^2 + K^2v^2$$

G and K values were obtained from the respective calibration curves Fig.(17-c) at constant E^2 as:

$$G = \frac{w}{u} \quad ; \quad K = \frac{w}{v}$$

Assumptions are made about the shape of the velocity signals to be able to evaluate mean and fluctuating velocities, because of the non linearity of the calibration curve. All the assumptions made are given in detail by Syred (58).

5.4.6 Analysis of Response Equations.

Considering the instantaneous velocity vectors acting on each of the four positions in Fig.(17-b), the four response equations and effective cooling velocities acting on each measuring position can be written as:

$$U_1^2 = v^2 + G^2 \frac{(w+u)^2}{2} + K^2 \frac{(w-u)^2}{2} \quad \ldots\ldots\ldots \quad (5.8)$$

$$U_2^2 = v^2 + G^2u^2 + K^2w^2 \quad \ldots\ldots\ldots \quad (5.9)$$

$$U_3^2 = v^2 + G^2\left(\frac{w-u}{2}\right)^2 + K^2\left(\frac{w+u}{2}\right)^2 \quad \ldots\ldots\ldots \quad (5.10)$$

$$U_4^2 = v^2 + G^2w^2 + K^2u^2 \quad \ldots\ldots\ldots \quad (5.11)$$

In order to solve three unknown values, u,v,w, only three equations are required out of four given above. Solving equations (5.8), (5.10) and (5.11) simultaneously the following equations are obtained for u, w, v.

$$u = \sqrt{\left[(U_1^2+U_3^2-2U_4^2)+\left((U_1^2+U_3^2-2U_4^2)^2 + (U_1^2-U_3^2)^2\right)^{\frac{1}{2}}\right]\frac{1}{2(G^2-K^2)}} \quad \ldots\ldots\ldots \quad (5.12)$$

$$w = \sqrt{\left[-(U_1^2+U_3^2-2U_4^2)+\left((U_1^2+U_3^2-2U_4^2)^2 + (U_1^2-U_3^2)\right)^{\frac{1}{2}}\right]\frac{1}{2(G^2-K^2)}} \quad \ldots\ldots\ldots \quad (5.13)$$

$$v = \sqrt{\frac{1}{2}\left[(U_1^2+U_3^2)-\frac{(G^2+K^2)}{(G^2-K^2)}\left((U_1^2+U_3^2-2U_4^2)^2+(U_1^2-U_3^2)^2\right)^{\frac{1}{2}}\right]}$$

Different sets of expressions for u ,w,v can be obtained from equations (5.8), (5.9) and (5.10). Depending on the probe positioning and the characteristics of the flow field either set of solutions can be chosen. It is advantageous to know the characteristics of the flow field beforehand so that the probe can be aligned in the most suitable direction, since the probe is most sensitive to the maximum velocity vector.

Detailed solution of the response equations for u,w,v and their evaluation from the relevant voltages are given in reference (58).

A computer programme has been writeen in FOCAL to solve the two different sets of equations and compare the results.
A flow chart of the programme is given in Appendix 4.

When a hot wire probe is used in a flow system which has a different temperature than the calibration temperature, which is often the case when the flow is generated by a blower, then it is necessary to correct the calibration data to take this effect into account. A method of correction is given in Appendix 2.

CHAPTER 6.

RESULTS AND DISCUSSION

6.1. Qualitative Flame Results.

Increase in flame length was one of the important indications of the flame interaction in the multiple burner arrangements. P(2) shows a photograph of the reference flame with moderate swirl (S=0.37). As can be seen from P(3) by the addition of a second burner at a separation of 0.77 D_E the overall visible flame length was increased. P(4) shows the overall visible flame length for a three burner system with the same separation and P(5) for a five burner system with a_1 = 0.77 D_E and a_2 = 1.50 D_E. When these photographs are compared the increase of the flame length due to the addition of another burner is clearly evident. P(6) and P(7) show two and three burner system at a closer separation (a = 0.25 D_E). Considerable flame lengthening, due to burner crowding, compared to reference flame is obvious. Comparison of P(6) and P(7) to P(3) and P(4) indicates the effect of burner separation on flame length.

Flame lengthening in multiple systems was found to be more pronounced at low swirl levels. In three and five burner systems neighbouring flames tended to divert from their original axes towards the centre flame and oscillations were set up particularly at the flame tips. At low swirl levels low turbulence intensities at the nozzle exit leads to instabilities in the flames.

6.2 Qualitative Results or Single Flame.

In most of the experiments presented in this chapter a moderate swirl level (S=0.37) was chosen. The single flame, which was taken as a reference flame for the multiple flames, was short, intense, steady and non-luminous. As the degree of swirl was reduced the flame length was increased and the flame started

becoming unsteady. This was most significant at swirl values under 0.2. With any further decrease in the degree of swirl the flame was lifted-off the burner rim and eventually was blown off. Accordingly the effect of any increase in swirl level was to reduce the flame length. Increasing the swirl beyond this level had no effect on the flame length. This critical swirl level was above 0.6 for the particular burner used. Experiments could not be carried out without swirl due to the extreme instability of non-swirling flames. To eliminate the effects of instability, swirl levels less than 0.2 were not employed in the multiple flame systems.

6.3 Flame Stability.

Before going into any detailed investigation of the multiple burner systems some preliminary single burner experiments had to be performed with burners having diffusers of different half angles in order to obtain a stable flame. The flame stability resulting from a certain burner geometry can be characterised by the blow-off velocity of the flame. With premixed flames it is the flow velocity of the fuel-air mixture above which the flame extinguishes. In the case of the particular diffusion flame used, the volumetric flow rate of the air is 12 times more than the volumetric flow rate of the fuel, therefore one has to refer to the air discharge velocity because air is the component which contributes the most to the flow. Fig.(18) shows the results of the blow-off tests performed with burners having 10°, 20°, 35° diffuser half angles at a high swirl level (S=0.57). As can be seen the burner with the 20° half angle diffuser showed higher stability in the fuel lean region compared to the others. Since the size of the recirculation zone is increased by increasing the diffuser angle to an optimum limit, the main advantage of using diffusers with

an optimum half angle is to obtain good flame stabilization at low degrees of swirl. In diffusers having narrow angles the flow is attached to the walls of the diffuser. As the angle gets larger than a critical value the flow separates from the walls of the diffuser and this reduces the advantages attained by the use of a diffuser.

Examination of the results of the blow-off limit tests showed that the most stable flame could be obtained by using a burner having a 20° half angle diffuser. Therefore burners having such diffusers were used throughout the rest of this investigation.

A series of blow-off tests were performed for different burner arrangements. Fig.(19) shows the result of the tests for two and three burner in line arrangements having a separation of $a = 0.25\ D_E$ and at moderate swirl level (S=0.37). Blow-off limits for the reference flame at the same swirl level are given for comparison. The reference flame was more stable in the fuel lean region. As the number of burners was increased the flame stability at the same equivalence ratio was reduced and the blow-off limit curves were shifted towards the fuel rich region with an increase in the number of flames.

Another factor which affects flame stability is the degree of swirl in the combustion air. It was observed that for three burner systems at low swirl levels ($S < 0.3$) and minimum separation ($a = 0.25\ D_E$) the centre flame lifted-off the burner rim and was blown-off frequently. At moderate ($0.3 < S < 0.5$) and high ($S > 0.5$) swirl levels, no blow-off due to flame interaction was found.

It is shown by previous workers (4), (53) that the direction of swirl in multiple jet arrangements plays an important role. If the adjacent jets are swirling in the same direction in other

words swirling "out of mesh" the overall stability of the system increases. That is because when the direction of rotation is the same in the region where two jets interact with each other, the directions of swirl velocity will be opposite and consequently the shear forces will be higher than "in mesh" swirling systems. Therefore burners swirling "out of mesh" have been used throughout this research.

While considering the effects of flame interaction the geometry of the burner arrangement must also be considered. Therefore at this point the terminology used for describing this geometry must be explained. As shown in Fig.(20) separation "a" is defined as the rim to rim distance of adjacent burners measured at the exit plane whereas pitch "P" is their centre to centre distance. These values are normalized into a dimensionless form by taking their ratio to the burner exit diameter. Thus

$$\bar{a} = a/D_E$$

$$\bar{P} = P/D_E$$

where

$\bar{a}$ = Separation constant.

$\bar{P}$ = Pitch constant.

However the most characteristic parameter for the flames is the throat diameter. Considering a multiple burner system with diffusers having large half angles, if the burners are placed so that they touch each other $\bar{a}$ will be equal to zero but the flames will not necessarily be in direct contact, particularly if they are contained only in the central region of the diffuser. Therefore axial and radial distances within the flame are normalised with the diameter of the burner throat (D_T) as x/D_T and r/R_T.

6.4 Quantitative Results on Flame Length.

Flame lengths were determined both by long exposure photography and by gas chromatographic analysis. The end of the flame was taken to be the point where CO concentration had decreased to 0.01%. Fig.(21) gives the flame lengths determined by gas chromatography as a function of burner separation and number of burners. As a consequence of flame interaction, the overall flame length was increased with a decrease in burner separation and increase in number of burners. These effects were more pronounced at low swirl levels.

When the flame lengths for the group of two burners were plotted against the reciprocal of separation at different swirl levels as in Fig.(22) and extrapolated to $1/a = 0$ the flame length of the group arrangement was, as expected, seen to be the same as that of a single flame at that swirl level.

The flame lengthening in multiple systems was due to delayed combustion and reduced entrainment rate of the ambient air. The air entrained into the flame provides extra oxygen for combustion. The presence of another flame in the near vicinity of a flame decreases the surface area which is in direct contact with the atmosphere and available for the entrainment of ambient air. Especially the centre flame of a multi flame arrangement has very little surface area in contact with the atmosphere and such flames were seen to be the longest of the sets having the same swirl and separation.

The observations made using stoichiometric air supply showed that the influence of burner separation and burner crowding were more pronounced in the fuel rich flames because any amount of air entrained into the flame would contribute to the combustion immensely. The flame lengths given in Fig.(21) are obtained

using 20% excess air. Therefore the effects of crowding and separation were less drastic, because any air entrained into the flame contributed less to the percentage of the air already present in the flame.

While comparing the lengths of different flames it was found to be more convenient to deal with a variable which compares the length of a multiple flame to that of a single flame at the same swirl rather than using the actual lengths of the flames expressed in conventional units of length. Therefore a dimensionless length factor L_R termed "percent relative length" has been defined as

$$L_R = \frac{L_m - L_s}{L_m} \times 100$$

where

L_s = Single flame length.

L_m = Multiple flame length.

L_R = Relative length in %.

When the dependance of this factor was studied it was found to vary inversely with the other dimensionless quantities like swirl (S) and separation ratio (R_s), defined as

$$R_s = (a/D_E)$$

where

a = Rim to rim distance of two adjacent burners.

D_E = Diameter of the burner exit.

Therefore a general equation in the form of

$$L_R = \frac{K}{R_s \cdot S}$$

was obtained where K is a proportionality constant.

This constant K was calculated by using the experimentally obtained flame lengths and was found to be 2 for a two burner

and 3 for a three burner system. Therefore the equation was reduced to

$$L_R = \frac{n}{R_s \cdot S}$$

where

n = Number of burners in a row.

It must be pointed out that this approximation is only valid for burners in line. For any different burner arrangement this relation will not hold due to the different entrainment characteristics.

6.5 Temperature Distributions.

Radial temperature profiles for a highly swirling reference flame at several axial positions are given in fig.(23). Since the swirling flames have a relatively cool central core, at the axial positions close to the burner exit the temperature maxima were located away from the burner axis. The maximum temperatures were found to be higher than in a non-swirling flame. Temperature maxima shifted towards the flame axis after about a distance of 2 D_T from the burner exit. At high swirl levels due to the presence of recirculation, hot combustion products from the downstream positions travel back to the nozzle exit and create higher pre-heat temperatures and thereby approach theoretical flame temperatures more closely.

The axial temperature profiles measured on the axis of the datum flame for two and three burner systems at a moderate swirl level (S = 0.37) and closest separation (a = 0.25 D_E) are given in Fig.(24). The temperature maxima were recorded further downstream in multiple systems as a result of the shifted reaction zone due to delayed combustion. Similarly slower decay of the temperature curves were noted, indicating slower cooling at the downstream positions of the multiple systems as a result of

reduced rate of entrainment of the surrounding air.

When the swirl level was decreased to S = 0.2, while all other variables were kept the same as in the previous case, the axial temperature profiles were as seen in Fig.(25). Since the reaction zone was shifted further away from the burner exit, at low swirl levels, due to reduced turbulent intensities, the combustion was delayed. As a result of that, the flames were longer and the temperature maxima were also shifted further downstream. Much slower decay of temperatures at the downstream positions were again due to reduced rate of entrainment of surrounding air. As can be seen from the figure these effects get more and more pronounced as the number of burners was increased.

The effect of swirl on the centre flame temperature in a three burner system with a separation of 0.25 D_E between the burners is shown in Fig.(26). At a moderate swirl level (S = 0.37) the temperature profile was more uniform and it gave a maximum near the burner exit, at about 2 D_T away from the exit plane and then decreased smoothly. At a higher swirl level (S = 0.57), the temperatures were lower near the burner exit, they gave a maximum at about 3 D_T away from the exit and then decayed much more rapidly compared to flames with lower swirl. Low temperatures near the burner exit were due to the cooling effect of the high rate of entrained surrounding air and better mixing encountered at high swirl levels as a result of the increased turbulent quantities near the burner exit. Combustion took place much more rapidly at high swirl levels therefore temperatures decayed much more rapidly at downstream positions. Recirculation of the hot combustion products at high swirl helped to preheat the fuel and air mixture and combustion was faster whereas at low swirl the temperatures near the burner exit were

also low but this is not due to high rate of entrained surrounding air and its cooling effect, but due to poorer mixing between fuel and combustion air supplied thus delayed combustion. When the mixing between air and fuel is poor at molecular level they form inflammable mixture much slower. Low turbulent intensities tend to leave the small pockets of fuel away from the contact of combustion air longer time therefore the reaction zone at low swirl levels was shifted away from the burner exit. The temperature maximas were reached at about 6 to 7 D_T downstream and then decayed very slowly. This slower decay is due to the low rate of entrainment of surrounding air owing to much lower turbulence levels at downstream positions.

In Fig.(27), again the effect of swirl on the centre flame temperature is shown for a five burner system. The centre and the outer burners were separated by $a_1 = 0.77\ D_E$ and the outer burners had a mutual separation of $a_2 = 1.50\ D_E$. The temperatures were recorded at the same swirl levels as in the three burner system. A very similar trend in axial temperature profiles was obtained as in Fig.(26) and the argument presented for the three burner case is also valid for this system. The maximum recorded temperature for the highly swirling flame system was shifted to $4\ D_T$ away from the exit plane as a consequence of the shifted reaction zone. The decay of temperature at the downstream position was much slower than it was in the three burner system at all of the three swirl levels chosen, i.e. in three burner system the temperatures at $X = 16\ D_T$ were about 1005, 655 and 550° C whereas in the five burner system at the same axial position the corresponding temperatures were about 1075, 970, 870° C for the swirl levels 0.2, 0.37 and 0.57 respectively. The only difference between the two systems was the increased number of burners.

Fig. (28) shows the effect of burner separation on the centre flame temperature in the three burner system, at a moderate swirl level (S = 0.37). Here the axial temperature profiles for two different separations and for the reference flame are given. As the separation was increased from a = 0.25 D_E to a = 0.77 D_E the temperature profile took a similar form to that of the reference flame. At a larger separation the shielding effect of the side flames on the centre flame was reduced, also from the aerodynamic point of view their mutual interference was less. Therefore the centre flame, although was not as free as a single flame, had a higher freedom compared to those with closer separation.

Fig. (29) shows the effect of burner crowding on radial flame temperature profiles measured at X = 1.8 D_T. The flames were moderately swirling (S = 0.37) and had a separation of 0.25 D_E. Two and three burner systems gave higher radial temperature profiles than a single flame. Higher temperatures on the axis between the burners were due to the presence of an adjacent burner. For the three burner system the temperature recorded on the centre burner axis was 1320° C whereas on the outer burner axis it was 1290° C. This was because the centre flame was entraining more hot combustion products whereas the outer burners were more free to entrain air at ambient temperature.

As in the case of the flame length results it was decided to deal with a variable which related the temperature in a multiple flame system to the temperature at the same point in a single flame which had the same degree of swirl. Therefore a dimensionless temperature factor T_R termed "percent relative temperature" has been defined as:

$$T_R = \frac{T_m - T_s}{T_s} \times 100$$

where

T_m = Multiple flame temperature.

T_s = Single flame temperature.

T_R = Relative temperature rise %.

These relative temperatures are calculated and plotted for a two burner system with a high swirl (S = 0.57) in Fig.(30). It is seen that as the separation between the burners was increased the relative temperature rise decreased owing to the combustion conditions approaching that of a free single flame; whereas when the two burners were brought closer together the actual temperatures and thus the relative temperatures increased. At an axial distance of 1.5 D_T, all relative temperatures were low because this was the point where combustion was most intense and the temperatures were highest in a single flame.

When these percent relative temperatures are plotted for two, three, four and five burner systems with S = 0.37 as in Fig. (31) they are seen to be even higher. Thus an increase in the number of burners increases the relative temperatures within a system.

When Figs. (30) and (31) are compared it is seen that in a two burner system with high swirl at axial positions further than X = 11 D_T, the relative temperature curves start falling whereas at a lower swirl level these curves are steeply rising at the same axial position. This indicates that at low swirl levels the temperatures are still rather high due to combustion being uncompleted as well as due to the reduction in the amount of entrainment of cold atmospheric air.

Fig.(31) also shows the effect of separation on relative temperature rise. The increase in relative temperatures indicate the increase in actual temperatures compared with the single flame when the burners are brought closer to each other.

In Fig.(32) isotherms for a single swirling flame and in Fig.(33.) isotherms for the three swirling flame system with a separation of a = 0.25 D_E are shown. When these two figures are compared, in the three burner system very high temperature zones at the early part of the flames and very slower decay of temperatures along the flames can be seen. At the same axial positions temperatures for the outer flame were lower than the centre flame. Isotherms were not symmetric around the axis between the burners because the centre and the outer flames behaved differently.

6.6 Gas Concentration Distributions.

The effect of burner crowding on radial gas concentrations measured at X = 2.2 D_T are shown in Fig.(34). The flames were swirling moderately (S = 0.37) and had a separation of a = 0.25 D_E. Oxygen concentrations are given in Fig.(34-a). At positions less than r = 1.5 R_T the single flame had a lower oxygen concentration than two and three flame systems. The reason for this is that the rate of combustion was higher in the single flame due to better mixing and oxygen was consumed more rapidly at the inner part of the flame. After r = 1.5 R_T O_2 concentration increased very rapidly due to high rate of entrainment of the surrounding air in the single flame and approached almost to atmospheric oxygen concentration at r = 4 R_T. In cases of the multiple flames O_2 concentration on the axis between the flames increased slightly and then decreased again due to the presence of another flame. Fig.(34-b) shows the radial variations of methane concentration in the same systems.

In case of the single flame the methane concentrations at the flame axis show that the majority of the gas injected has already been mixed and reacted with the combustion air while the small amounts of gas which have been deflected and travelled towards

the edge of the flame have remained unreacted. In the multiple flame systems methane concentrations on the centre of the flame were much higher compared to the single case as a result of poorer mixing between fuel and combustion air and thus slower combustion. As a consequence of flame interaction resulting in reduced amount of entrainment much higher methane concentrations were recorded on the axis between the burners. The corresponding carbon monoxide and hydrogen concentrations are given in Fig. (34-c) and Fig. (34-d) respectively. These gases were not supplied with the fuel but produced in the flame as an intermediate product (CO) or due to cracking of methane (H_2) where combustion is not complete. The fact that their concentrations on the flame centre as well as at the edges of the flames are much higher in the multiple systems indicate the presence of flame interaction. All these radial concentration profiles indicate that the rate of entrainment of the surrounding air and the rate of mixing were greatly reduced due to the crowding effect in the multiple systems. The presence of higher fuel concentrations (CH_4, H_2 and CO) at the flame edges of the multiple systems was partly due to reduced entrainment and consequently a reduced dilution effect; and partly due to retarded combustion as a result of the presence of the low shear region on the axis between the burners as a consequence of flame interaction.

The effect of burner separation on radial gas concentrations for two and three burner systems measured at $X = 2.2\ D_T$ and moderate swirl level are shown in Fig. (35) and Fig. (36) respectively. [O_2 concentrations in Fig. (35-a) and Fig. (36-a), CH_4 concentrations in Fig. (35-b) and Fig. (36-b), CO concentrations in Fig. (35-c) and Fig. (36-c), H_2 concentrations in Fig. (35-d) and Fig. (36-d)]. As the separation between the burners was increased

the radial variations of the gas concentrations approached to that of a single flame. Lower oxygen and fuel (CH_4, CO, H_2) concentrations near the flame centre encountered at a wider separation of a = 0.77 D_E indicate that by moving burners further apart the mixing and the rate of combustion were improved greatly. Since each flame had more surface area available for entrainment of the surrounding air the concentrations near the flame edges showed the presence of larger quantities of entrained air. The effect of separation on the combustion of a three burner system was much more pronounced compared to that on a two burner system.

In Fig. (37) the effect of burner crowding on axial distributions of gas concentrations are shown. In the multiple systems as a consequence of flame interaction the combustion was delayed as indicated by slower decay of methane along the axis Fig. (37-a) as well as the presence of high CO and high H_2 concentrations, Fig. (37-b) and (37-c). The presence of high H_2 and CO concentrations which are intermediate products of combustion were due to the partial oxidation of methane. High concentration of carbon monoxide is consistent with the expected reduction of the rate of mixing of the fuel and the combustion air. The amount of ambient air entrained was less in the multiple systems as indicated by lower O_2 concentrations at the downstream positions as shown in Fig. (37-a). As expected this resulted in higher CO_2 concentration as shown in Fig. (37-b) due to less dilution of combustion products.

Fig. (38) shows the effect of burner crowding on axial gas concentrations at a lower swirl level (S = 0.2), when the burners were separated by 0.25 D_E. The concentration profiles show a similar trend as in the previous case. But due to the reduced degree of swirl the rate of combustion was even more delayed as

shown by much slower decay of CH_4 concentration Fig.(38-b), along the axis and the presence of higher CO concentration Fig.(38-a) near the burner exit as well as along the axis. The measured O_2 concentration Fig.(38-a) and CO_2 concentration Fig.(38-b) at the downstream positions indicated slower rate of entrainment of surrounding air compared to a higher swirling system. As was indicated in the flame length results these flames tend to be very much longer than moderately and highly swirling flames. When the concentration profiles of a low swirl system Fig.(38) is compared with that of a higher swirl system Fig.(37), the effect of burner crowding on the scale of interaction was found to be more pronounced at low swirl levels. Similar effects on axial oxygen, methane and carbon monoxide concentrations for the three burner system with a separation of $a = 0.25\ D_E$ are seen in Fig.(39). These results are given for two different swirl levels.

The effect of separation on axial distribution of the concentrations of oxygen, carbon monoxide, methane and carbon dioxide is shown in Figs. (40-a) and (40-b) respectively for the three burner system ($S = 0.37$). At the closer separation $a = 0.25\ D_E$, the flames affected each other more than at the wider separation, $a = 0.77\ D_E$. Allen (4) showed that in multiple jet systems at closer separations due to the aerodynamic interaction the velocity gradients along the jet axis were very much lower. These low velocity gradient regions were associated with lower turbulent intensities and subsequently these lead to poorer mixing. The occurrance of the measured gas concentrations were in close agreement with Allen's aerodynamic results. The presence of higher methane and carbon monoxide concentration at the closer separation at any axial station showed that the turbulent intensities were reduced by bringing the burners closer to each other. The increase in the

rate of entrainment by moving the burners further apart was indicated by higher recorded O_2 concentrations at almost all axial positions.

Fig.(41-a) and Fig.(41-b) again show the effect of separation on axial $CO-O_2$ and CH_4-CO_2 concentrations respectively, for two burner system (S = 0.2). Comparison of these figures with the groups of Figs.(40) and (41) shows that the effect of separation gets more pronounced with a decrease in the degree of swirl.

6.7 Gas Concentration Distributions for the Single Flame.

Radial profiles of gas concentrations for the single swirling flame (S = 0.37) which was taken as a reference flame in most of the experiments are presented in Fig.(42) at three different axial stations. In Fig.(42-a) very rapid decay of methane concentration on the burner axis can be seen. At an axial station inside the burner diffuser X = -0.31 D_T the centre methane concentration was about 75% and within one throat diameter distance due to very rapid combustion and high rates of mixing this concentration was reduced to about 0.75% at X = 0.62 D_T. Isothermal velocity measurements showed that radial velocity components were quite high in the cold jet Fig. (43-c) and these would be even higher in the flame due to acceleration caused by the combustion. Therefore the presence of high methane concentration on the flame edges can be attributed to this high radial component of velocity such that part of the fuel was carried away towards the flame edge before it had a chance to be burnt. Even though the concentrations at the flame edges were not very high; consideration must be given to the fact that because of the high rate of entrainment of the surrounding air the dilution effects will be more pronounced. This can be seen to be true from the oxygen concentrations given in Fig.(42-d). Therefore

the presence of 6% methane in this oxygen rich region is equivalent to much higher methane concentrations in a region where the entrainment effects are less pronounced.

Part of the unburnt fuel in the form of carbon monoxide (as an intermediate product of combustion) and hydrogen (product of cracking) are given in Figs.(42-b) and (42-c) respectively. They both show very similar profiles at the same axial stations. High concentrations of CO and H_2 were present where the methane concentration was low and vice versa. When these results are compared to the amplitudes of temperature fluctuations measured by Apak (69) Fig(45) it is seen that there was a close resemblance between the plots of the amplitudes of temperature fluctuations and the concentration profiles for methane within a same flame.

Fig.(42-e) shows the profiles of CO_2 concentration. As would be expected there was very little CO_2 inside the diffuser where combustion had just started. It reached a higher level at an axial station of $X = 0.62\ D_T$ where the rate of combustion was very high as could be seen from methane concentration profile in Fig.(42-a). At an axial station of $X = 2.18\ D_T$ CO_2 concentration was slightly decreased due to dilution as a result of the high rate of entrainment of the surrounding air and also the profile was spread over a larger cross sectional area. Fig.(42-f) shows the profiles of N_2 concentration. The regions which have more entrained air can be seen where the N_2 concentration has approached to atmospheric nitrogen concentration.

6.8 Isothermal Velocity Distributions for the Single Jet.

Three mean velocity components in a cold annular air jet of a single burner measured by a hot wire anemometer are presented in this section. The velocities are normalized by initial annular jet velocity which was calculated at the throat section from the total air input.

Fig. (43-a) shows the radial profiles of the relative mean axial velocity for a moderately swirling annular air jet (S = 0.37) at four different axial stations. Velocity maxima were recorded away from the burner axis. These profiles are very similar in nature to the mean axial velocity profiles measured by Dvorak (70) under burning conditions Fig. (46) using a laser dopler anemometer. The velocities were considerably higher under burning conditions due to the expansion and thus the acceleration associated with combustion. It must also be noted that in the isothermal velocity measurements the central fuel jet was not present and subsequently neither was its contribution to the overall system. Negative velocitie were recorded near the burner exit both in cold and hot systems. The presence of a recirculation zone at this swirl level (S = 0.37) was not expected from a jet without a divergent diffuser.

The presence of recirculation at low swirl levels is a characteristic of the burners with a diffuser. The reverse flow zone created helps to stabilize the flame inside the diffuser by recirculating hot combustion products and pre-heating the cold fuel and air issuing into the diffuser. The fuel jet was also noted to spread radially outwards under the effect of the induced internal reverse flow zone and when ignited gave a rapidly mixed intense flame as was verified by gas concentration measurements shown in Fig. (42).

In Figs. (43-b) and (43-c) radial distributions of relative mean tangential and radial velocity components respectively for the same system at the same axial stations. At the burner exit (X = 0), each mean velocity component gave a maximum at a radial distance corresponding to $r/R_E = 1$ which shows the effect of the burner diffuser on the velocity distribution. All the mean

velocity components decayed very rapidly in the axial direction.

Relative mean axial, tangential and radial velocity distributions for a highly swirling (S = 0.57) cold annular air jet are given in Fig.(44-a), (44-b) and (44-c) respectively at three different axial stations. Again maximum mean velocities were recorded at $r/R_E = 1$ near the jet exit.

In general any increase in the degree of swirl increases the angle of spread of the jet thereby increasing the total available surface area per unit volume of the jet for mixing with the surrounding fluid.

The velocity gradients near the jet exit are usually larger at high swirl levels giving rise to higher shear stresses. Turbulent intensities and consequently the rate of mixing also increases with increasing the degree of swirl. A highly swirling jet dissipates its turbulent energy much faster and at a shorter distance from the exit compared to one with a lower swirl therefore the velocites, the velocity gradients and resulting shear terms will be less than they are in a weakly swirling jet at an axial station away from the jet exit. The changeover point at which the turbulence parameters of a swirling jet change from being larger than they are for a weakly swirling jet, to smaller is typically 3 and 5 jet diameters for the swirl numbers between S = 0 to S = 0.6 as stated by Allen (4).

Radial profiles of mean axial velocity component at several axial stations as measured by Dvorak (70) with the laser dopler anemometer, in the same burner system under burning conditions is given in Fig.(46). A recirculation zone existed near the burner exit. Velocities near the flame edges were found to be almost doubled in magnitude compared to the isothermal velocity measurements given in Fig.(43) measured by hot wire anemometer.

Apak (69) measured average temperatures and amplitudes of fluctuations with relevance to the formation of oxides of nitrogen in the same burner system at two different swirl levels (S = 0.37 and S = 0.57). Amplitudes of temperature fluctuations as measured by Apak are shown in Fig. (45) in order to give complete picture of the single flame used in the multiple flame studies. Apak concluded that on the flame axis the amplitudes of temperature fluctuations were dependent on the magnitude of average temperature such that higher the average temperature larger was the amplitude and vice versa.

6.9 Degree of Oxidation.

Degree of oxidation, defined in Chapter (1), in the flames was calculated using the measured gas chromatographic data. It was taken as a good measure showing the degree of completion of combustion. The degree of oxidation along the flame axis for single, two and three flame systems at a moderate swirl level (S = 0.37) are given in Fig. (47). In the case of a single flame, oxidation is almost complete at positions about eight throat diameters downstream from the burner exit whereas in multiple systems the oxidation is found to be incomplete at distances twice this value. This is an indication of delayed combustion in multiple systems as a consequence of interaction. This delay besides being due to reduced rate of entrainment is also due to improper mixing of the combustion air with the fuel. Allen (4) showed that in multiple jet systems due to the presence of neighbouring jets the local velocities within a flame increased with corresponding decrease in velocity gradients and shear stress terms. Because the mixing within a flame is mostly as a result of turbulent eddies set up by shear forces, lack of these causes improper mixing. Since the rate of entrainment is similarly

reduced the rate of oxidation is grossly reduced. In Fig.(48) the effect of separation on degree of oxidation along the centre flame axis in a three burner system at a moderate swirl level is seen. At a closer separation where a = 0.25 D_E, the increase in the degree of oxidation is much slower than it is in the case of a larger separation where a = 0.77 D_E. At a large separation although the mixing and the entrainment rates were reduced compared to that of a single flame, as a result of reduced turbulence intensity and due to the presence of adjacent flames, they were appreciably higher than they are at a close proximity system.

In Fig.(49) the degrees of oxidation along the flame axis are given for a system which has a lower swirl (S = 0.2) and closest separation (a = 0.25 D_E). The progress of combustion in these cases is even slower than it is in the previous case. Since with any reduction in swirl the turbulence intensity is also reduced, this leads to poorer mixing and thus to delayed combustion which is seen as a longer flame length.

Effect of burner crowding on radial degree of oxidation at an axial station of X = 2.2 D_T is shown in Fig.(50). In the three burner system each flame was separated by 0.25 D_E. The degree of oxidation on the flame axis was very low in the three burner system compared to the single flame, since the progress of combustion is much slower in the multiple systems due to flame interaction. At about r = 2.5 R_T both single and multiple flames have a low degree of oxidation region and then it again increases at the flame edges. That increase is much faster and nearer to complete combustion in single flame whereas it is comparatively slower in three flame system because of the presence of another flame nearby. The low degree of oxidation

region in the single flame corresponds to the region where turbulence intensities are low in a cold single jet as measured by Allen (4).

Much lower values of the degree of oxidation in the three burner system implies further reduction in the turbulence intensities as a result of flame interaction.

6.10 Dilution and Mixing Factors.

In this section some factors calculated depending on the measured gas concentration data have been presented. The definitions of these factors have been given in section (1.6.5).

Fig.(51) shows the change in the degree of dilution with the number of burners. When the value of the dilution factor is greater than 1.0 the point in question is in the fuel rich region. When this value approaches to zero the medium reaches to the atmospheric conditions. M_D = 1 indicates no entrainment of the surrounding air. The single flame shows a very short fuel rich zone. It entrains the surrounding air very rapidly and approaches to almost atmospheric conditions at about 10 D_T downstream. Two and three burner systems show a different behaviour. The fuel rich zone extends up to 6 D_T in the two burners and 8 D_T in the three burners whereas it is less than 1 D_T in the single flame. At about 16 D_T the dilution in the multi burner systems have only progressed half way. Effect of number of burners on the radial values of the dilution factor is given in Fig.(52). The single flame does not show any fuel rich zone at that particular axial position. Beyond r = 2 R_T it entrains air very rapidly and approaches to complete dilution. In the three flame system a fuel rich zone appears at the centre of the centre flame which extends up to r = R_T and before it is diluted to a considerable extent the fuel concentration again increases under the effect of the adjacent flame. The increase starts before the axis between the burners where the interaction is most intense.

The dilution factor along the single flame axis and along the centre flame axis of the three burner arrangement at a lower swirl level (S = 0.2) are shown in Fig.(53). The flames tend to

have a longer fuel rich zone at low swirl. In the single flame this fuel rich zone extends up to 6 D_T and in the three burner arrangement up to 9 D_T. Both flame systems show a slower approach to atmospheric conditions compared to the corresponding flames Fig.(51), at a higher swirl level.

These results show that the degree of dilution at a flame point decreases as the number of burners increases and the degree of swirl decreases.

Fig.(54) shows the radial distribution of the aerodynamic mixing factor (M_A) and Fig.(55) shows the corresponding stoichiometric mixing factor (M_S). In a single flame, at the same axial position, M_S is always equal or greater than unity which indicates the presence of just sufficient or excess amount of air over that required to complete the combustion. In the three flame arrangement M_S is always less than unity which indicates insufficient amount of air to complete the combustion. The value of M_A at the centre of the single flame is equal to unity where the mixing between the fuel and the combustion air is completed. Between the centre and $r = 2.5\ R_T$ the mixing between the fuel and the input air is not yet complete but not far from the complete mixing, beyond $r = 2.5\ R_T$, the flame entrains great amounts of atmospheric air. This has also been shown by the dilution factor in Fig.(52). The three burner system is far from the complete mixing at all points, at this particular axial position. The mixing of the fuel with the combustion air is very low especially near the axis of the centre flame and around the axes of the adjacent flames. The value of the stoichiometric mixing factor reaches to almost unity at about $r = 1.5\ R_T$ where the dilution factor is also about unity.

When the adjacent burners are far apart the large scale mixing between the fuel and the air increases greatly. Fig.(56) shows the effect of burner separation on aerodynamic mixing factor for the three burner system. The burner arrangement with the separation of a = 0.77 D_E shows appreciably better mixing compared to the arrangement having a separation of a = 0.25 D_E.

Schematic flow patterns for a single swirling flame and for three swirling flame system have been postulated from the measured and computed data coupled with visual observations obtained by introducing NaCl into the flames and are given in Figs.(57-a) and (57-b) respectively. As shown in Fig.(57-b), mass transfer between the adjacent jets is expected but the amount and the direction of the mass transfer needs to be studied separately to prove the validity of this postulation.

CHAPTER 7.

CONCLUSIONS

An experimental study of the interaction in the multiple turbulent gaseous diffusion flames was the main concern of the research programme. The influence of the number of burners, their separation and the degree of swirl on the interaction of the multiple flames for different configurations has been investigated. A single flame has been studied as a reference flame to provide information for the comparison with the multiple systems.

Multiple flames were found to be less stable against blow-off compared to a single flame and the blow-off limit curves shifted towards the fuel rich region as the swirl was reduced. At low swirl levels and minimum separation the centre flames were lifted off the burner rim and were frequently blown-off.

Considerable increase in the flame length was one of the indications of the flame interaction in the multiple burner arrangements. As a consequence of the flame interaction overall visible flame length increased with a decrease in the burner separation and increase in the number of burners. These effects were even more pronounced at low swirl levels. In the three and the five burner systems neighbouring flames tended to diverge from their original axes towards the centre flame and oscillations were set up particularly at the flame end. At separations more than four exit diameters no visible flame lengthening was observed.

Changing the burner spacing and the number of burners resulted in very distinct changes in the flame temperatures. The temperatures measured on the axis of the datum flame, show that the temperature maxima are recorded at further downstream

in the multiple systems as a result of the shifted reaction zone due to delayed combustion. Slower decay of the temperature curves indicate slower cooling at the downstream positions of the multiple systems. Beyond $a = 2 D_E$ no effect of neighbouring flames on flame temperature are noticeable.

The gas concentration measurements all indicate that with the burner crowding the rate of entrainment of the surrounding air and the rate of mixing are greatly reduced. Presence of high unburnt fuel and low oxygen concentrations on the axis between the flames is due to reduced entrainment and consequently reduced dilution effect; and partly retarded combustion as a result of the expected low turbulence intensities. In the multiple systems the decay of the methane concentration is slower, and the rate of carbon monoxide formation is higher along the flame axis compared to the single flame. These effects are more pronounced at closer separations and at low degree of swirl. At separations larger than $a = 2 D_E$ no interaction is noticeable.

Swirl greatly increases the mixing characteristics and consequently the rate of combustion of a flame particularly in the region close to the nozzle. The multiple flames that have a low degree of swirl show markedly higher interaction than the moderate or highly swirling flame systems. The degree of swirl also increases the rate of combustion by increasing the rate of entrainment of the surrounding air into the flames.

The multiple flame systems show a slower approach to complete combustion indicated by $N = 1$. The dilution factor tends to be higher at the downstream positions of the multiple systems which indicates a smaller amount of the entrainment of the surrounding air.

The degree of dilution at a flame point is decreased as the number of burners is increased and the degree of swirl is decreased.

When the adjacent burners are far apart the large scale mixing between the fuel and the air is increased greatly.

The following general conclusions can be drawn from the results of this investigation:

1. Multiple flames are less stable against blow-off, central flames can be lifted-off the burner rim when surrounded by other flames.

2. For flames separated by more than two burner exit diameters there was no significant interaction. As flames are brought together from $X/D_E = 2$ interaction increases and reaches a maximum when burners are adjacent to one another.

3. Burner crowding reduces large scale mixing and entrainment of air from the surroundings, thus delaying the combustion.

4. Swirl greatly increases the mixing characteristics and the rate of combustion within a flame.

5. The interaction effects become more pronounced as the swirl number is decreased.

6. Burners with 20 degrees diffuser half angle show better stability compared to burners with smaller or larger angled diffusers.

7. In predicting flame length for multiple burners, account must be taken of the increase in flame length as a consequence of separation distance of other flames. Increase in flame lengths can result in severe damage to combustion chambers.

CHAPTER 8.

RECOMMENDATIONS FOR FUTURE WORK

The scope of this research project was proposed by the Ministry of Defence (Ships) which was partly a continuation of the investigation carried out by Allen (4), who has provided isothermal data on multiple jet systems. But the systems studied were not the same in the two investigations thus it is difficult to relate these two sets of results. In order to complete the set of data on multiple jet systems under burning conditions measurement of flame velocities with the laser doppler technique developed within the Department (70) would be most valuable to provide information on a newly explored field of combustion.

A study of the mixing characteristics under burning conditions in the same multiple jet system would be very interesting. A radioactive tracer gas technique can be used for this purpose. To measure the amount of mass transferred between the adjacent flames a tracer gas can be injected into a burner and its presence and concentration can be searched for in the surrounding burners. This investigation can be done both for "in mesh" and "out of mesh" swirling jet systems.

There are certain difficulties associated with incorporating swirl and combustion. Whereas much progress in the field of turbulence models is currently taking place, very little attention is paid on recirculating combustion systems. The present investigation accompanied with (69) and (70) presents a set of data (time mean concentrations, mean temperatures and amplitudes of temperature fluctuations, mean and fluctuating three component velocities under cold and burning conditions) for a single swirling diffusion flame with recirculation. These data can be

used to test the validity of an existing combustion model or for the formulation of a new model. The most valuable attempt would be to extend the turbulence model for chemically reacting system developed by Bray (75), (76), (77), to cover swirling diffusion flames with recirculation. The above mentioned data can help to construct and check the validity of the model.

An investigation can be performed in order to make an exact calculation of the radiation from the multiple flames under various conditions. In order to make an exact calculation of the radiation from the flames and the gases, it is necessary to know the temperature, the relative positions of emitting and absorbing media and their emissivities and absorbtivities as well as the local velocities. The local emissivities of luminous, turbulent diffusion flames are little known. If a sufficiently accurate calculation of the burning rate and the distribution of the combustion products could be made, the temperature field and the distribution of emissivity would be obtained. The emission of a luminous flame depends on the number of carbon particles, and their number varies greatly with the conditions under which the combustion occurs. It is influenced, for instance by the mixing of air and the combustible gases and by the temperature of both components. As long as these conditions cannot be predicted, there is no possibility of calculating the radiation from a flame exactly. The faint bluish shine which natural gas emits and which is called "chemoluminosity" arises from the chemical reactions within the gaseous components. Such flames do not have a high radiating ability, but under certain conditions, such as when the number of burners are increased or when the swirl level is decreased some luminosity is observed in the flames, due to

the formation of carbon particles which glow in the flame and give it the yellowish colour, thus increasing the rate of radiation from the flames. A study of the amount of radiation heat loss from the multiple flame systems can have both practical and theoretical value.

REFERENCES

1. Hardcastle, J.W., "Downwards and Sideways Firing in a Naval Boiler" Proc.Symp. on Comb. in Marine Boilers, Inst.Fuel, Jan. 1968, pp.273-279.

2. Hardcastle, J.W., "Combustion and Multiple Burners" International Flame Research Foundation Aerodynamics Panel, Doc.No. A/30/c/15, April, 1967.

3. Miss Macnair, E.J., "Problems of Multiple Burners", International Flame Research Foundation, Doc.Nr. G14/a/1, 1967, Ijmuiden, Holland.

4. Allen, R.A., "Aerodynamics and Interaction of Single and Multiple Jets with Swirl" Ph.D. Thesis. Dept. of Chem.Eng. and Fuel Tech., Sheffield University, England, 1970.

5. Chigier, N.A. and Chervinsky, A., "Experimental Investigation of Swirling Vortex Motion in Jets". Jnl.Appl.Mech. 1967, pp.443-451, Trans.ASME 34, E,2.

6 Lee, Shao-Lin.,"Axisymmetrical turbulent swirling jet". Jnl. Appl.Mech. 32 Trans.A.S.M.E., Ser.E, 1965, pp.258-262.

7. Craya, A. and Darrigal, M., "Turbulent Swirling Jet" Physics of Fluids Supplement (1967), Vol.10, pt. 9, pp.197-199.

8. Laurence, J.C., "Intensity Scale and Spectra of Turbulence in Mixing region of Free Subsonic Jet", N.A.C.A., T.N.3561, Dec.1955.

9. Rose, G.W., "A swirling round turbulent jet", Trans.ASME. 84E, J.Appl.Mech. 29, 1962, pp.615-625.

10. Ricou, F.P. and Spalding, D.B., "Measurements of entrainment by axisymmetrical turbulent jets", J.Fluid Mech. 1961, II, 1, pp.21-32.

11. Beér, J.M. and Chigier, N.A., "Combustion Aerodynamics", Applied Science Pub.Ltd., London, 1972.

12. Chigier, N.A. and Beér, J.M., "The Flow Region near the Nozzle in Double Concentric Jets", Trans.ASME, 86D, J.Basic Eng., 1964, 4, pp.797-804.

13. Hawthorne, W.R., Weddel, D.S. and Hottel, H.C., "Mixing and Combustion in turbulent gas Jets", Third Symposium on Combustion, Flames and Explosion Phenomena, pp.266-288, Williams and Wilkins, Baltimore, 1951.

14. Longwell, J.P., Chenevey, S.E., Clark, W.W. and Frost, E.E., "Flame stabilization by baffles in high velocity gas streams", Third Symposium on Combustion, Flame and Explosion Phenomena, Baltimore, 1949, pp.40-44.

15. Longwell, J.P., "Flame stabilization by bluff bodies and turbulent flames in ducts." Fourth Symp. on Combustion, Flame and Explosion Phenomena, Baltimore, 1953, pp.90-97.

16. Lewis, B. and von Elbe, G., "Combustion, Flames and Explosions of Gases", Academic Press, New York, 1951, revised 1961.

17. Wohl, K., Kapp, N.M. and Gazley, C., "Stability of open flames", Third Symposium on Combustion, Williams and Wilkins, Baltimore, 1949, p.3.

18. Williams, G.C., Hottel, H.C. and Scurlock, A.C., "Flame Stabilisation and propagation in high Velocity gas Streams." Third Symposium on Combustion, Williams and Wilkins, Baltimore, 1949, p.21.

19. Bafuwa, G.G. and Maccallum, N.R.L., "Flame Stabilization in Swirling Jets", Combustion Institute European Symposium, 1973, Sheffield. pp.565-570.

20. Hottel, H.C. and Hawthorne, W.R., Third Symposium on Combustion, Williams and Wilkins, Baltimore, 1949, p.254.

21. Guenther, R., "Gaswärme" 1966, 15, p.376.

22. Chigier, N.A. and Beér, J.M., "Velocity and Static pressure distributions in swirling air jets issuing from annular and divergent nozzles", Trans.ASME, 86D, J.Basic Eng., 1965, 4, pp.788-798.

23. Swithenbank, J. and Chigier, N.A., Twelfth Symposium (International) on Combustion, p.1154, The Combustion Institute, Pittsburg, Penna. 1969.

24. Dugger, G.L. and Heimel, S., 1952, NACA TN 2624.

25. Gaydon, A.G. and Wolfhard, H.G., "Flames", Chapman and Hall, London, 1960.

26. Fricker, N. and Leuckel, W., "Swirl Stabilization of high jet momentum natural gas flames, and the optimization of burner design", International Flame Research Foundation, 1971, Doc.No. F35/a/4^{2}, Ijmuiden, Holland.

27. Hemsath, K., "Mixing factors and degree of oxidation: definitions and formulae for computation", International Flame Research Foundation, 1965, Doc.No. G.00/a/1^{1}, Ijmuiden, Holland.

28. Chigier, N.A. and Chervinsky, A., "Experimental and theoretical study of turbulent swirling jets issuing from a round orifice", Israel, J.Tech. 1966, 4, pp.44-54.

29. Narain, J.P. and Uberoi, M.S., "The swirling turbulent plume", University of Colorado, Dept. of Aerospace Engineering Sciences, Departmental Report No. 3525.

30. Chigier, N.A. and Chervinsky, A., "Aerodynamic study of turbulent burning free jets with swirl", Eleventh Symposium (International) on Combustion, The Combustion Institute, Pittsburgh, Penna., 1967, p.489.

31. Beér, J.M. and Chigier, N.A., "Swirling jet flames issuing from an annular burner", 5 me Journee d'Etudes sur les Flammes, Paris, 1963; also Doc.No. K20/a/91, International Flame Research Foundation, Ijmuiden, Holland, 1963.

32. Beér, J.M., "On the stability and combustion intensity of pressure jet oil flames", Combustion, 1965, 37, pp.27-44.

33. Kerr, N.M. and Fraser, D., "Swirl part I, effect on axi-symmetrical turbulent jets; part II, effect on flame performance and modelling of swirling flames", J.Inst.Fuel, 1965, 38, No. 299, pp.519-538.

34. Fricker, N. and Leuckel, W., "Flow and mixing patterns in gas flames with swirl in the annular air stream", International Flame Research Foundation, Doc.No. G02/a/18, Ijmuiden, Holland.

35. Leuckel, W., "The effect of swirl on ignition and combustion behaviour of turbulent diffusion flames", International Flame Research Foundation, Doc.No. K.20/a/4, Ijmuiden, Holland.

36. Beltagui, S.A. and Maccallum, N.R.L., "Aerodynamics of swirling flames - vane generated type", Combustion Institute European Symposium, Sheffield, 1973, pp.559-564.

37. Laurence, J.C. and Benninghoff, J.M., "Turbulence measurements in multiple interfering air jets", NACA. TN.4029, Dec.1957.

38. Corrsin, S., "Investigation of the behaviour of parallel two dimensional air jets", NACA.W.R.4H24, 1944.

39. Jung Von. R., "Grandzüge der von parallel schlitzbrennern ausgehenden rauchgasstromung und feuerranmen" Mitt der Vereinigung der Grosshesselbesitzer Heff. 90, 1964.

40. Knystautas, R., "The turbulent jet from a series of holes in line", The Aeronautical Quarterly. Vol.XV. Feb.1964, pp.1-29.

41. Koestel, A. and Austin, J.B., "Air Velocities in two Parallel Ventilating Jets", Heating Piping and Air Conditioning, Feb.1959.

42. Whaley, H., "A fundamental study of flow characteristics and heat transfer in multiple burner oil fired marine boilers". Ph.D. Thesis - Sheffield University, 1965.

43. Miller, D.R. and Comings, E.W., "Force-momentum fields in a dual jet flow", J.Fluid Mech., V.7. pt.2, 1969. p.237.

44. Glahn, U.H., Groesbeck, D.E. and Huff, R.G., "Peak axial-velocity decay with single and multi element nozzles". AIAA 10th Aerospace Sciences Meeting, San Diego, California, Jan.1972.

45. Wright, F.H., "Multiple flame holder array: Flame interactions", Jnl.Amer.Rocket Soc., 29, 1959, pp.143-144.

46. Godridge, A.M., "A comparison of RFO flame characteristics in test facilities and operational plant", Combustion Institute European Symposium, Sheffield, 1973, pp.657-662.

47. Zietz, U., Lübben, M., Baumgärtet, G. and Fetting, F., "Flow phenomena, mixing and stability of enclosed multi-jet turbulent diffusion flames", Institut für Technische Chemie der Technischen Universität, Hanover.

48. Putnam, A.A. and Speich, C.F., "A model study of the interaction of multiple turbulent diffusion flames", Ninth Symposium (International) on Combustion, Academic Press, New York, 1963, pp.867-877.

49. Thomas, P.H., Baldwin, R. and Heselden, A.J.M., "Buoyant diffusion flames: Some measurements of air entrainment, heat transfer and flame merging", Tenth Symposium (International) on Combustion, The Combustion Institute, Pittsburg, Penna., 1965, pp.983-996.

50. Huffman, K.G., "The interaction and merging of flames from burning liquids", Ph.D. Thesis, University of Oklahoma graduate College, 1967.

51. Braunschweig, S.T., "Multiple flames in near and far region ", International Flame Research Foundation, Doc.No. F.24/ga/4, Ijmuiden, Holland, 1971.

52. Tucker, A.C.N., "A first approach to the deviation of swirling jets in multi-burner systems", Esso Research Centre, Doc.No. G02/ca/10.

53. Fricker, N., Van Heyden, L. and Michelfelder, S., "Investigations into the Combustion of Natural Gas in multi-burner Systems", International Flame Research Foundation, Doc.No. F35/a/5, Ijmuiden, Holland, 1971.

54. Hinze, J.O., "Turbulence", McGraw Hill Book Comp.Ltd., New York, 1959.

55. Schlicting, Dr. H., "Boundary Layer Theory" Sixth Edition, McGraw Hill, 1968.

56. Bird, R.B., Stewart, W.E. and Lightfoot, E.W., "Transport Phenomena", Wiley, 1965.

57. Lumley, J.L., "Fluid Mechanics of internal flow", G. Souran ed., p.152, Elsevier, 1967.

58. Syred, N., "Velocity measurements in turbulent flow fields", Sheffield University, Departmental report, FTCE/27/NS/12/70.

59. Fristrom, R.M. and Westenberg, A.A., "Flame Structure", McGraw-Hill Book Comp.Ltd., New York, 1965.

60. Weinberg, F.J., "Optics of Flames", Butterworths, London, 1963.

61. Bradley, D. and Matthews, K.J., "Measurement of High Gas Temperatures with fine wire thermocouples", Jnl.Mech.Eng. Science, Vol.10, pp.299-305, 1968.

62. Bradley, D. and Entwistle, A.G., "Determination of the emissivity, for total radiation, of small diameter platinum-10% rhodium wires in the temperature range 600-1450°C", Brit.J.Appl.Phys. Vol.12, p.708, 1961.

63. Bradley, D. and Entwistle, A.G., "The total hemispherical emittance of coated wires", Brit.J.Appl.Phys. 17, p.1155, 1966.

64. Shevla, R.A., "Estimated viscosities and thermal conductivities of gases at high temperatures", NASA, TR R-132, 1962, U.S. Government Printing Office.

65. Bretsznajder, S., "Prediction of transport and other physical properties of fluids", Int.Series of Monographs in Chem.Eng. V.11, Pergamon Press, 1971.

66. Kent, J.H., "A noncatalytic coating for platinum rhodium thermocouples", Combustion and Flame, Vol.14, pp.279-281, 1970.

67. Penny and Giles Data Recorders Manual, "An automatic chromatograph for combustion gas analysis", Issue No. 1, P.G. P.112, 1969.

68. Lilley, D.G., "Turbulent swirling flame prediction", AIAA paper presented at the AIAA 6th Fluid and Plasma Dynamics Conference, Palm Springs, California, 1973.

69. Apak, S.C., "The relation between the formation of nitrogen oxides and the temperature fluctuations", University of Sheffield, Department of Chem.Eng. & Fuel Tech. Dissertation, 1973.

70. Dvorak, K., Unpublished Work, University of Sheffield, Dept. of Chem.Eng. and Fuel Tech.

71. Davies, T.W., "A study of the aerodynamics of the recirculation zone formed in a free annular air jet", Ph.D. Thesis, Sheffield University, Dept. of Chem.Eng. and Fuel Tech., 1969.

72. DISA Operating Manual Type D5501 Anemometer.

73. Bearman, P.W., "Corrections for the effect of ambient temperature drift on hot-wire measurements in incompressible flow", DISA Information No. 11, 1971, pp.25-30.

74. Davies, P.O.A.L. and Fisher, M.J., "Heat transfer from electrically heated cylinders", Proc.Roy.Soc. A280, p.486, 1965.

75. Bray, K.N.C., "Equations of turbulent combustion I fundamental equations of reacting turbulent flow", University of Southampton AASU Report No. 331, 1973.

76. Bray, K.N.C., "Equations of turbulent combustion II boundary layer approximation", University of Southampton, AASU Report No. 331, 1973.

77. Bray, K.N.C., "Kinetic energy of turbulence in flames", University of Southampton AASU Report No. 332, 1974.

78. Kim, W.J. and Manning, F.S., "Turbulence energy and intensity spectra in a baffled, stirred vessel". J.A.I.Ch.Eng. V.10, 1964, pp.747-752.

P.(1.a) Babcock & Wilcox Marine Boiler.

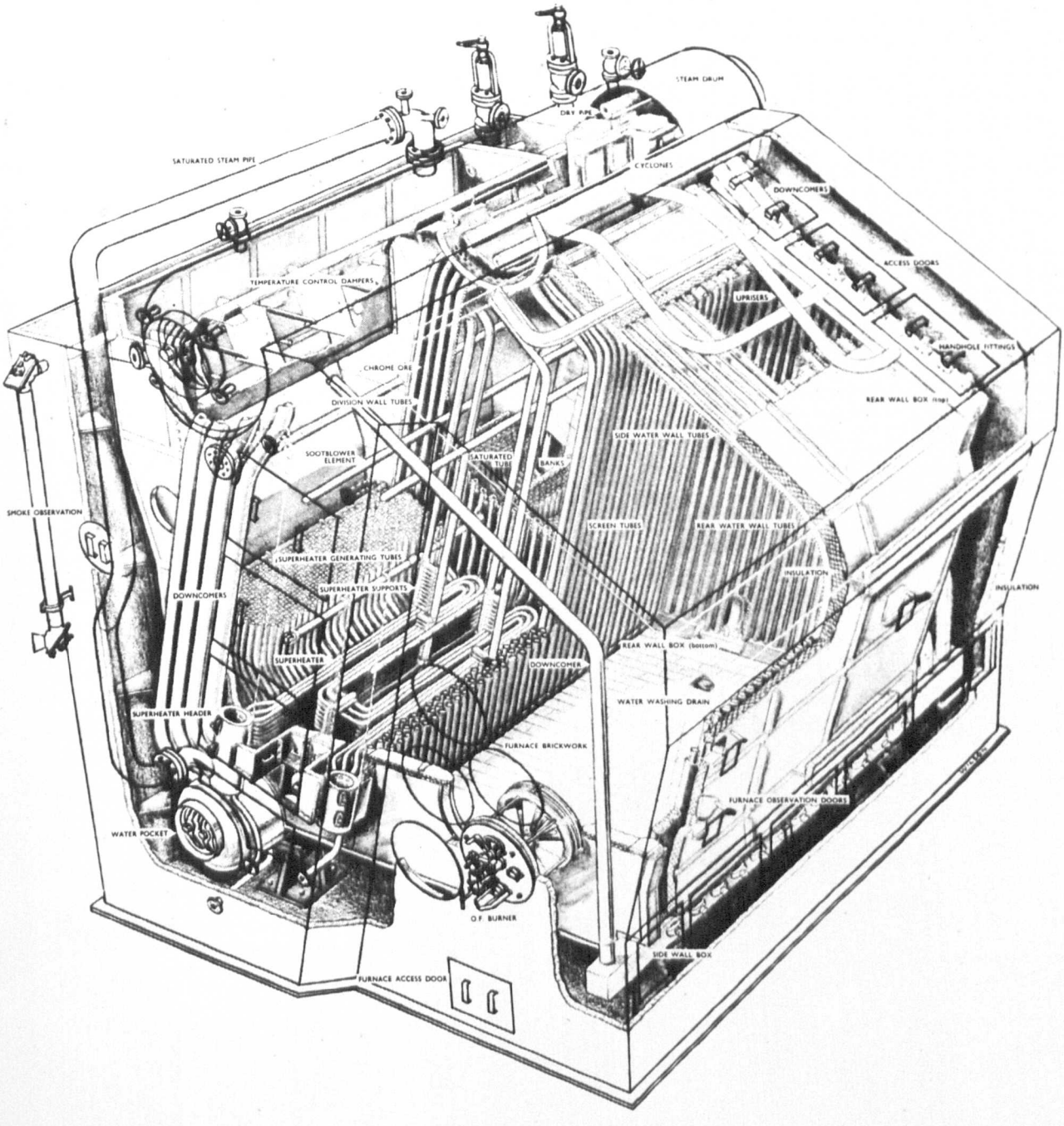

P.I.a. BABCOCK & WILCOX LIMITED TYPICAL MARINE SELECTABLE SUPERHEAT BOILER

P.(1.b.) Experimental Apparatus.

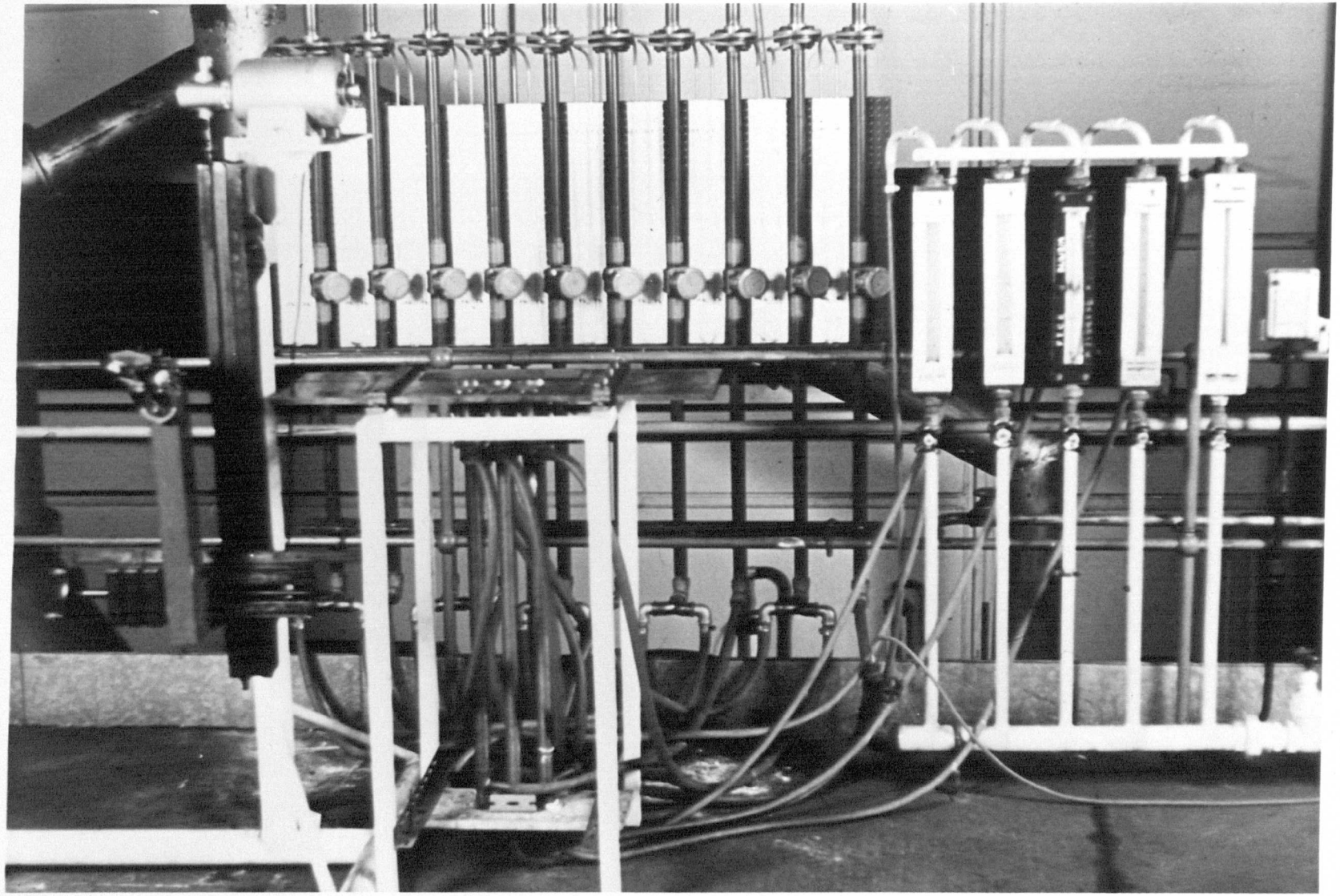

P. 1-b

P.(2) Single Flame (S = 0.37).

P.(3) Two Flames (S = 0.37), (a = 0.77 D_E).

P.(4) Three Flames (S = 0.37), (a = 0.77 D_E).

P-2

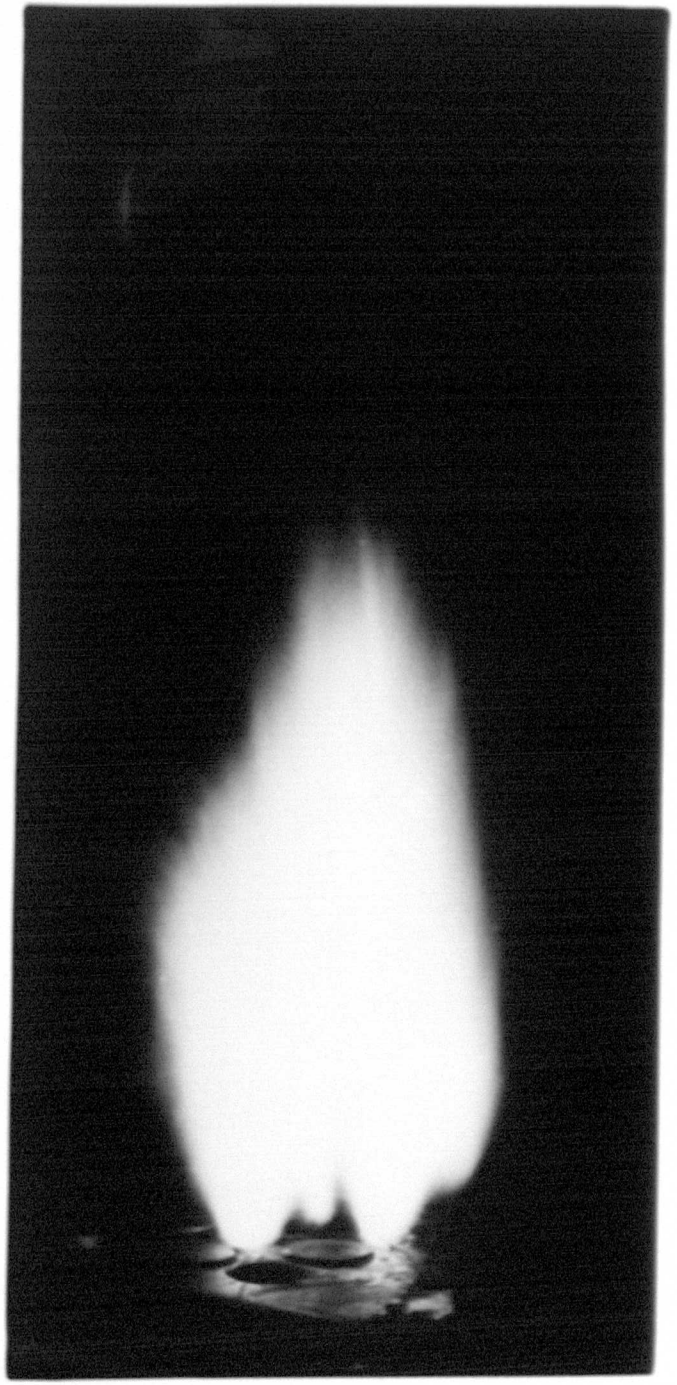

P-3

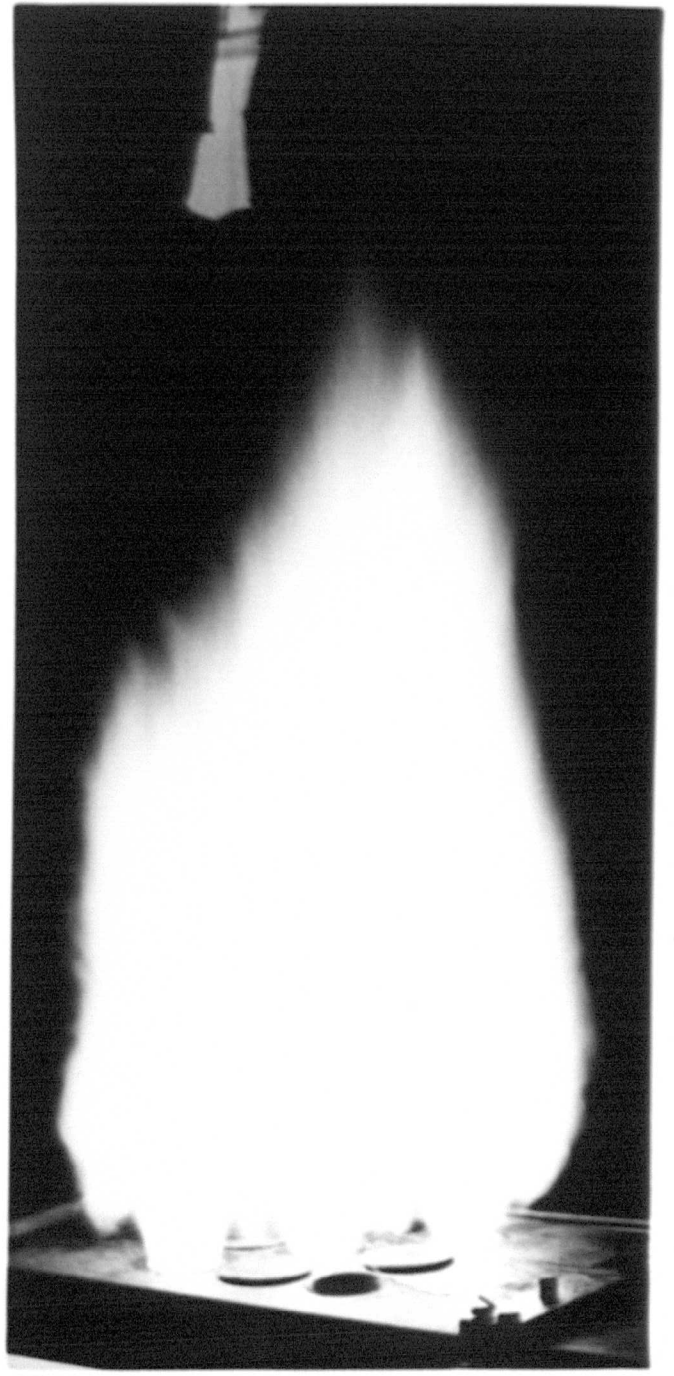

P-4

P.(5) Five flames ($S = 0.37$), ($a_1 = 0.77\ D_E$, $a_2 = 1.50\ D_E$).

P.(6) Two flames ($S = 0.37$), ($a = 0.25\ D_E$).

P.(7) Three flames ($S = 0.37$), ($a = 0.25\ D_E$).

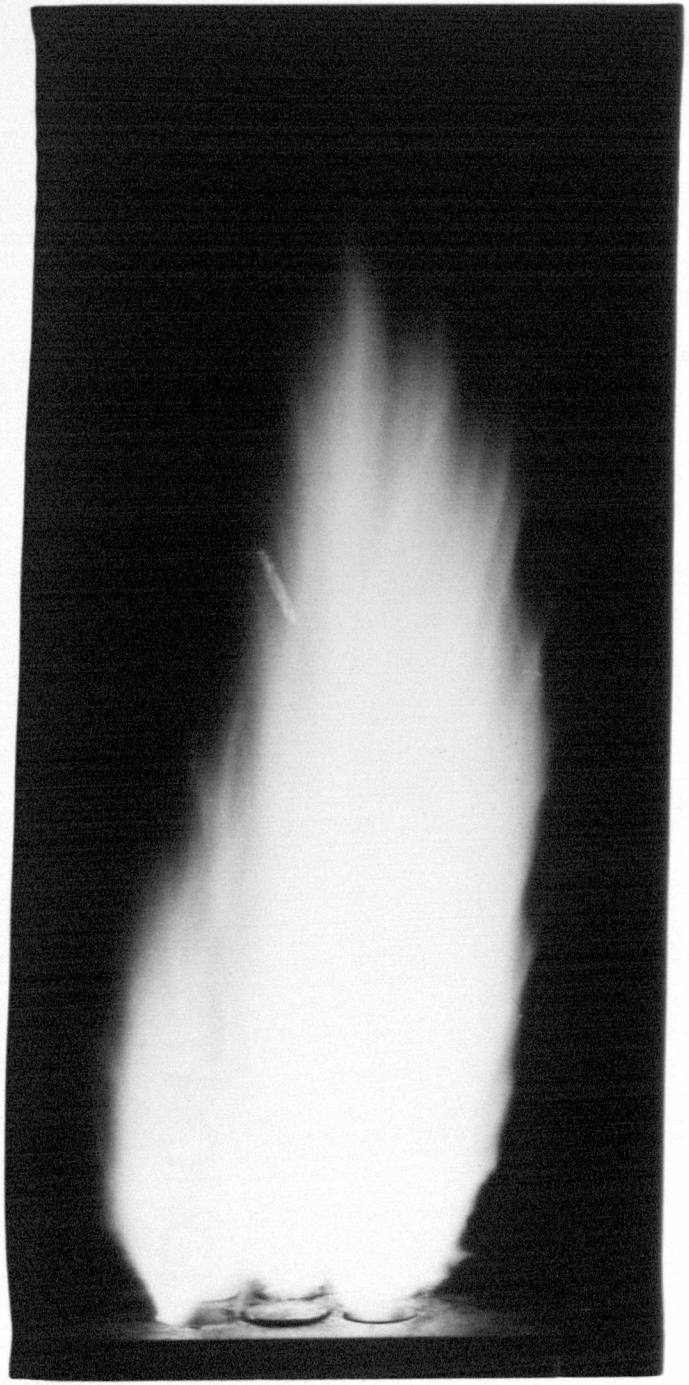

P-5

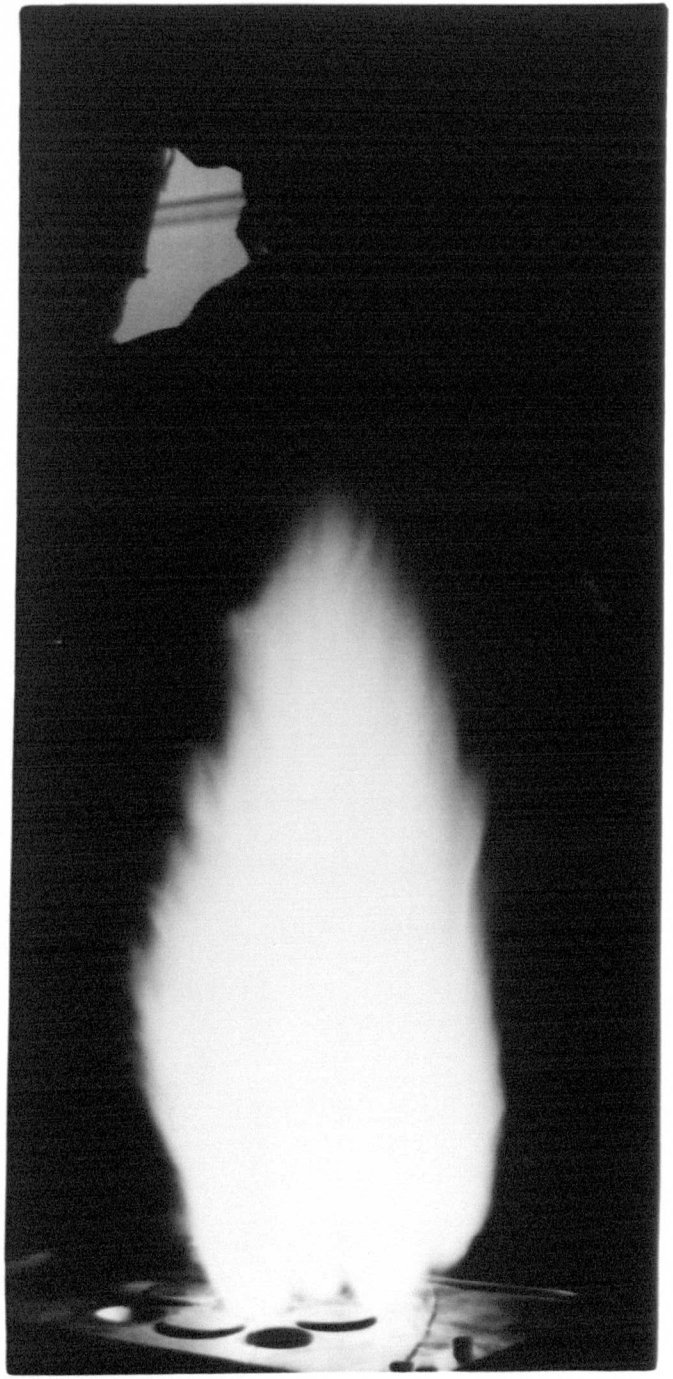

P-6

P-7

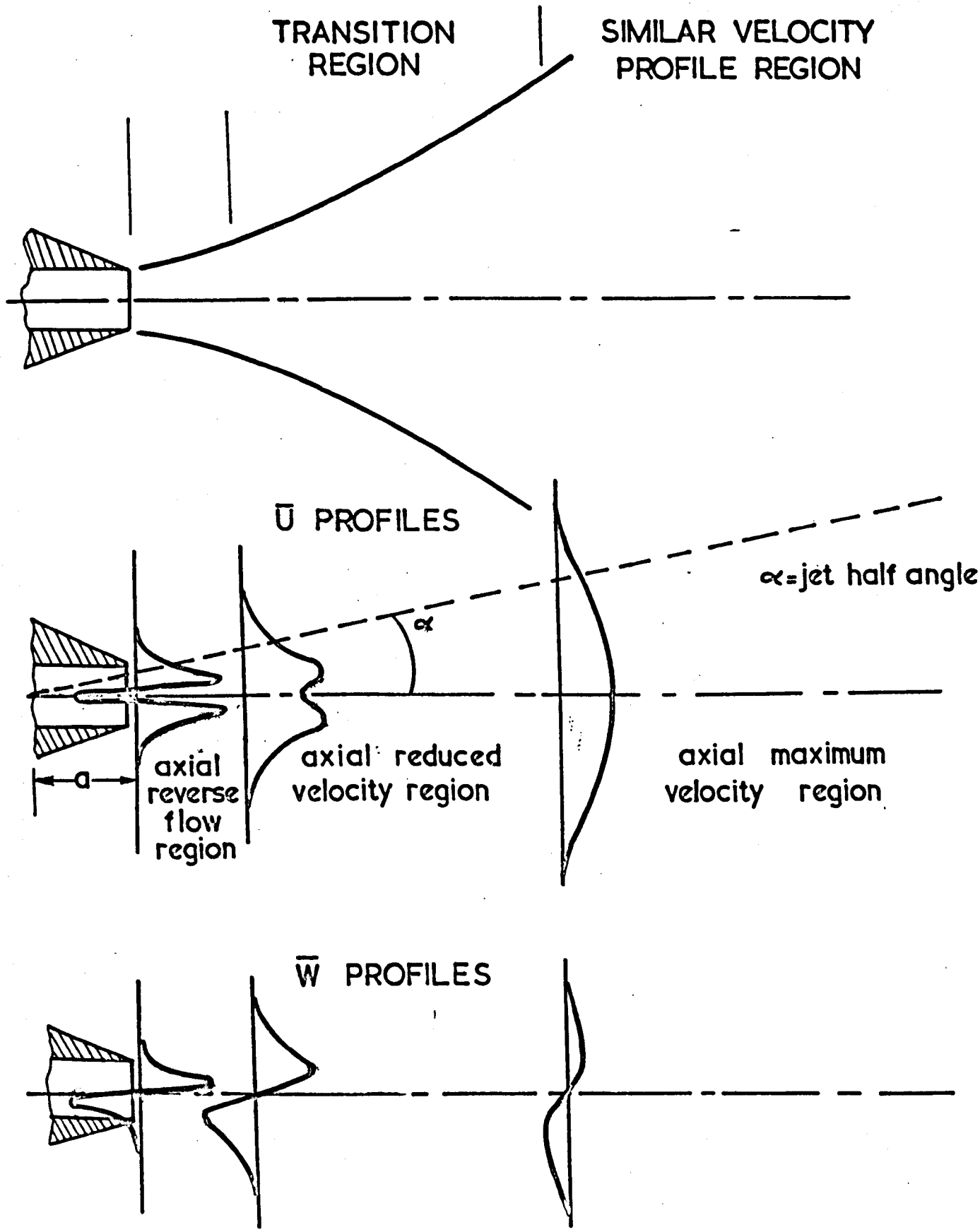

FIG. 1 REGIONS OF A STRONGLY SWIRLING JET.

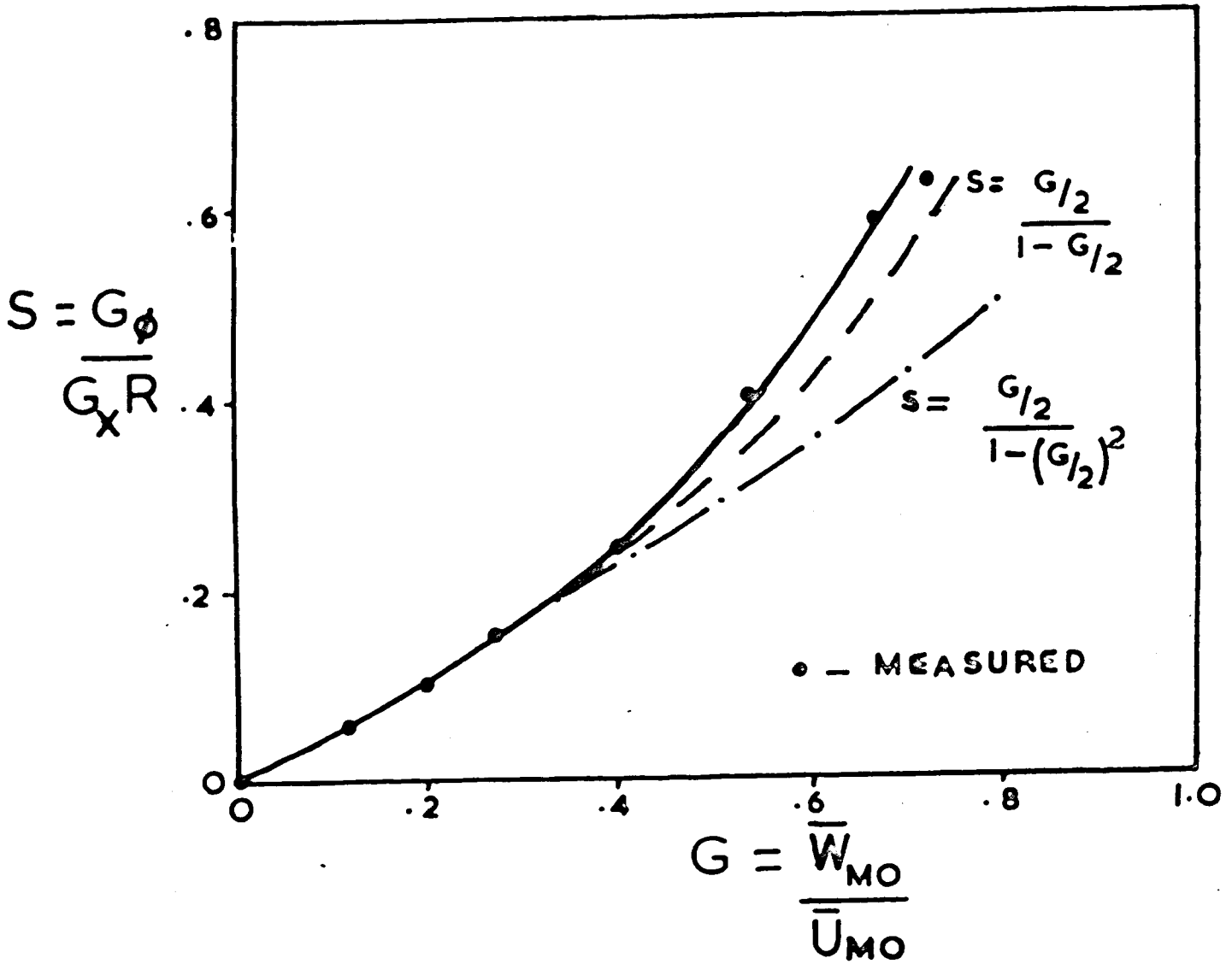

Fig. 2 Swirl parameters (Chigier & Chervinsky)

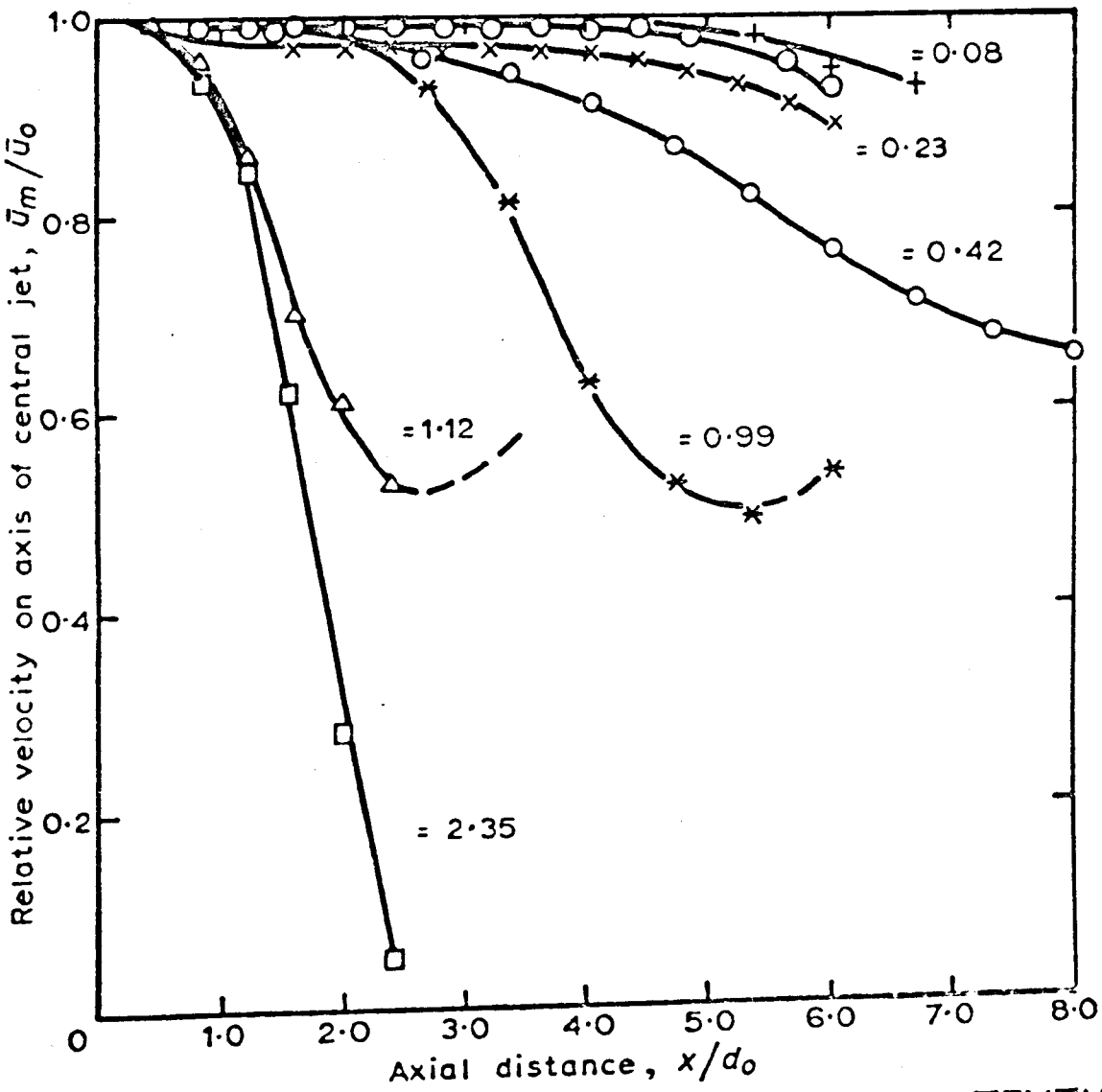

FIG.3 INFLUENCE OF THE ANNULAR JET ON THE POTENTIAL CORE AND DECAY OF THE CENTRAL JET. (From Chigier & Béer)

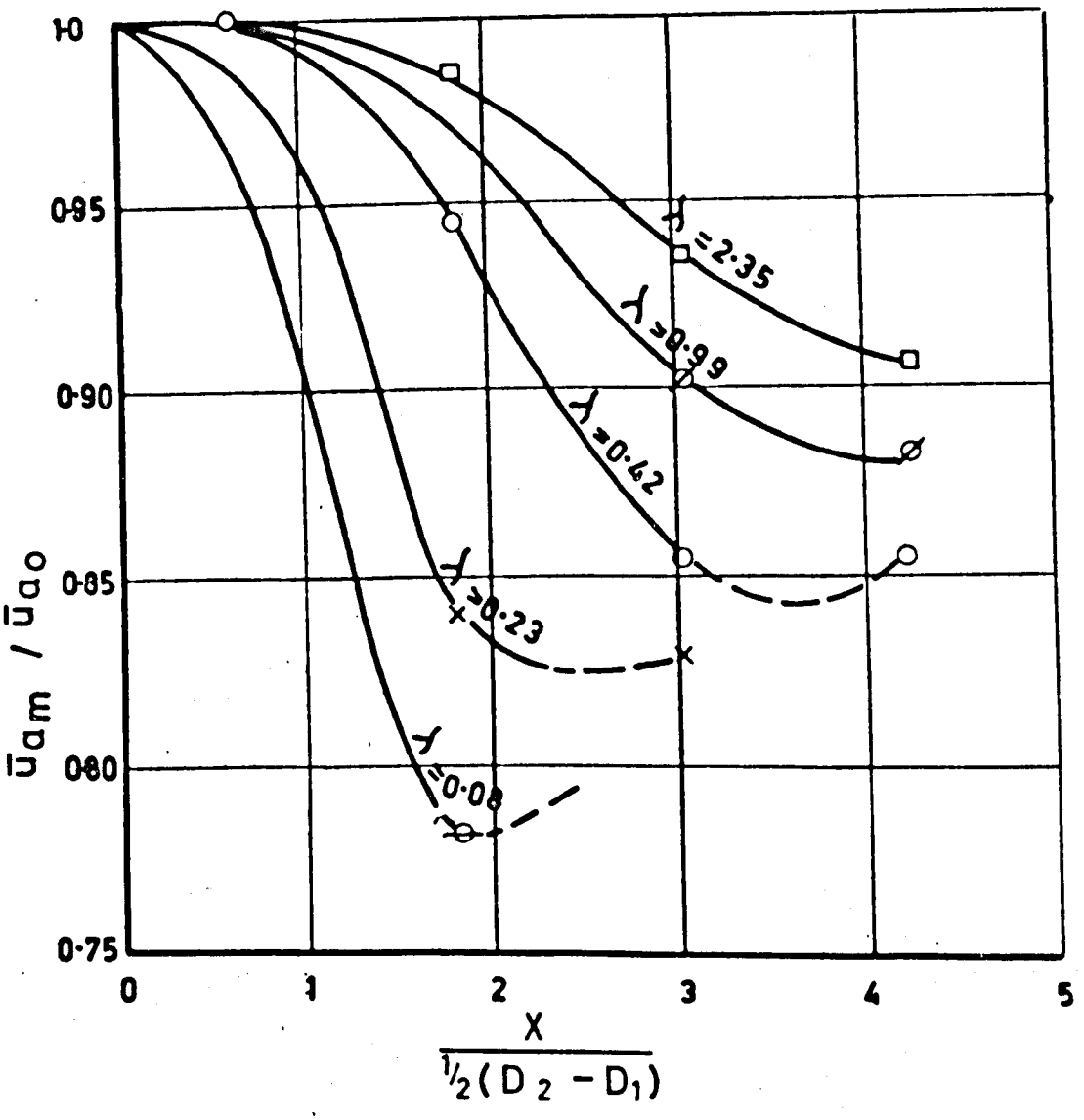

FIG. 4 INFLUENCE OF CENTRAL JET ON POTENTIAL CORE AND DECAY OF ANNULAR JET. (From Chigier & Béer)

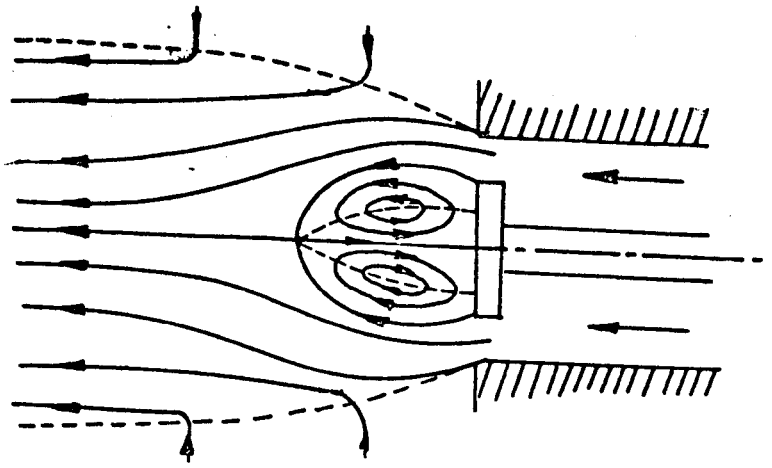

FIG. 5 Internal recirculation in the wake flow behind a bluff body.

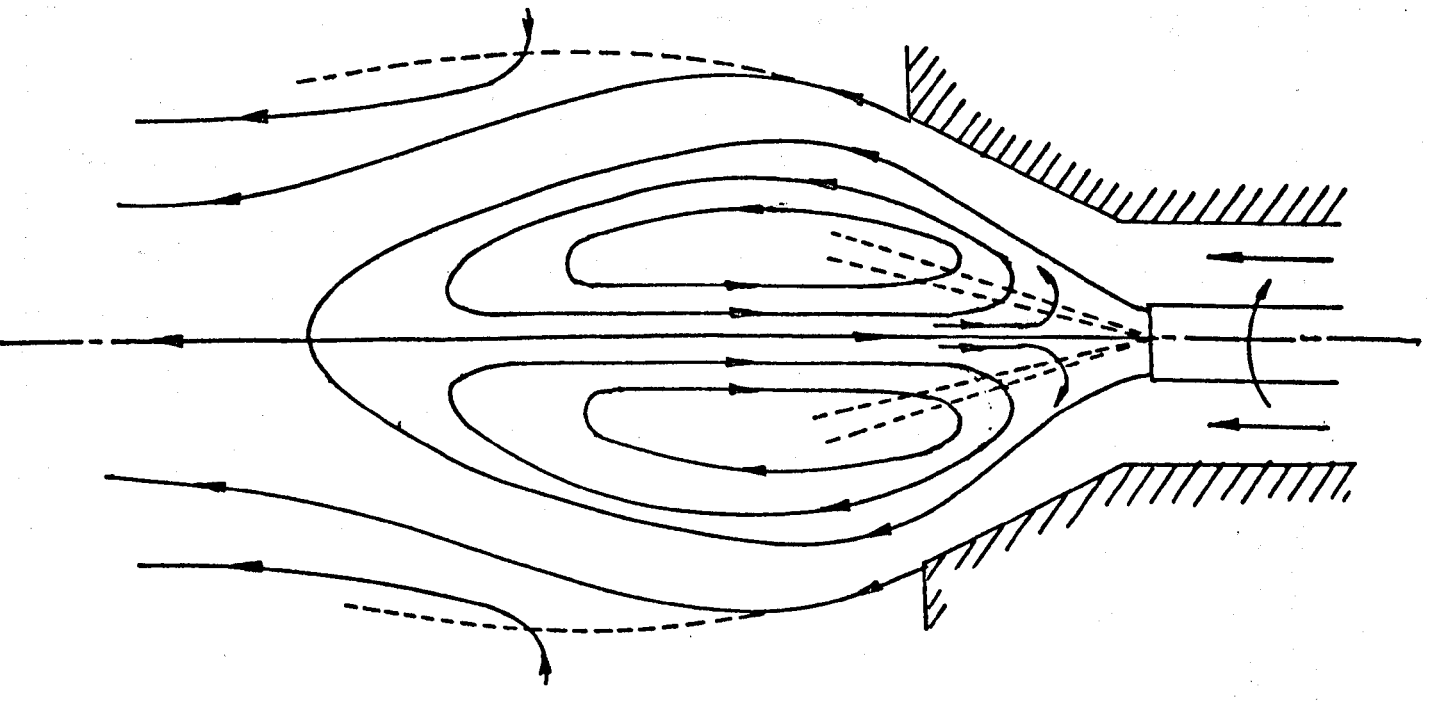

FIG. 6 Annular swirling flame jet with internal recirculation.

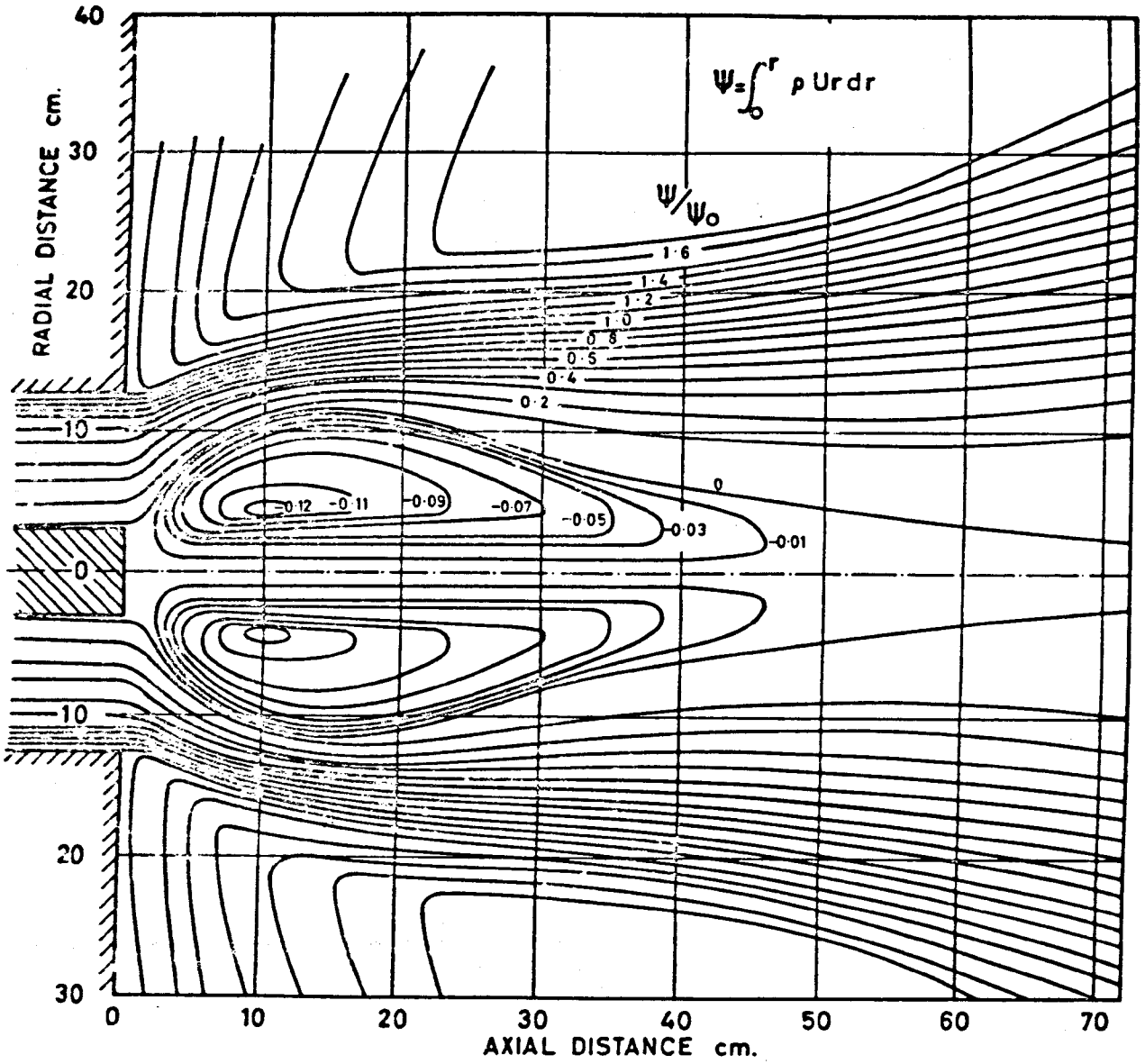

FIG.7 STREAMLINES OF FLOW IN THE VORTEX REGION OF A STRONGLY SWIRLING JET. (From Chigier and Béer)

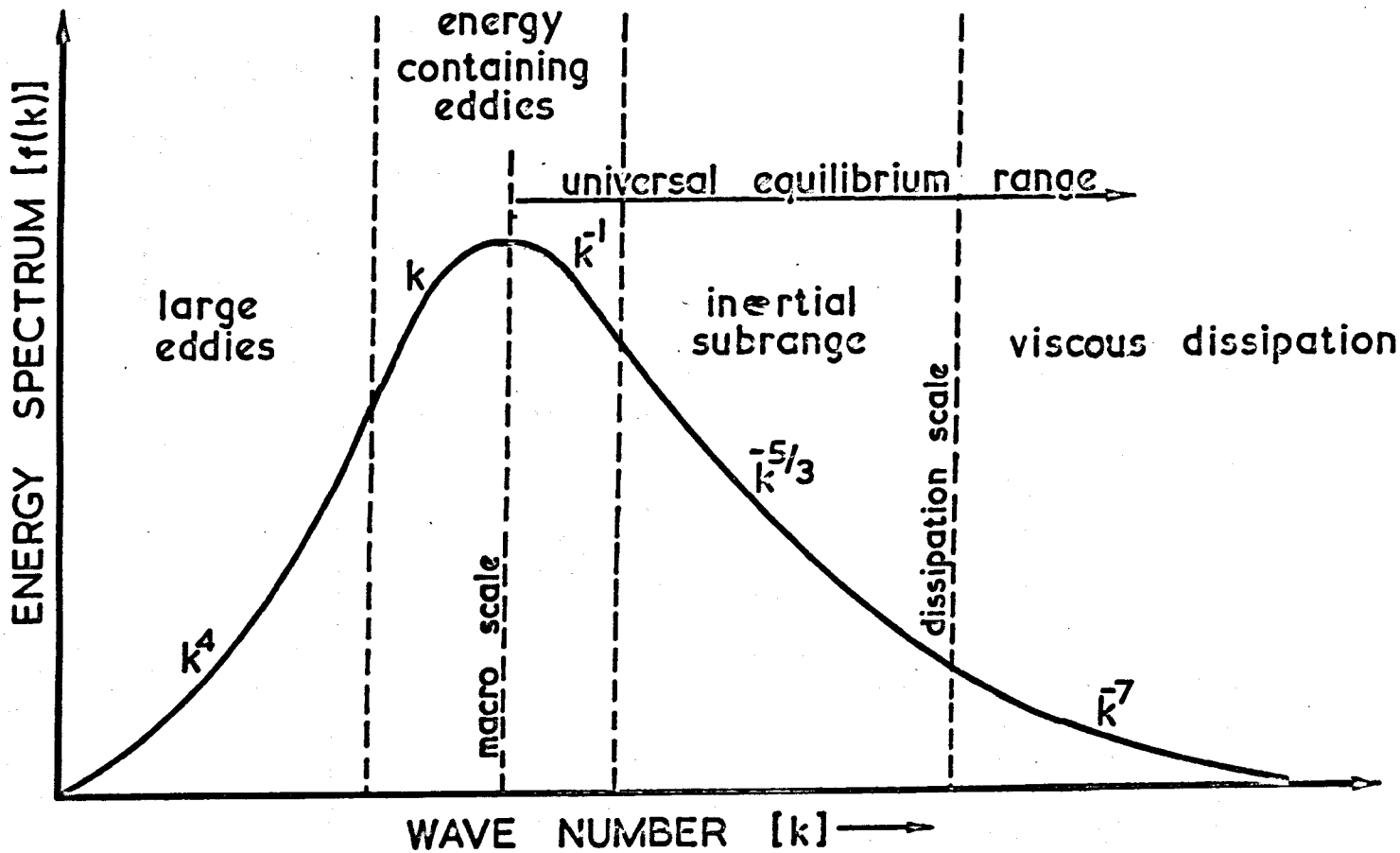

FIG. 8 THEORETICAL ENERGY SPECTRUM.
(Kim & Manning, Ref. 78)

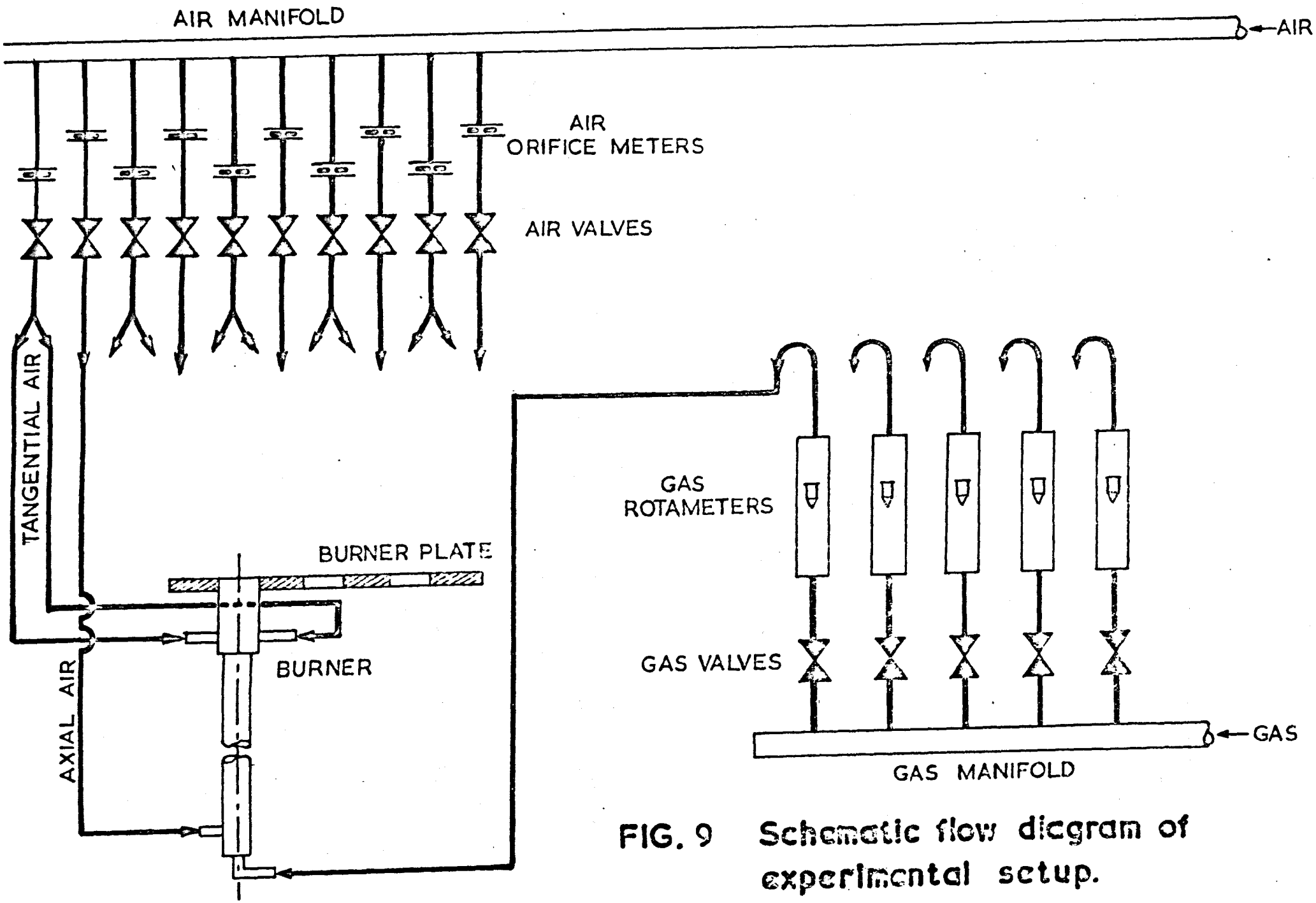

FIG. 9 Schematic flow dicgram of experimental setup.

FIG. 10

DOUBLE CONCENTRIC EXPERIMENTAL BURNER.

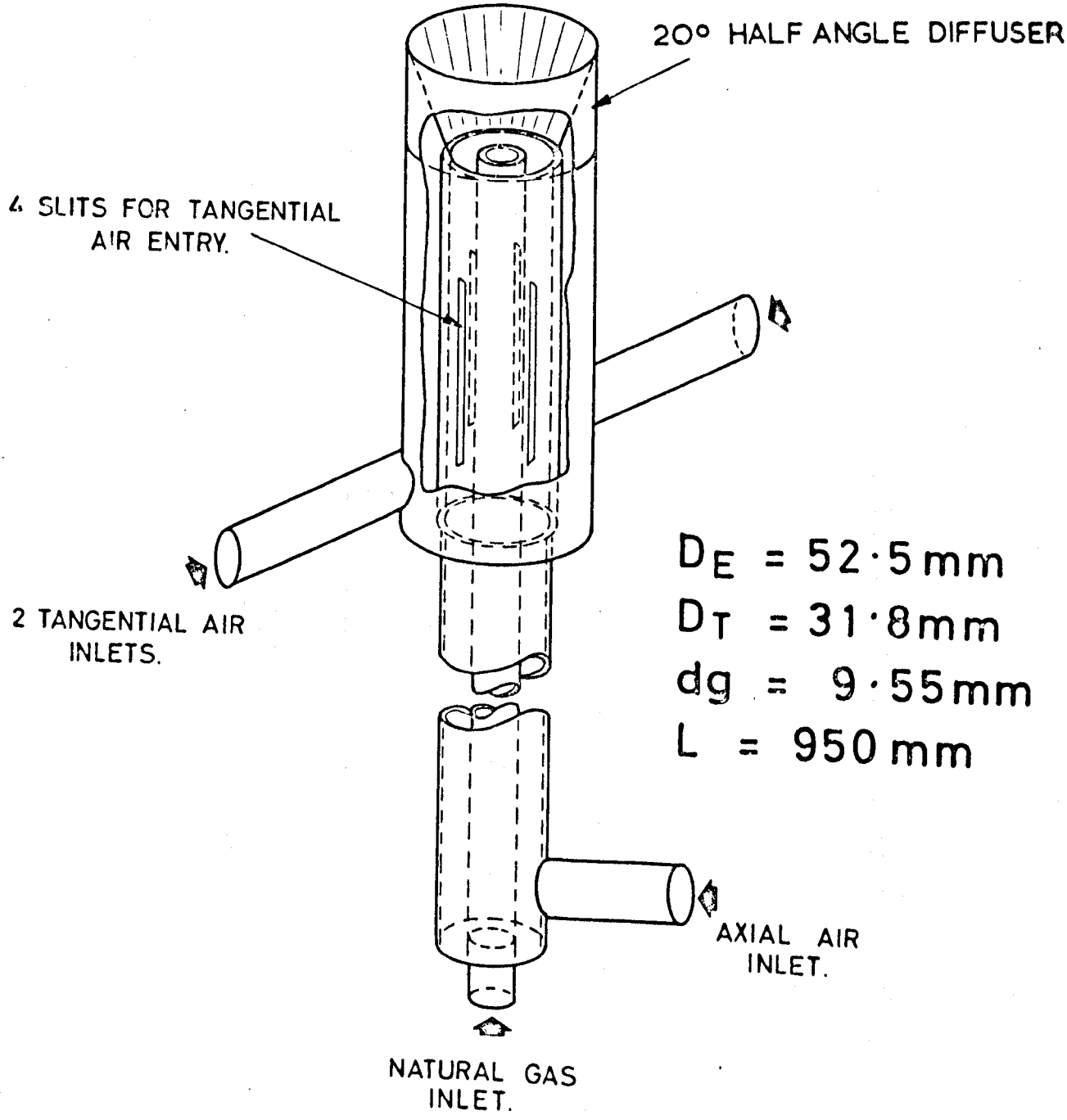

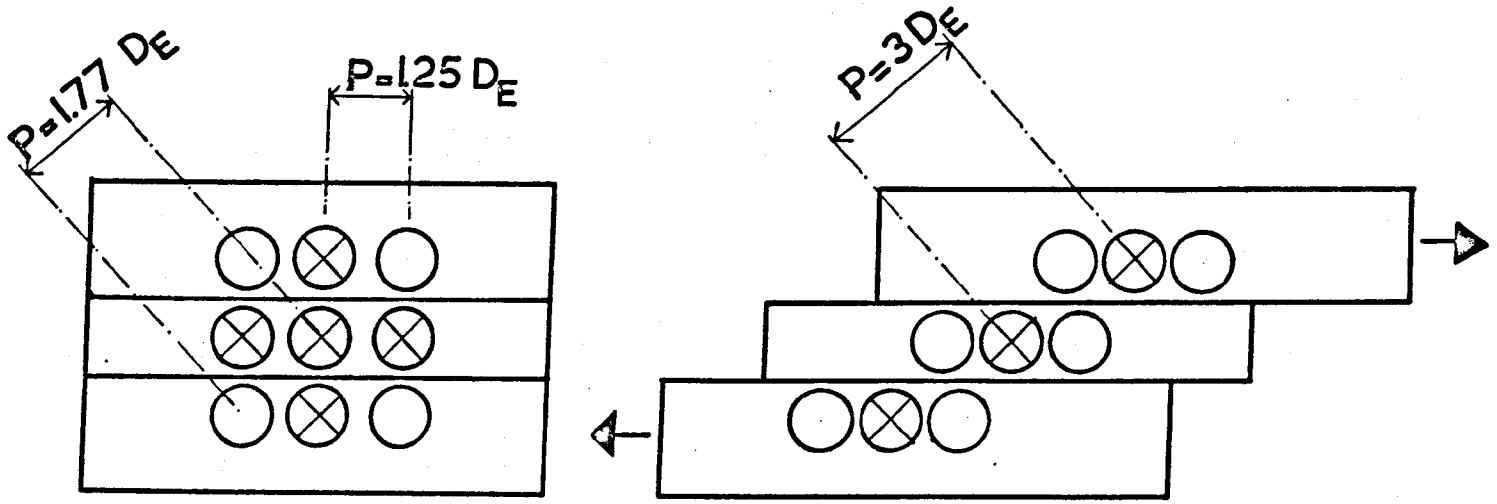

FIG.11 :Movable burner plate and alternate burner positions

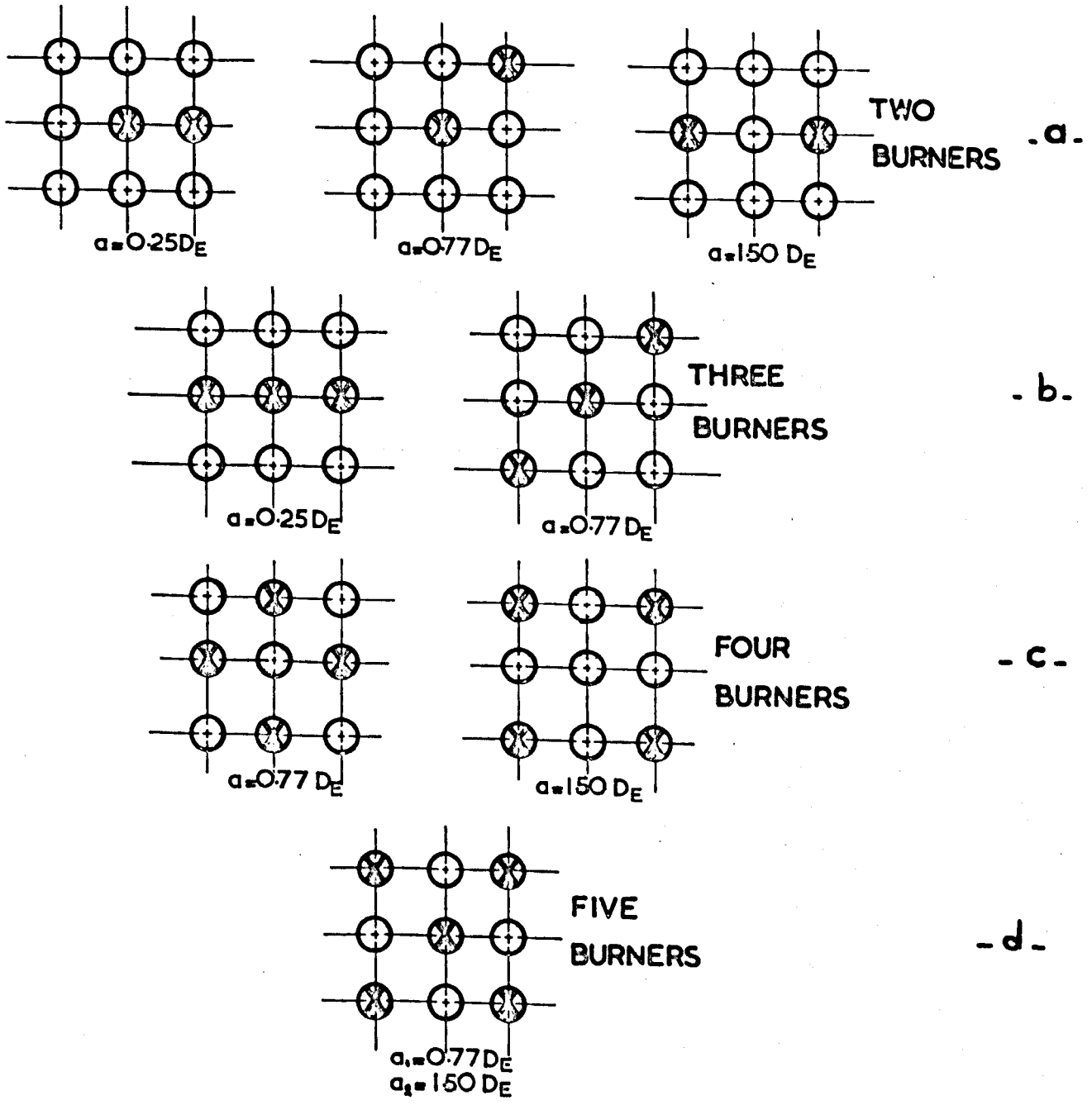

FIG.12 BURNER ARRENGMENTS EMPLOYED.

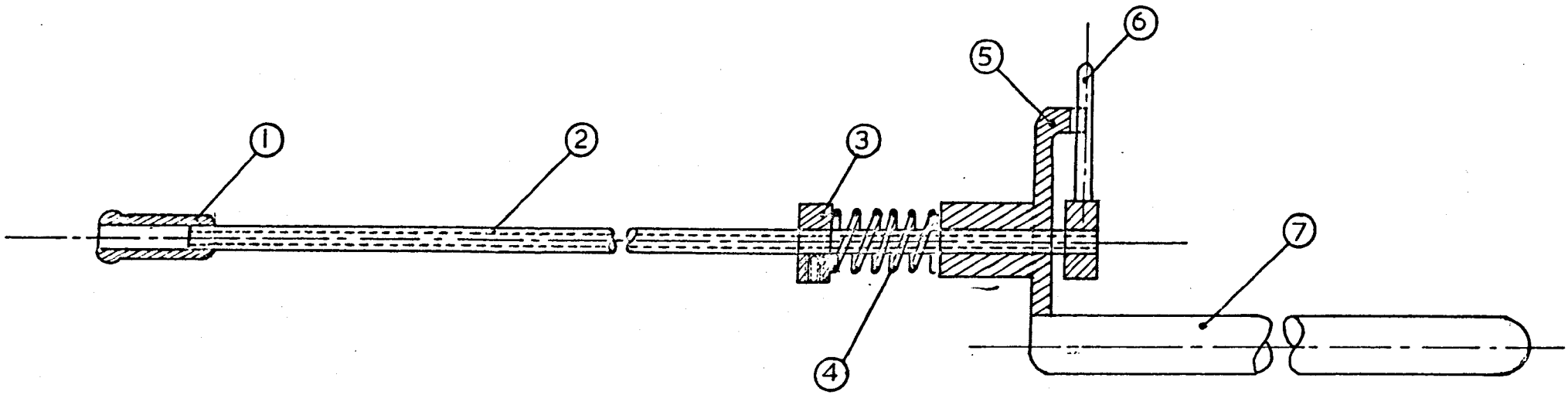

FIG. 13 PROBE SUPPORT HOLDER.

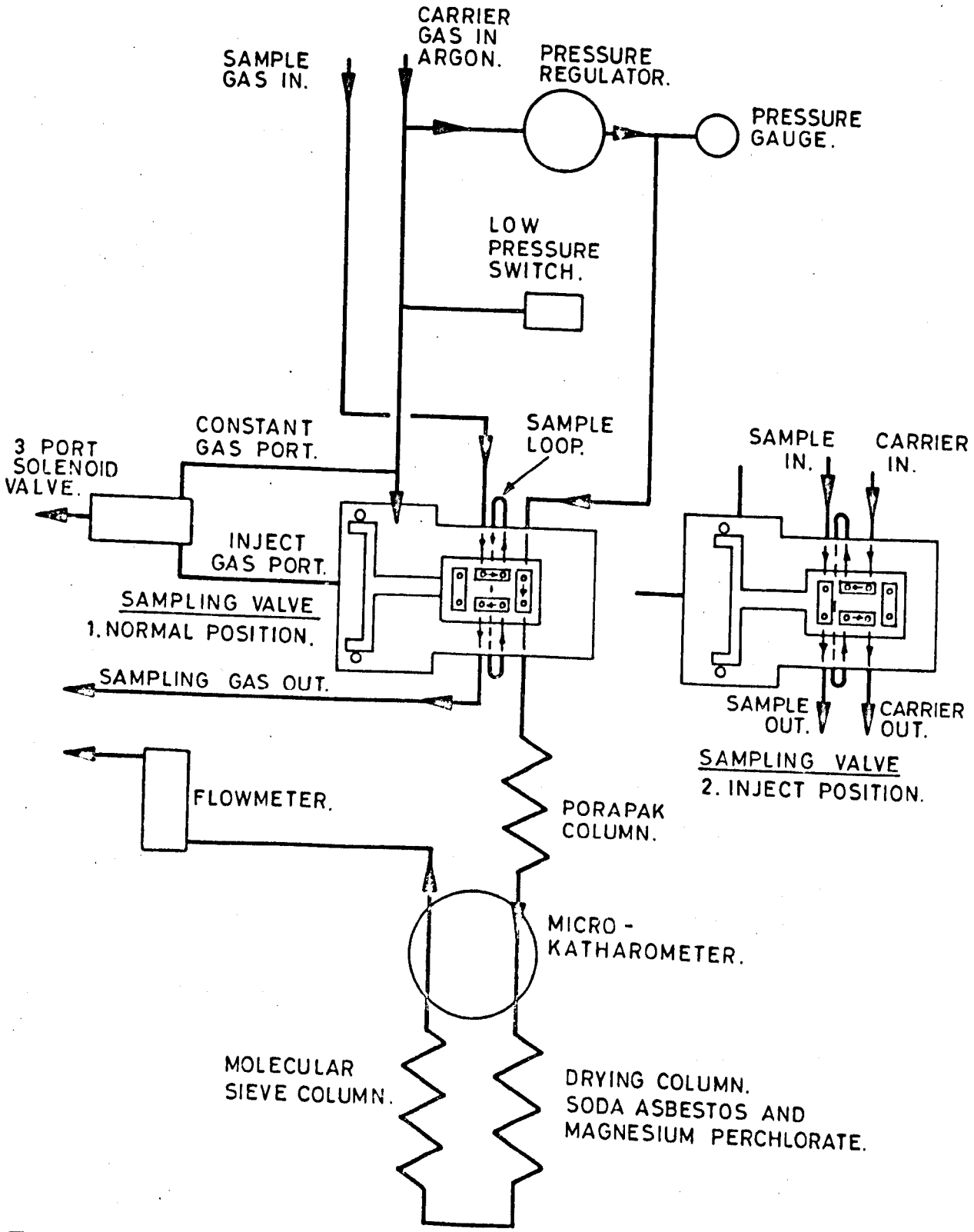

FIG. 14 SHEMATIC DIAGRAM OF THE FLOW THROUGH THE GAS CHROMATOGRAPH.

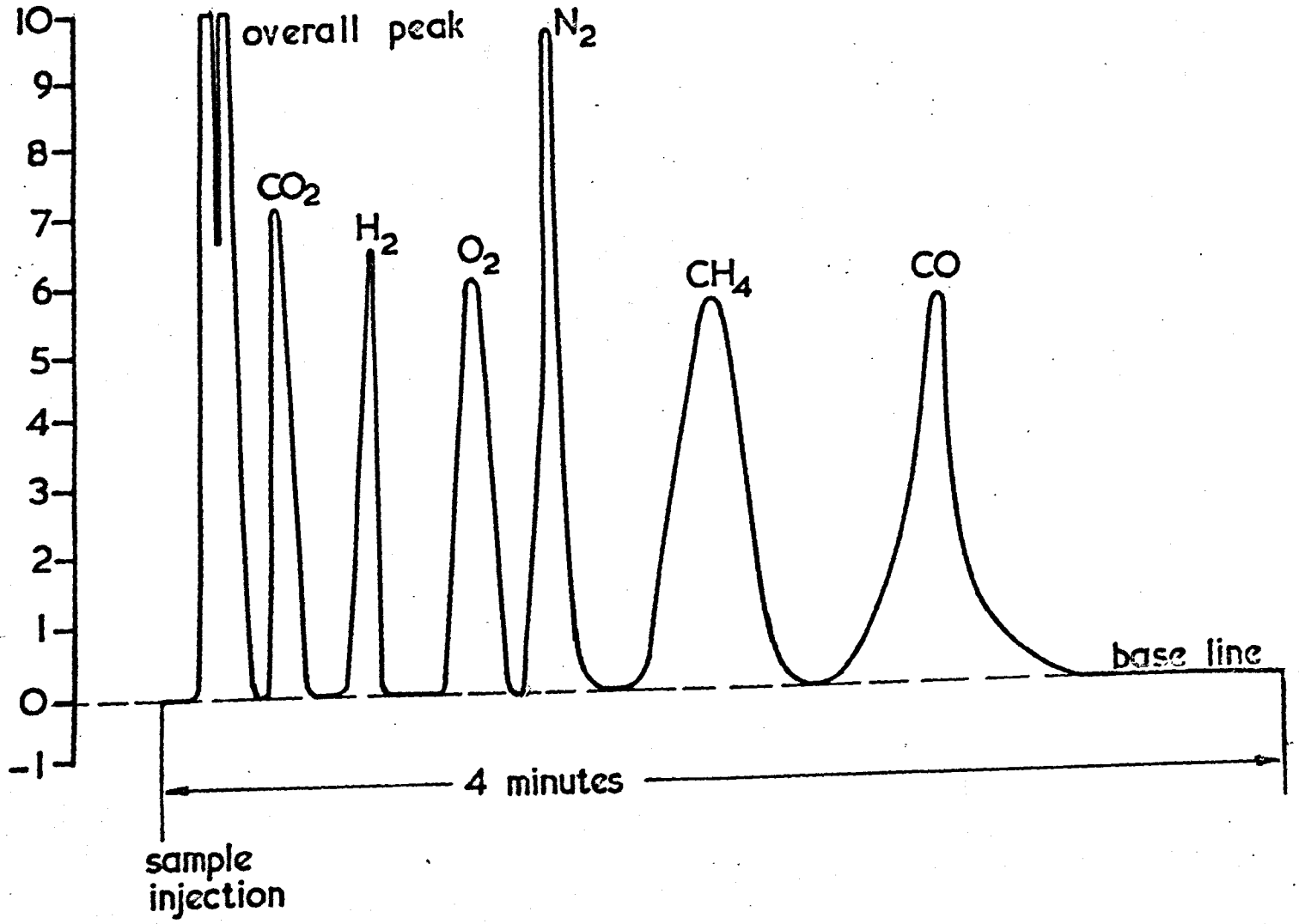

FIG. 15-a A TYPICAL CHROMATOGRAM OF A FLAME SAMPLE.

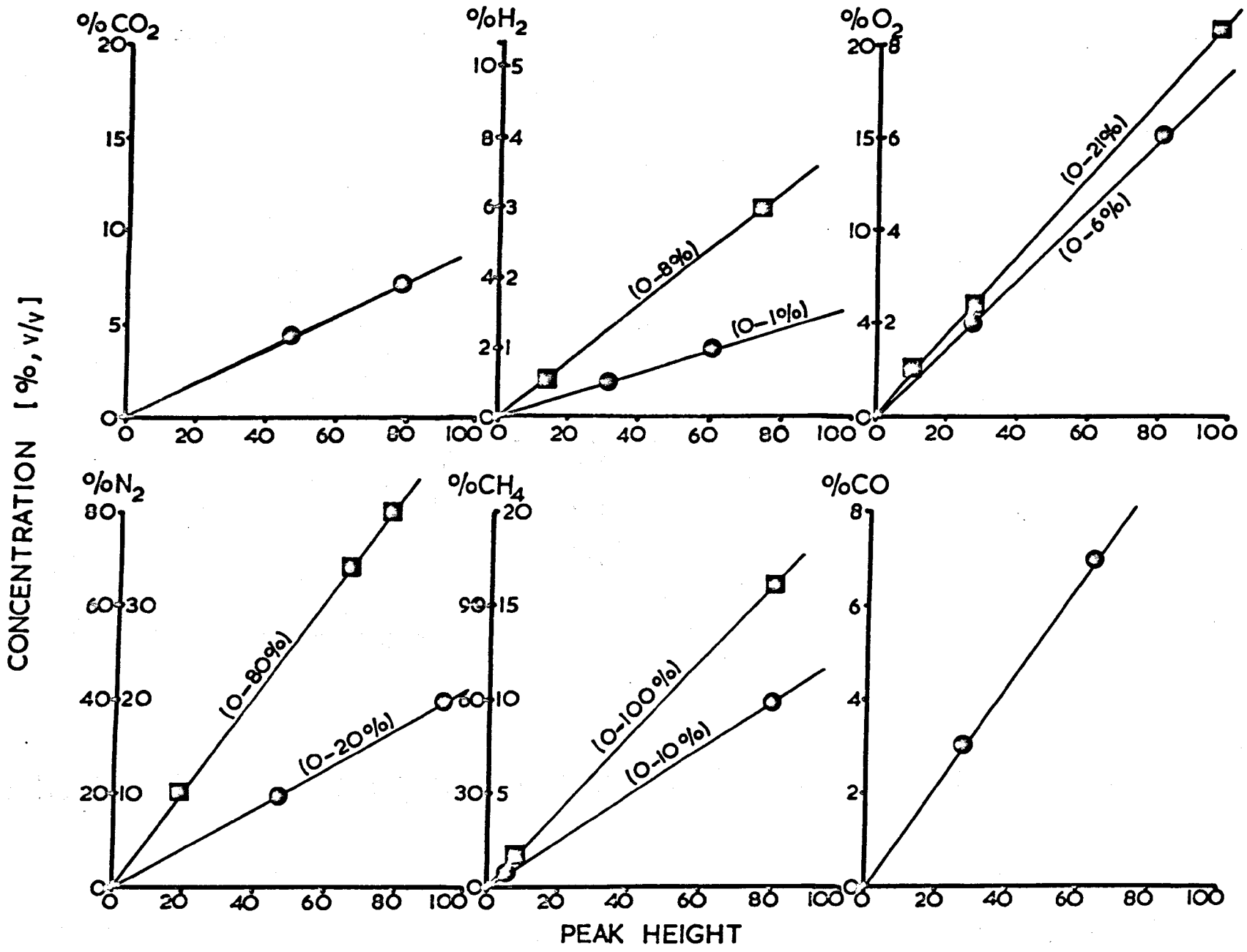

FIG. 15-b TYPICAL CALIBRATION DATA FROM STANDARD GAS SAMPLE.

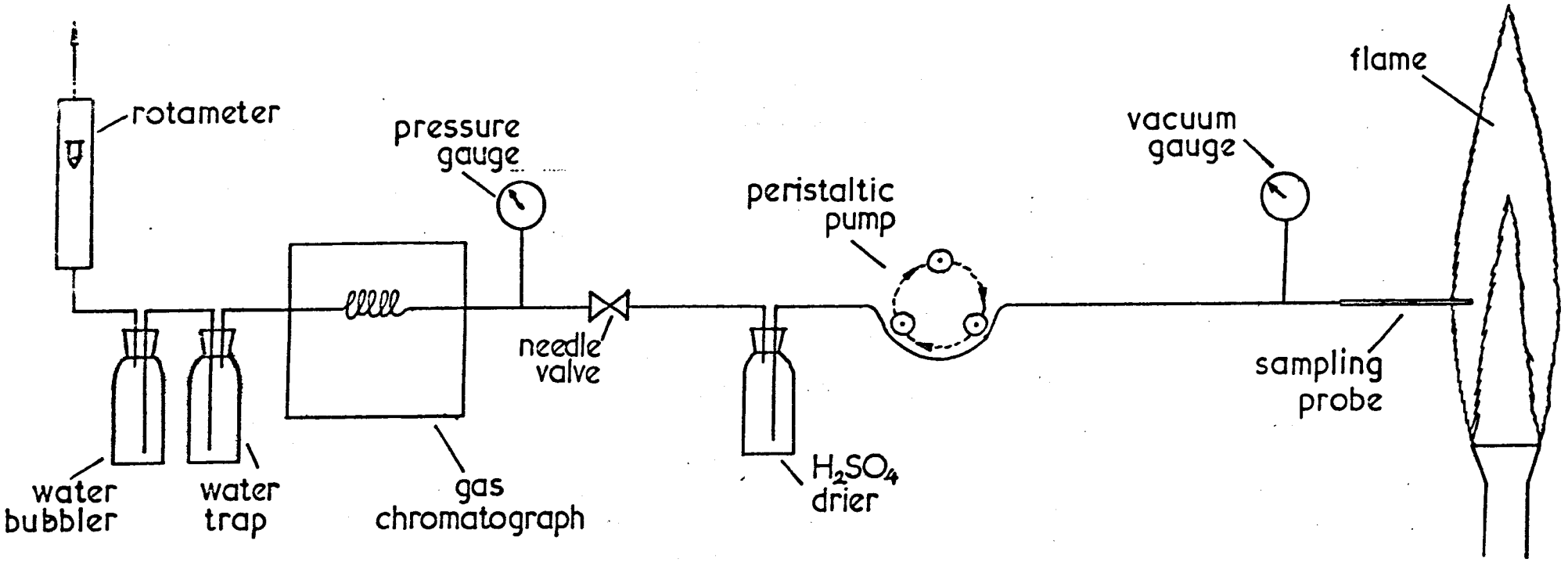

FIG. 16 Schematic representation of the gas sampling system.

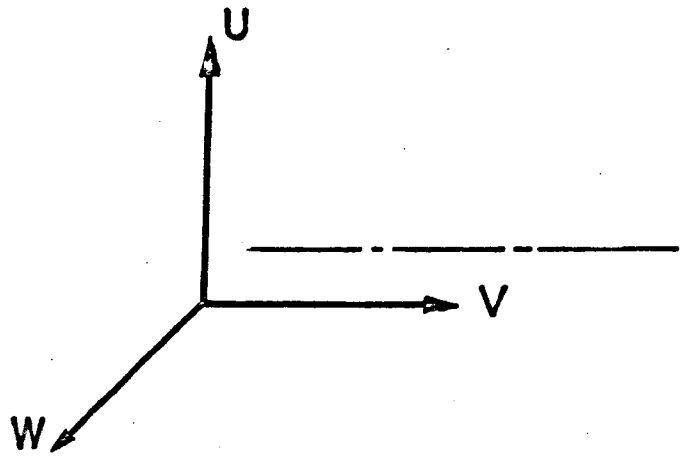

THE COORDINATE SYSTEM, THE RROBE BEING PARALLEL TO V AXIS.

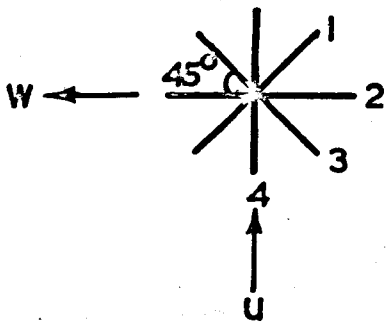

PROBE MEASURING POSITIONS.

FIG.17-a THE FOUR POINT MEASURING TECHNIQUE.

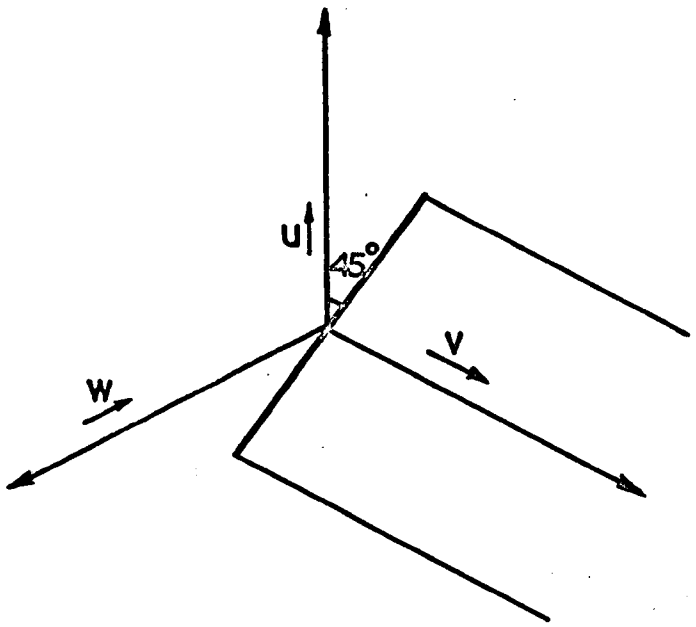

POSITION 1

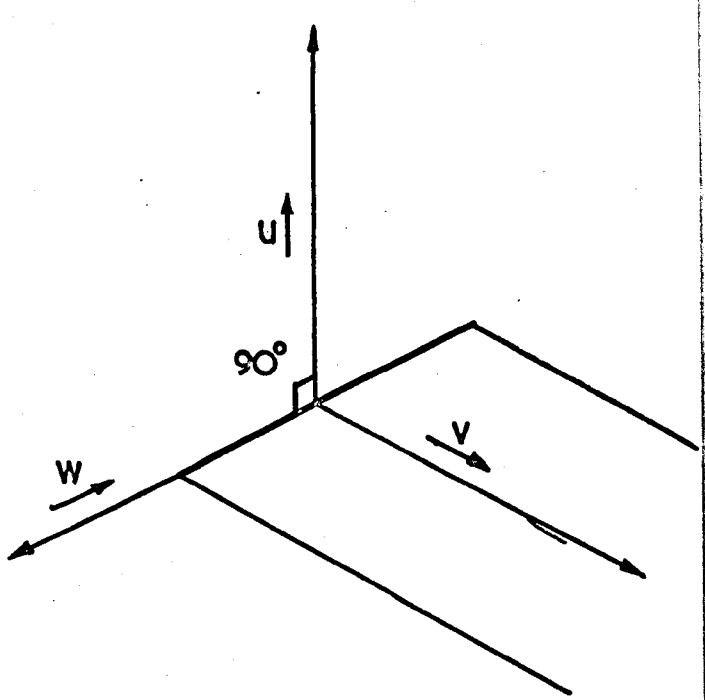

POSITION 2

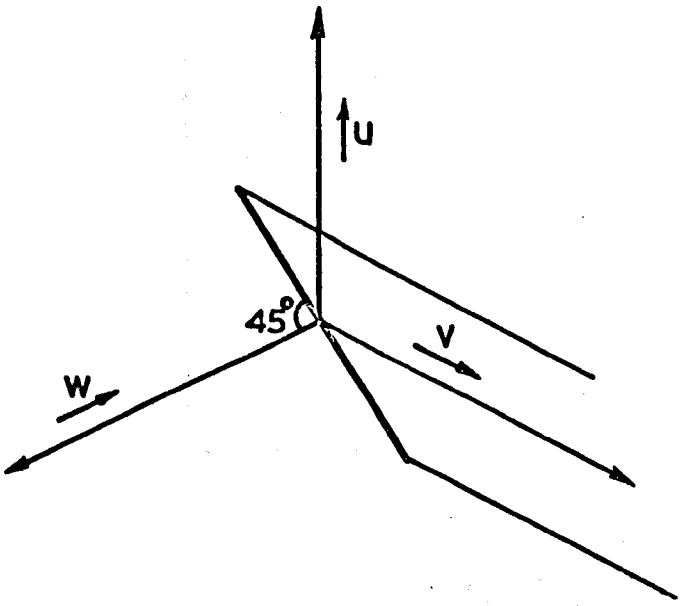

POSITION 3

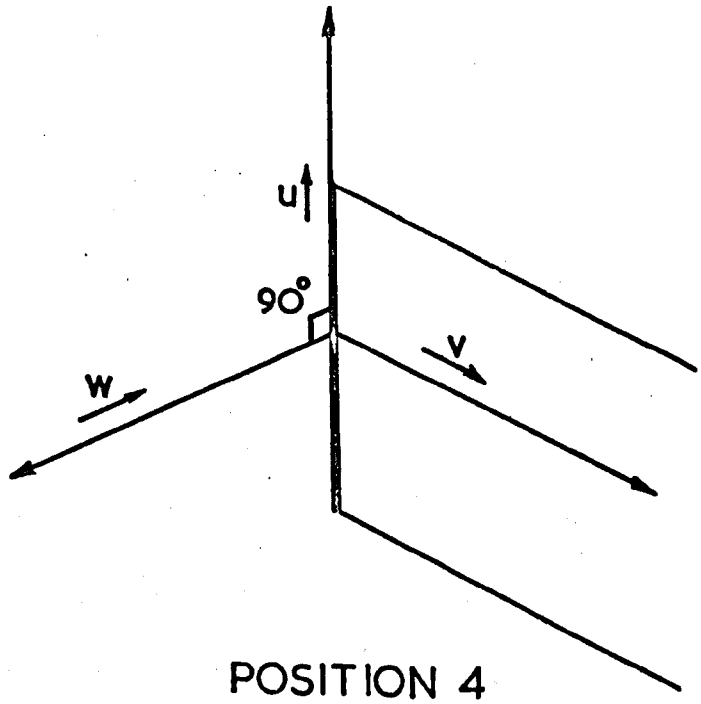

POSITION 4

FIG.17-b VELOCITY VECTORS ACTING ON VARIOUS PROBE POSITIONS.

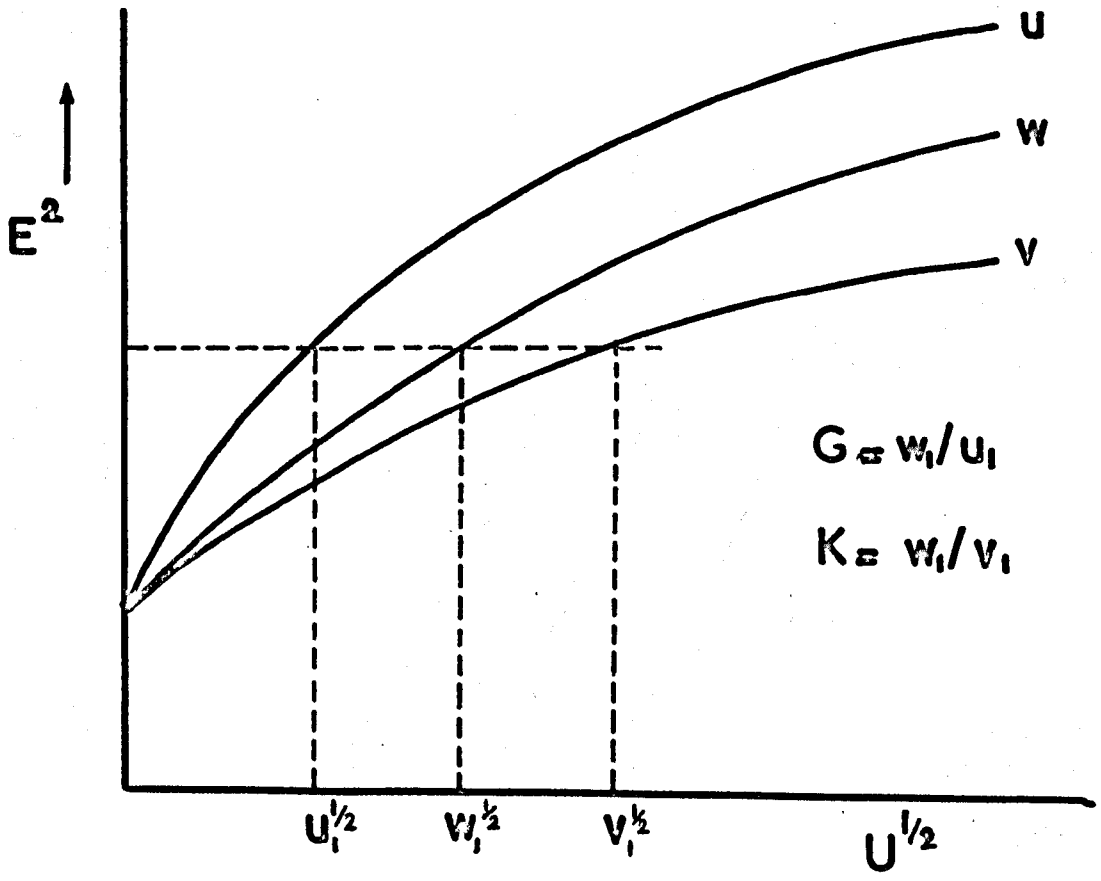

FIG.17-c CALIBRATION CURVES FOR THE THREE DIFFERENT DIRECTIONS.

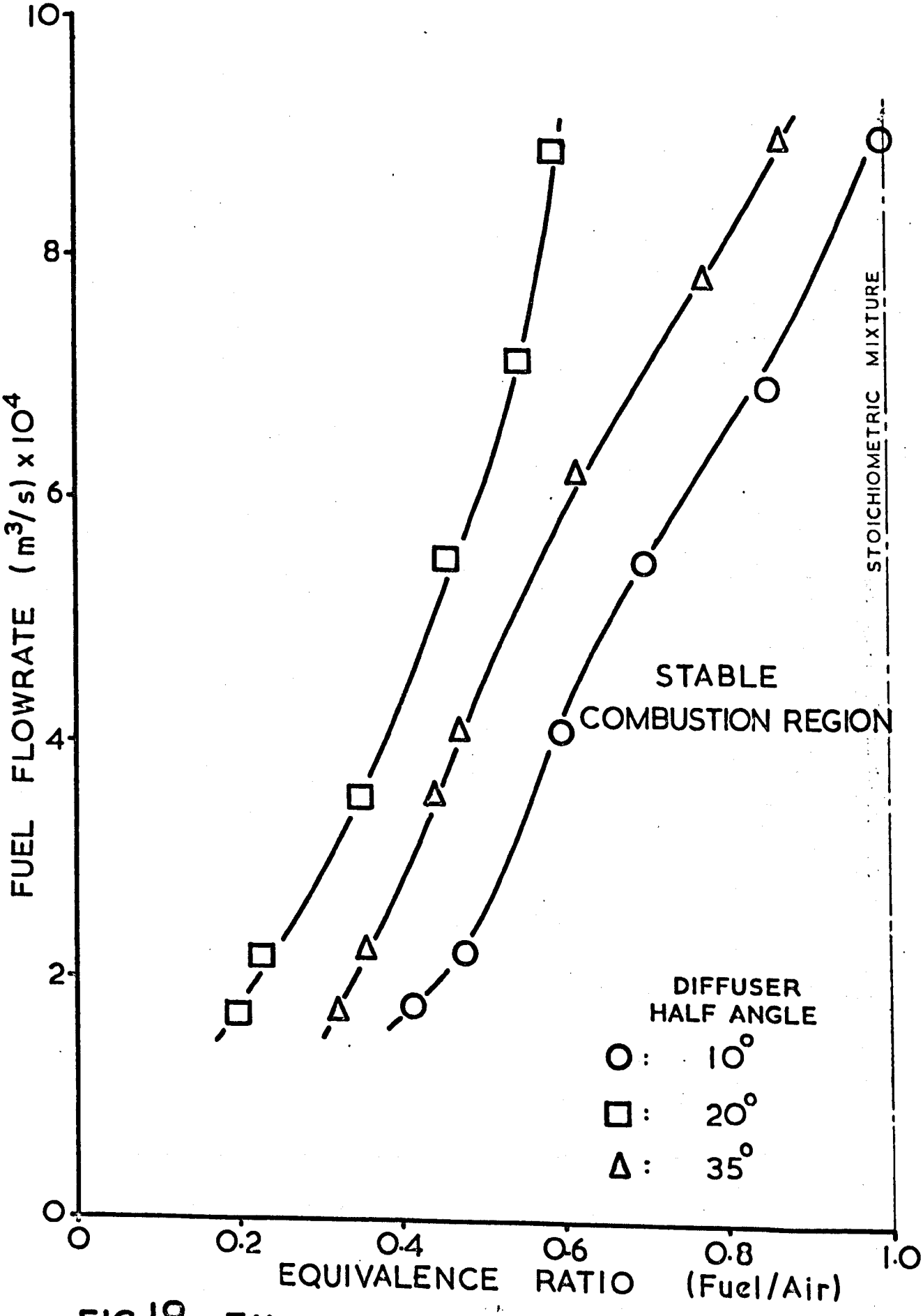

FIG.18: Effect of diffuser half angle on blow-off for a single swirling flame. (S=0.57)

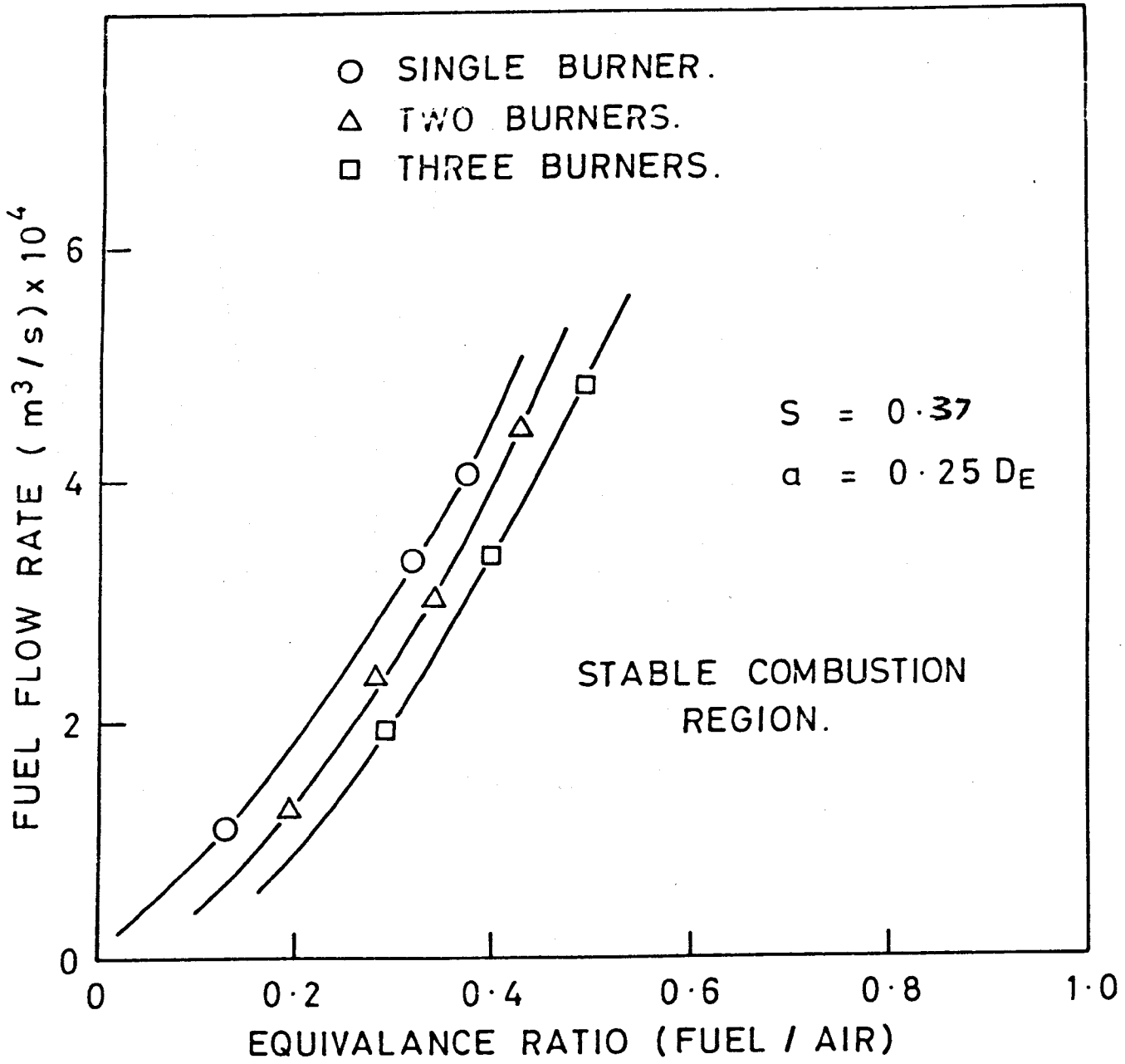

FIG. 19 COMPARISON OF BLOW OFF LIMITS.

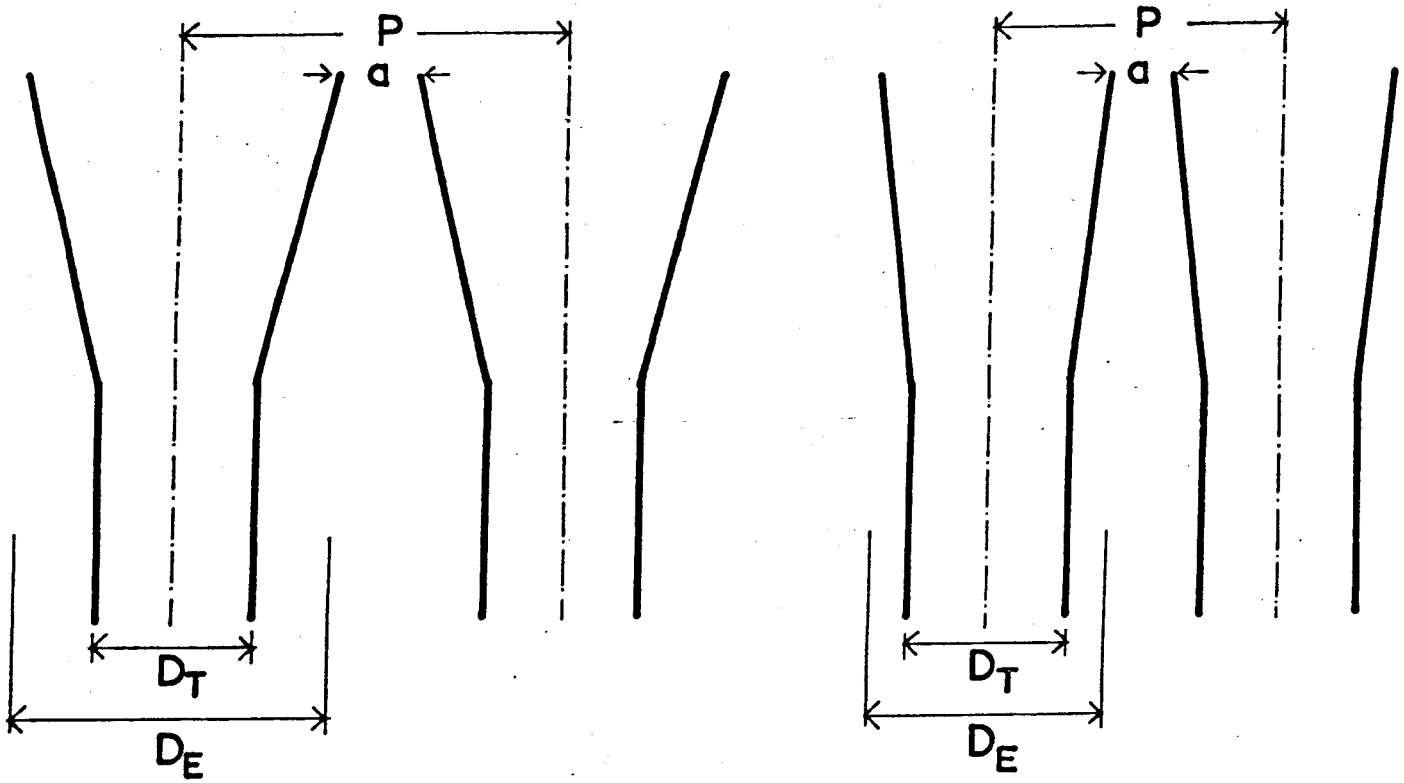

FIG. 20: Burners with different angle of diffuser exits.

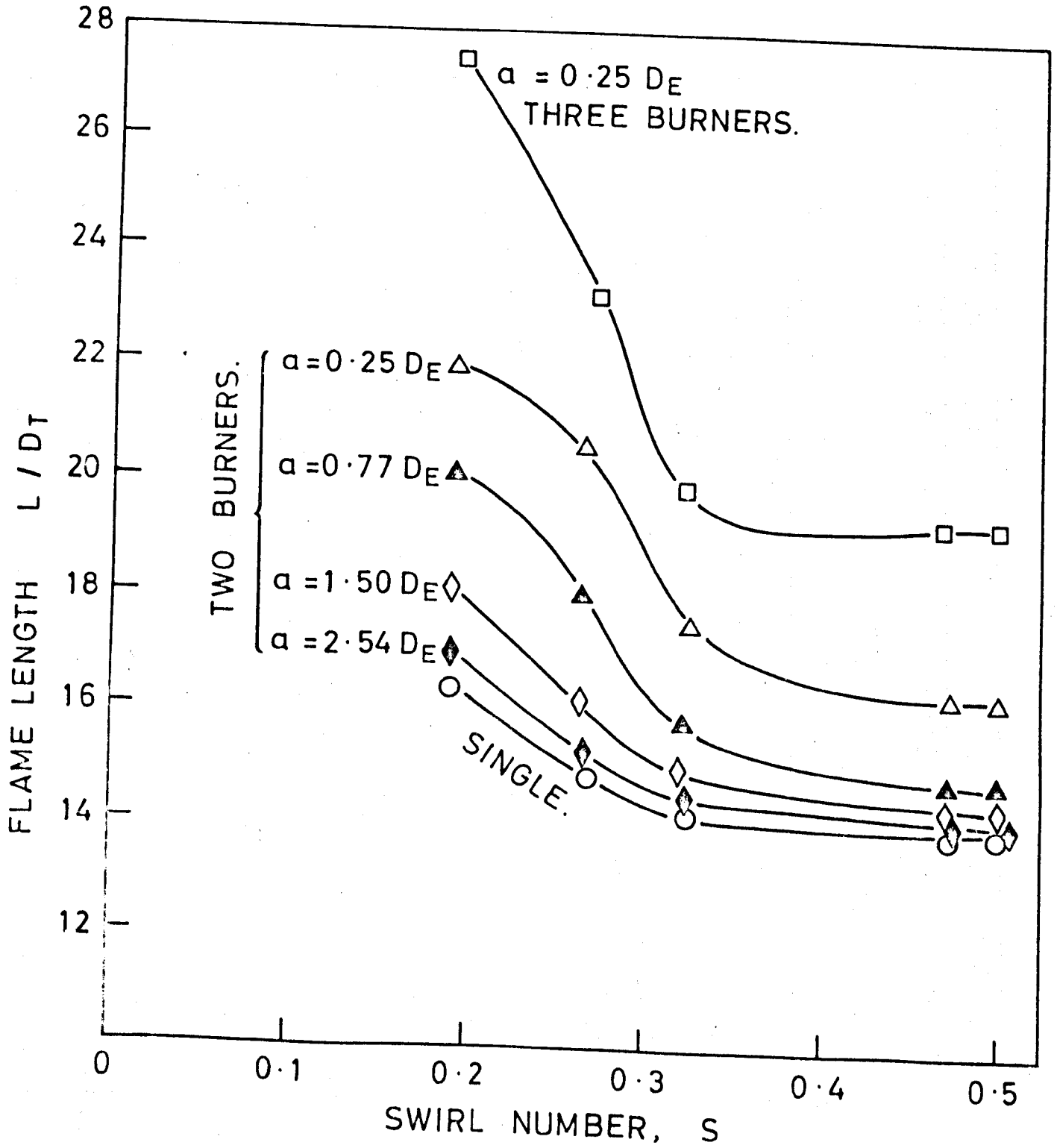

FIG 21 EFFECT OF BURNER SEPARATION AND NUMBER OF BURNERS ON FLAME LENGTH.

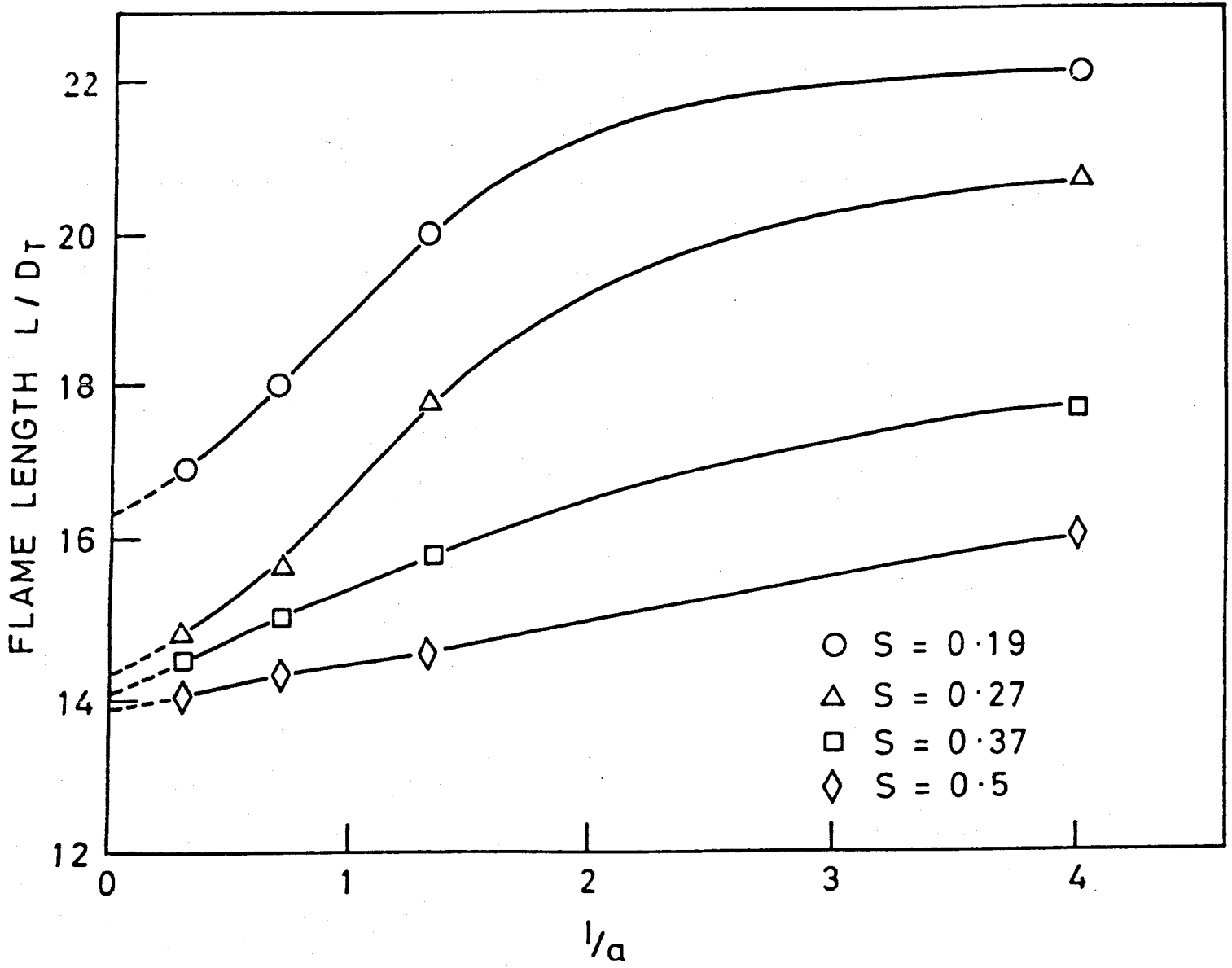

FIG. 22 CHANGE OF FLAME LENGTH WITH SEPARATION AT DIFFERENT SWIRL LEVELS FOR THE GROUP OF TWO BURNERS.

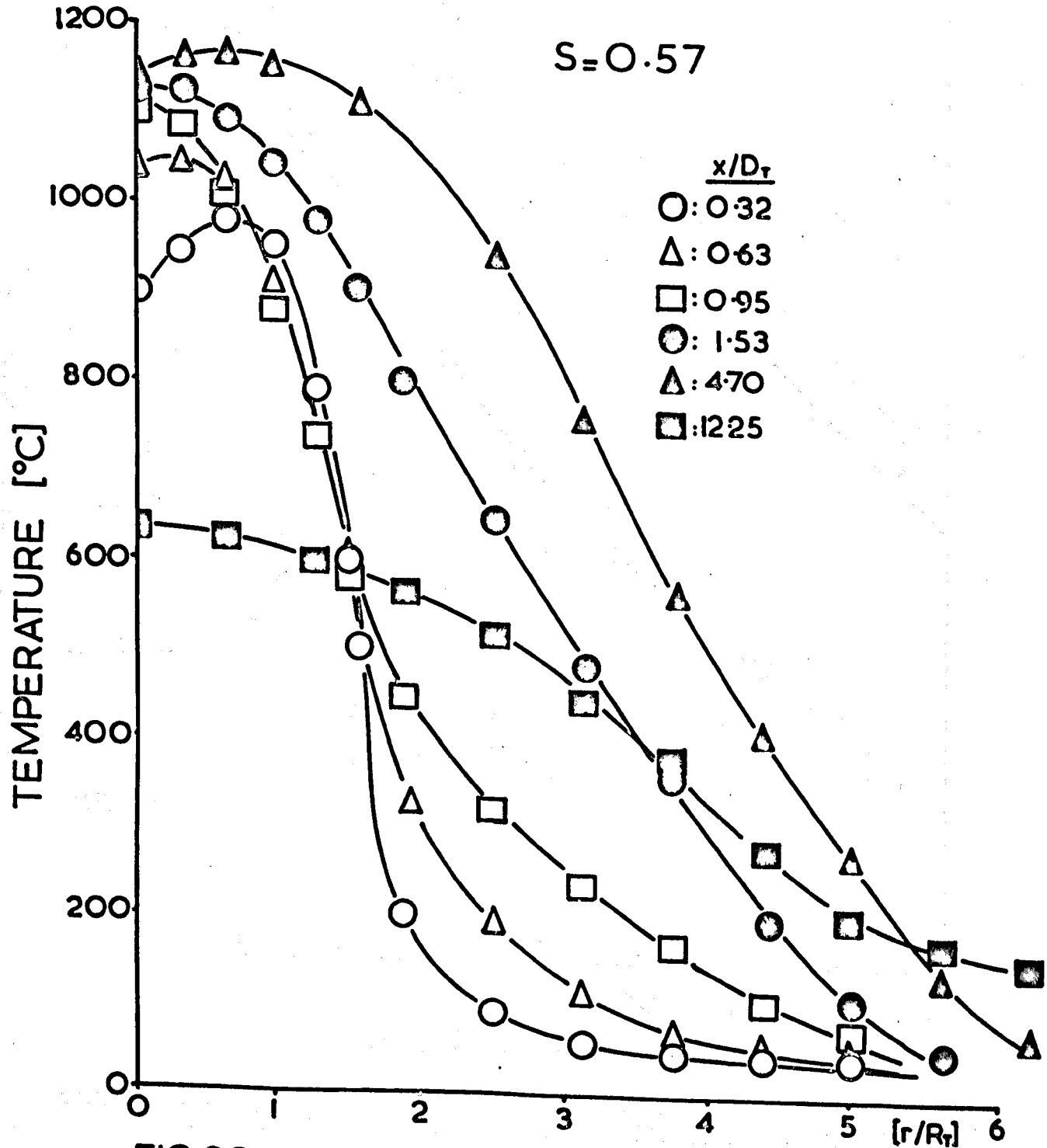

FIG.23 RADIAL TEMPERATURE DISTRIBUTIONS IN A HIGHLY SWIRLING SINGLE JET.

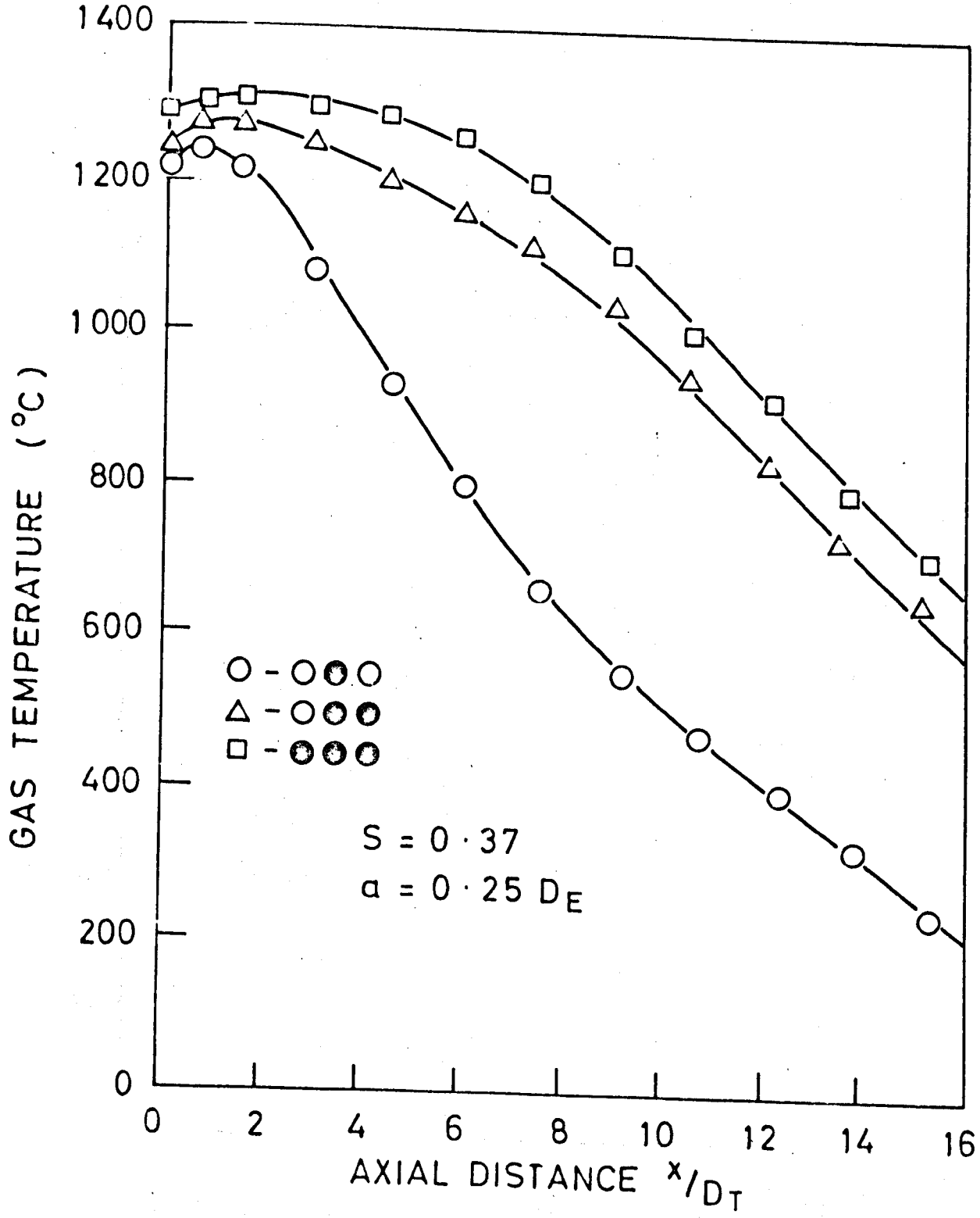

FIG.24 EFFECT OF BURNER CROWDING ON FLAME TEMPERATURE MEASURED ON AXIS OF DATUM FLAME.

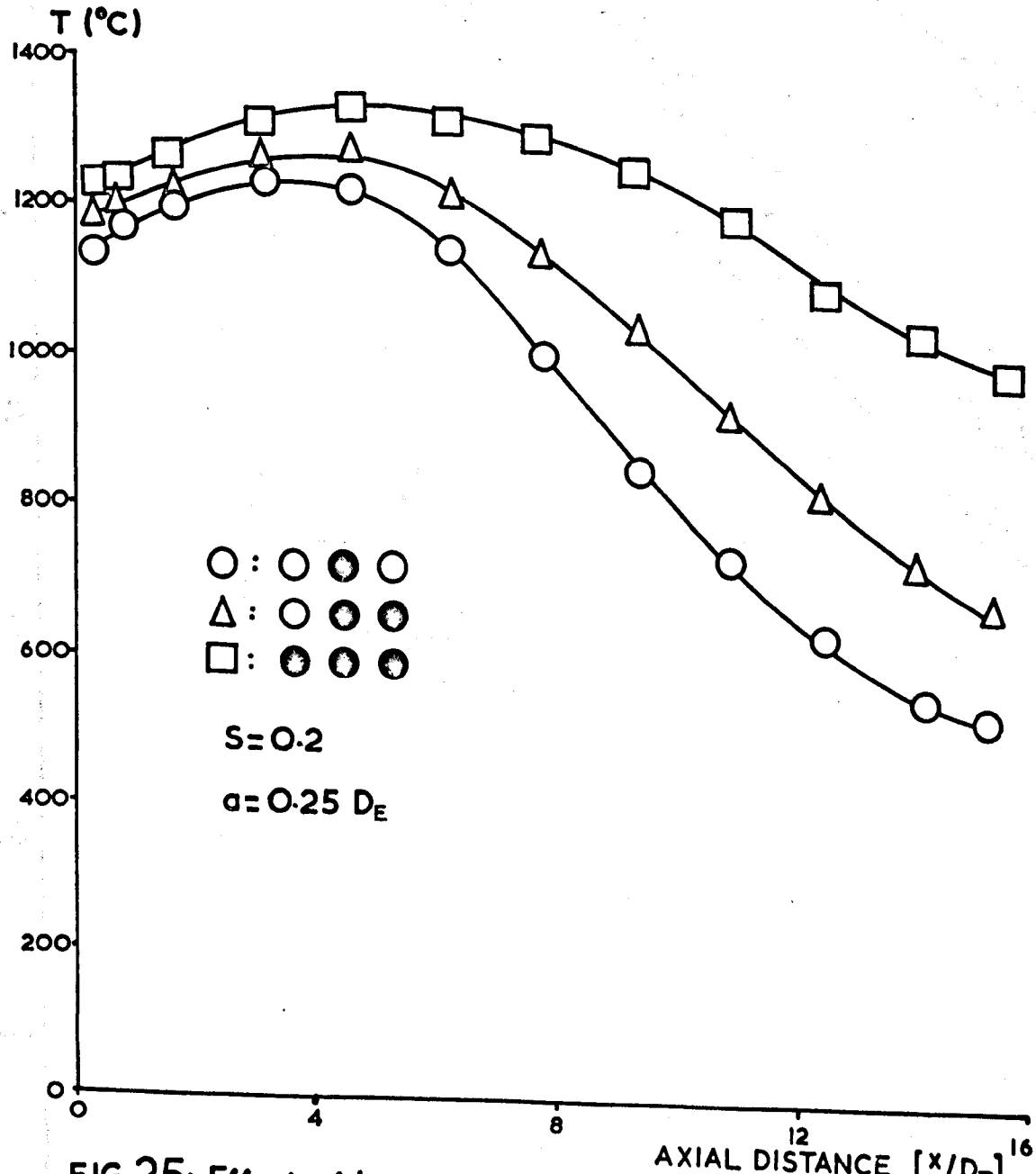

FIG.25: Effect of burner crowding on flame temperature measured on axis of datum flame at low swirl.

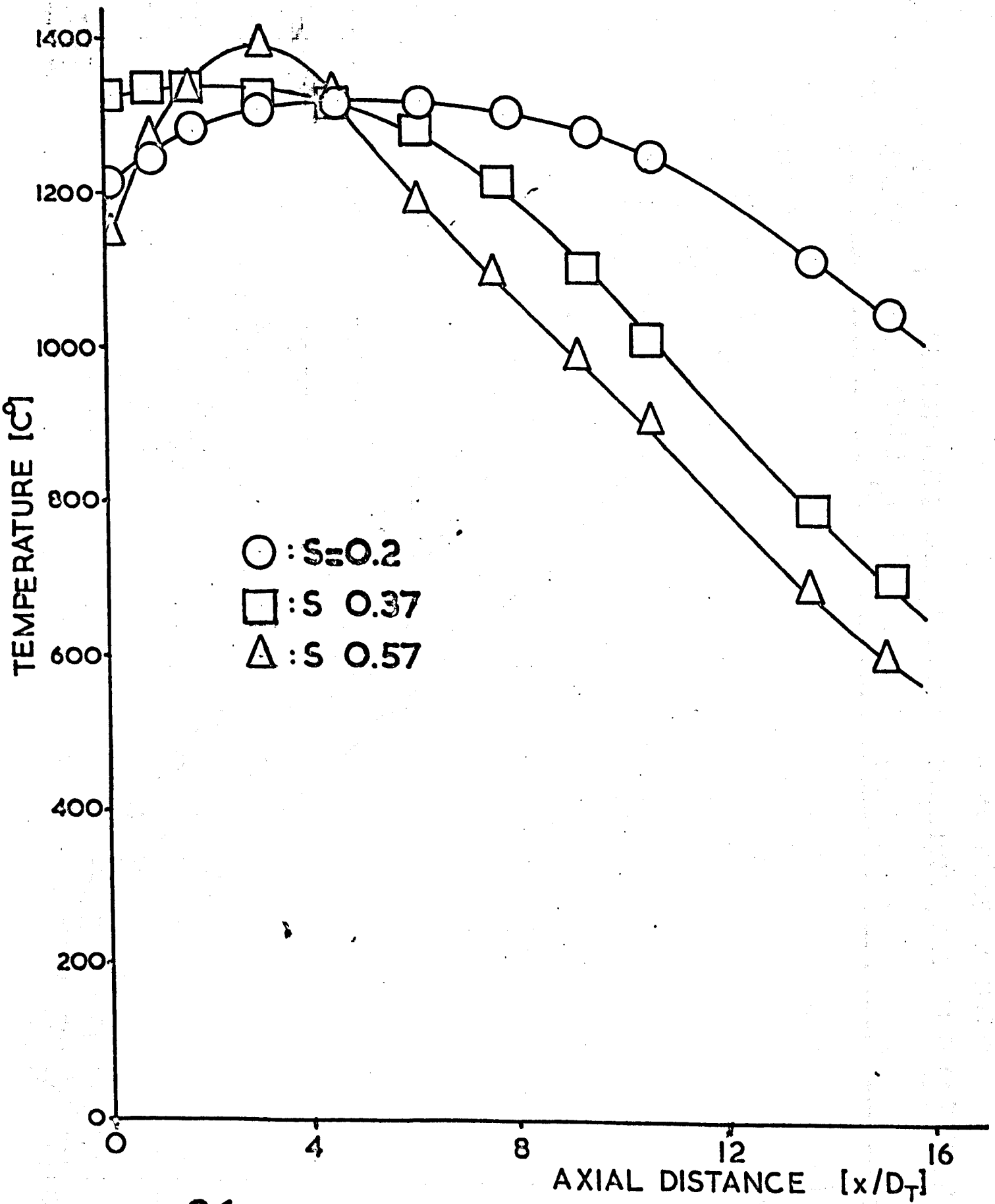

FIG.26: Effect of swirl on centre flame temperature in three burner system with a: 0·25D_E.

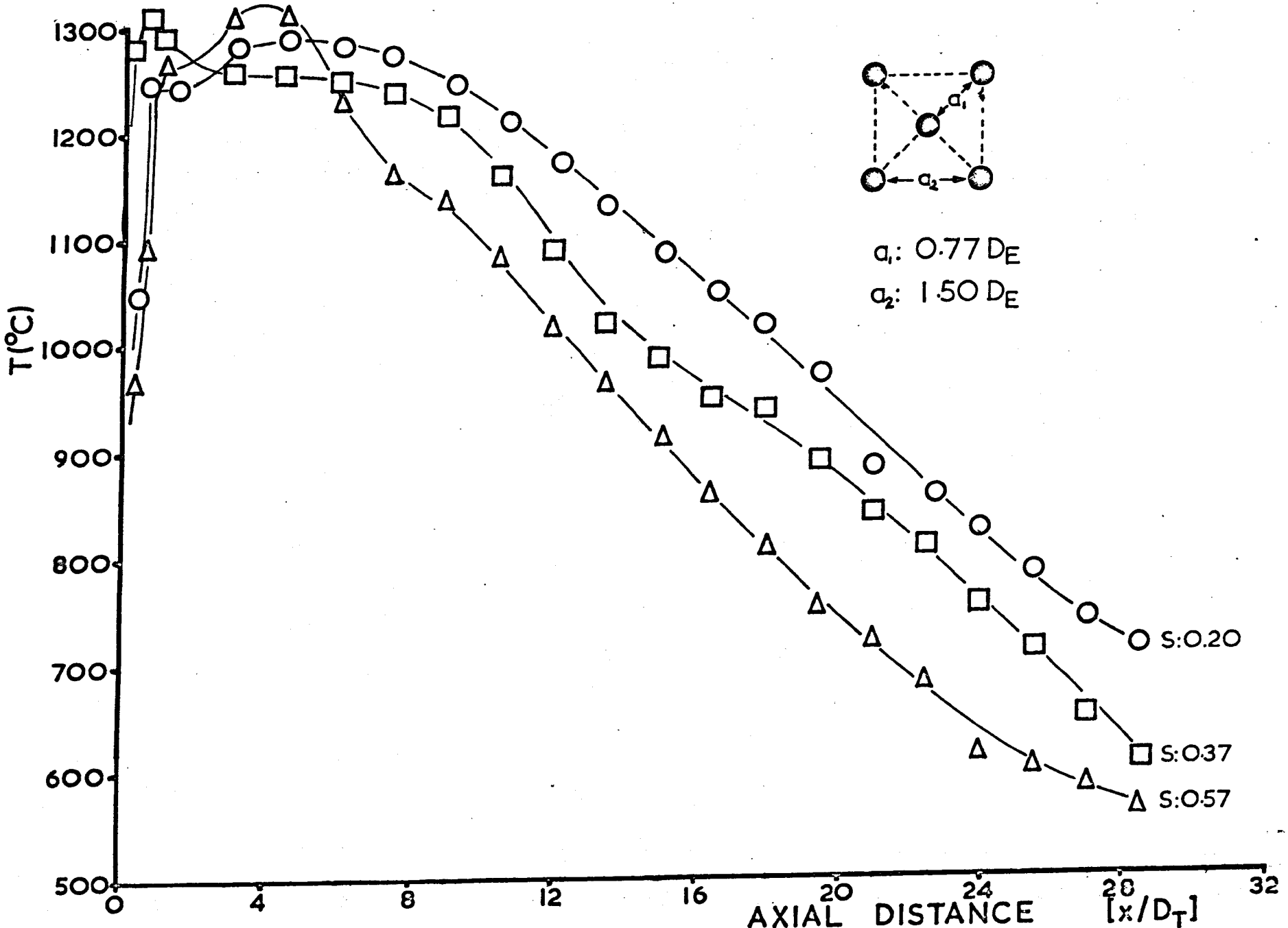

FIG. 27: Effect of swirl on centre flame temperature in a five burner system.

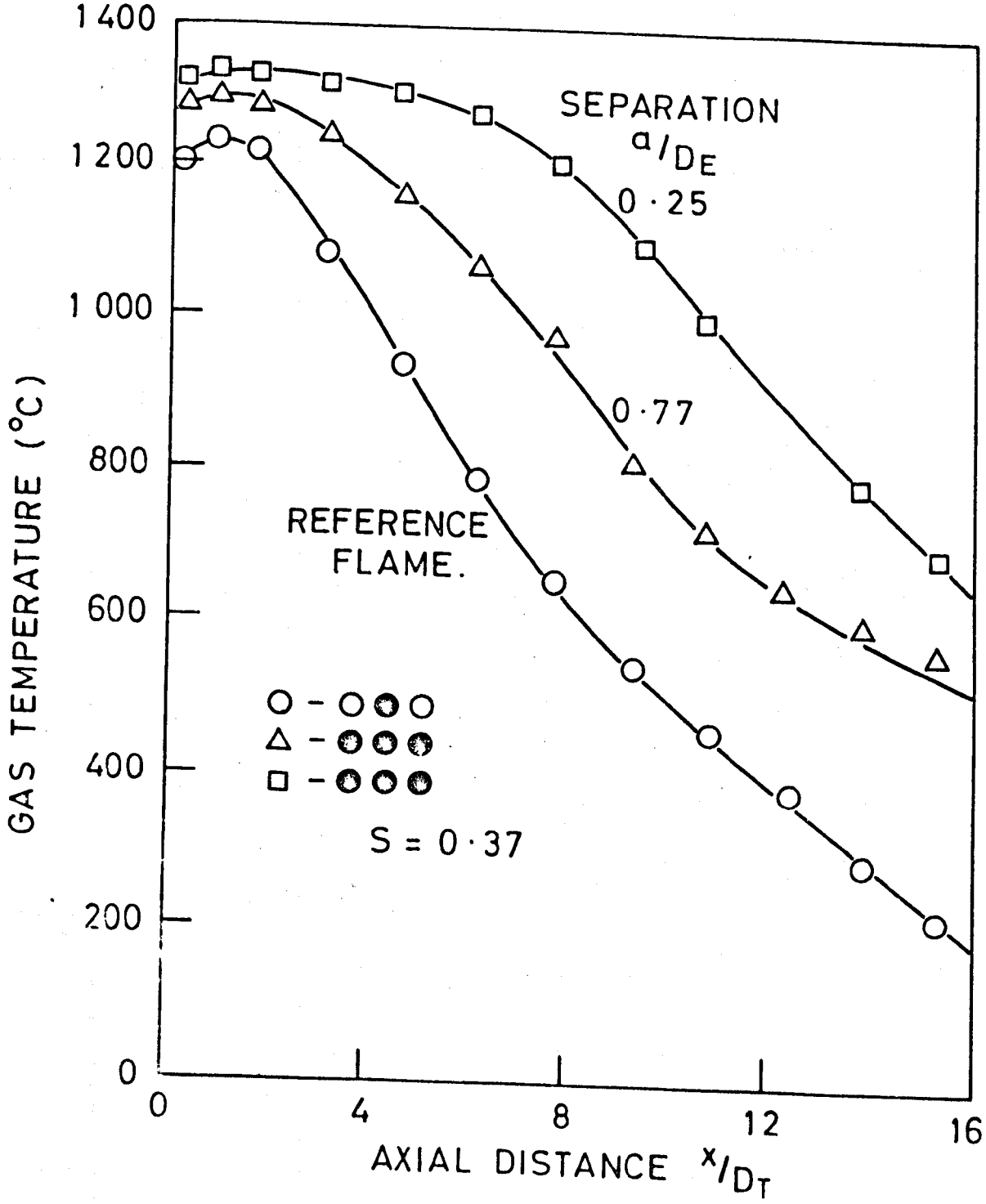

FIG.28 EFFECT OF BURNER SEPARATION ON CENTRE FLAME TEMPERATURE IN THREE BURNER SYSTEM.

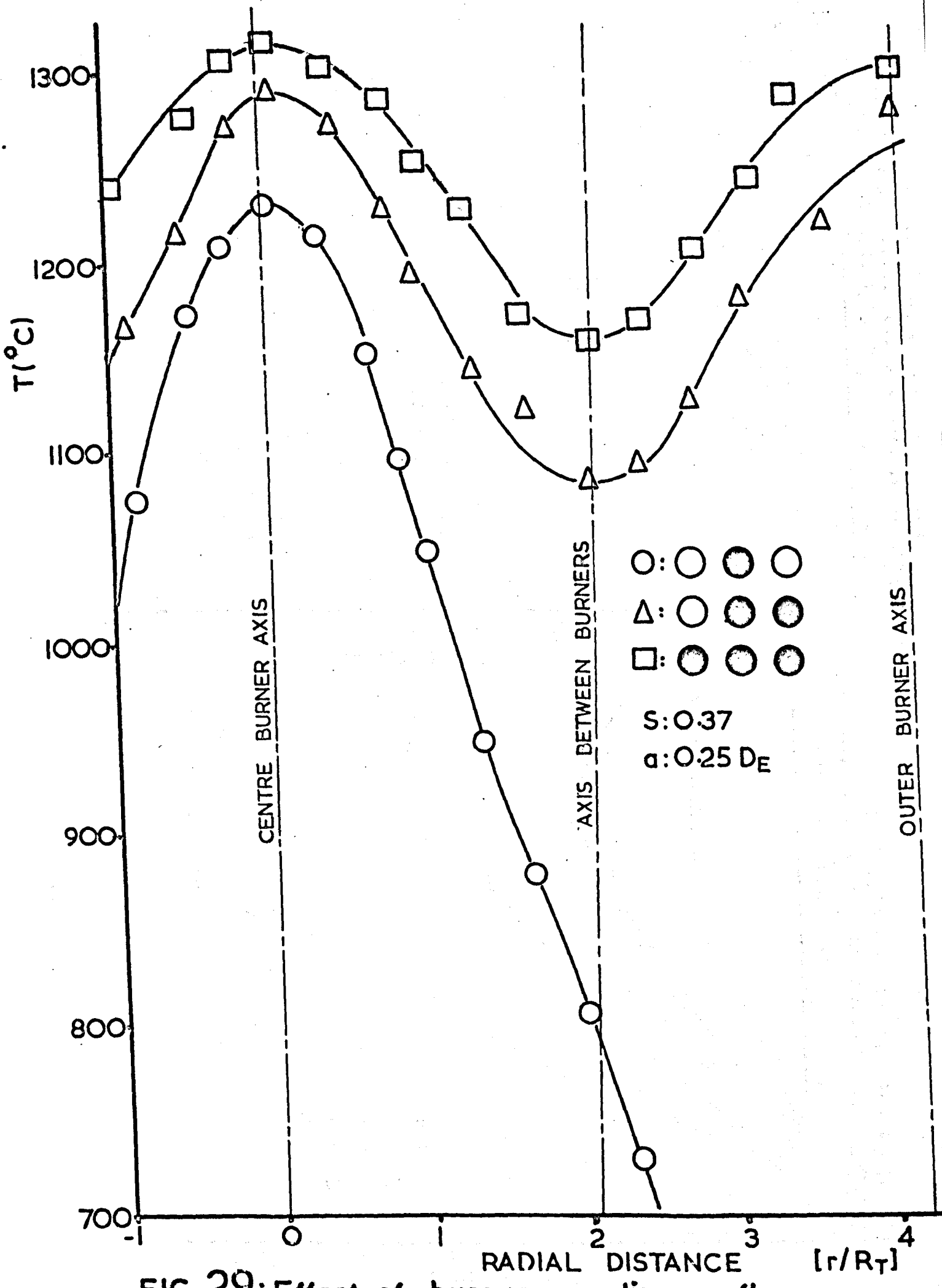

FIG.29: Effect of burner crowding on flame temperature at $x = 1.8\ D_T$

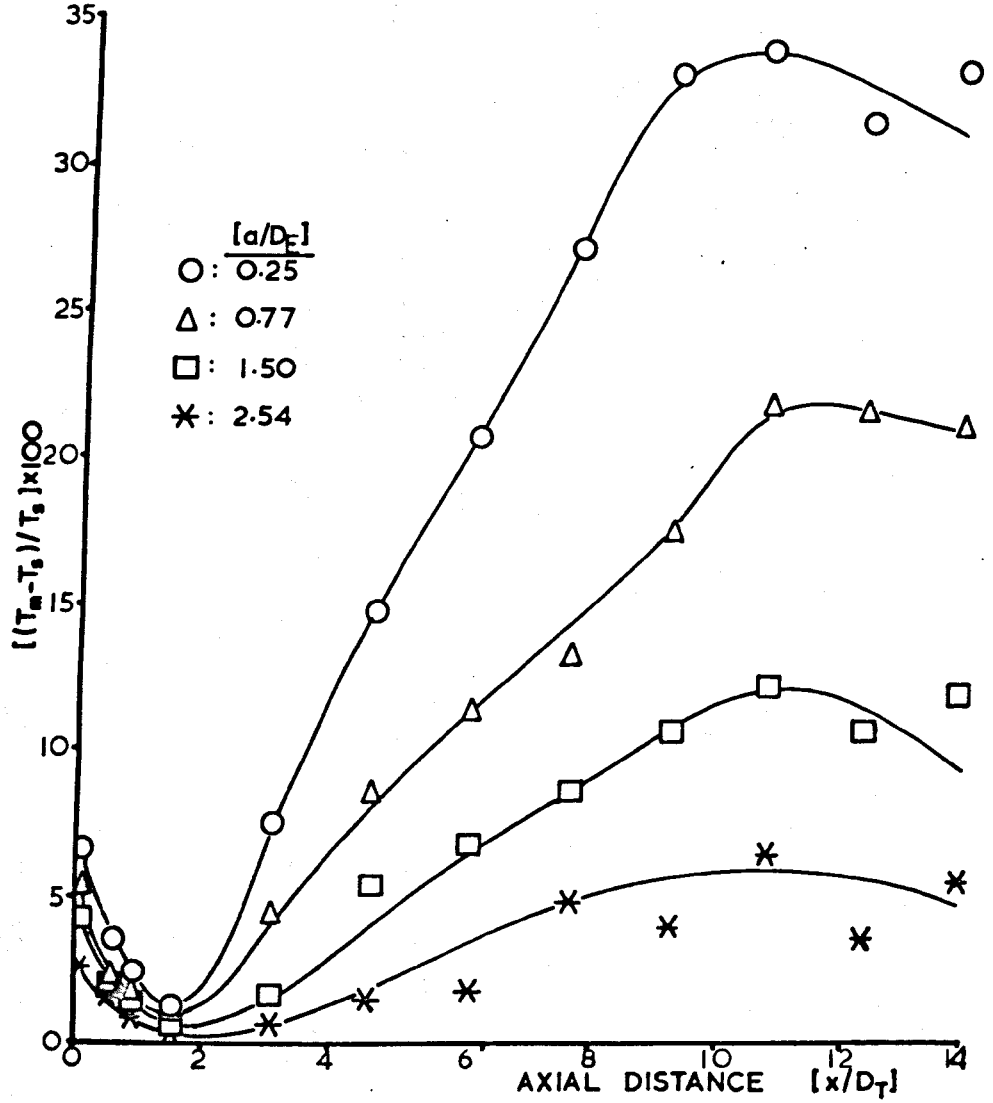

FIG.30: Effect of burner separation on percent temperature rise for two burner system. (S:0.57)

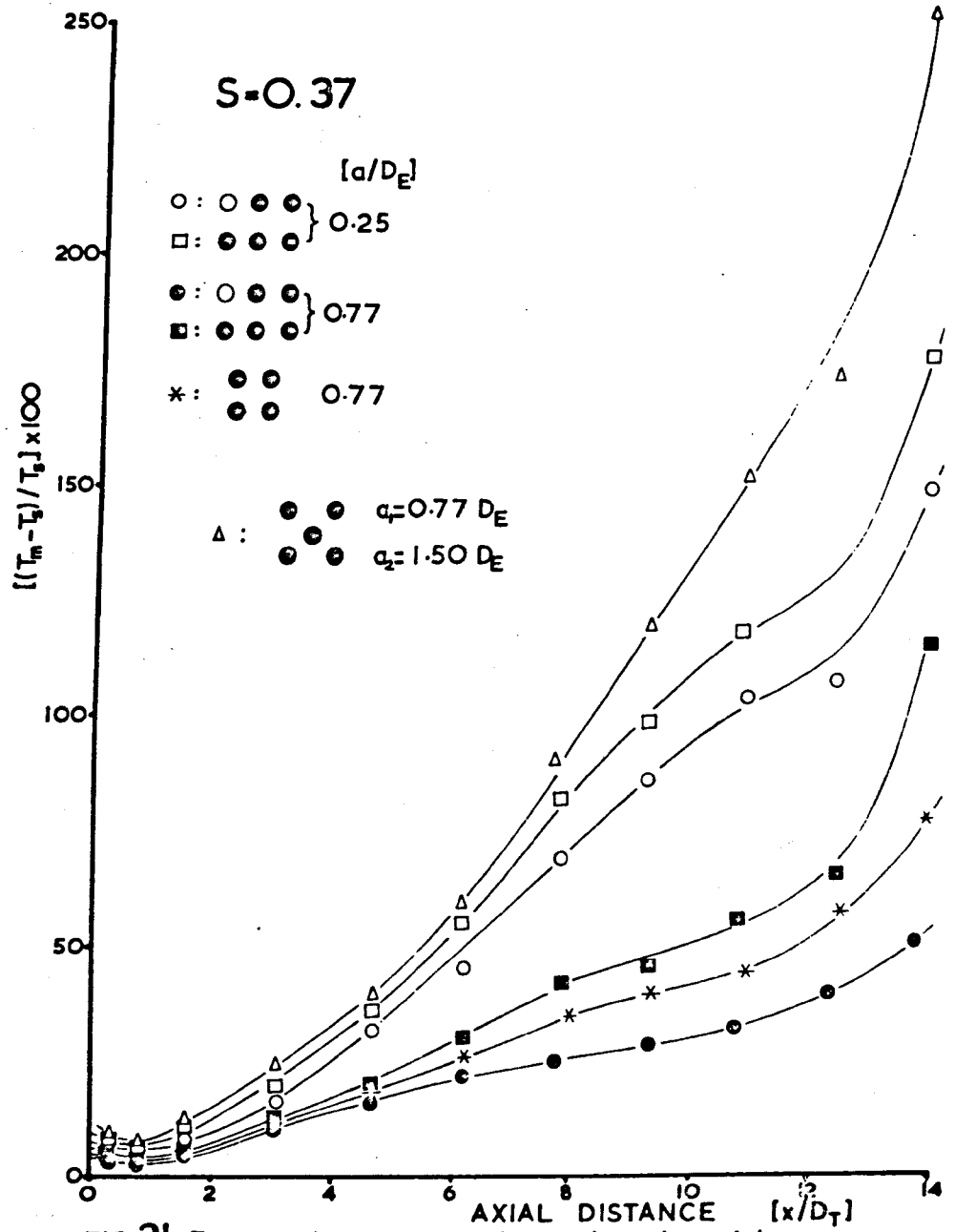

FIG.31: Effect of burner separation and number of burners on percent temperature rise for different burner arrays.

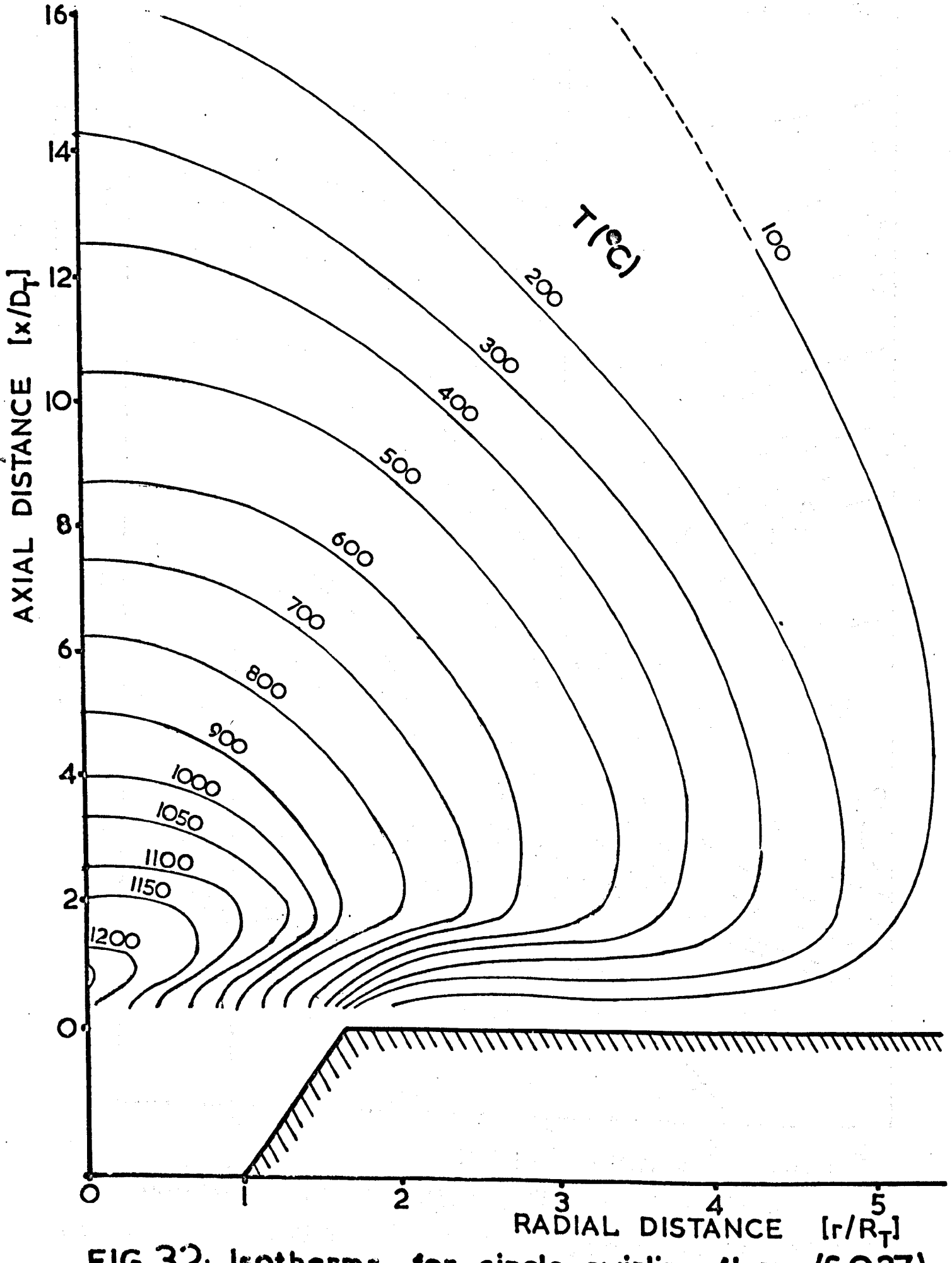

FIG.32: Isotherms for single swirling flame. (S:0.37)

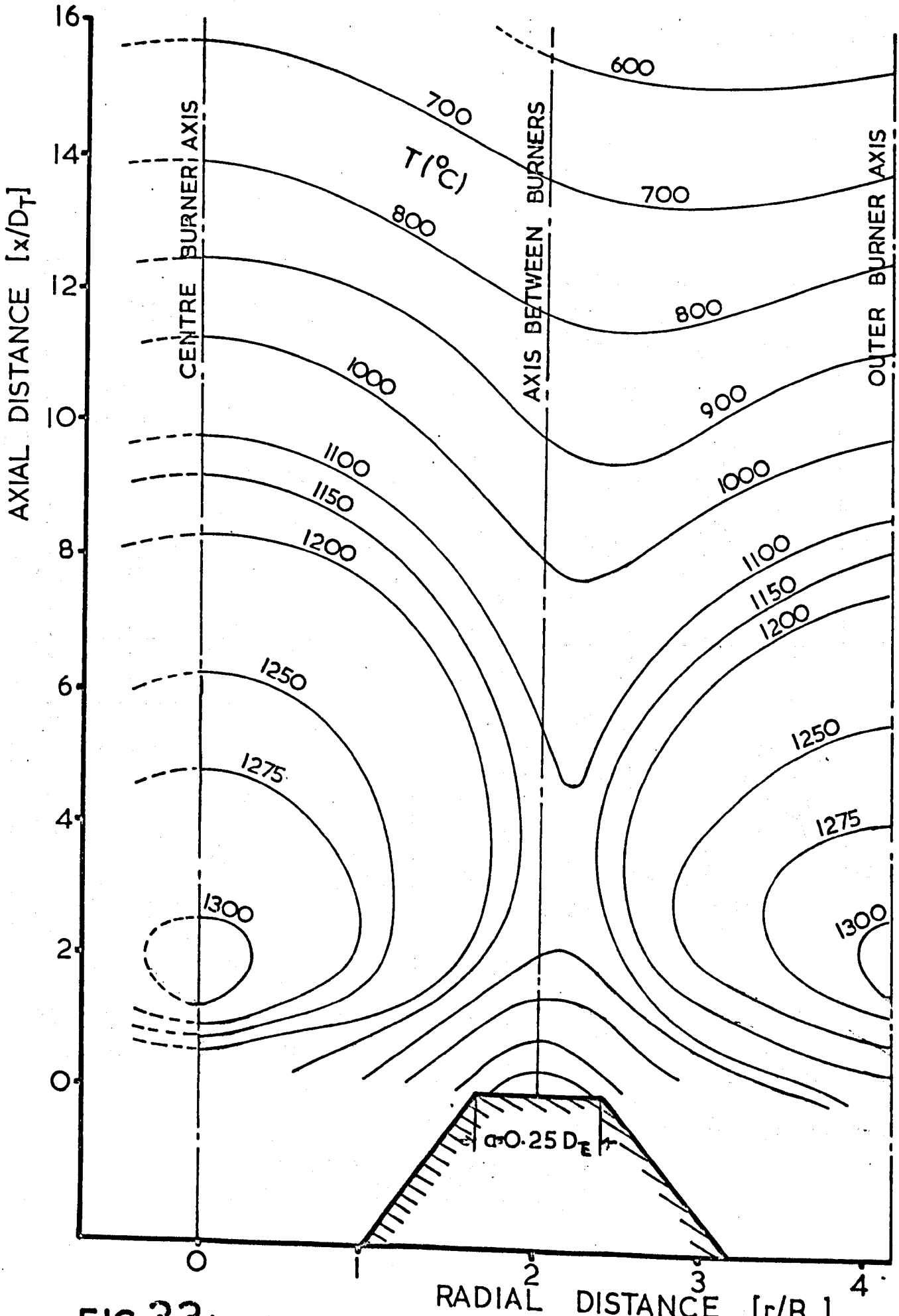

FIG.33 isotherms between flames for a three swirling burner system. (S:0.37, a:0.25 D_E)

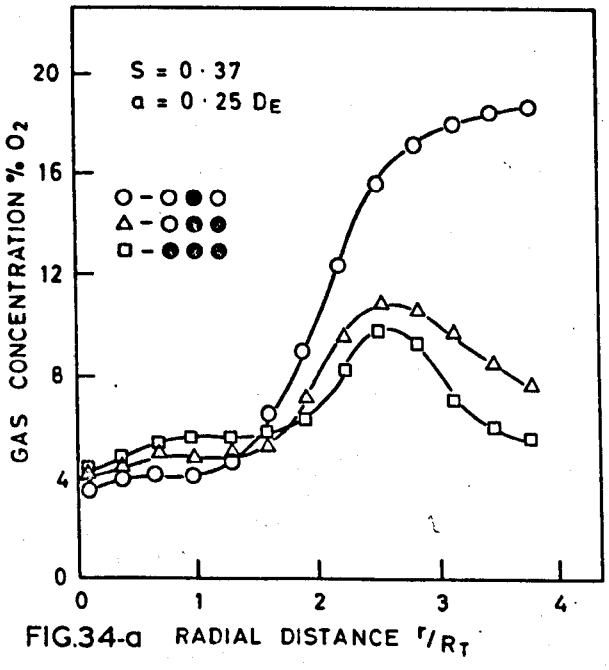

FIG.34-a

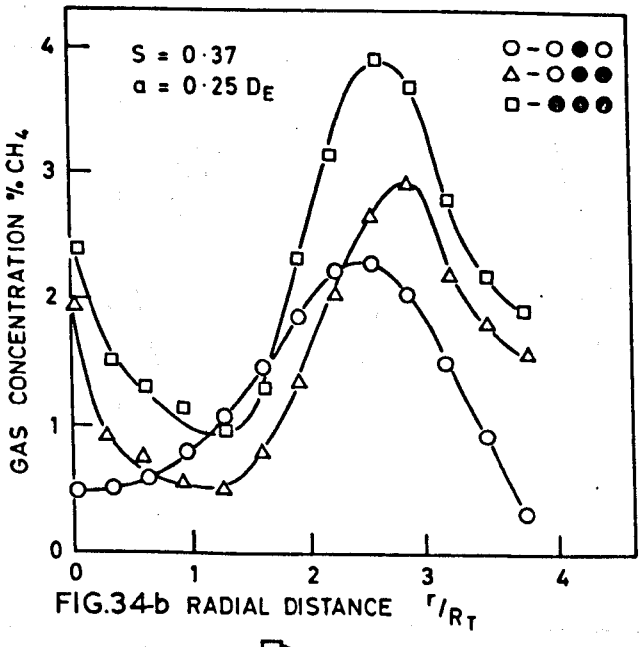

FIG.34-b

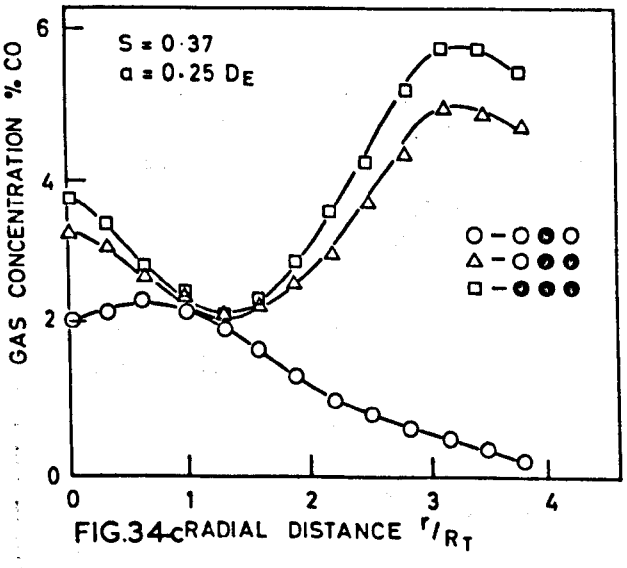

FIG.34-c

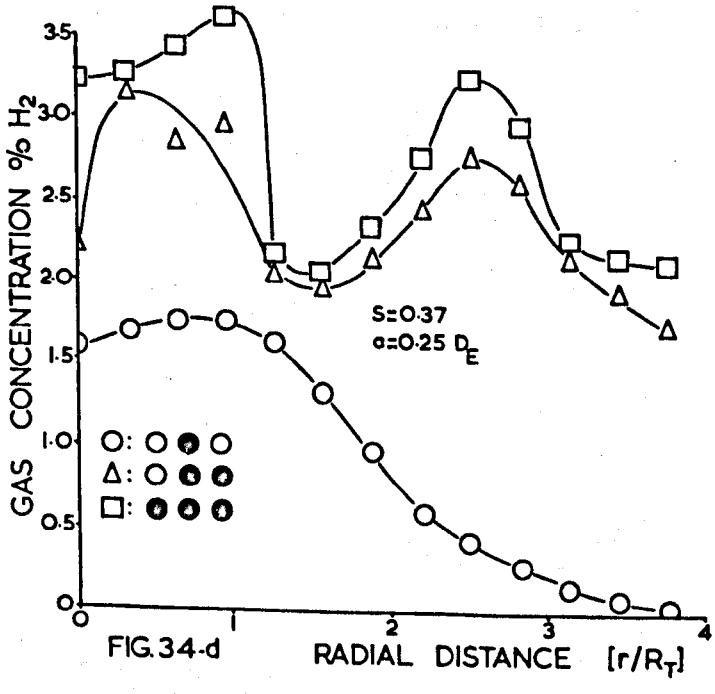

FIG.34-d

FIG.34: EFFECT OF BURNER CROWDING ON GAS CONCENTRATIONS AT X = 2·2 D_T.

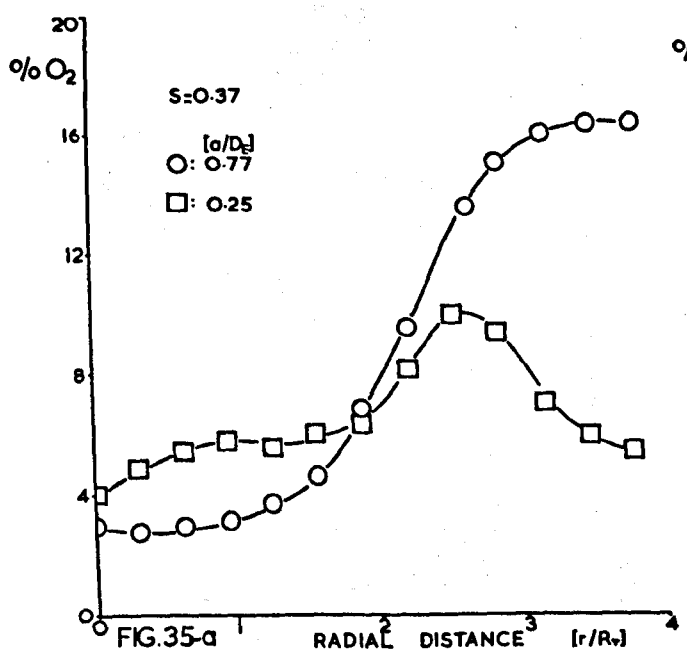

FIG.35-a

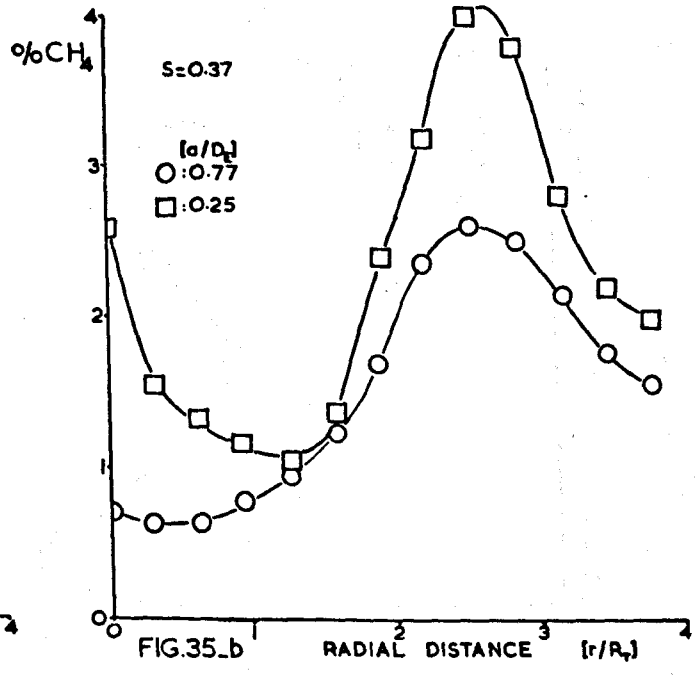

FIG.35_b

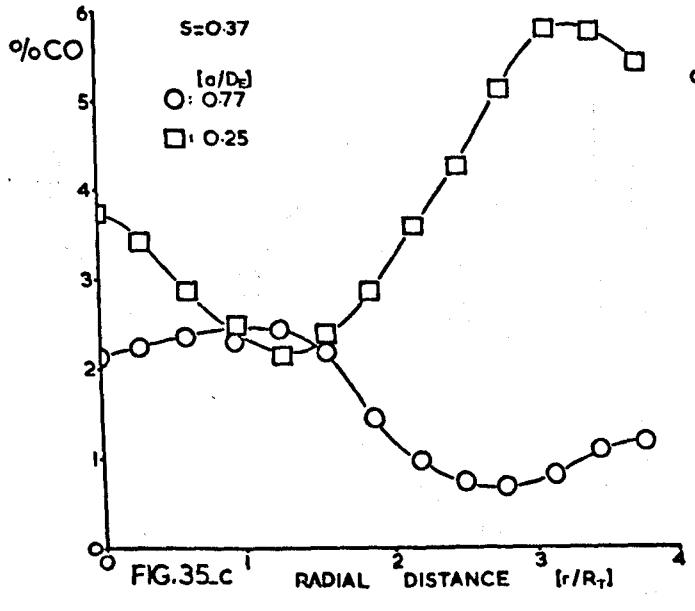

FIG.35_c

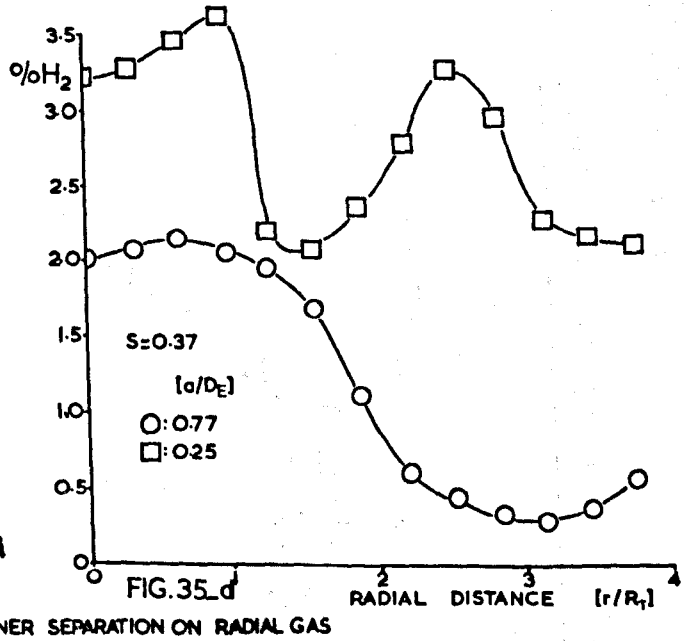

FIG.35_d

FIG. 35 EFFECT OF BURNER SEPARATION ON RADIAL GAS CONCENTRATIONS AT X=2·2 D_T IN A THREE BURNER SYSTEM.

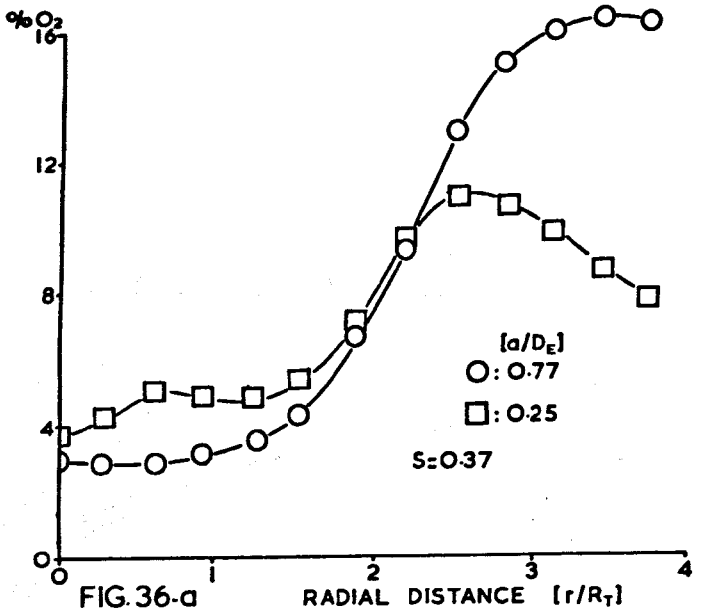

FIG. 36-a

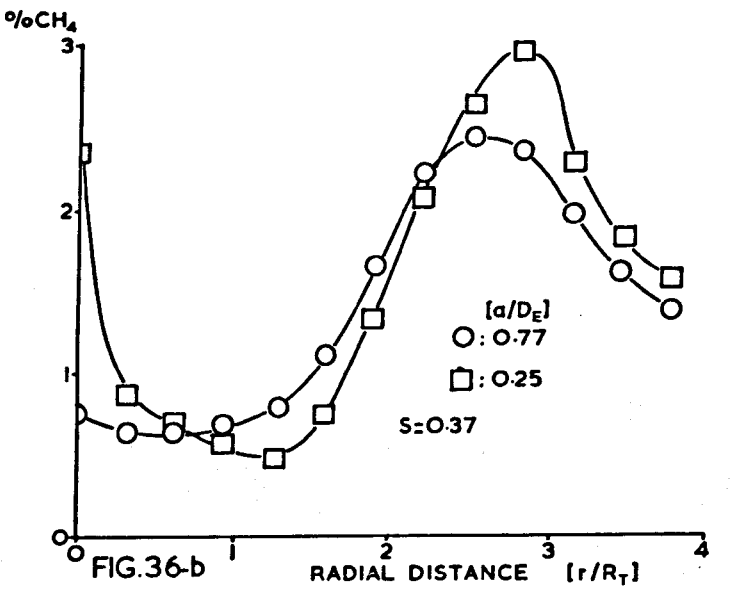

FIG. 36-b

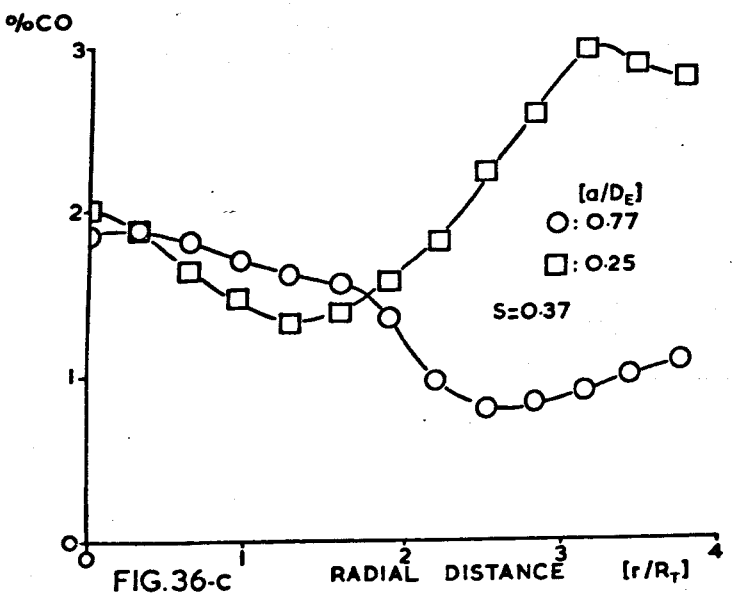

FIG. 36-c

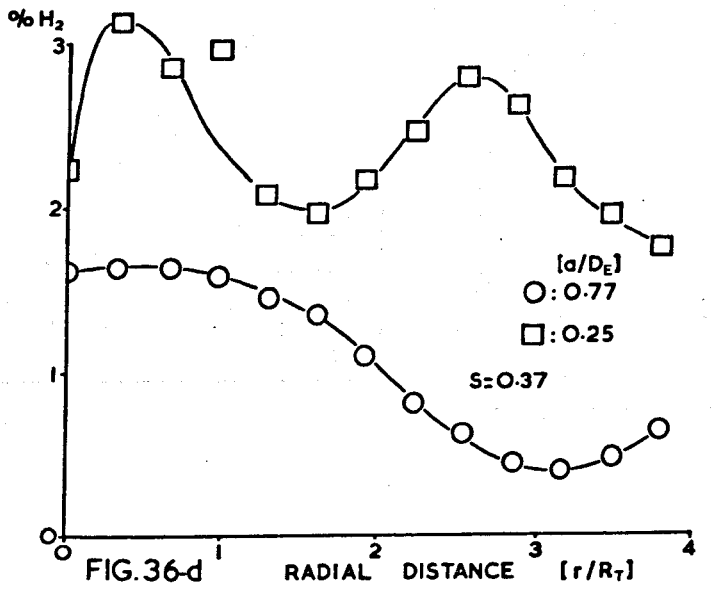

FIG. 36-d

FIG. 36: EFFECT OF SEPARATION ON RADIAL GAS CONCENTRATIONS IN TWO BURNERS

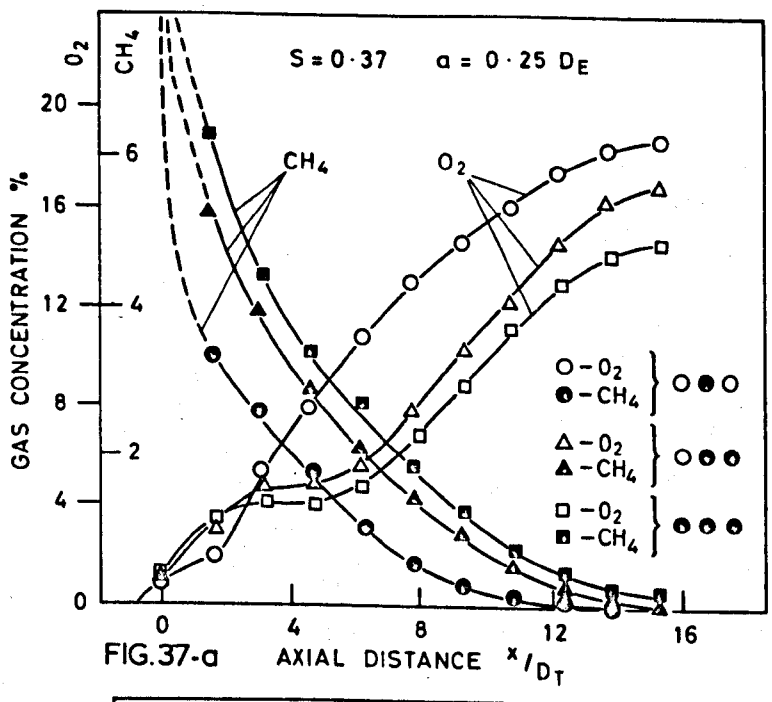

FIG.37-a

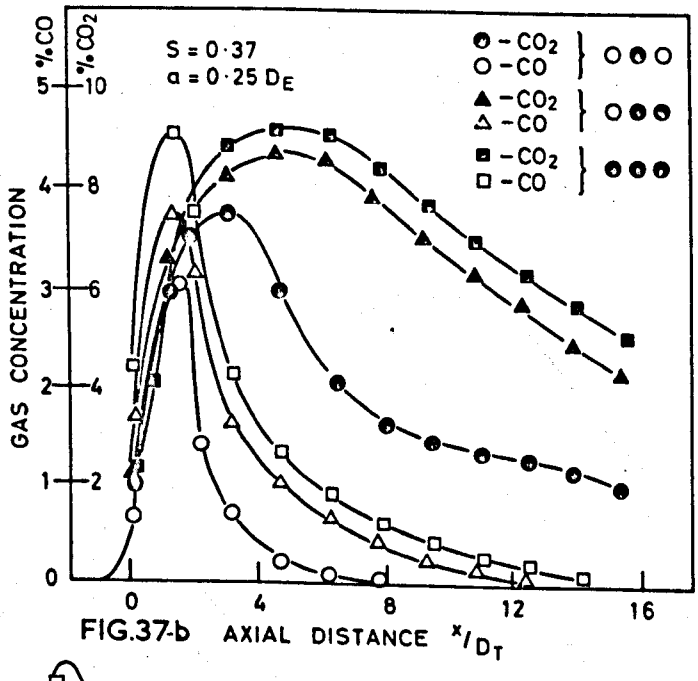

FIG.37-b

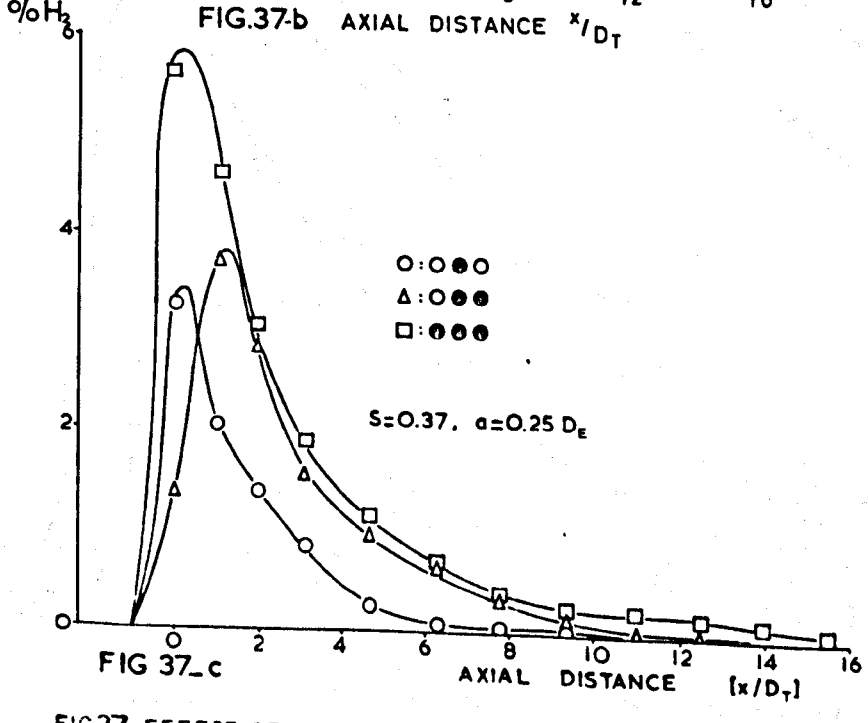

FIG 37_c

FIG37: EFFECT OF BURNER CROWDING ON AXIAL GAS CONCENTRATIONS.

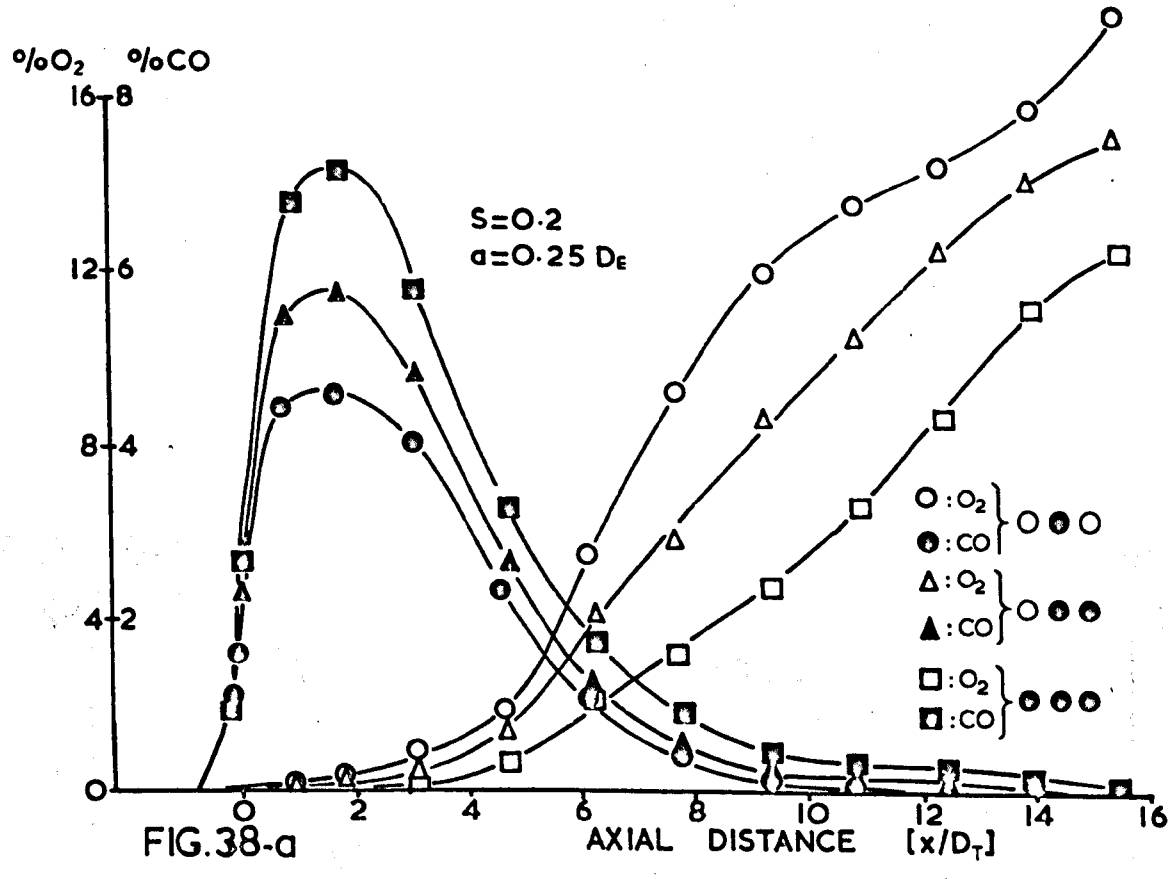

FIG.38-a

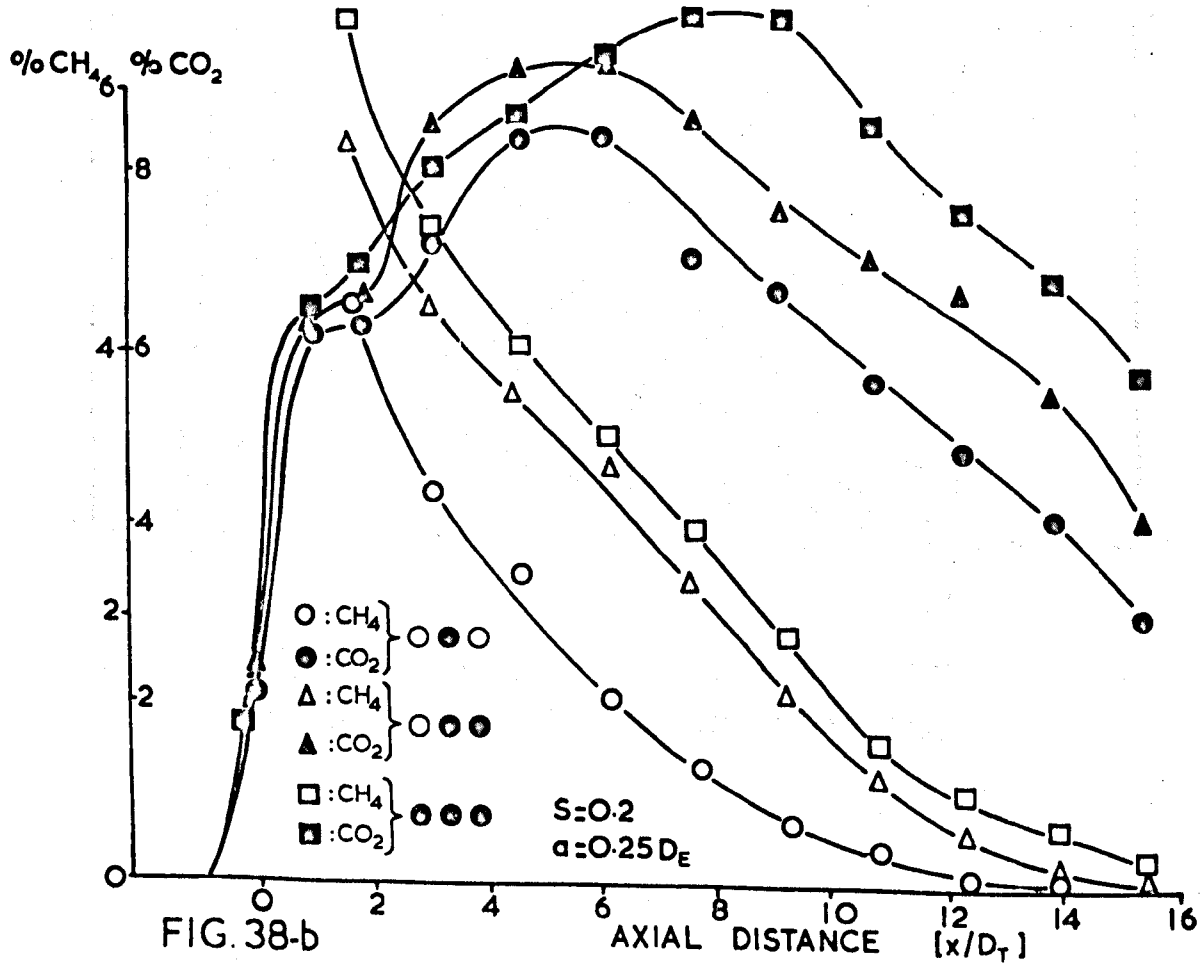

FIG.38-b

FIG.38: EFFECT OF BURNER CROWDING ON AXIAL GAS CONCENTRATIONS AT LOW SWIRL LEVEL

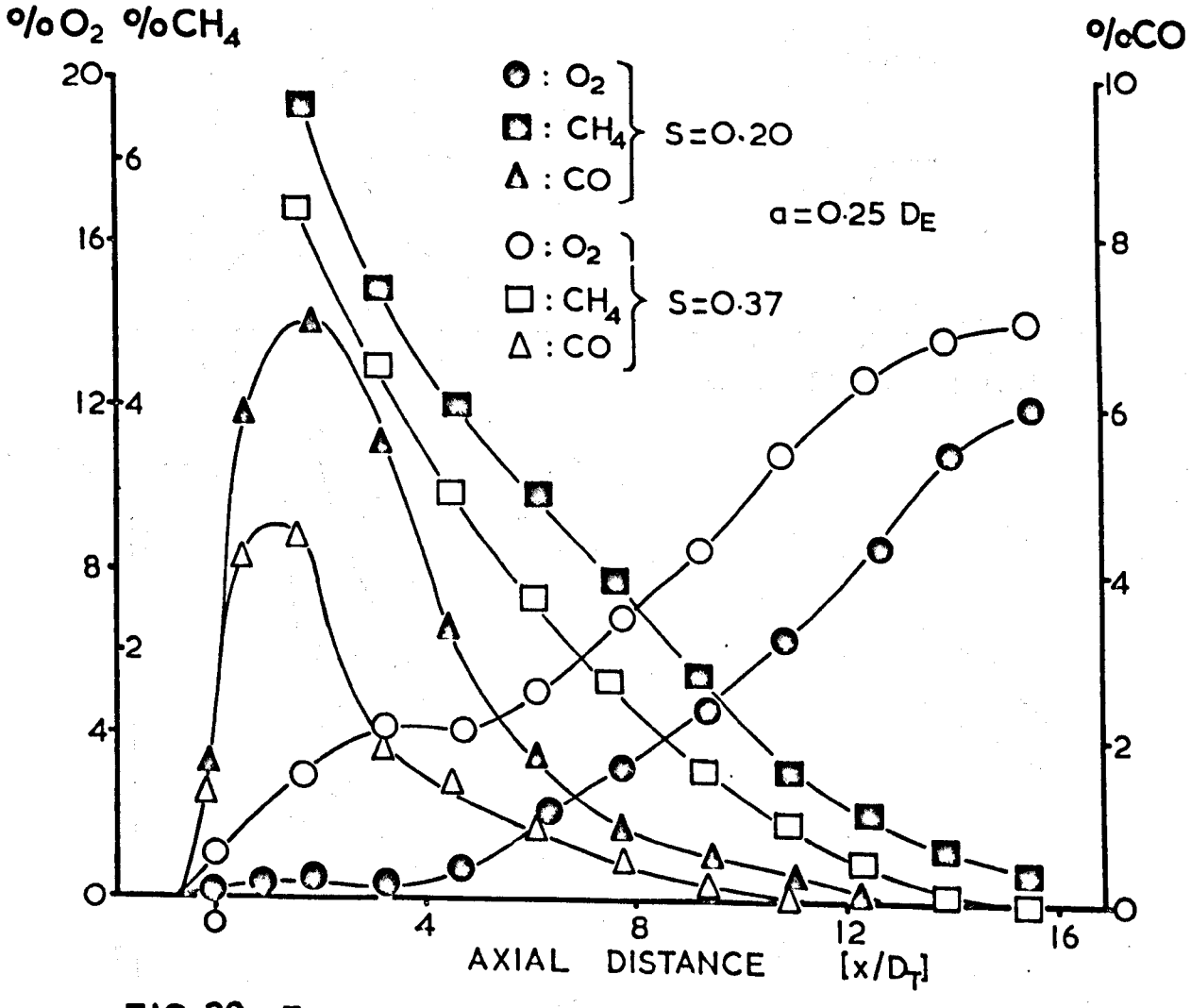

FIG. 39: Effect of swirl on O_2, CH_4 and CO concentrations in three burner system.

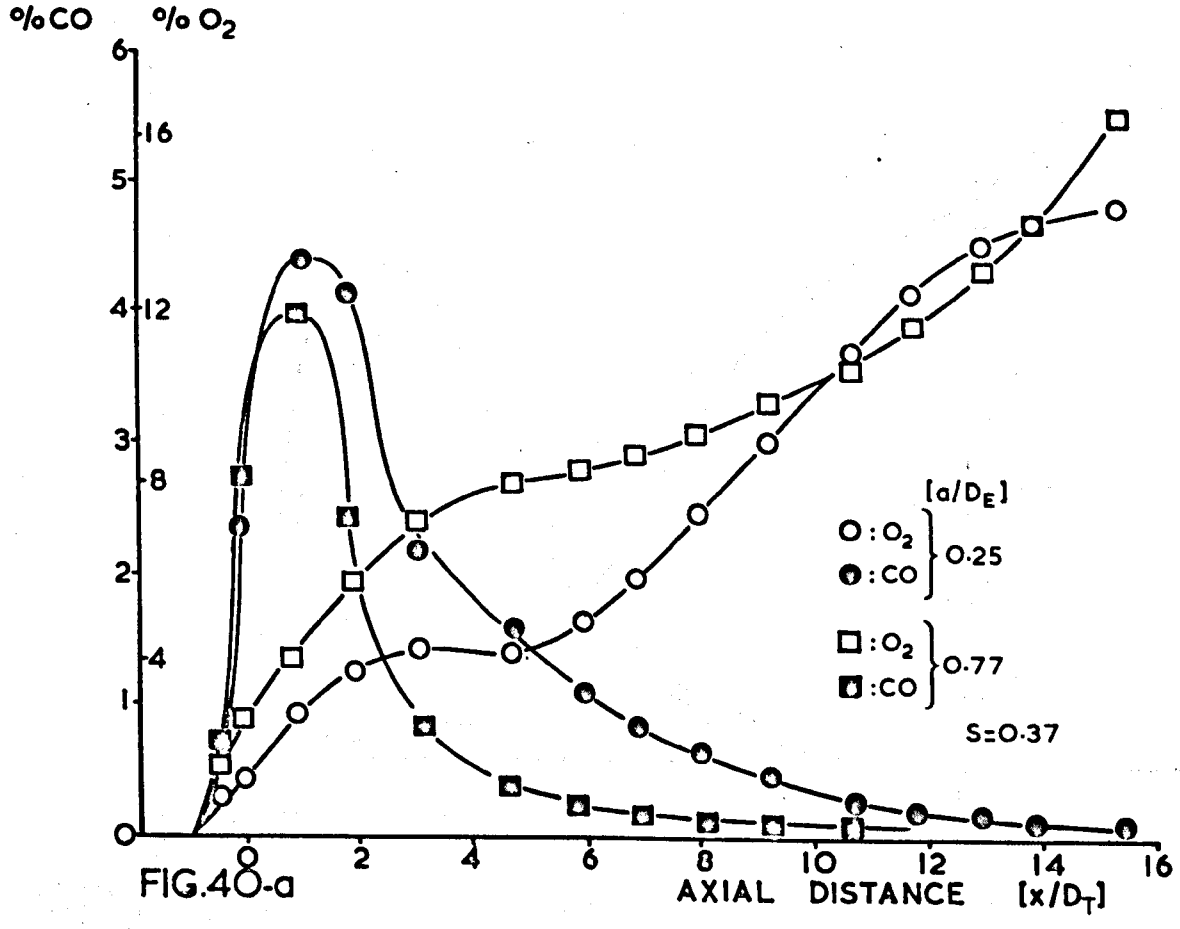

FIG.40-a

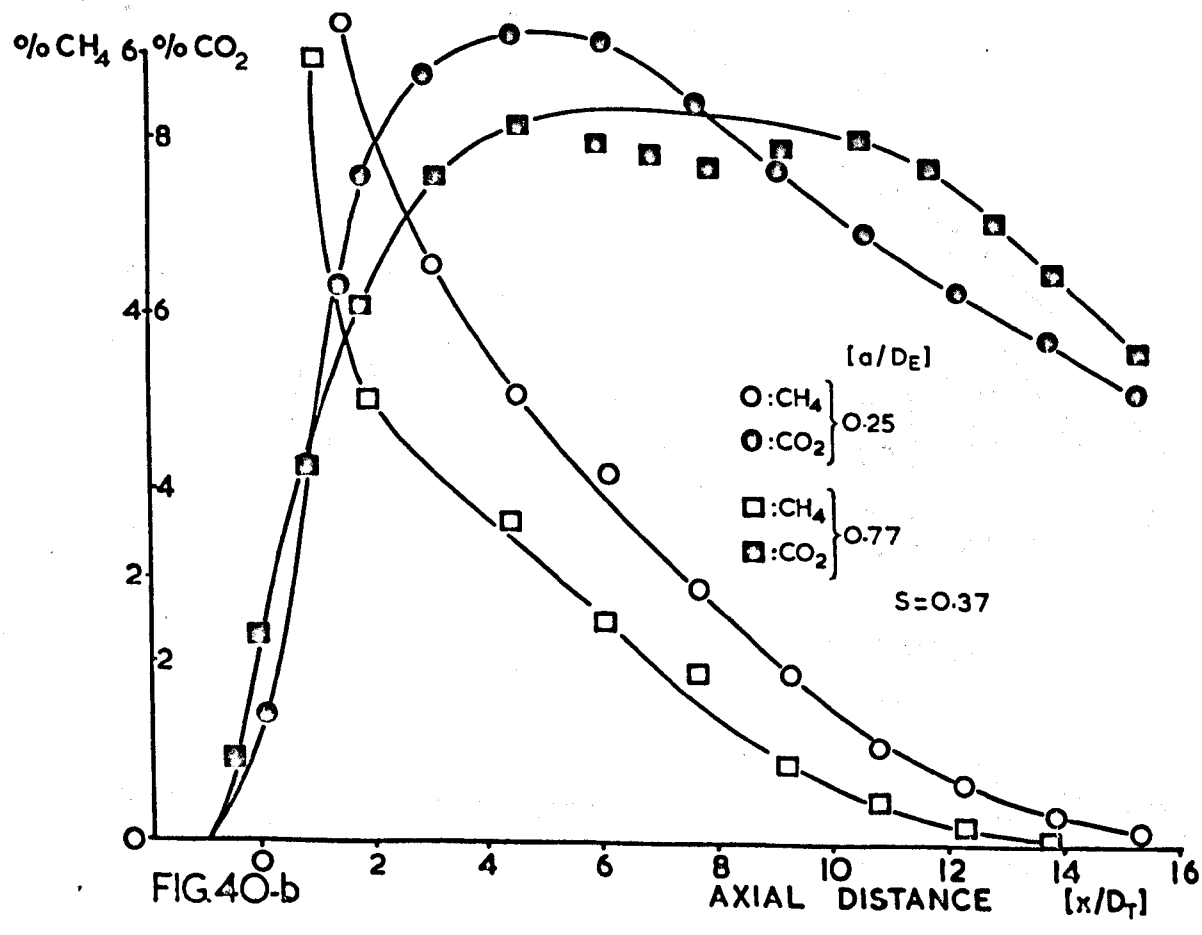

FIG.40-b

FIG.40 EFFECT OF BURNER SEPARATION ON AXIAL GAS CONCENTRATIONS IN A THREE BURNER SYSTEM.

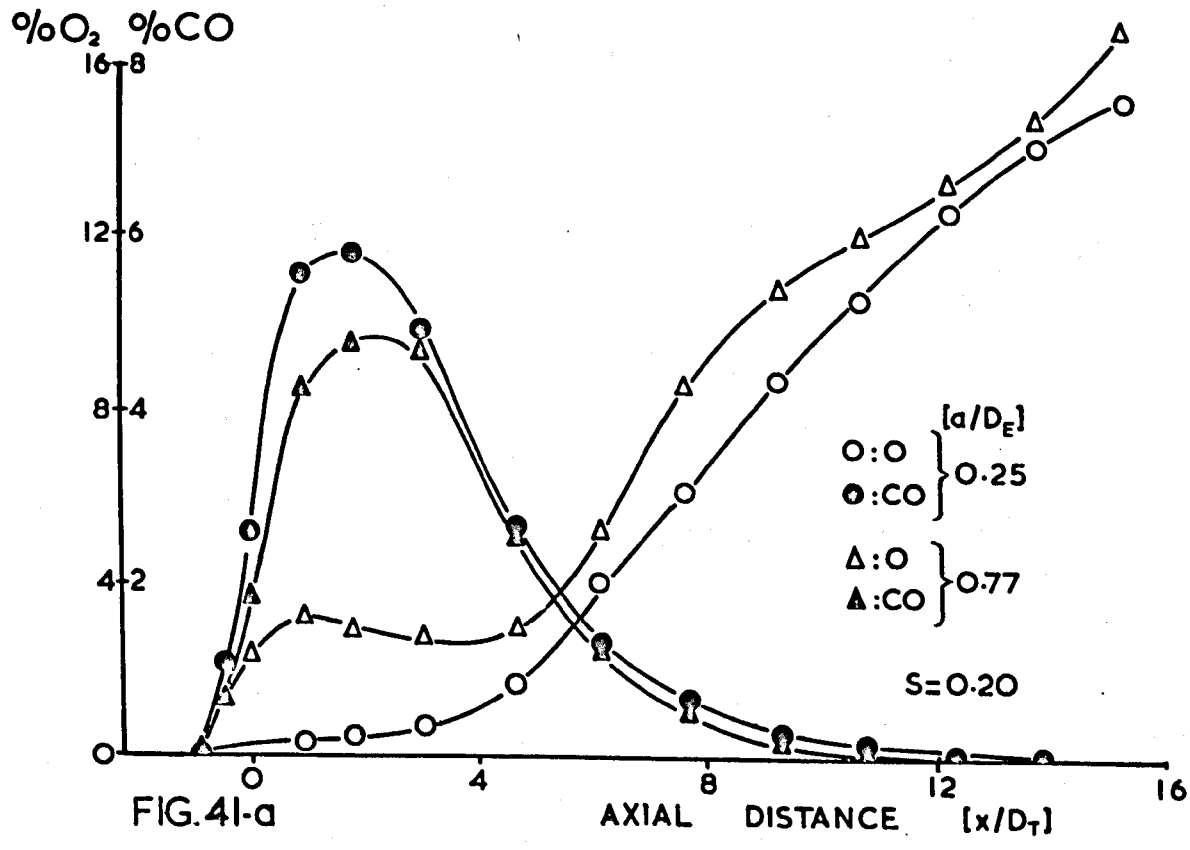

FIG.41-a

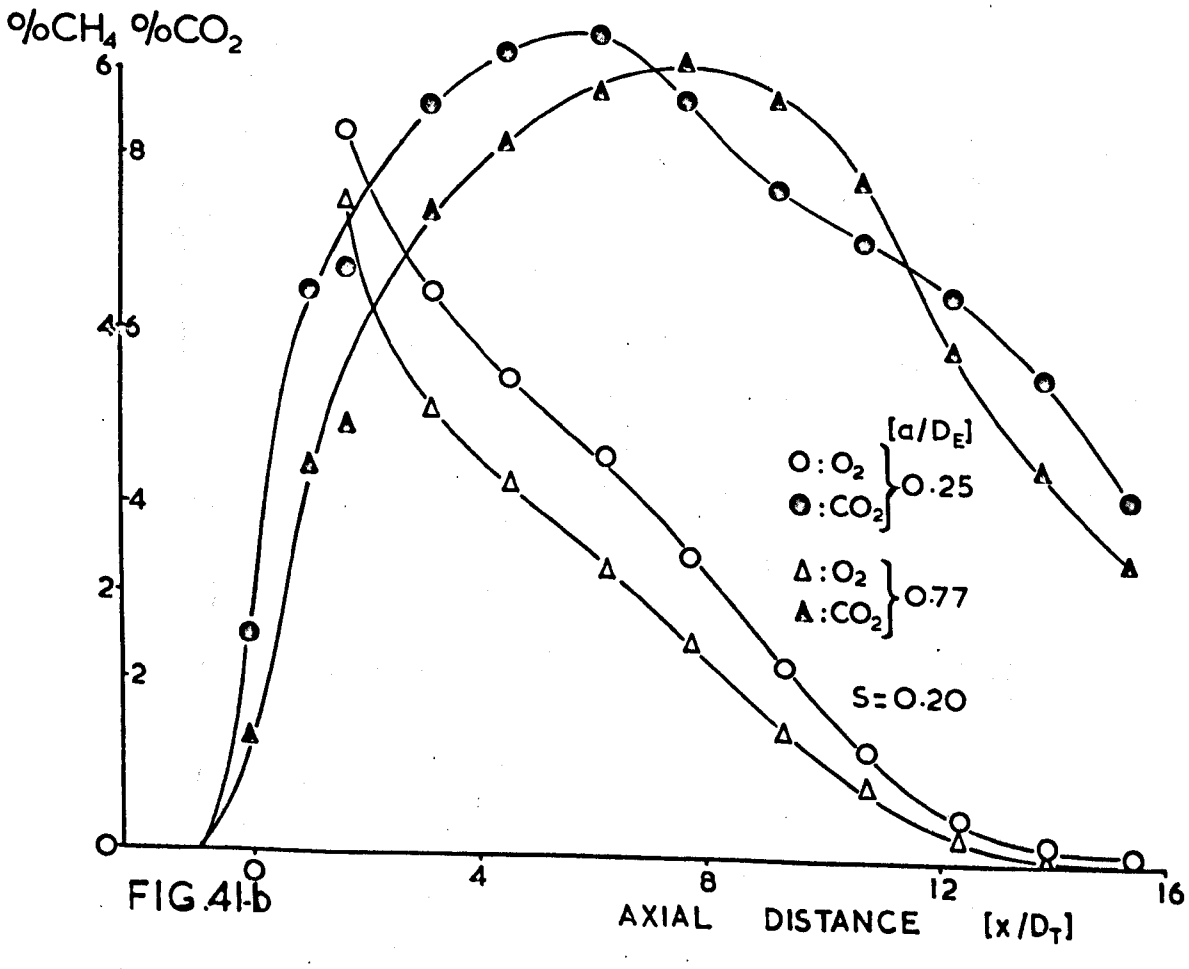

FIG.41-b

FIG. 41 EFFECT OF BURNER SEPARATION ON AXIAL GAS CONCENTRATIONS IN A THREE BURNER SYSTEM AT LOW SWIRL.

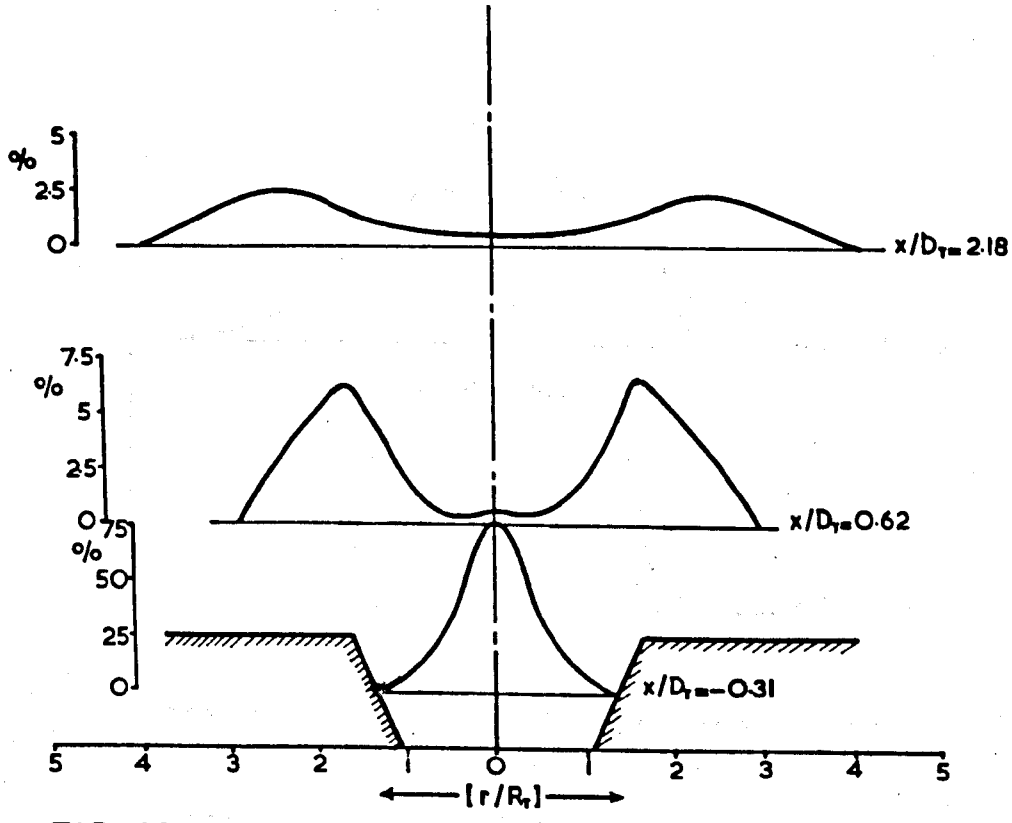

FIG 42-a Radial profiles of CH_4 concentration. at S=0.37.

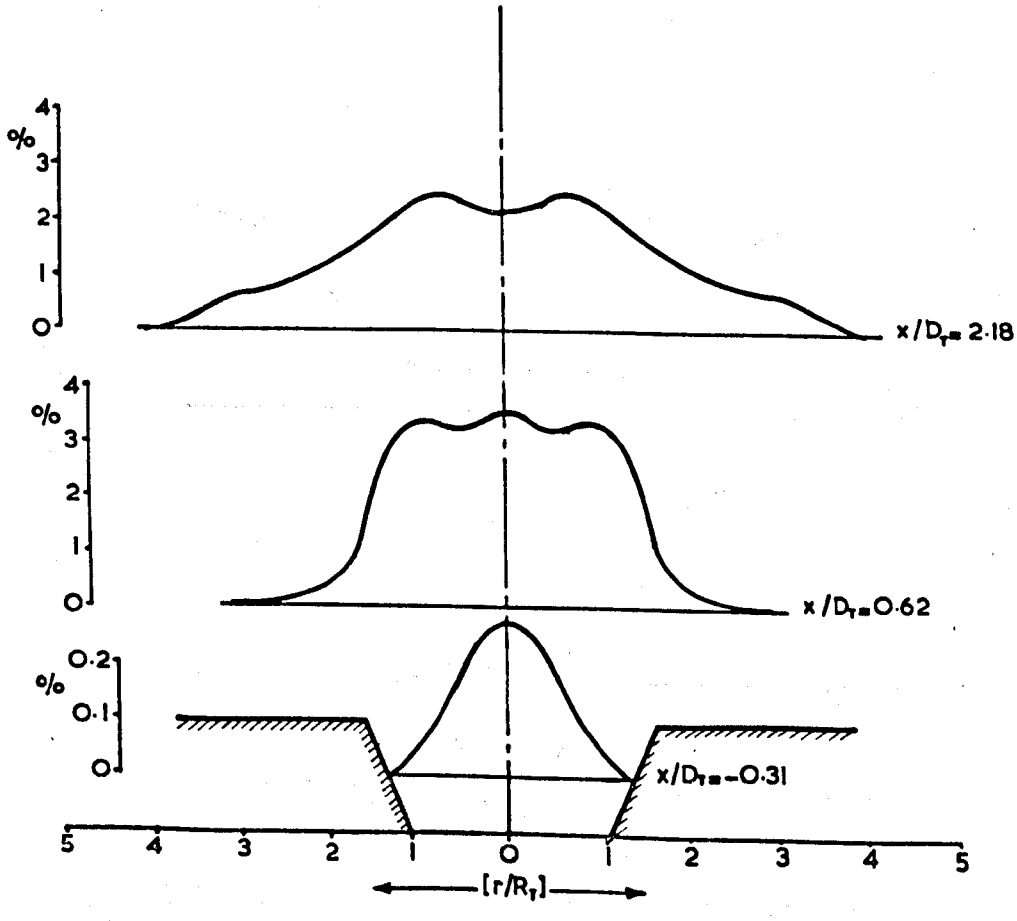

FIG 42-b Radial profiles of CO concentration.

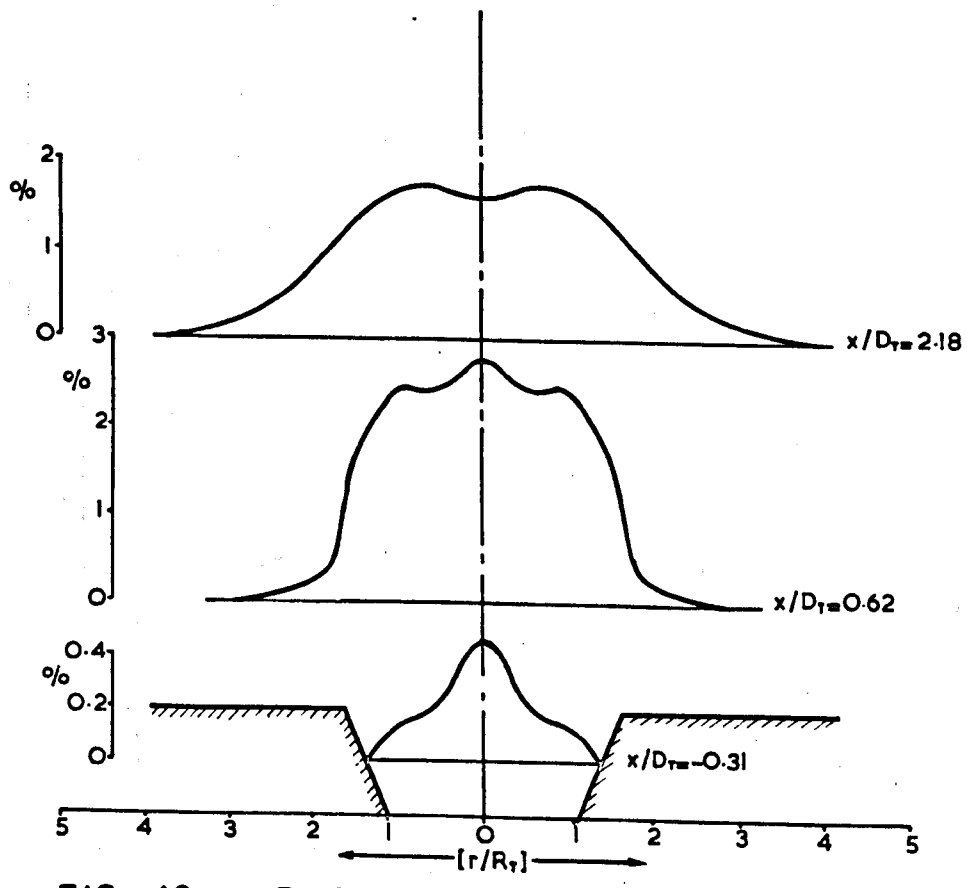

FIG. 42-c Radial profiles of H_2 concentration.

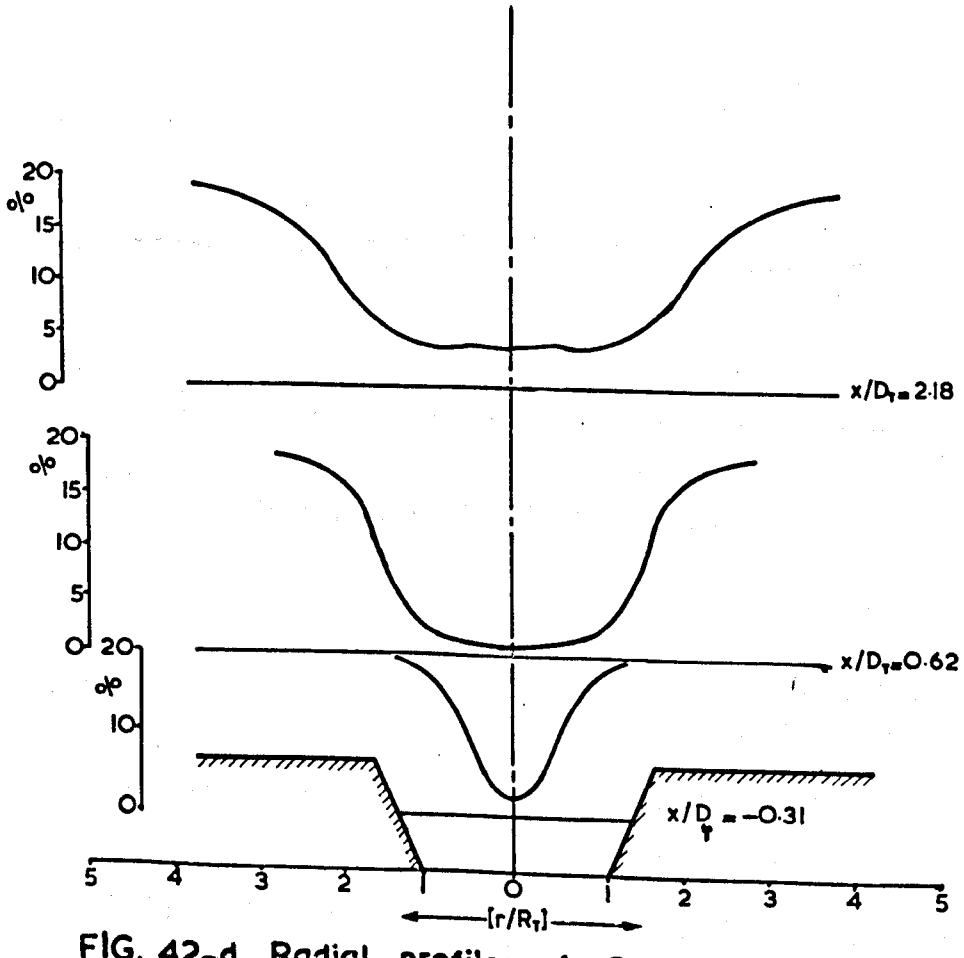

FIG. 42-d Radial profiles of O_2 concentration.

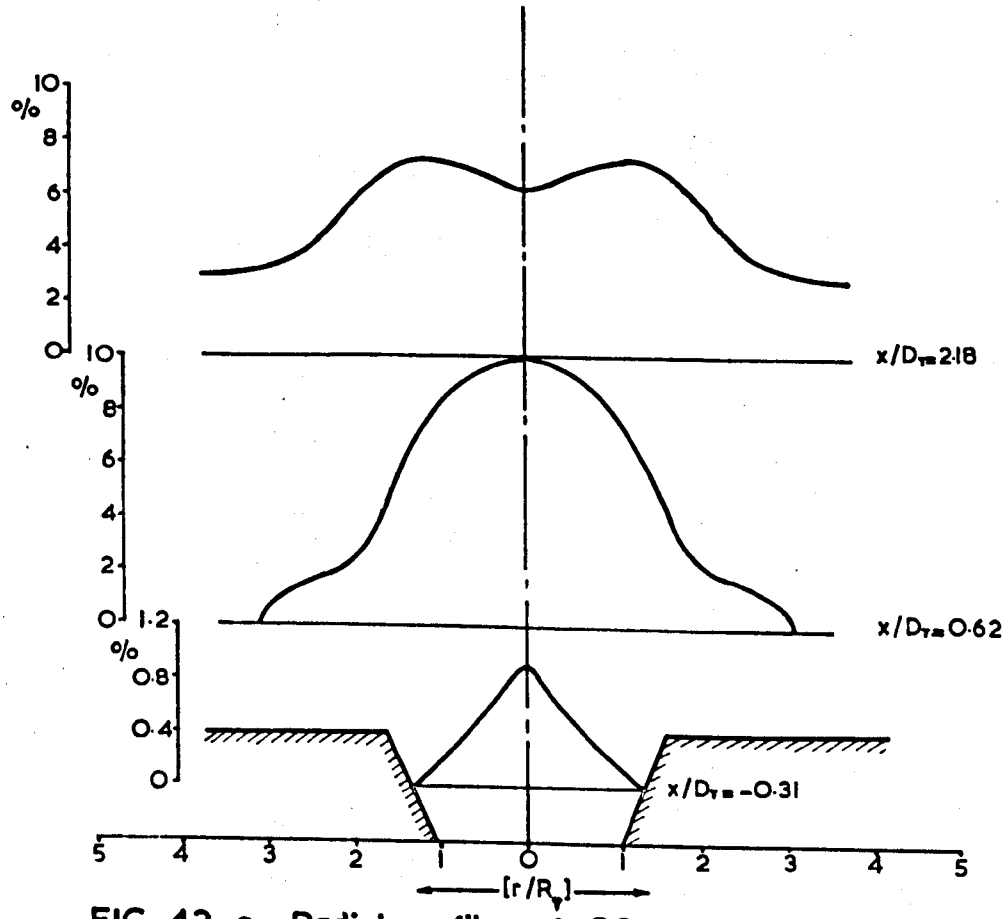

FIG. 42-e Radial profiles of CO_2 concentration.

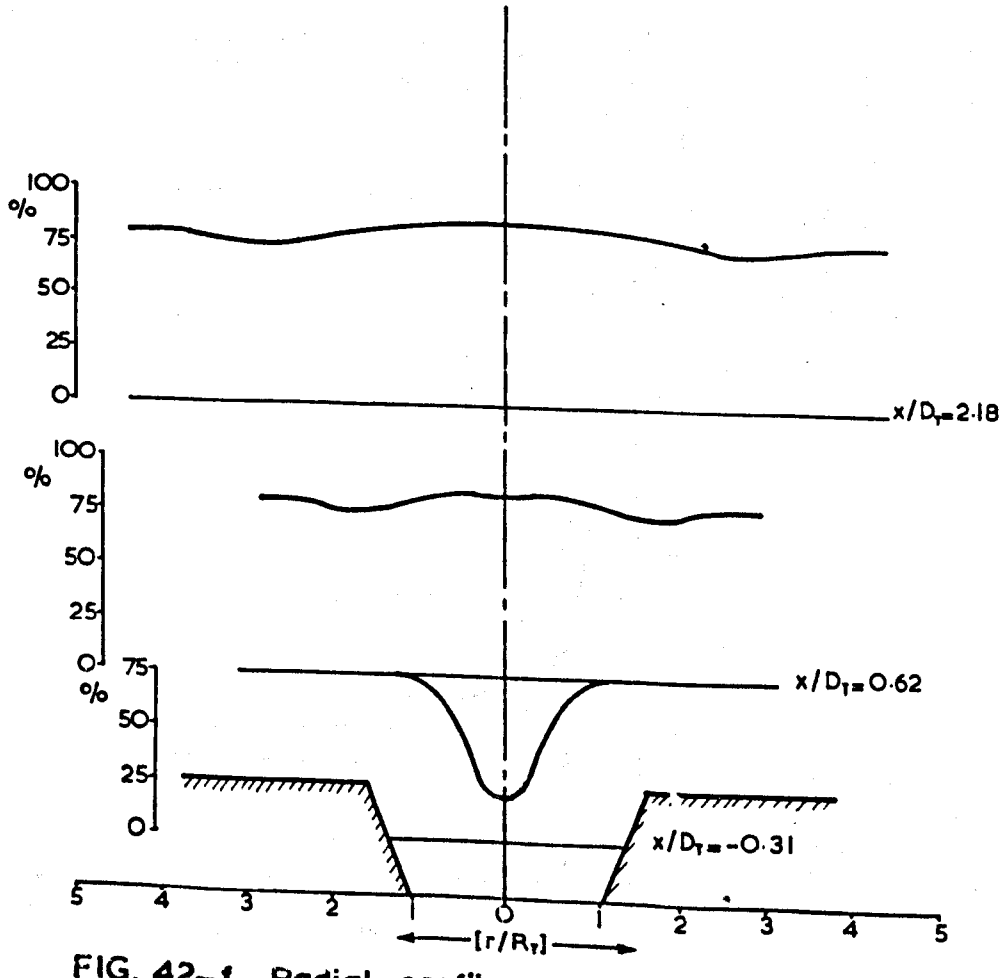

FIG. 42-f Radial profiles of N_2 concentration.

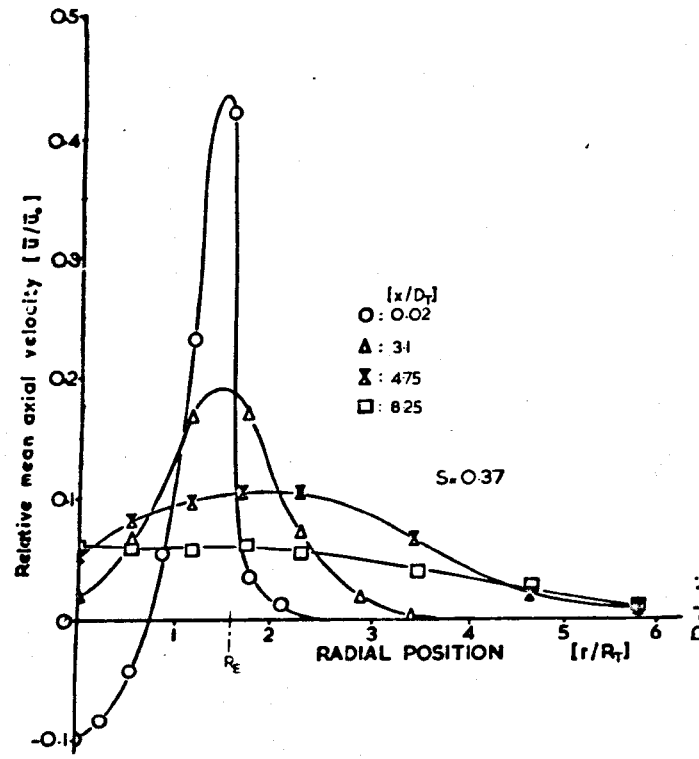

FIG. 43-a

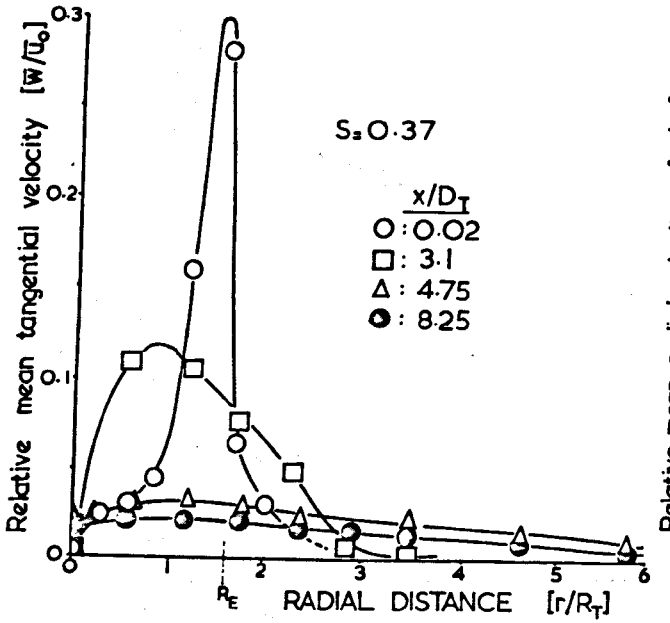

FIG. 43-b

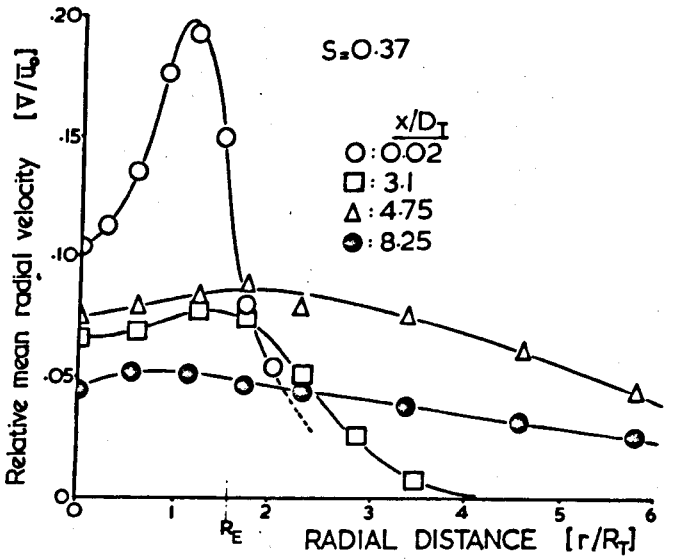

FIG. 43-c

FIG.43 Isothermal velocity distributions in the annular section of a single jet.

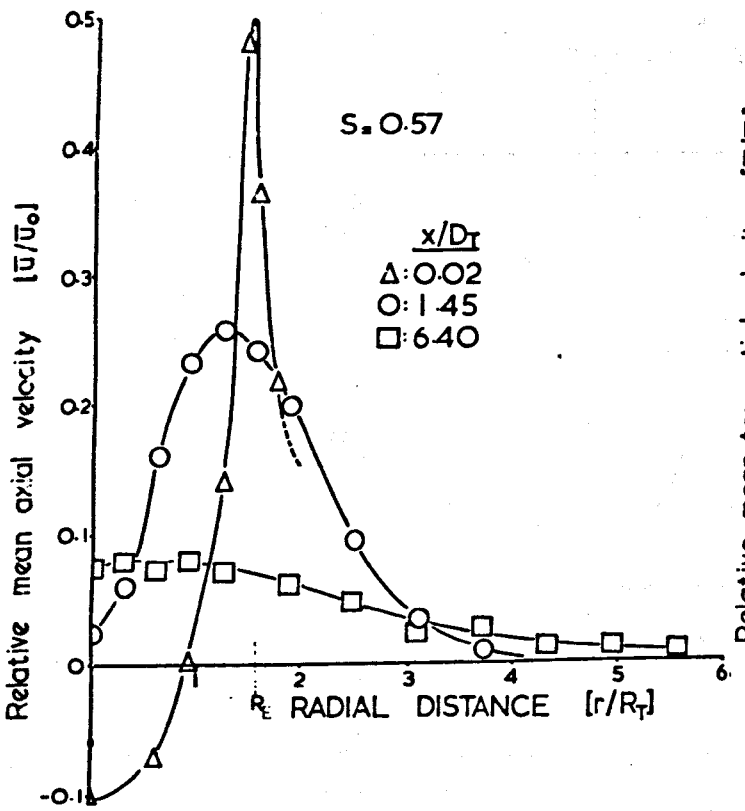

FIG. 44-a

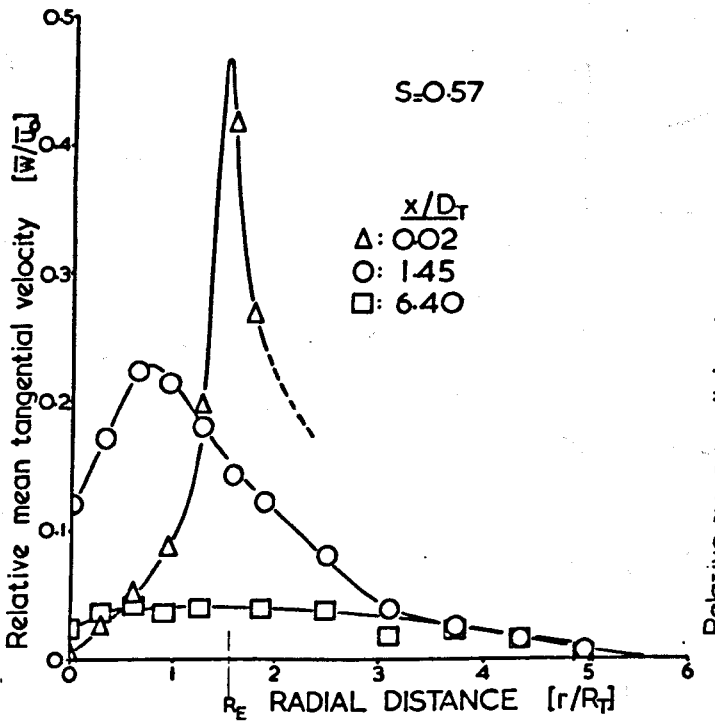

FIG. 44-b

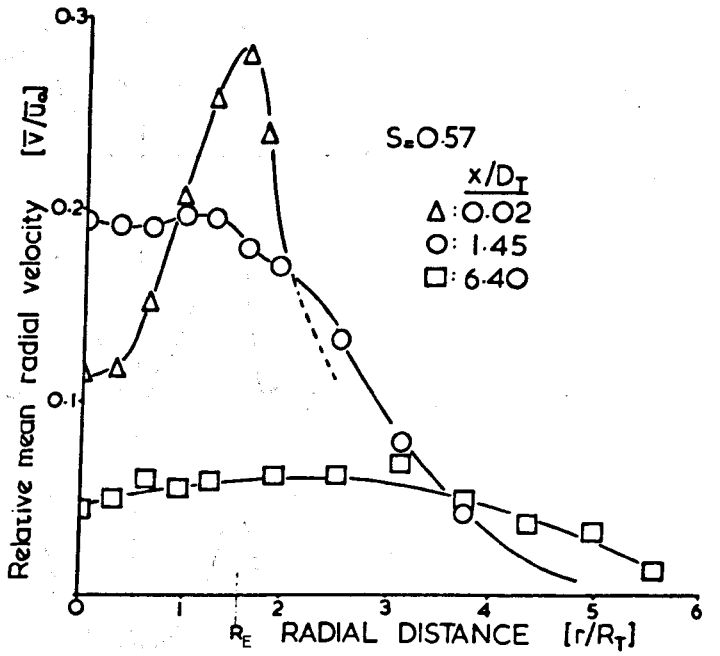

FIG. 44-c

FIG. 44 ISOTHERMAL VELOCITY DISTRIBUTIONS IN THE ANNULAR SECTION OF A SINGLE JET AT A HIGH SWIRL LEVEL (S=0.57).

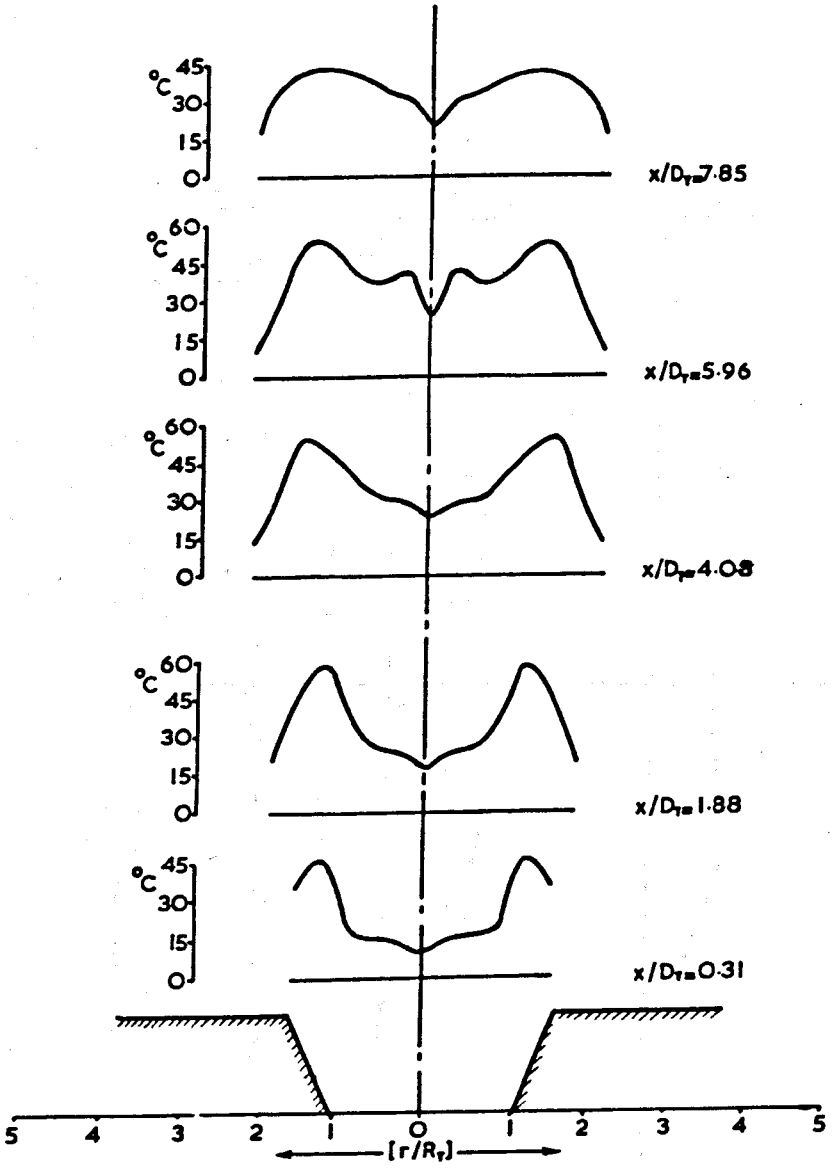

FIG. 45-a RADIAL PROFILES OF TEMPERATURE FLUCTUATIONS FOR S=0.37. (From Apak)

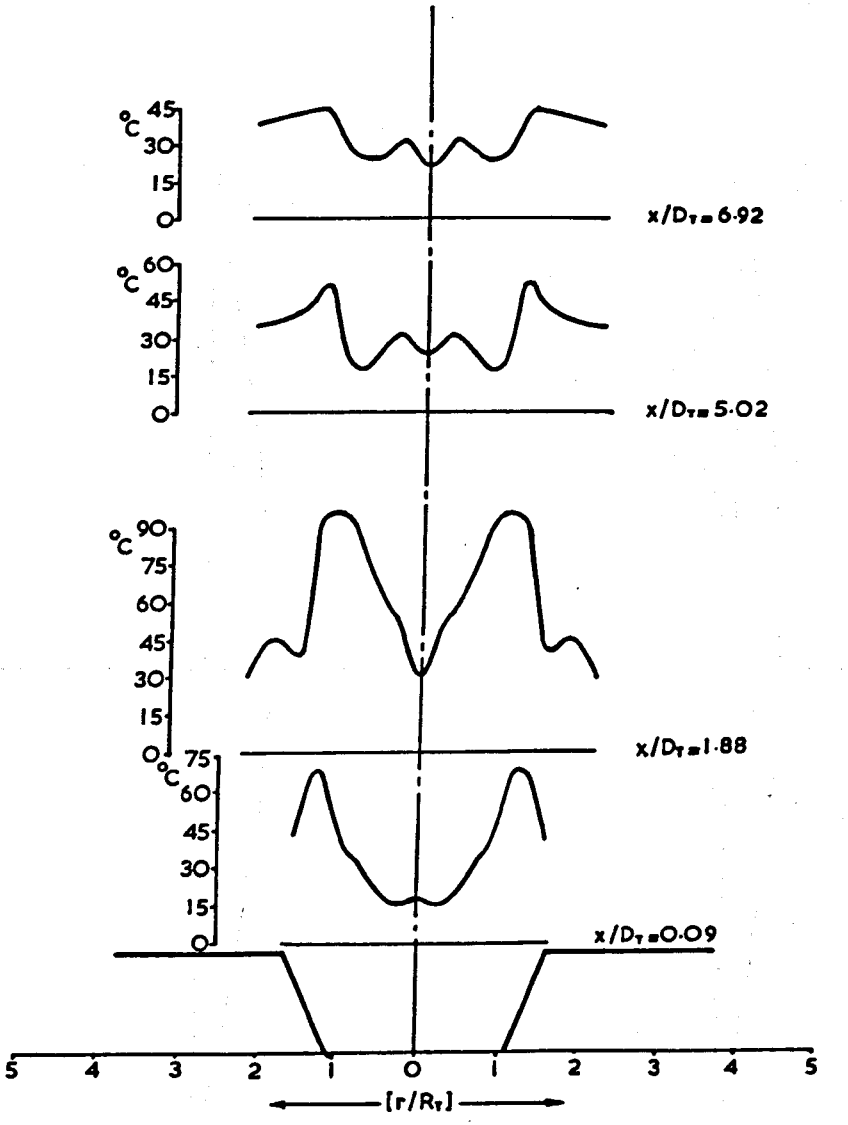

FIG. 45-b RADIAL PROFILES OF TEMPERATURE FLUCTUATIONS FOR S=0.57. (From Apak)

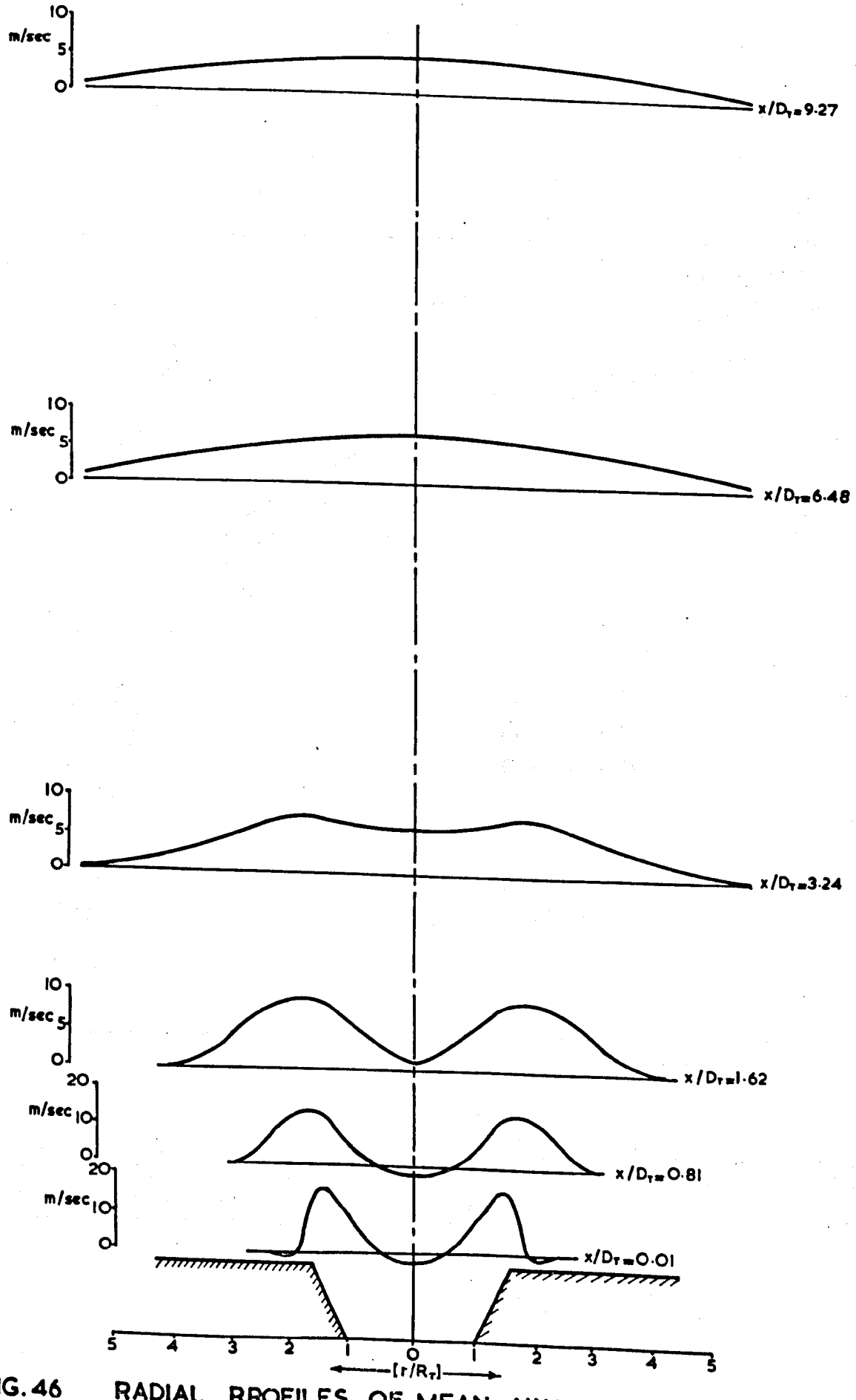

FIG. 46 RADIAL RROFILES OF MEAN AXIAL VELOCITY, ($\bar{U}$) FOR S = 0·37. (From Dvorak)

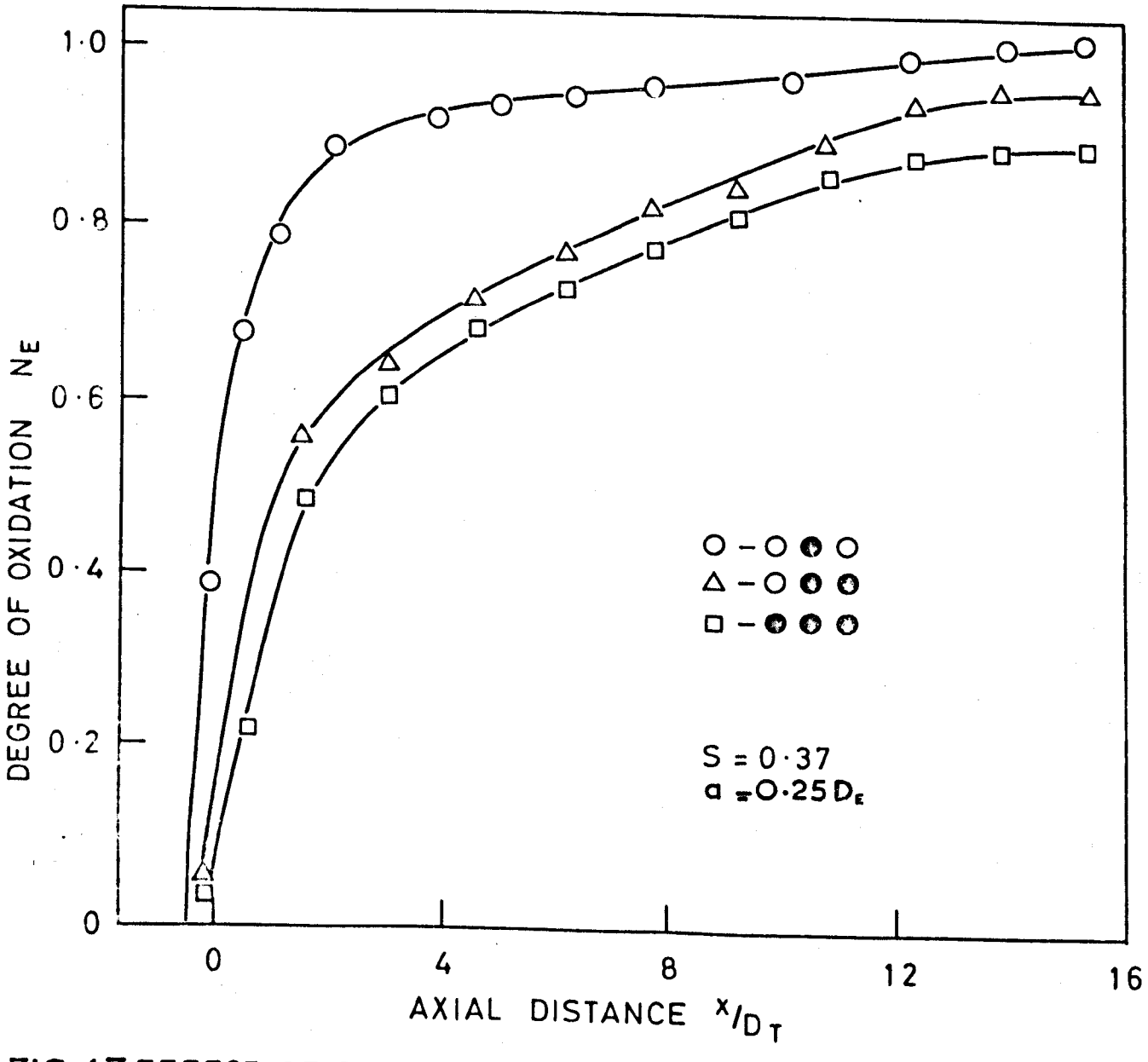

FIG. 47 EFFECT OF BURNER CROWDING ON DEGREE OF OXIDATION ALONG THE DATUM FLAME AXIS.

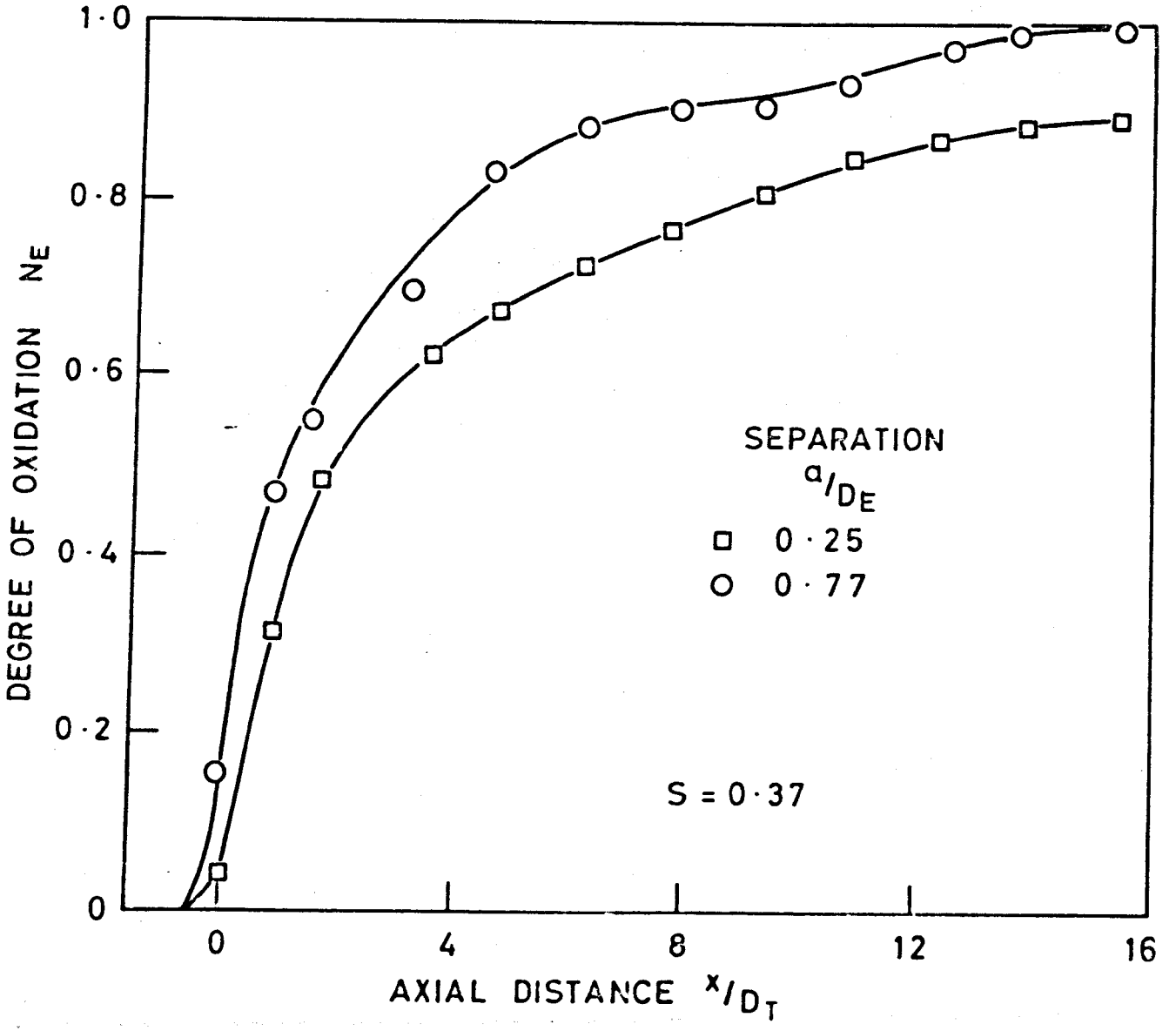

FIG. 48 EFFECT OF SEPARATION ON DEGREE OF OXIDATION ALONG THE CENTRE FLAME AXIS IN THREE BURNER SYSTEM.

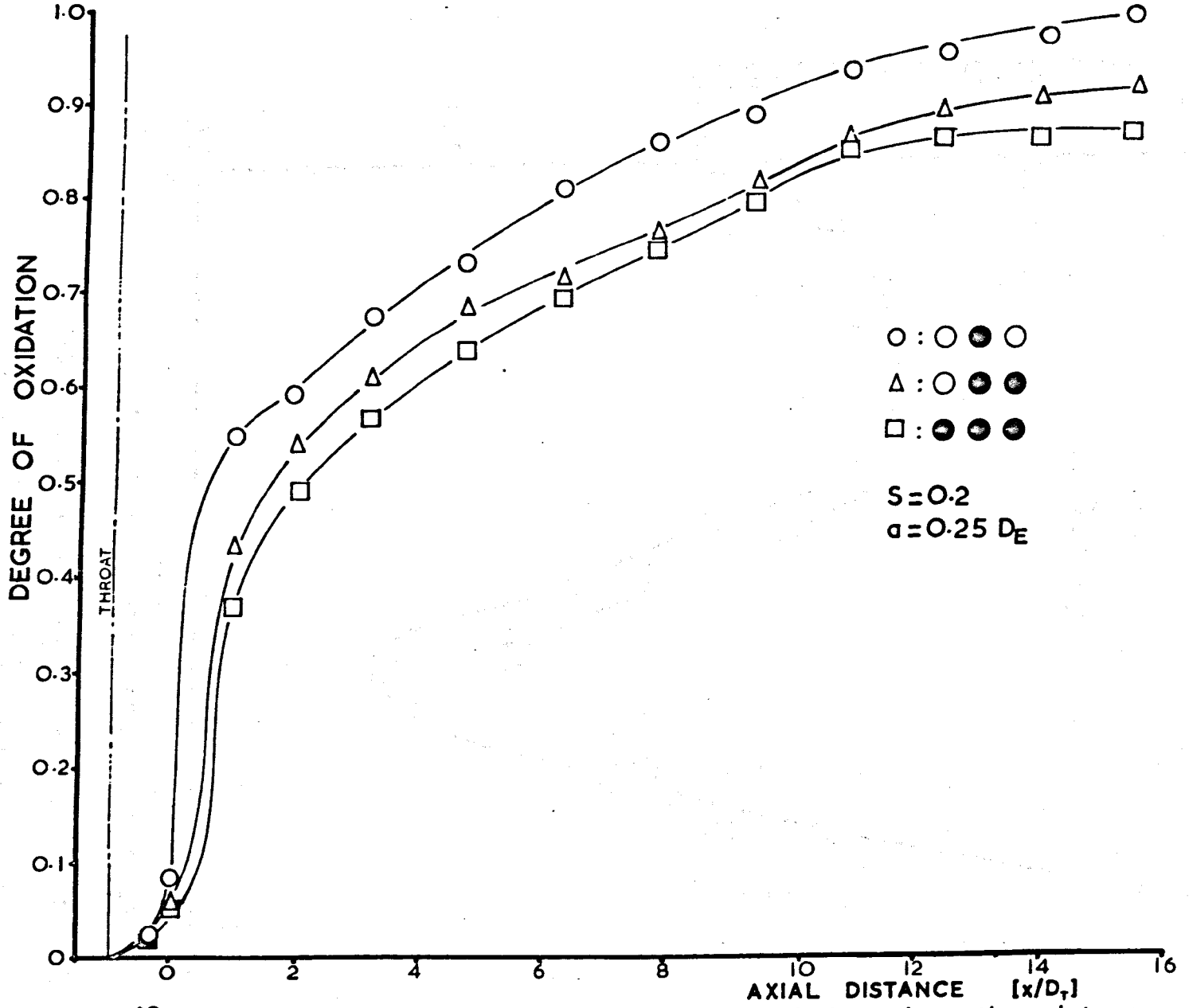

FIG.49: Effect of burner crowding on degree of oxidation along the datum flame axis at low degree of swirl.

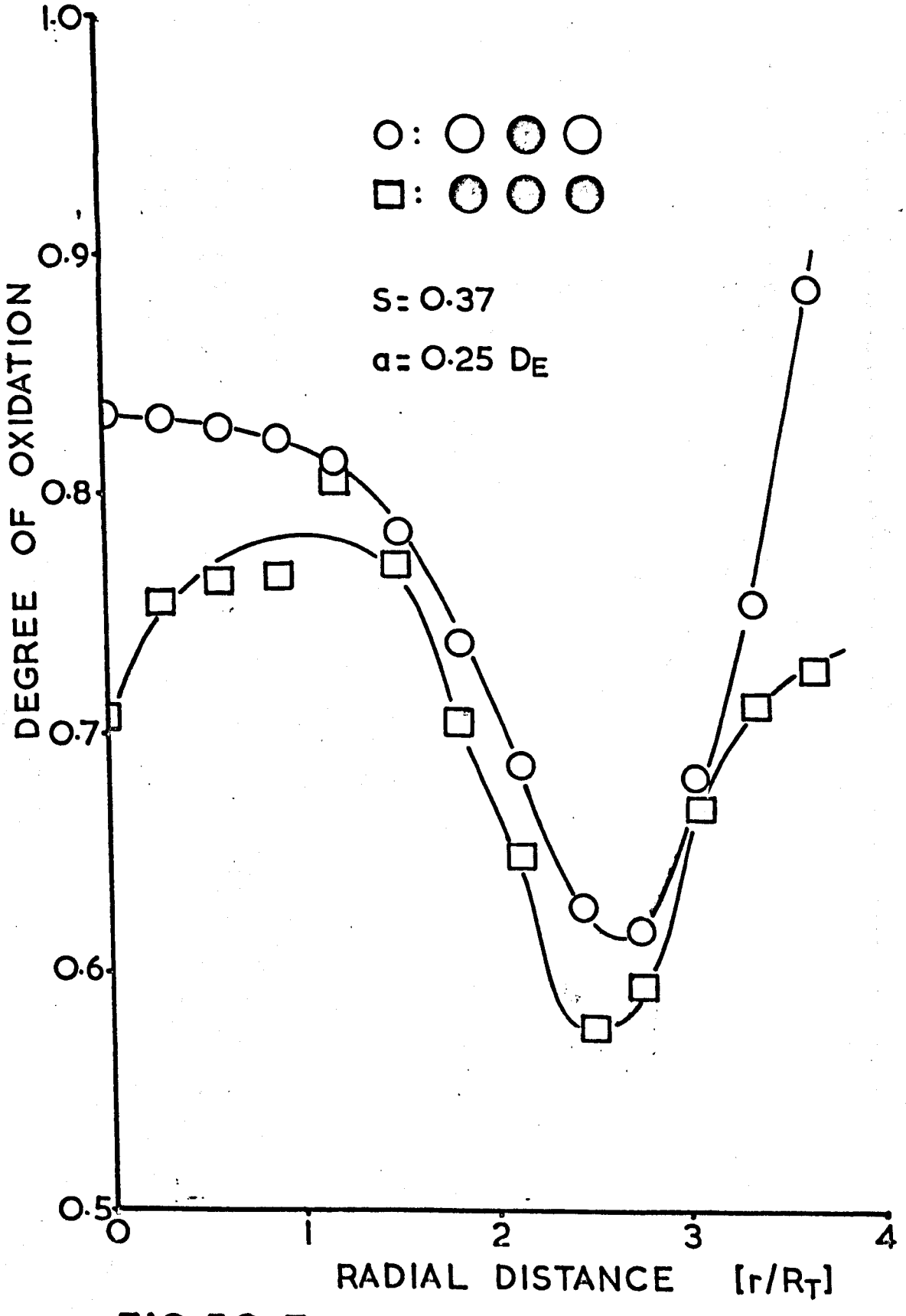

FIG. 50: Effect of burner crowding on degree of oxidation at $x/D_T = 2.2$.

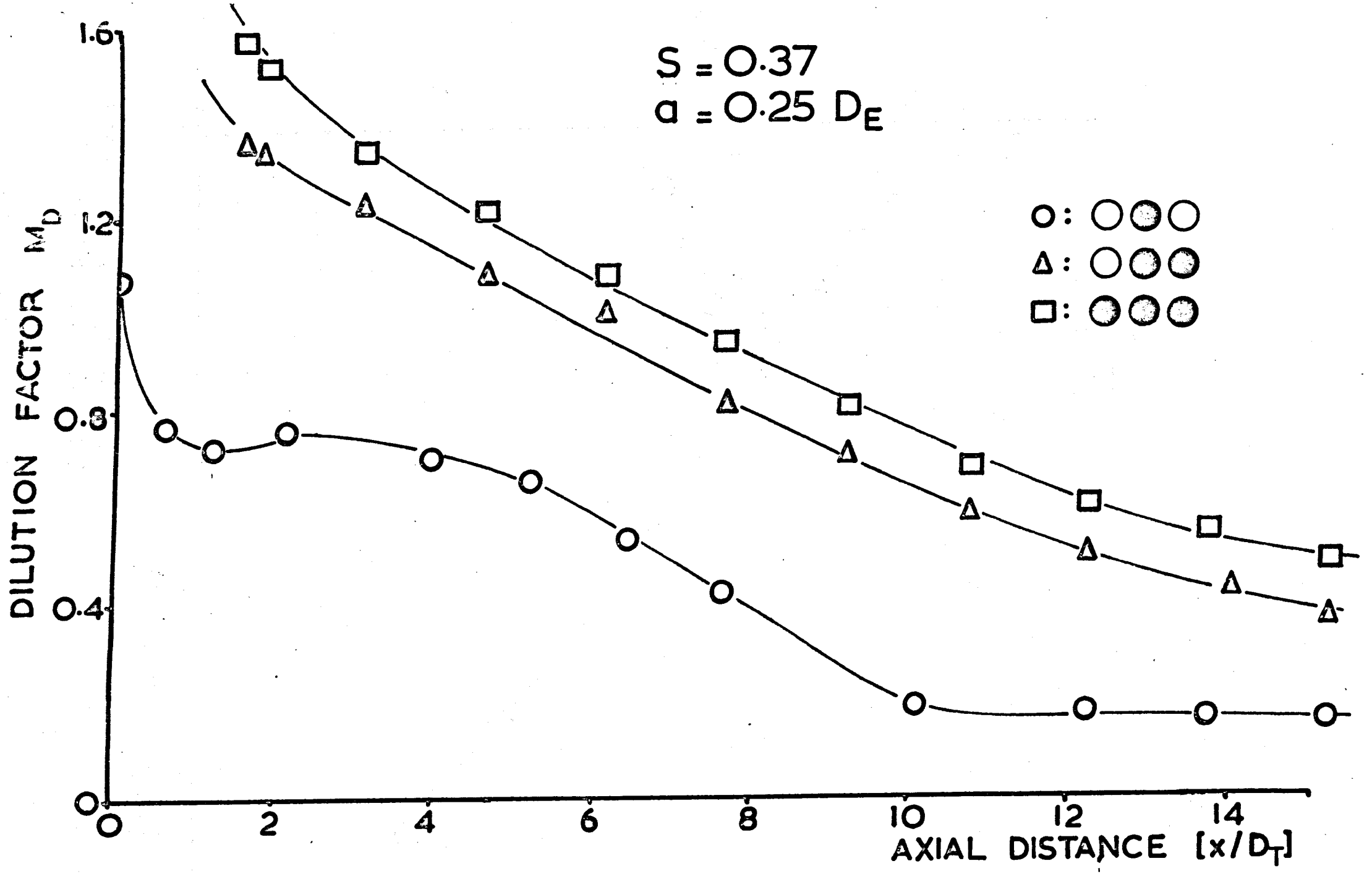

FIG. 51 Effect of burner crowding on degree of dilution.

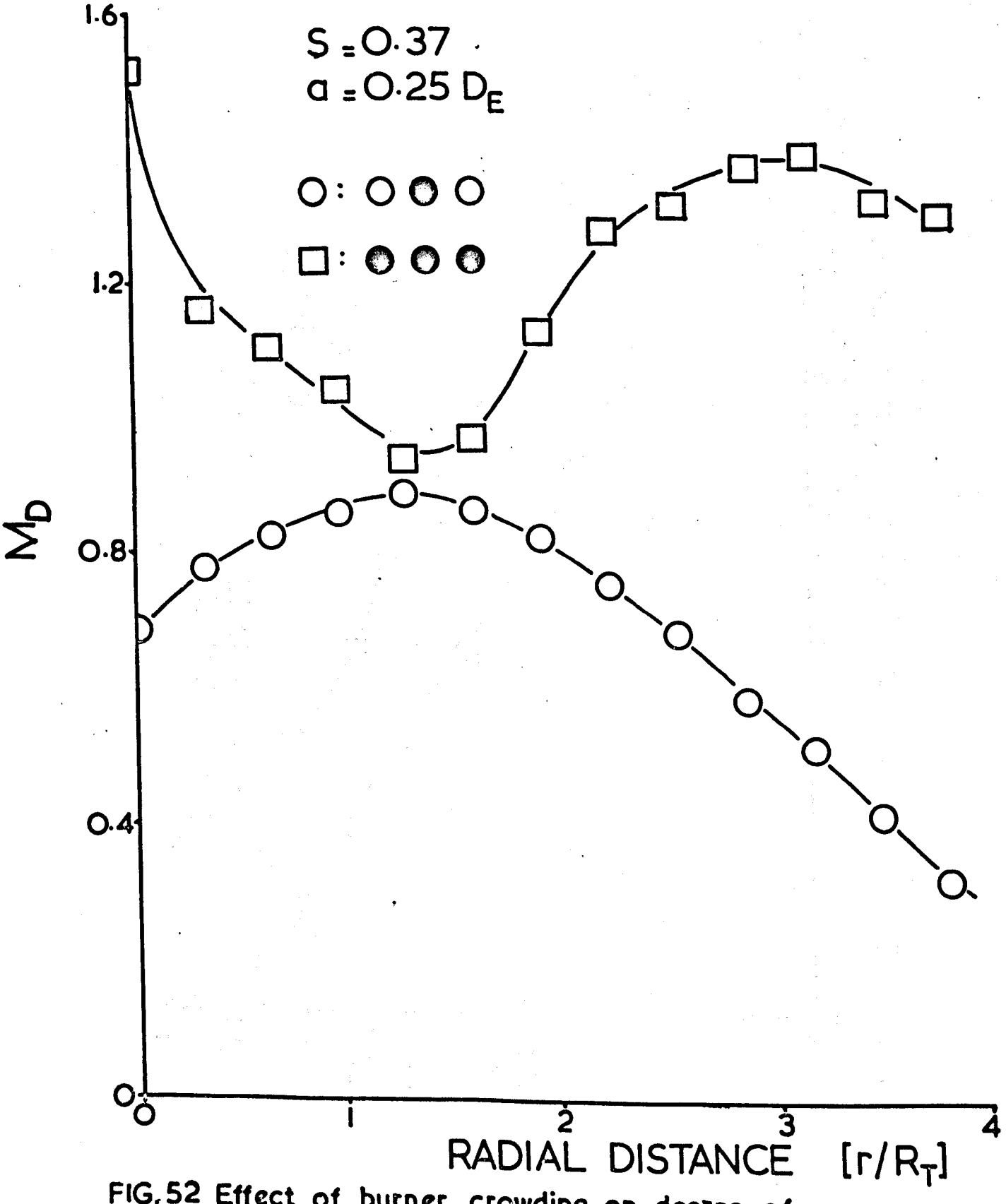

FIG. 52 Effect of burner crowding on degree of dilution at $x/D_T = 2.2$.

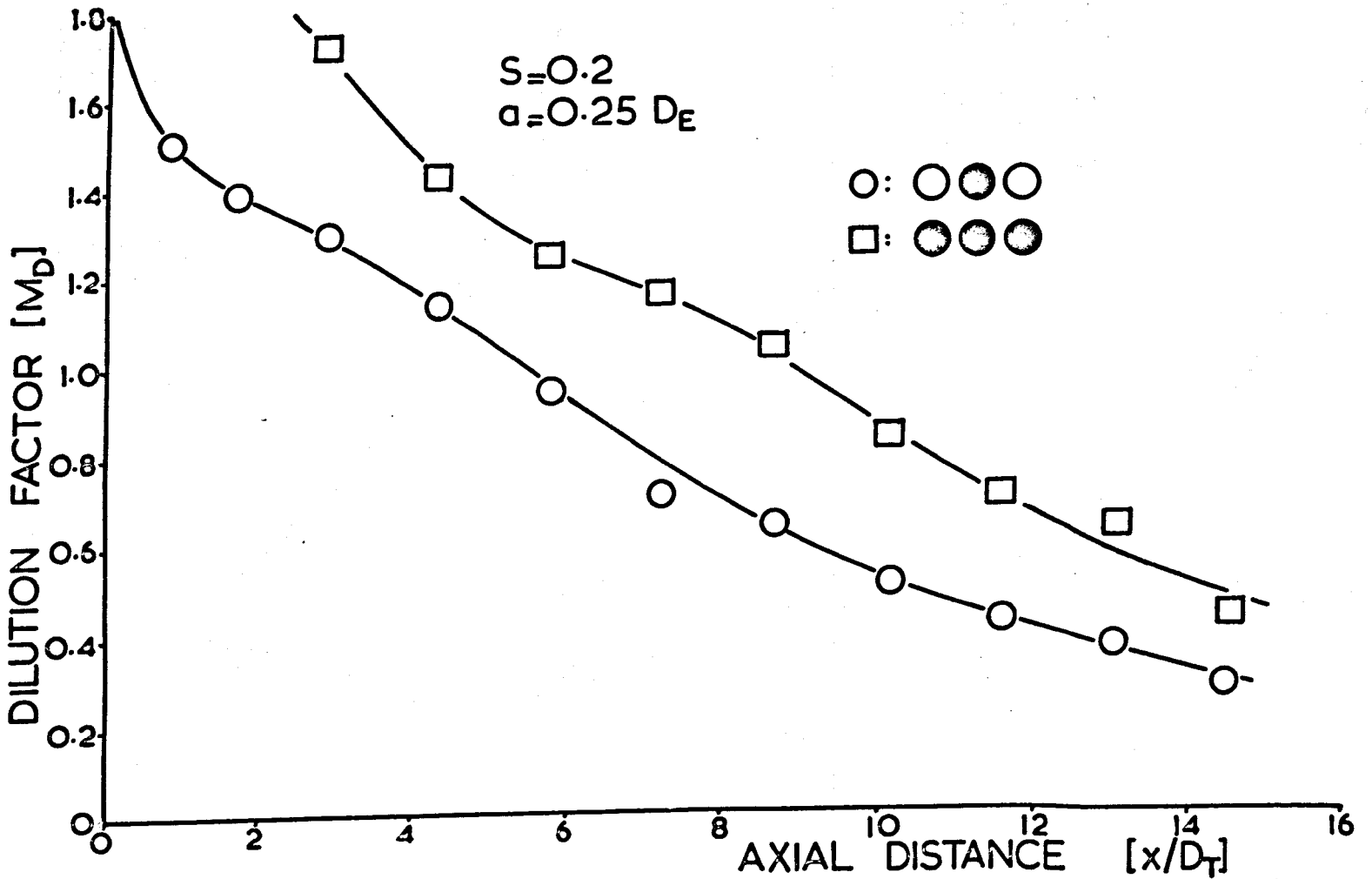

FIG.53 Effect of burner crowding on dilution factor at low swirl level.

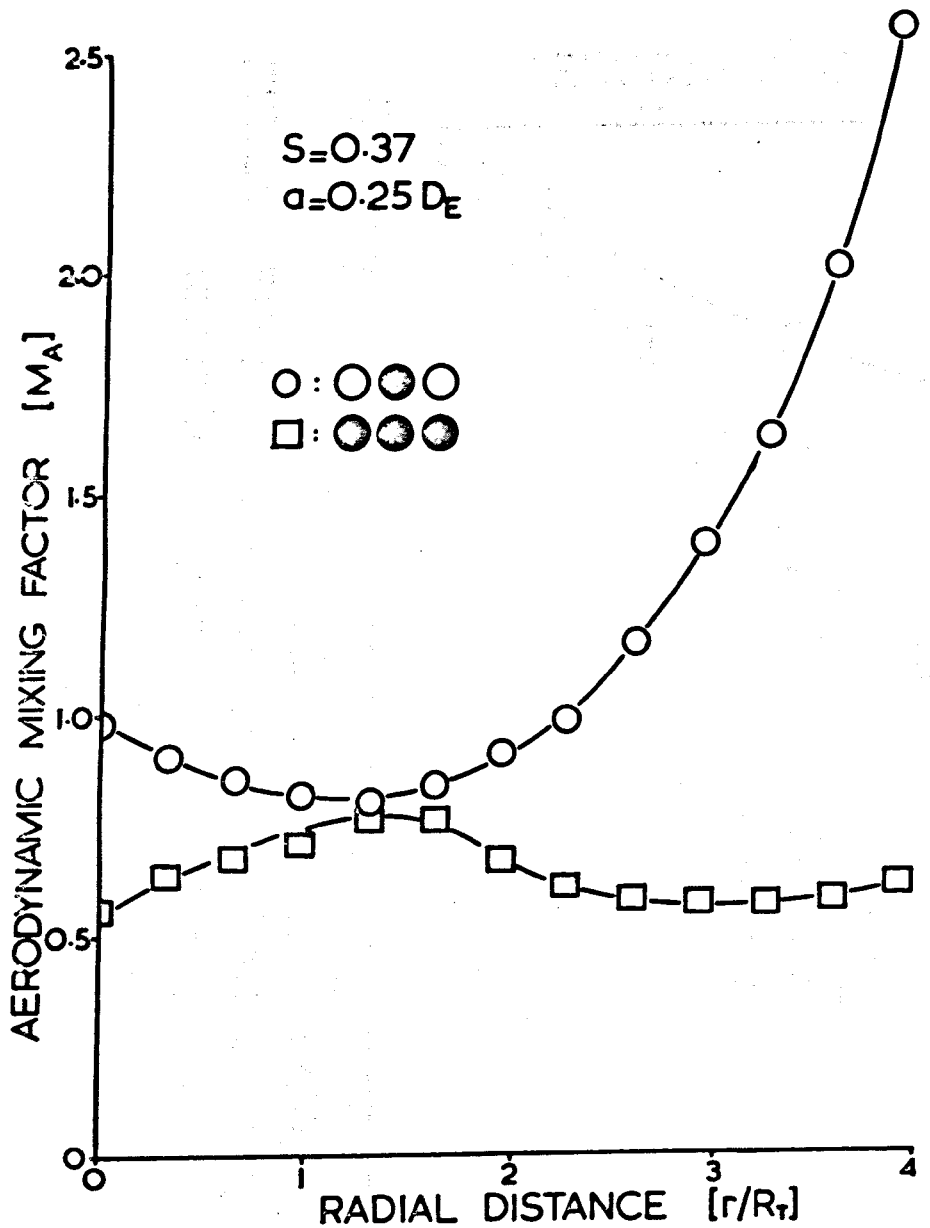

FIG.54 Effect of burner crowding on aerodynamic mixing factor at x/D_T=2·2.

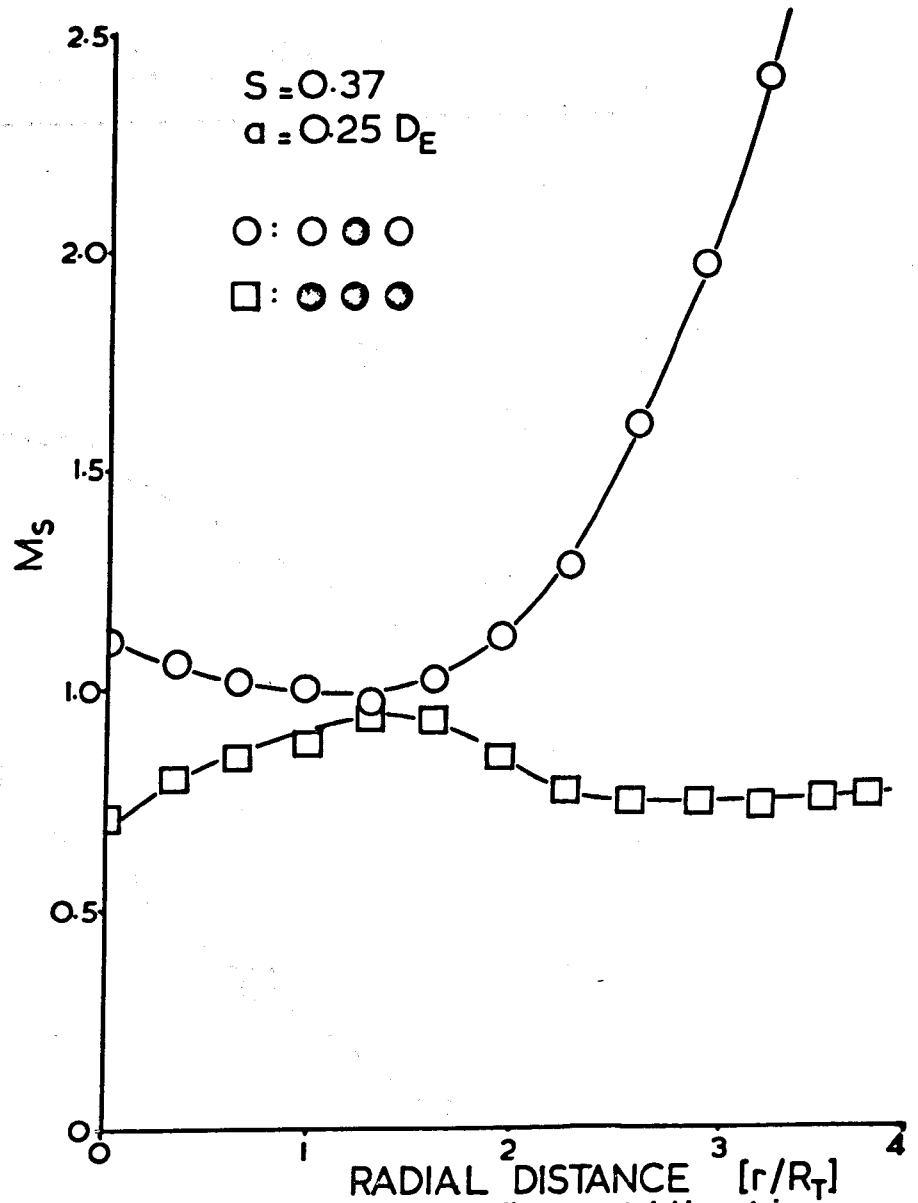

FIG.55 Effect of burner crowding on stoichiometric mixing factor at x/D_T=2·2.

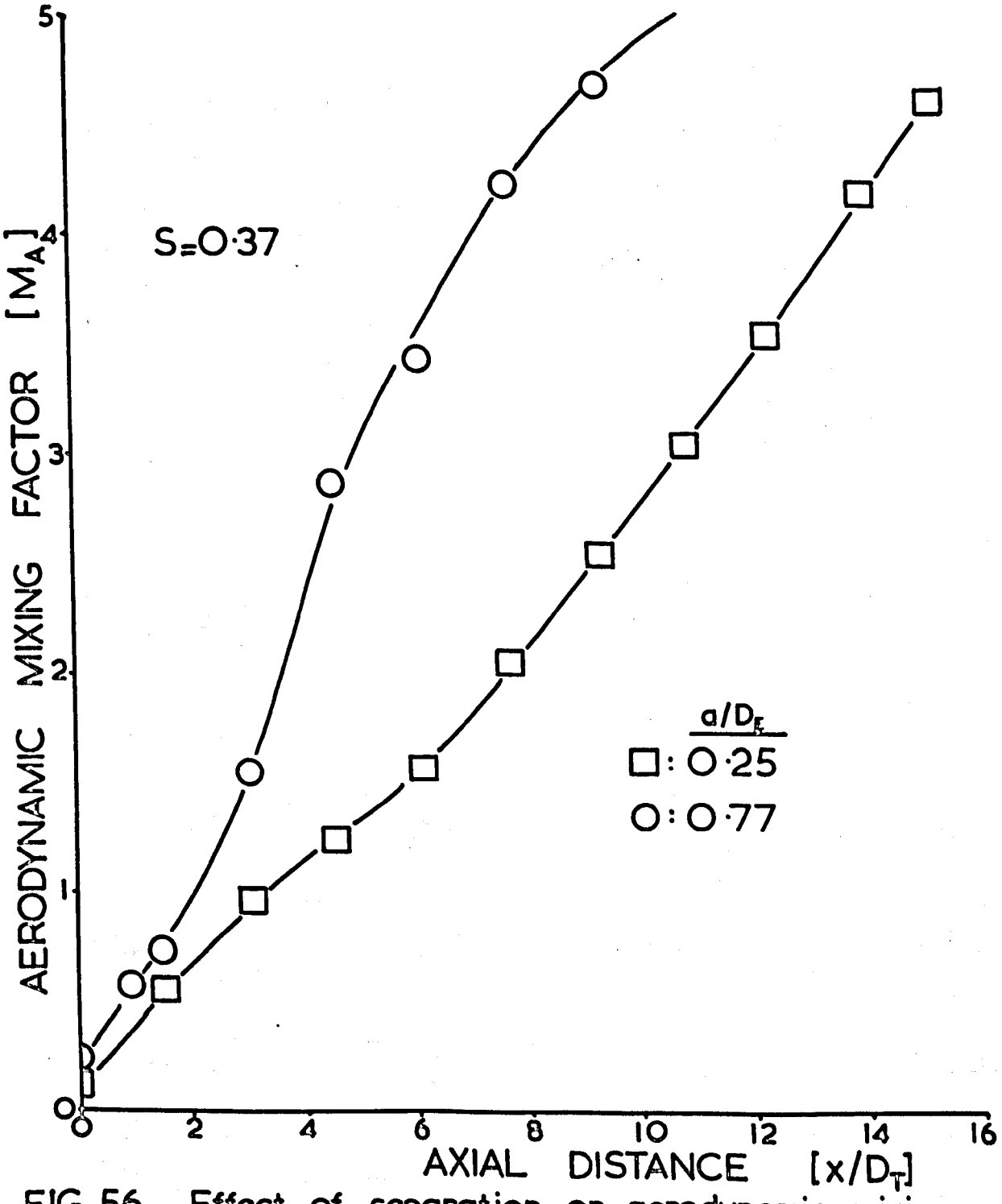

FIG. 56 Effect of separation on aerodynamic mixing factor in a three burner system.

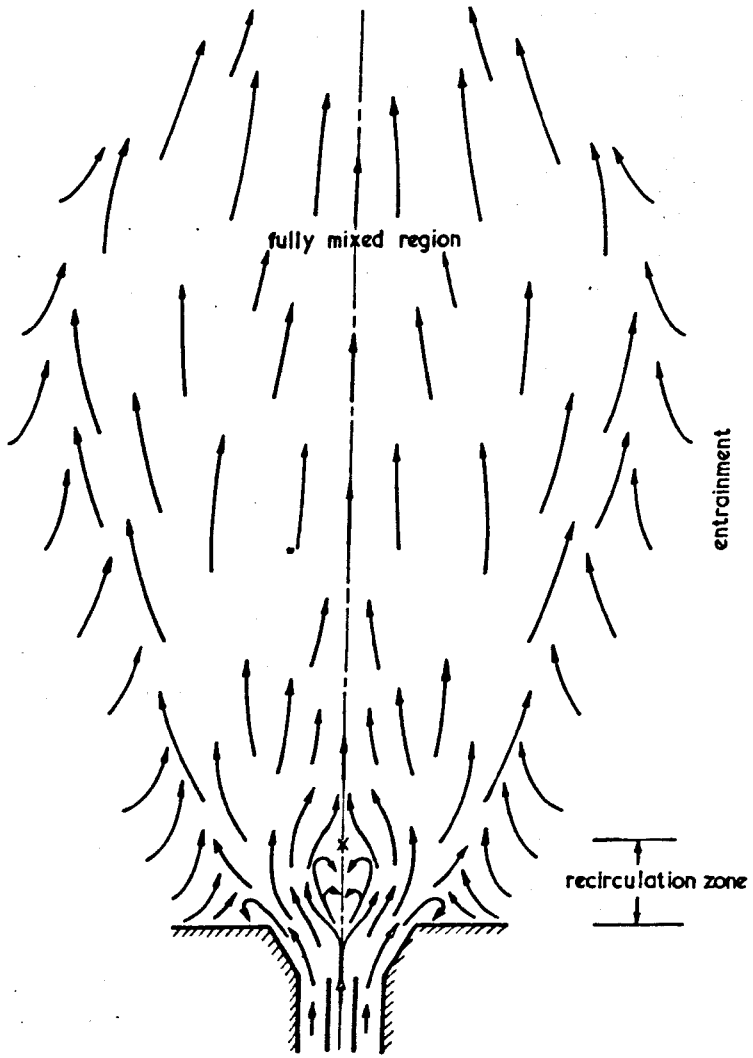

FIG.57-a Schematic flow patterns in a single swirling flame.

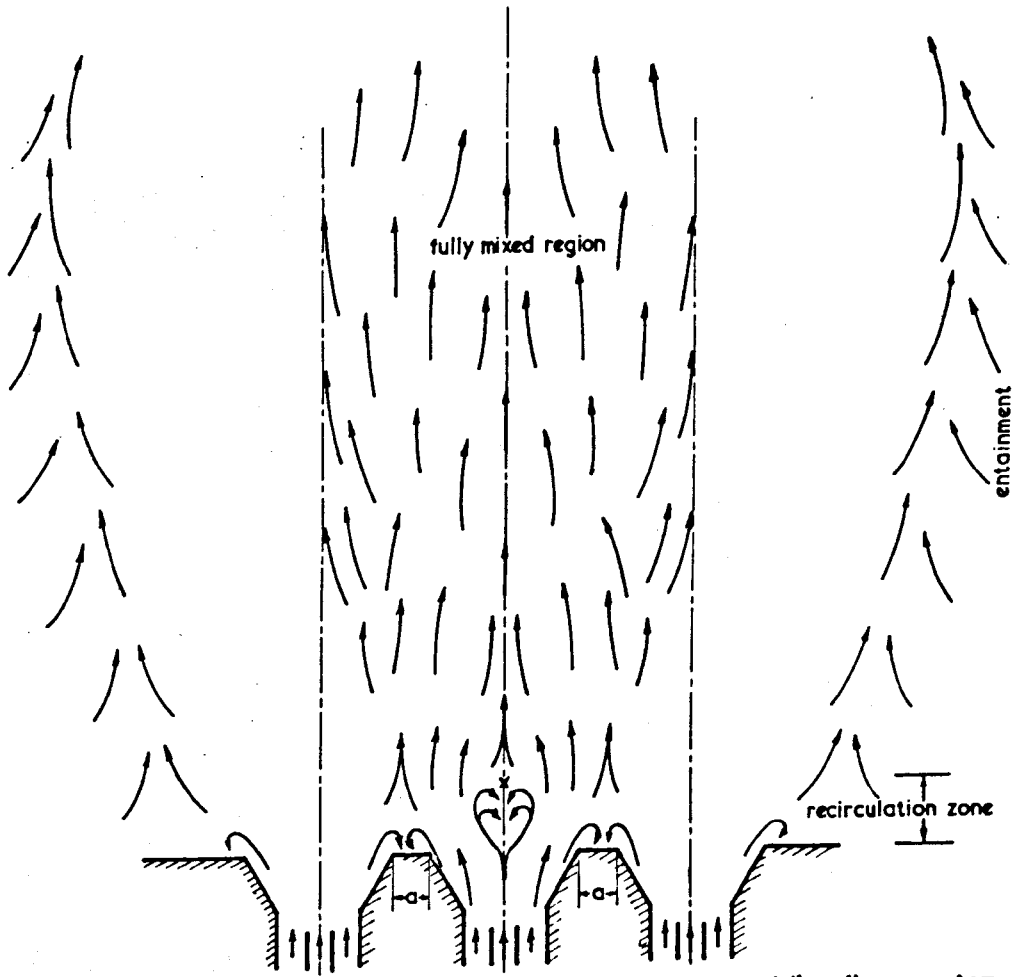

FIG.57-b Schematic flow patterns in a three swirling flame system.

APPENDIX 1.

COMPOSITION OF NATURAL GAS

	Bacton	Easington
N_2	1.54	1.20
CO_2	0.05	0.50
CO	-	-
H_2	-	-
CH_4	94.2	94.3
C_2H_6	3.30	3.20
C_3H_8	0.61	0.58
iso-C_4	0.08	0.08
n-C_4	0.12	0.11
C_5	0.07	0.06
CV (Btu/sft^3 dry)	1043	1042
S.G. (dry/dry air)	0.591	0.594

Natural gas was supplied from two terminals, and the figures quoted (% v/v) are an average of one month's results. The major difference between the two gases is the CO_2 content. Chromatographic analysis for CO_2 is a quick check on gas source.

APPENDIX 2.

CORRECTION OF WIRE CONSTANTS FOR VARIATIONS IN GAS TEMPERATURE

When a hot wire probe is used in a flow of a different temperature than the calibration temperature, which is often the case when the flow is generated by a fan, then it is essential to correct the calibration data to take this effect into account.

A constant-temperature hot wire anemometer is designed to maintain the temperature of the wire constant under changing ambient flow conditions. Therefore observation of the output voltage of a hot-wire anemometer only does not help to separate effects due to change in flow velocity or a change in flow temperature. There are many situations, as it has been in this research, where the ambient temperature of the flow does not remain constant and where considerable error can be introduced into the measurement of flow velocity.

The basic response of the hot wire anemometer can be described by King's law, which relates the Nussult number Nu, to the Reynolds number, Re, of the flow around the wire.

$$Nu = A' + B' \, Re^{\frac{1}{2}} \quad \ldots\ldots\ldots \quad (A2.1)$$

where

$$Nu = \frac{E^2}{R_w \, \ell \, k \, (T_w - T_a)} \qquad Re = \frac{\rho U d}{\mu}$$

A' and B' are wire constants, R_w is wire resistance E is the bridge voltage, ℓ is hot-wire length. From equation (A2.1)

$$E^2 = R_w \, \ell \, k(T_w - T_a)A' + R_w \, \ell k \, (T_w - T_a)B' \, \left(\frac{\rho U d}{\mu}\right)^{\frac{1}{2}} \quad \ldots\ldots\ldots \quad (A2.2)$$

In the above equation, k, ρ and μ are all evaluated at temperature T which is a temperature characteristic of the flow around the wire. For air the group $k(\rho/\mu)^{\frac{1}{2}}$ has a very little

dependence (54) on fluid temperature. Thus for a wire at a fixed temperature equation (A2.2) becomes:

$$E^2 = k\,(T_w - T_a)A'' + (T_w - T_a)B''\,U^{\frac{1}{2}} \quad \ldots\ldots\ldots \quad (A2.3)$$

The flow properties have been evaluated at the wire surface temperature T_w, as suggested by Davies and Fisher (74). At a constant wire temperature equation (A2.3) becomes

$$E^2 = A + B\,U^{1/n} \quad \ldots\ldots\ldots \quad (A2.4)$$

At two different ambient temperatures hot wire anemometer response equation will be (73)

$$E_m^2 = A + B\,U^{\frac{1}{2}} + C \quad \text{at temperature } T_{a_1} \quad \ldots\ldots\ldots \quad (A2.5)$$

$$E_m^2 = A_1 + B_1 U^{\frac{1}{2}} + C_1 \quad \text{at temperature } T_{a_2} \quad \ldots\ldots\ldots \quad (A2.6)$$

where

$$\frac{A}{A_1} = \frac{B}{B_1} = \frac{C}{C_1} = \frac{T_w - T_{a_1}}{T_w - T_{a_2}} \quad \ldots\ldots\ldots \quad (A2.7)$$

let $$\frac{T_{a_1} - T_{a_2}}{T_{a_1}} = \varepsilon$$

and $$\frac{T_w}{T_{a_1}} = \theta$$

where θ is the overheat ratio. Therefore equation (A2.7) can be written as follows:

$$\frac{A}{A_1} = \frac{B}{B_1} = \frac{C}{C_1} = \frac{\theta - 1}{\theta - 1 + \varepsilon} = \frac{\sigma}{\sigma + \varepsilon} \quad \ldots\ldots \quad (A2.8)$$

where $\sigma = \theta - 1$

Substituting eq.(A2.8) back into eq.(A2.4) gives

$$E_m^2 = A\,\frac{(\sigma + \varepsilon)}{\sigma} + B\,\frac{\sigma + \varepsilon}{\sigma}\,U^{1/n} \quad \ldots\ldots\ldots (A2.9)$$

Now let

$$E_m = E_c + \delta E \quad \ldots\ldots\ldots \quad (A2.10)$$

where E_c = the bridge voltage in the absence of any temperature change.

δE = variation in bridge voltage with the temperature change.

Substituting eq.(A2.10) into eq.(A2.5)

$$(E_m - \delta E)^2 = A + B\, U^{\frac{1}{2}} \quad \ldots\ldots\ldots\ldots \quad (A2.11)$$

and combining equations (A2.11) and (A2.9)

$$E_m^2 = (1 + \frac{\varepsilon}{\sigma})\ (E_m - \delta E)^2$$

and

$$E_m = (1 + \frac{\varepsilon}{\sigma})^{\frac{1}{2}}\ E_c \quad \ldots\ldots\ldots\ldots \quad (A2.12)$$

If the changes in stream temperature, $(T_{a_1} - T_{a_2})$, is small compared with the difference between wire temperature and stream temperature, that means ε/θ is small, thus equation (A2.12) becomes

$$E_c \simeq E_m\ (1 - \frac{\varepsilon}{2\sigma}) \quad \ldots\ldots\ldots\ldots \quad (A2.13)$$

By substituting the value of E_c in equation (A2.5) the correct velocity can be found.

APPENDIX 3.

The programme is written in Focal and calculates the actual gas temperature by solving equation (5.3) for T_G. To do this the physical properties of the gas at the point had to be known.

The concentrations measured by the gas chromatograph are at dry basis. First the water content is calculated by making N_2, O_2 and carbon balance and all concentrations are converted to wet basis. Mixture viscosity and thermal conductivity are calculated using Wilke and Mason-Saxena equations, as given in Ref. (65), respectively. Mixture density, molecular weight and specific heat are calculated by taking a weighed average of these properties at the temperature and pressure in question.

Using these computed properties mixture heat transfer coefficient and effective junction emissivities are calculated to be inserted into equation (5.3).

Having fed the necessary data aerodynamic and stoichiometric mixing factors and degree of oxidation are also calculated in this programme.

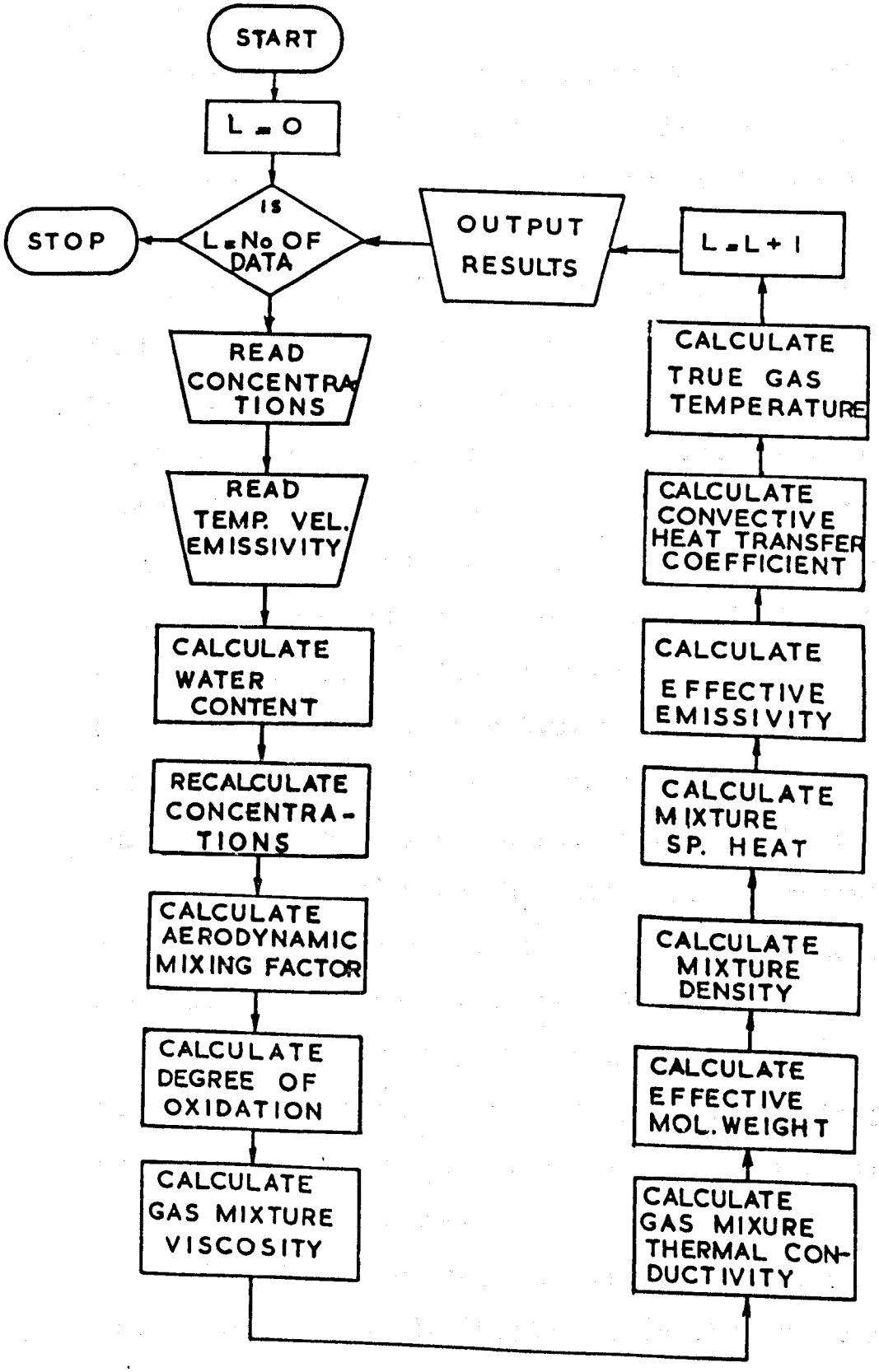

FLOW DIAGRAM OF THE COMPUTER PROGRAM FOR CORRECTON OF RECORDED TEMPERATURES.

APPENDIX 4.

Two programmes are written in FOCAL to calculate the isothermal velocities of the annular air stream. First programme calculates the calibration constants to be used in the second programme for calculating the three component mean velocities.

Programme (1) calculates the calibration constants A,B,C in the calibration equation (5.6). First the ambient temperature, pressure and a set of calibration data (anemometer D.C. voltage E and NPL pitot pressure readings in m.m. H_2O corresponding to flowrates) are fed. Then the computer converts the pressures to flowrate data and does a least squares fit on the given data to obtain the constants A,B,C. As a check on the calculated constants the D.C. voltages are recalculated using equation (5.6) and compared to the D.C. voltages previously fed in as data. Within the calibration range used comparison of two sets of voltages show a very close fit of the calibration equation.

Programme (2) uses the calibration constants calculated by the previous programme to compute mean and fluctuating velocities depending on the hot wire anemometer data.

Because the voltage readings of a hot wire anemometer are highly dependent on the flow temperatures a temperature correction is introduced for voltages to take into account the changes in temperature.

After this the programme is a straight forward solution of the equations (5.12), (5.13) and (5.14), for mean velocities and the equations given by Syred (58) for the turbulent parameters.

Since this programme assumes that the three out of the four output voltages are in phase the errors in computation of the turbulent parameters can be grossly in error and therefore they are not used for any interpretation.

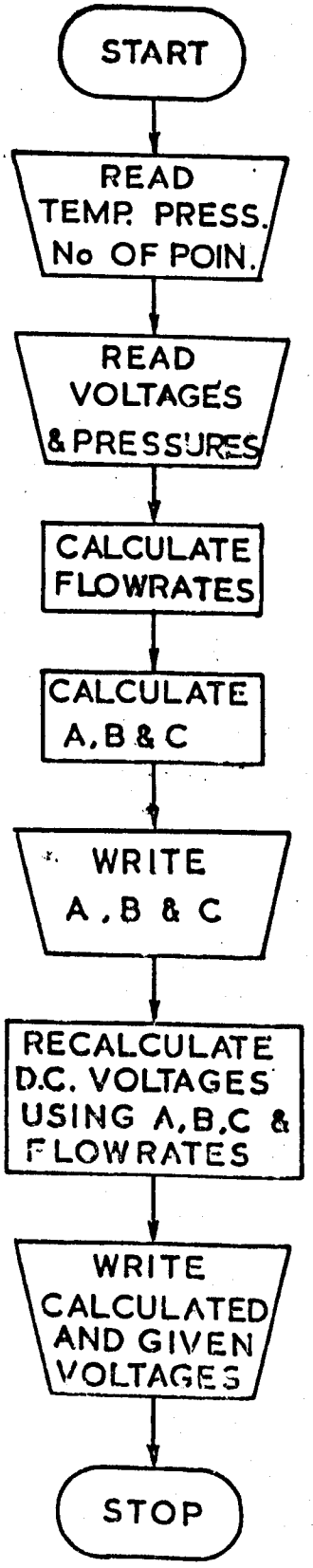

PROGRAM-1 FLOW DIAGRAM OF COMPUTER PROGRAM FOR CALCULATING THE CABRATION CONSTANTS.

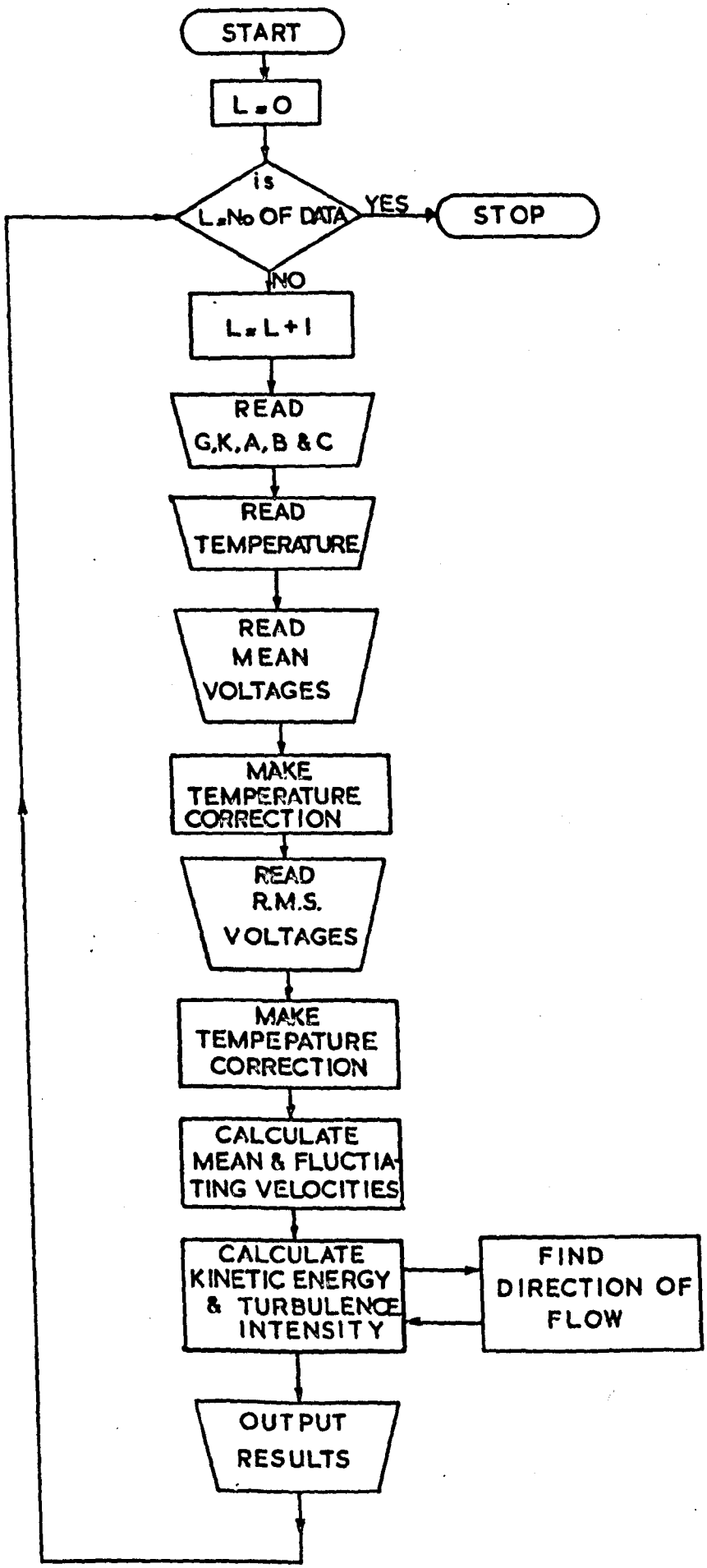

FLOW DIAGRAM OF THE PROGRAM FOR CALCULATING THE VELOCITIES.

PROGRAM - 2